

Plume Tracking Field and Model Analysis of Discharges from the Encina Ocean Outfall and San Elijo Ocean Outfall

18 November 2022

Submitted to:

Chris Trees
Director of Operations
San Elijo Joint Powers Authority



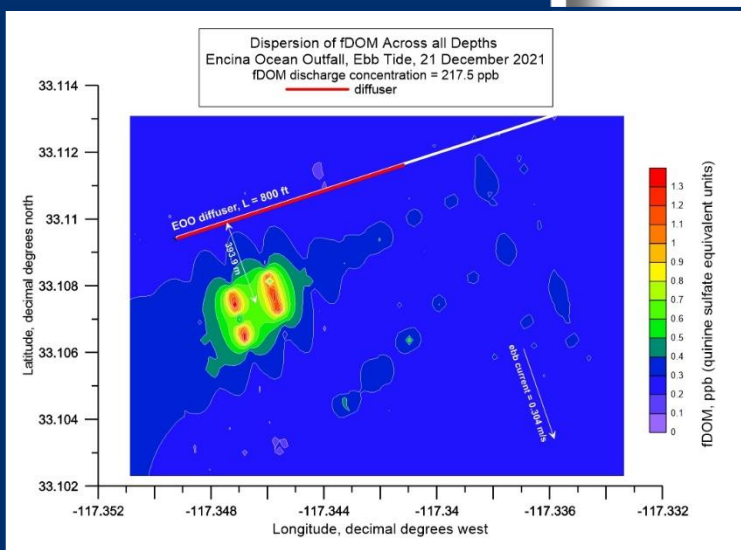
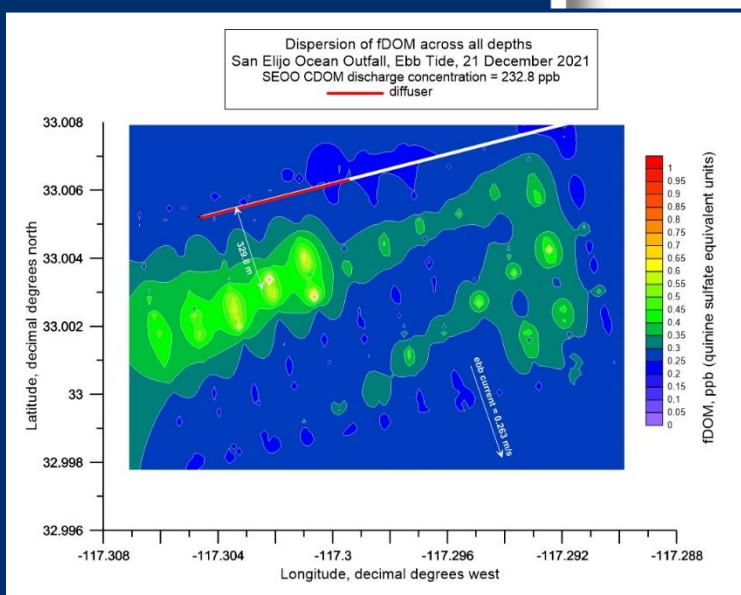
Alicia Appel
Director of Environmental Compliance
Encina Wastewater Authority



Nicki Branch
Laboratory Superintendent
City of Escondido



Submitted by:
Scott Jenkins, Ph.D.
Makrom Shatila, P.E.
Michael Baker International





ACKNOWLEDGEMENTS

Michael Baker International would like to extend a special thank you to all San Elijo Joint Powers Authority (SEJPA), Encina Wastewater Authority (EWA), and City of Escondido personnel and staff who were key to the successful completion of this outfall AUV plume tracking study.



Michael Baker International also wishes to acknowledge the contribution of the subconsultants involved with this project. Below is a list of each subconsultant and their associated tasks, which were essential to completing this study successfully:



- **MBC Aquatic Sciences:** Work Plan and water quality data collection services.



- **Orca Maritime:** Provided research vessel (R/V Benthic Cat) and Autonomous Underwater Vehicle (AUV), including operations and data collection.



TABLE OF CONTENTS

Executive Summary	ES-1
1 Introduction	1-1
1.1 Fluid Mechanics and Regulatory Standards of Effluent Dilution	1-3
1.2 Outfall Survey Methods	1-5
1.3 CDOM/fDOM Calibration	1-11
2 Plume Tracking Results for Encina Ocean Outfall (EOO)	2-1
2.1 First EOO Deployment - 21 September 2021.....	2-1
2.2 Second EOO Deployment - 20 December 2021	2-26
2.3 Third EOO Deployment - 2 March 2022.....	2-55
3 Plume Tracking Results for San Elijo Ocean Outfall (SEOO)	3-1
3.1 First SEOO Deployment – 23 September 2021	3-1
3.2 Second SEOO Deployment – 21 December 2021	3-26
3.3 Third SEOO Deployment - 3 March 2022.....	3-44
4 NPDES Permit Discussion	4-1
5 Summary of Findings	5-1
6 Conclusions	6-1
7 References	7-1

APPENDICES

APPENDIX-A: Discharge Logs for the EOO on 21 September, 20 December 2021, and 2 March 2022

APPENDIX-B: Discharge Logs for the SEOO on 23 September, 21 December 2021, and 3 March 2022

APPENDIX-C: EOO - Plumes 20 Text file Output

APPENDIX-D: SEOO - Plumes 20 Text file Output

LIST OF TABLES

Table 1: Comparison of SEOO and EOO Features.....	ES_1
Table 2: Summary of Comparison of SEOO and EOO Features	ES-2
Table 3: Iver3 AUV Specifications	1-7
Table 4: Iver3 AUV Subsystems	1-7
Table 5: Iver3 AUV fDOM Sensor Specifications	1-8
Table 6: Summary of Comparison of SEOO and EOO Features	2-1
Table 7: Plumes 20 (UM3) Initialization of EOO Ebb tide Ambient Conditions on 20 December 2021 with Ambient Current	2-43
Table 8: Plumes 20 (UM3) Output of EOO Dilution Factor (D_{fDOM}) during Ebb Tide on 20 December 2021 with Ambient Current (Final D_{fDOM} solution highlighted in yellow)	2-44
Table 9: Plumes 20 (UM3) Initialization of EOO Flood tide Ambient Conditions on 20 December 2021 with Ambient Current	2-52
Table 10: Plumes 20 (UM3) Output of EOO Dilution Factor (D_{fDOM}) during Flood Tide on 20 December 2021 with Ambient Current (Final D_{fDOM} solution highlighted in yellow)	2-53
Table 11: Plumes 20 (UM3) Initialization of EOO Ebb tide Ambient Conditions on 2 March with Ambient Current..	2-72
Table 12: Plumes 20 (UM3) Output of EOO Dilution Factor (D_{fDOM}) during Ebb Tide on 2 March 2022 with Ambient Current (Final D_{fDOM} solution highlighted in yellow)	2-73
Table 13: Plumes 20 (UM3) Initialization of EOO flood tide Ambient Conditions on 2 March with Ambient Current	2-82
Table 14: Plumes 20 (UM3) Output of EOO Dilution Factor (D_{fDOM}) during Flood Tide on 2 March 2022 with Ambient Current (Final D_{fDOM} solution highlighted in yellow)	2-84
Table 15: Plumes 20 (UM3) Initialization of SEOO Ebb Tide Ambient Conditions on 21 December 2021 with Ambient Current.....	3-41
Table 16: Plumes 20 (UM3) Output of SEOO Dilution Factor (D_{fDOM}) during Ebb Tide on 21 December 2021 with Ambient Current (Final D_{fDOM} solution highlighted in yellow)	3-42

LIST OF FIGURES

Figure 1.1.1: Schematic diagram of the rising wastewater plume pancaking at the pycnocline (trapping level) and spreading laterally along the base of the pycnocline under the influence of its residual momentum and internal wave mass transport.....	1-4
Figure 1.1.2: Schematic of jet merging due to axial expansion of each of the 200 jets during the initial phase of discharge from the SEOO diffuser, when the momentum flux of each jet exceeds the buoyancy of the effluent. Image from CORMIX v-12 near-field simulation of the SEOO diffuser.	1-5
Figure 1.2.1: Three-Dimensional Data Model of fDOM collected with the Iver3 AUV. AUV track lines are shown in black.	1-6
Figure 1.2.2: Schematic of AUV out and return legs along any given track line in the AUV survey pattern, in order to capture the vertical structure of the plume while maximizing transit time in regions of maximum horizontal spreading.....	1-7
Figure 1.2.3: Iver3 Autonomous Underwater Vehicle (AUV)	1-7
Figure 1.2.4: Sea-Bird SBE 19plusV2 CTD and typical shipboard casting equipment.....	1-8
Figure 1.2.5: The 2 MHz Nortek ADCP with rigid mount for deployment from the R/V Benthic Cat.....	1-8
Figure 1.2.6: Research Vessel (R/V) Benthic Cat (Source: Orca Maritime).....	1-9
Figure 1.2.7: Eureka Handheld fDOM Probe with iPad data recorder for onshore sampling of the treated wastewater effluent prior to discharge and typical autosampler provided by EWA.	1-10
Figure 1.2.8: Onshore SEOO Sampling Site at Cardiff State Beach (not used) (Source: SEJPA).....	1-10
Figure 1.2.9: Onshore EOO Sampling Site at EWPCF (Source: EWA).....	1-10
Figure 1.3.1: Correlation function between the YSI / Xylem EXO f/DOM sensor in the AUV which measures fDOM in QSU vs. the Sea-bird BE 19plusV2 CTD which measures fDOM in relative fluorescence units (RFU) at the stationary monitoring stations.	1-12
Figure 2.1.1: EOO Survey boxes and sampling stations for the first AUV deployment, 21 September 2021	2-3
Figure 2.1.2: Salinity/Temperature/Density depth profiles derived from CTD casts on 19 September 2021 at Station EOO-Ebb, prior to the AUV survey of the plume dispersion from EOO on 21 September 2021 during ebb tide.....	2-4
Figure 2.1.3: Vertical profiles of natural background fDOM concentrations measured during the first deployment at the far-field ebb tide monitoring station “EOO-EBB,” located 2 kilometers northwest of EOO along the -160 ft. MLLW depth contour, cf. yellow dot in Figure 2.1.1	2-5
Figure 2.1.4: Vertical profiles of natural background fDOM concentrations measured during the first deployment at the far-field flood tide monitoring station “EOO-Flood,” located 2 km southeast of EOO along the -160 ft. MLLW depth contour, cf. orange dot in Figure 2.1.1	2-6
Figure 2.1.5: Time series of depth averaged current derived from ADCP measurements at EOO during ebb-tide AUV survey on 21 September 2021.....	2-8
Figure 2.1.6: Time series of depth averaged current derived from ADCP measurements at EOO during flood-tide AUV survey on 21 September 2021.....	2-8

Figure 2.1.7: Bathymetric contour map overlaid onto the EOO survey boxes (solid black lines) and the EOO ebb-tide AUV survey track lines (dotted white lines). Note the extreme bathymetric depression of the head of the Carlsbad Submarine Canyon that encroaches on the northern end of the EOO flood tide survey box. As tidal currents flow across the Carlsbad Submarine Canyon, this bathymetric depression excites internal waves whose cross-shore oscillations produce the high current spikes in the ADCP records on 21 September 2021 (cf. **Figure 2.1.5** and **Figure 2.1.6**)..... 2-9

Figure 2.1.8: AUV track lines as flown during ebb tide surveys of the discharge plume from EOO during the first deployment, 21 September 2021. The total dimension of the AUV surveyed area on ebb tide was 2000 m in the along shore direction and 1000 m in the cross-shore direction or a total surveyed area of approximately 494.3 acres. Note, at 30° N latitude, 1° longitude = 93,453.2 m, while 1° latitude = 110,904.4 m..... 2-10

Figure 2.1.9: Contour plot of AUV measurements of fDOM at the trapping level during ebb tide surveys of the discharge plume from EOO. EOO discharge rate = 24.17 mgd; End-of-pipe discharge concentration of fDOM = 248.71 ppb (QSU); End of pipe discharge salinity = 0.85 psu; Trapping level (pycnocline depth) = 26.24 ft MSL; Mean ebb tide current = 0.288 m/s (0.56 kts) toward the southeast..... 2-11

Figure 2.1.10: Calibrated CFD simulation of the plume dispersion through the water column from EOO. CFD simulation calibrated to AUV measurements of fDOM along the track line #3 during ebb tide on 21 September 2021. CFD simulation based on EOO discharge rate = 26.318 mgd; End-of-pipe discharge concentration of fDOM_(x=0) = 248.71 ppb (QSU); Trapping level (pycnocline depth) = 26.24 ft MSL; Mean ebb tide current = 0.288 m/s (0.56 kts) toward the southeast. 2-14

Figure 2.1.11: Full depth contour plot (aka, heat map) of AUV measurements of fDOM during ebb tide surveys of the discharge plume from the EOO. EOO discharge rate = 24.17 mgd; End-of-pipe discharge concentration of fDOM = 248.71 ppb (QSU); End of pipe salinity = 0.85 psu; Mean ebb tide current = 0.288 m/s (0.56 kts) toward the southeast. 2-15

Figure 2.1.12: Full depth contour plot (aka, heat map) of the signal to noise ratio (SNR) of fDOM during the AUV ebb tide surveys of the discharge plume from the EOO. EOO discharge rate = 24.17 mgd; End-of-pipe discharge concentration of fDOM = 248.71 ppb (QSU); End of pipe salinity = 0.85 psu; Mean ebb tide current = 0.288 m/s (0.56 kts) toward the southeast. 2-16

Figure 2.1.13: Full depth contour plot (aka, heat map) of the dilution factor (D_{fDOM}) of fDOM during the AUV ebb tide surveys of the discharge plume from the EOO. EOO discharge rate = 24.17 mgd; End-of-pipe discharge concentration of fDOM = 248.71 ppb (QSU); End of pipe salinity = 0.85 psu; Mean ebb tide current = 0.288 m/s (0.56 kts) toward the southeast 2-17

Figure 2.1.14: Full depth composite contour plot (aka, heat map) of AUV measurements of salinity during ebb tide surveys of the discharge plume from EOO. EOO discharge rate = 24.17 mgd; End-of-pipe discharge salinity = 0.85 psu; Mean ebb tide current = 0.288 m/s (0.56 kts) toward the southeast. 2-20

Figure 2.1.15: AUV track lines as flown during flood tide surveys of the discharge plume from EOO during the first deployment, 21 September 2021. The total dimension of the AUV surveyed area on flood tide was 2000 m in the along shore direction and 1000 m in the cross-shore direction or a total surveyed area of approx. 494.3 acres. Note, at 30° N latitude, 1° longitude = 93,453.2 m, while 1° latitude = 110,904.4 m. 2-21

Figure 2.1.16: Full depth contour plot (aka, heat map) of AUV measurements of fDOM during flood tide surveys of the discharge plume from EOO. EOO discharge rate = 26.318 mgd; End-of-pipe discharge concentration of fDOM = 248.71 ppb (QSU); End of pipe salinity = 0.85 psu; Mean ebb tide current = 0.265 m/s (0.52 kts) toward the northwest..... 2-22

- Figure 2.1.17:** Full depth contour plot (aka, heat map) of the signal to noise ratio (SNR) of fDOM during flood tide AUV surveys of the discharge plume from EOO. EOO discharge rate = 26.318 mgd; End-of-pipe discharge concentration of fDOM = 248.71 ppb (QSU); End of pipe salinity = 0.85 psu; Mean ebb tide current = 0.265 m/s (0.52 kts) toward the northwest. 2-23
- Figure 2.1.18:** Full depth contour plot (aka, heat map) of the dilution factor (D_{fDOM}) of fDOM during flood tide AUV surveys of the discharge plume from EOO. EOO discharge rate = 26.318 mgd; End-of-pipe discharge concentration of fDOM = 248.71 ppb (QSU); End of pipe salinity = 0.85 psu; Mean ebb tide current = 0.265 m/s (0.52 kts) toward the northwest. 2-24
- Figure 2.1.19:** Full depth composite contour plot (aka, heat map) of AUV measurements of salinity during flood tide surveys of the discharge plume from EOO. EOO discharge rate = 26.318 mgd; End-of-pipe discharge concentration of salinity = 0.85 psu; Mean ebb tide current 0.265 m/s (0.52 kts) toward the northwest. 2-25
- Figure 2.2.1:** EOO Survey boxes and sampling stations for second AUV deployment, 19-21 December 2021 2-27
- Figure 2.2.2:** Side-scan sonar survey image of EOO used to obtain precision geo-referenced coordinates along the length of the pipeline and diffuser. 2-29
- Figure 2.2.3:** Salinity/Temperature/Density depth profiles derived from CTD casts on 19 December 2021 used to program the AUV surveys of the plume dispersion from EOO on 20 December 2021. 2-30
- Figure 2.2.4:** Vertical profiles of natural background fDOM concentrations measured during the second deployment at the far-field ebb tide monitoring station “EOO-EBB,” located 2 km northwest of EOO along the -160 ft. MLLW depth contour, cf. yellow dot in **Figure 2.2.1**. 2-31
- Figure 2.2.5:** Vertical profiles of natural background fDOM concentrations measured during the second deployment at the far-field flood tide monitoring station “EOO-FLOOD,” located 2 kilometers southeast of EOO along the -160 ft. MLLW depth contour, cf. orange dot in **Figure 2.2.1**. 2-32
- Figure 2.2.6:** Time series of depth averaged current derived from ADCP measurements at EOO during ebb-tide AUV survey on 20 December 2021..... 2-34
- Figure 2.2.7:** Time series of depth averaged current derived from ADCP measurements at EOO during flood-tide AUV survey on 20 December 2021..... 2-34
- Figure 2.2.8:** AUV track lines as flown during ebb tide surveys of the discharge plume from EOO during the second deployment, 20 December 2021. The total dimension of the AUV surveyed area on ebb tide was 707.1 m in the longshore (shore parallel) direction and 1,414.2 m on the cross-shore (on/off shore) direction or a total surveyed area of approximately 247.1 acres. Note, at 30° N latitude, 1° longitude = 93,453.2 m, while 1° latitude = 110,904.4 m. 2-36
- Figure 2.2.9:** Full depth contour plot (aka, heat map) of AUV measurements of fDOM during surveys of the discharge plume from EOO during ebb tide on 20 December 2021. Average EOO discharge rate =31.20 mgd during ebb tide; End-of-pipe discharge concentration of fDOM = 217.5 ppb (QSU); End of pipe salinity = 0.96 psu; Trapping level (pycnocline depth) = -13.1 ft MSL; Mean ebb tide current = 0.304 m/s (0.59 kts) toward the southeast. 2-37
- Figure 2.2.10:** Full depth contour plot (aka, heat map) of the Signal to Noise Ratio (SNR) of fDOM during AUV surveys of the discharge plume from EOO during ebb tide on 20 December 2021. Average EOO discharge rate =31.20 mgd during ebb tide; End-of-pipe discharge concentration of fDOM = 217.5 ppb (QSU); End of pipe salinity = 0.96 psu; Trapping level (pycnocline depth) = -13.1 ft MSL; Mean ebb tide current = 0.304 m/s (0.59 kts) toward the southeast. 2-38

- Figure 2.2.11:** Full depth contour plot of the (aka, *heat map*) dilution factor (D_{fDOM}) of fDOM during AUV surveys of the discharge plume from EOO during ebb tide on 20 December 2021. Average EOO discharge rate =31.20 mgd during ebb tide; End-of-pipe discharge concentration of fDOM = 217.5 ppb (QSU); End of pipe salinity = 0.96 psu; Trapping level (pycnocline depth) = -13.1 ft MSL; Mean ebb tide current = 0.304 m/s (0.59 kts) toward the southeast. 2-39
- Figure 2.2.12:** Full depth composite contour plot (aka, *heat map*) of AUV measurements of salinity during surveys of the discharge plume from EOO during ebb tide on 20 December 2021. Average EOO discharge rate =31.20 mgd during ebb tide; End of pipe salinity = 0.96 psu; Trapping level (pycnocline depth) = -13.1 ft MSL; Mean ebb tide current = 0.304 m/s (0.59 kts) toward the southeast. 2-41
- Figure 2.2.13:** Plumes 20 solution of discharge plume trajectories for discharges of 31.2 mgd of EOO effluent at a discharge salinity of $S_{(x=0)} = 0.96$ psu, per operating conditions and water mass temperature/salinity profiles during ebb tide on 20 December 2021. Plumes 20 simulation performed based on ambient current = 0.304 m/s per ADCP measurements. For the 20 December 2021 conditions, the ZID (completion of initial dilution) is defined by the maximum horizontal excursion of trajectories from the origin. From the maximum horizontal spreading of the plume, the ZID extends from $X = 0.0$ m to $X = 197$ m so that ZID = 197 m. 2-45
- Figure 2.2.14:** AUV track lines as flown during flood tide surveys of the discharge plume from EOO during the second deployment, 20 December 2021. The total dimension of the AUV surveyed area on flood tide was 707.1 m in the longshore (shore parallel) direction and 1,414.2 m on the cross-shore (on/off shore) direction or a total surveyed area of approximately 247.1 acres. Note, at 30° N latitude, 1° longitude = 93,453.2 m, while 1° latitude = 110,904.4 m. 2-46
- Figure 2.2.15:** Full depth contour plot (aka, *heat map*) of AUV measurements of fDOM during surveys of the discharge plume from EOO during flood tide on 20 December 2021. Average EOO discharge rate =29.70 mgd during flood tide; End-of-pipe discharge concentration of fDOM = 217.5 ppb (QSU); End of pipe salinity = 0.96 psu; Trapping level (pycnocline depth) = -13.1 ft MSL; Mean flood tide current = 0.211 m/s (0.41 kts) toward the northwest. 2-47
- Figure 2.2.16:** Full depth contour plot (aka, *heat map*) of the Signal to Noise Ratio (SNR) of fDOM during AUV surveys of the discharge plume from EOO during flood tide on 20 December 2021. Average EOO discharge rate =29.70 mgd during flood tide; End-of-pipe discharge concentration of fDOM = 217.5 ppb (QSU); End of pipe salinity = 0.96 psu; Trapping level (pycnocline depth) = -13.1 ft MSL; Mean flood tide current = 0.211 m/s (0.41 kts) toward the northwest. 2-49
- Figure 2.2.17:** Full depth contour plot (aka, *heat map*) of the Dilution Factor(D_{fDOM}) of fDOM during AUV surveys of the discharge plume from EOO during flood tide on 20 December 2021. Average EOO discharge rate =29.70 mgd during flood tide; End-of-pipe discharge concentration of fDOM = 217.5 ppb (QSU); End of pipe salinity = 0.96 psu; Trapping level (pycnocline depth) = -13.1 ft MSL; Mean flood tide current = 0.211 m/s (0.41 kts) toward the northwest. 2-50
- Figure 2.2.18:** Full depth composite contour plot (aka, *heat map*) of salinity during AUV surveys of the discharge plume from EOO during flood tide on 20 December 2021. Average EOO discharge rate =29.70 mgd during flood tide; End of pipe salinity = 0.96 psu; Trapping level (pycnocline depth) = -13.1 ft MSL; Mean ebb tide current = 0.211 m/s (0.41 kts) toward the northwest. 2-51

- Figure 2.2.19:** Plumes 20 solution of discharge plume trajectories for discharges of 29.7 mgd of EOO effluent at a discharge salinity of $S_{(x=0)} = 0.96$ psu, per operating conditions and water mass temperature/salinity profiles during flood tide on 20 December 2021. Plumes 20 simulation performed based on ambient current = 0.211 m/s per ADCP measurements. For the 20 December 2021 conditions, the ZID (zone within which initial dilution is completed) is defined by the maximum horizontal excursion of trajectories from the origin. From the maximum horizontal spreading of the plume, the ZID extends from $X = 0.0$ m to $X = 120$ m so that ZID = 120 2-54
- Figure 2.3.1:** EOO Survey boxes and sampling stations for the third AUV deployment, 1-2 March 2022 2-56
- Figure 2.3.2:** Salinity/Temperature/Density depth profiles derived from CTD casts on 1 March 2022 used to program the AUV surveys of the plume dispersion from the Encina Ocean Outfall during ebb and flood tides on 2 March 2022 2-59
- Figure 2.3.3:** Vertical profiles of natural background fDOM concentrations measured during the third deployment at the far-field flood tide monitoring station “EOO-Ebb,” located 2 kilometers southeast of EOO along the -160 ft. MLLW depth contour, cf. orange dot in **Figure 2.3.1** 2-60
- Figure 2.3.4:** Vertical profiles of natural background fDOM concentrations measured during the third deployment at the far-field flood tide monitoring station “EOO-Flood,” located 2 kilometers southeast of EOO along the -160 ft. MLLW depth contour, cf. orange dot in **Figure 2.3.1** 2-61
- Figure 2.3.5:** Time series of depth averaged current derived from ADCP measurements at EOO during ebb-tide AUV survey on 2 March 2022. 2-62
- Figure 2.3.6:** Time series of depth averaged current derived from ADCP measurements at EOO during flood-tide AUV survey on 2 March 2022 2-62
- Figure 2.3.7:** AUV track lines as flown during ebb tide surveys of the discharge plume from EOO during the second deployment, 2 March 2022. The total dimension of the AUV surveyed area on ebb tide was 707.1 m in the longshore (shore parallel) direction and 1,414.2 m on the cross-shore (on/off shore) direction or a total surveyed area of approximately 247.1 acres. Note, at 30° N latitude, 1° longitude = 93,453.2 m, while 1° latitude = 110,904.4 m..... 2-64
- Figure 2.3.8:** Full depth contour plot (aka, *heat map*) of AUV measurements of fDOM during surveys of the discharge plume from EOO during ebb tide on 2 March 2021. Average EOO discharge rate = 27.6 mgd during ebb tide; End-of-pipe discharge concentration of fDOM = 261.8 ppb (QSU); End of pipe salinity = 0.82 psu; Trapping level (pycnocline depth) = -26.9 m (-88.3 ft) MSL; Mean ebb tide current = 0.526 m/s (1.02 kts) toward the southeast. 2-65
- Figure 2.3.9:** Full depth contour plot (aka, *heat map*) of the Signal to Noise Ratio (SNR) of fDOM during AUV surveys of the discharge plume from EOO during ebb tide on 2 March 2021. Average EOO discharge rate = 27.6 mgd during ebb tide; End-of-pipe discharge concentration of fDOM = 261.8 ppb (QSU); End of pipe salinity = 0.82 psu; Trapping level (pycnocline depth) = -26.9 m (-88.3 ft) MSL; Mean ebb tide current = 0.526 m/s (1.02 kts) toward the southeast. 2-66
- Figure 2.3.10:** Full depth contour plot of the (aka, *heat map*) dilution factor (D_{fDOM}) of fDOM during AUV surveys of the discharge plume from EOO during ebb tide on 2 March 2021. Average EOO discharge rate = 27.6 mgd during ebb tide; End-of-pipe discharge concentration of fDOM = 261.8 ppb (QSU); End of pipe salinity = 0.82 psu; Trapping level (pycnocline depth) = -26.9 m (-88.3 ft) MSL; Mean ebb tide current = 0.526 m/s (1.02 kts) toward the southeast. 2-67

Figure 2.3.11: Full depth composite contour plot (aka, *heat map*) of AUV measurements of salinity during surveys of the discharge plume from EOO during ebb tide on 2 March 2021. Average EOO discharge rate = 27.6 mgd during ebb tide; End-of-pipe discharge concentration of fDOM = 261.8 ppb (QSU); End of pipe salinity = 0.82 psu; Trapping level (pycnocline depth) = -26.9 m (-88.3 ft) MSL; Mean ebb tide current = 0.526 m/s toward the southeast. 2-69

Figure 2.3.12: Full depth contour plot (aka, *heat map*) of the Signal to Noise Ratio (SNR) of salinity during AUV surveys of the discharge plume from EOO during ebb tide on 2 March 2021. Average EOO discharge rate = 27.6 mgd during ebb tide; End-of-pipe discharge concentration of fDOM = 261.8 ppb (QSU); End of pipe salinity = 0.82 psu; Trapping level (pycnocline depth) = -26.9 m (-88.3 ft) MSL; Mean ebb tide current = 0.526 m/s toward the southeast. 2-70

Figure 2.3.13: Plumes 20 solution of discharge plume trajectories for discharges of 27.6 mgd of EOO effluent at a discharge salinity of $S_{(x=0)} = 0.82$ psu, per operating conditions and water mass temperature/salinity profiles during ebb tide on 2 March 2022. Plumes 20 simulation performed based on ambient current = 0.526 m/s per ADCP measurements. For the 2 March 2022 conditions, the ZID (zone within which initial dilution is completed) is defined by the maximum horizontal excursion of trajectories from the origin. From the maximum horizontal spreading of the plume, the ZID extends from $X = 0.0$ m to $X = 224$ m so that $ZID = 224$ m. 2-74

Figure 2.3.14: AUV track lines as flown during flood tide surveys of the discharge plume from EOO during the second deployment, 2 March 2022. The total dimension of the AUV surveyed area on flood tide was 707.1 m in the longshore (shore parallel) direction and 1,414.2 m on the cross-shore (on/off shore) direction or a total surveyed area of approximately 247.1 acres. Note, at 30° N latitude, 1° longitude = 93,453.2 m, while 1° latitude = 110,904.4 m..... 2-75

Figure 2.3.15: Full depth contour plot (aka, *heat map*) of AUV measurements of fDOM during surveys of the discharge plume from EOO during flood tide on 2 March 2021. Average EOO discharge rate = 24.2 mgd during flood tide; End-of-pipe discharge concentration of fDOM = 261.8 ppb (QSU); End of pipe salinity = 0.82 psu; Trapping level (pycnocline depth) = -26.9 m (-88.3 ft) MSL; Mean flood tide current = 0.261 m/s (0.51 kts) toward the northwest. 2-76

Figure 2.3.16: Full depth contour plot (aka, *heat map*) of Signal to Noise Ratio (SNR) of fDOM during AUV surveys of the discharge plume from EOO during flood tide on 2 March 2021. Average EOO discharge rate = 24.2 mgd during flood tide; End-of-pipe discharge concentration of fDOM = 261.8 ppb (QSU); End of pipe salinity = 0.82 psu; Trapping level (pycnocline depth) = -26.9 m (-88.3 ft) MSL; Mean flood tide current = 0.261 m/s (0.51 kts) toward the northwest. 2-78

Figure 2.3.17: Full depth contour plot (aka, *heat map*) of Dilution Factor (D_{fDOM}) of fDOM during AUV surveys of the discharge plume from EOO during flood tide on 2 March 2021. Average EOO discharge rate = 24.2 mgd during flood tide; End-of-pipe discharge concentration of fDOM = 261.8 ppb (QSU); End of pipe salinity = 0.82 psu; Trapping level (pycnocline depth) = -26.9 m (-88.3 ft) MSL; Mean flood tide current = 0.261 m/s (0.51 kts) toward the northwest. 2-79

Figure 2.3.18: Full depth composite contour plot (aka, *heat map*) of AUV measurements of salinity during surveys of the discharge plume from EOO during flood tide on 2 March 2021. Average EOO discharge rate = 24.2 mgd during flood tide; End-of-pipe discharge concentration of fDOM = 261.8 ppb (QSU); End of pipe salinity = 0.82 psu; Trapping level (pycnocline depth) = -26.9 m (-88.3 ft) MSL; Mean flood tide current = 0.261 m/s (0.51 kts) toward the northwest. 2-80

- Figure 2.3.19:** Full depth contour plot (aka, *heat map*) of the Signal to Noise Ratio (SNR) of salinity during AUV surveys of the discharge plume from EOO during flood tide on 2 March 2021. Average EOO discharge rate = 24.2 mgd during flood tide; End-of-pipe discharge concentration of fDOM = 261.8 ppb (QSU); End of pipe salinity = 0.82 psu; Trapping level (pycnocline depth) = -26.9 m (-88.3 ft) MSL; Mean flood tide current = 0.261 m/s (0.51 kts) toward the northwest. 2-81
- Figure 2.3.20:** Plumes 20 solution of discharge plume trajectories for discharges of 24.2 mgd of EOO effluent at a discharge salinity of $S_{(x=0)} = 0.82$ psu, per operating conditions and water mass temperature/salinity profiles during ebb tide on 2 March 2022. Plumes 20 simulation performed based on ambient current = 0.261 m/s per ADCP measurements. For the March 2022 conditions, the ZID (zone within which initial dilution is completed) is defined by the maximum horizontal excursion of trajectories from the origin. From the maximum horizontal spreading of the plume, the ZID extends from $X = 0.0$ m to $X = 120$ m so that ZID = 120 m. 2-85
- Figure 3.1.1:** SEOO Survey boxes and sampling stations for the first AUV deployment, 23 September 2021..... 3-2
- Figure 3.1.2:** Salinity/Temperature/Density depth profiles derived from CTD casts on 19 September 2021 used to program the AUV survey of the plume dispersion from SEOO on 23 September 2021 during flood tide. 3-4
- Figure 3.1.3:** Vertical profiles of natural background fDOM concentrations measured during the first deployment at the far-field flood tide monitoring station “SEOO-FLOOD”, located 2 km southeast of SEOO along the -140 ft. MLLW depth contour, cf. orange dot in **Figure 3.1.1**..... 3-5
- Figure 3.1.4:** Vertical profiles of natural background fDOM concentrations measured during the first deployment at the far-field ebb tide monitoring station “SEOO-EBB”, located 2 km northwest of SEOO along the -140 ft. MLLW depth contour, cf. yellow dot in **Figure 3.1.1**..... 3-6
- Figure 3.1.5:** Time series of depth averaged current derived from ADCP measurements at SEOO during flood-tide AUV survey on 23 September 2021..... 3-8
- Figure 3.1.6:** Time series of depth averaged current derived from ADCP measurements at SEOO during ebb-tide AUV survey on 23 September 2021..... 3-8
- Figure 3.1.7:** AUV track lines as planned for flood tide surveys of the discharge plume from SEOO. 3-9
- Figure 3.1.8:** AUV track lines as flown during flood tide surveys of the discharge plume from SEOO. The total dimension of the AUV surveyed area on ebb tide was 2000 m in the along shore direction and 1000 m in the cross-shore direction or a total surveyed area of approximately 494.3 acres. Note, at 30° N latitude, 1° longitude = 93,453.2 m, while 1° latitude = 110,904.4 m. 3-10
- Figure 3.1.9:** Contour plot of AUV measurements of fDOM at the trapping level during flood tide surveys of SEOO. SEOO discharge rate = 9.473 mgd; End-of-pipe discharge concentration of fDOM = 206.04 ppb (QSU); Trapping level (pycnocline depth) = 38.7 ft MSL; End of pipe salinity = 1.92 ppt; Mean flood tide current = 0.326 m/s (0.63 kts) toward the northwest. 3-11
- Figure 3.1.10:** Calibrated CFD simulation of the plume dispersion through the water column from SEOO. CFD simulation calibrated to AUV measurements of fDOM along the track line #3 during flood tide as shown in **Figure 3.1.8**. CFD simulation based on SEOO discharge rate = 9.5 mgd; End-of-pipe discharge concentration of fDOM = 206 ppb (QSU); End of pipe salinity = 1.92 psu; Trapping level (pycnocline depth) = 38.7 ft MSL; Mean flood tide current = 0.326 m/s (0.63 kts) toward the northwest; Ambient ocean fDOM concentration at the trapping level=0.45 to 0.65 ppb (QSU). 3-13

- Figure 3.1.11:** Full depth contour plot (aka, heat map) of AUV measurements of fDOM during surveys of SEOO during flood tide on 23 September 2021. Average SEOO discharge rate = 9.473 mgd during flood tide; End-of-pipe discharge concentration of fDOM = 206.04 ppb (QSU); End of pipe salinity = 1.92 psu; Trapping level (pycnocline depth) = 38.7 ft MSL; Mean flood tide current = 0.326 m/s (0.63 kts) toward the northwest. 3-14
- Figure 3.1.12:** Full depth contour plot (aka, heat map) of the fDOM signal to noise ratio (SNR) from AUV surveys of SEOO during flood tide on 23 September 2021. Average SEOO discharge rate = 9.473 mgd during flood tide; End-of-pipe discharge concentration of fDOM = 206.04 ppb (QSU); End of pipe salinity = 1.92 psu; Trapping level (pycnocline depth) = 38.7 ft MSL; Mean flood tide current = 0.326 m/s (0.63 kts) toward the northwest. 3-16
- Figure 3.1.13:** Full depth contour plot (aka, heat map) of the dilution factor (D_{fDOM}) of fDOM from AUV surveys of SEOO during flood tide on 23 September 2021. Average SEOO discharge rate = 9.473 mgd during flood tide; End-of-pipe discharge concentration of fDOM = 206.04 ppb (QSU); End of pipe salinity = 1.92 psu; Trapping level (pycnocline depth) = 38.7 ft MSL; Mean flood tide current = 0.326 m/s (0.63 kts) toward the northwest. 3-17
- Figure 3.1.14:** Full depth composite contour plot (aka, heat map) of salinity during AUV surveys of SEOO during flood tide on 23 September 2021. Average SEOO discharge rate = 9.473 mgd during flood tide; End of pipe salinity = 1.92 psu; Trapping level (pycnocline depth) = 38.7 ft MSL; Mean flood tide current = 0.326 m/s (0.63 kts) toward the northwest. 3-18
- Figure 3.1.15:** AUV track lines as flown during ebb tide surveys of the discharge plume from SEOO. Ebb tide survey was truncated to only 3 track lines due to problems with seawater in the fuel of the AUV support vessel. The total dimension of the AUV surveyed area on flood tide was 2000 m in the along shore direction and 500 m in the cross-shore direction or a total surveyed area of approximately 247.2 acres. Note, at 30° N latitude, 1° longitude = 93,453.2 m, while 1° latitude = 110,904.4 m. 3-20
- Figure 3.1.16:** Full depth contour plot (aka, heat map) of AUV measurements of fDOM from surveys of the discharge plume from SEOO during ebb tide on 23 September 2021. Average SEOO discharge rate = 10.44 mgd during flood tide; End-of-pipe discharge concentration of fDOM = 206.04 ppb (QSU); End of pipe salinity = 1.87 psu Trapping level (pycnocline depth) = 38.7 ft MSL; Mean ebb tide current = 0.373 m/s (0.72 kts) toward the southeast. 3-21
- Figure 3.1.17:** Full depth contour plot (aka, heat map) of the fDOM signal to noise ratio (SNR) from AUV surveys of the discharge plume from SEOO during ebb tide on 23 September 2021. Average SEOO discharge rate = 10.44 mgd during flood tide; End-of-pipe discharge concentration of fDOM = 206.04 ppb (QSU); End of pipe salinity = 1.87 psu Trapping level (pycnocline depth) = 38.7 ft MSL; Mean ebb tide current = 0.373 m/s (0.72 kts) toward the southeast. 3-22
- Figure 3.1.18:** Full depth contour plot (aka, heat map) of the fDOM dilution factor (D_{fDOM}) from AUV surveys of the discharge plume from SEOO during ebb tide on 23 September 2021. Average SEOO discharge rate = 10.44 mgd during flood tide; End-of-pipe discharge concentration of fDOM = 206.04 ppb (QSU); End of pipe salinity = 1.87 psu Trapping level (pycnocline depth) = 38.7 ft MSL; Mean ebb tide current = 0.373 m/s (0.72 kts) toward the southeast. 3-23
- Figure 3.1.19:** Full depth composite contour plot (aka, heat map) of salinity during AUV surveys of the discharge plume from SEOO during ebb tide on 23 September 2021. Average SEOO discharge rate = 10.44 mgd during ebb tide; End of pipe salinity = 1.92 psu; Trapping level (pycnocline depth) = 38.7 ft MSL; Mean ebb tide current = 0.373 m/s (0.72 kts) toward the southeast. 3-25
- Figure 3.2.1:** SEOO Survey boxes and sampling stations for second AUV deployment, 21 December 2021 3-27

Figure 3.2.2: Side-scan sonar survey of SEOO used to obtain precision coordinates along the length of the pipeline and diffuser 3-29

Figure 3.2.3: Salinity/Temperature/Density depth profiles derived from CTD casts on 19 December 2021 used to program the AUV survey of the plume dispersion from SEOO on 21 December 2021 during ebb tide. 3-30

Figure 3.2.4: Vertical profiles of natural background fDOM concentrations measured during the second deployment at the far-field flood tide monitoring station “SEOO-EBB”, located 2 km northwest of SEOO along the -140 ft. MLLW depth contour, cf. yellow dot in **Figure 3.2.1**. 3-31

Figure 3.2.5: Time series of depth averaged current derived from ADCP measurements at SEOO during ebb-tide AUV survey on 21 December 2021. 3-33

Figure 3.2.6: AUV track lines on 21 December 2021 as flown during ebb tide surveys of the discharge plume from SEOO. Note, at 30° N latitude, 1° longitude = 93,453.2 m, while 1° latitude = 110,904.4 m..... 3-34

Figure 3.2.7: Full depth contour plot (aka, heat map) of AUV measurements of fDOM from surveys of SEOO during ebb tide on 21 December 2021. Average SEOO discharge rate = 12.63 mgd during flood tide; End-of-pipe discharge concentration of fDOM = 232.8 ppb (QSU); End of pipe salinity = 1.097 psu; Trapping level (pycnocline depth) = -13.1 ft MSL; Mean ebb tide current = 0.263 m/s (0.51 kts) toward the southeast.. 3-35

Figure 3.2.8: Full-depth contour plot (aka, heat map) of the signal to noise ratio (SNR) of fDOM during AUV surveys of SEOO during ebb tide on 21 December 2021. Average SEOO discharge rate = 12.63 mgd during flood tide; End-of-pipe discharge concentration of fDOM = 232.8 ppb (QSU); End of pipe salinity = 1.097 psu; Trapping level (pycnocline depth) = -13.1 ft MSL; Mean ebb tide current = 0.263 m/s (0.51 kts) toward the southeast..... 3-36

Figure 3.2.9: Full depth contour plot (aka, heat map) of the dilution factor, (D_{fDOM}) of fDOM during AUV surveys of SEOO during ebb tide on 21 December 2021. Average SEOO discharge rate = 12.63 mgd during flood tide; End-of-pipe discharge concentration of fDOM = 232.8 ppb (QSU); End of pipe salinity = 1.097 psu; Trapping level (pycnocline depth) = -13.1 ft MSL; Mean ebb tide current = 0.263 m/s (0.51 kts) toward the southeast..... 3-39

Figure 3.2.10: Full depth composite contour plot (aka, heat map) of salinity during AUV surveys of the discharge plume from SEOO during ebb tide on 21 December 2021. Average SEOO discharge rate = 12.63 mgd during flood tide; End-of-pipe discharge concentration of fDOM = 232.8 ppb (QSU); End of pipe salinity = 1.097 psu; Trapping level (pycnocline depth) = -13.1 ft MSL; Mean ebb tide current = 0.263 m/s (0.51 kts) toward the southeast. 3-40

Figure 3.2.11: Plumes 20 solution of discharge plume trajectories for discharges of 12.63 mgd of SEOO effluent at discharge salinity of $S_{(x=0)} = 1.097$ psu, per operating conditions and water mass temperature/salinity profiles during flood tide on 21 December 2021. Plumes 20 simulation performed based on ambient current = 0.263 m/s per ADCP measurements. ZID is defined by the maximum horizontal excursion of trajectories from the origin. From the maximum horizontal spreading of the plume, the ZID extends from $X = 0.0$ m to $X = 126$ m so that ZID = 126 m..... 3-43

Figure 3.3.1: Survey boxes and sampling stations for the second AUV deployment, 3 March 2022, at the San Elijo Ocean Outfall..... 3-46

Figure 3.3.2: Salinity/Temperature/Density depth profiles derived from CTD casts on 1 March 2022 used to program the AUV survey of the plume dispersion from SEOO on 3 March 2021 during ebb and flood tides. 3-48

Figure 3.3.3: Vertical profiles of natural background fDOM concentrations measured during the third deployment at the far-field ebb tide monitoring station “SEOO-EBB”, located 2 km northwest of SEOO along the -140 ft. MLLW depth contour, cf. yellow dot in **Figure 3.3.1** 3-49

Figure 3.3.4: Vertical profiles of natural background fDOM concentrations measured during the third deployment at the far-field flood tide monitoring station “SEOO-Flood”, located 2 km southeast of SEOO along the -140 ft. MLLW depth contour, cf. orange dot in **Figure 3.3.1**..... 3-50

Figure 3.3.5: Time series of depth averaged current derived from ADCP measurements at SEOO during ebb-tide AUV survey on 21 December 2021..... 3-52

Figure 3.3.6: Time series of depth averaged current derived from ADCP measurements at SEOO during flood-tide AUV survey on 21 December 2021..... 3-52

Figure 3.3.7: AUV track lines on 3 March 2022 as flown during ebb tide surveys of the discharge plume from SEOO. Note, at 30°N latitude, 1° longitude = 93,453.2 m, while 1° latitude = 110,904.4 m..... 3-53

Figure 3.3.8: Full depth contour plot (aka, heat map) of AUV measurements of fDOM from surveys of SEOO during ebb tide on 3 March 2022. Average SEOO discharge rate = 8.806 mgd during ebb tide; End-of-pipe discharge concentration of fDOM = 204.34 ppb (QSU); End of pipe salinity = 0.71 psu; Trapping level (pycnocline depth) =26.9 m (-88.3 ft) MSL; Mean ebb tide current = 0.472 m/s (0.92 kts) toward the southeast..... 3-54

Figure 3.3.9: Full-depth contour plot (aka, heat map) of the signal to noise ratio (SNR) of fDOM during AUV surveys of SEOO during ebb tide on 3 March 2022. Average SEOO discharge rate = 8.806 mgd during ebb tide; End-of-pipe discharge concentration of fDOM = 204.34 ppb (QSU); End of pipe salinity = 0.71 psu; Trapping level (pycnocline depth) = -26.9 m (-88.3 ft) MSL; Mean ebb tide current = 0.473 m/s (0.92 kts) toward the southeast. 3-56

Figure 3.3.10: Full depth contour plot (aka, heat map) of the dilution factor, (D_{fDOM}) of fDOM during AUV surveys of SEOO during ebb tide on 3 March 2022. Average SEOO discharge rate = 8.806 mgd during ebb tide; End-of-pipe discharge concentration of fDOM = 204.34 ppb (QSU); End of pipe salinity = 0.71 psu; Trapping level (pycnocline depth) = -26.9 m (-88.3 ft) MSL; Mean ebb tide current = 0.473 m/s (0.92 kts) toward the southeast..... 3-57

Figure 3.3.11: Google Earth image of the San Elijo Lagoon whose tidal inlet is located 660 m (2,165 ft.) north of the headworks of the San Elijo Ocean Outfall, (located by the green and red lines). 3-59

Figure 3.3.12: Storage rating function of the newly restored San Dieguito Lagoon, (cf. AECOM, 2016, “Environmental Impact Report/Environmental Impact Statement for the San Elijo Lagoon Restoration Project”). Annotations in blue designate the tidal range and tidal discharge volume from the lagoon during ebb tide on 3 March 2022 3-60

Figure 3.3.13: CORMIX v-11 Simulation of the discharge plume from the San Elijo Lagoon during ebb tide on 3 March 2022. Average SEOO discharge rate = 8.806 mgd during ebb tide; End-of-pipe discharge concentration of fDOM = 204.34 ppb (QSU); End of pipe salinity = 0.71 psu; Trapping level (pycnocline depth) = -26.9 m (-88.3 ft) MSL; Mean ebb tide current = 0.472 m/s (0.92 kts) toward the southeast. 3-61

Figure 3.3.14: AUV track lines on 3 March 2022 as flown during flood tide surveys of the discharge plume from SEOO. Note, at 30° N latitude, 1° longitude = 93,453.2 m, while 1° latitude = 110,904.4 m. 3-63

- Figure 3.3.15:** Full depth contour plot (aka, heat map) of AUV measurements of fDOM from surveys of SEOO during flood tide on 3 March 2022. Average SEOO discharge rate = 11.851 mgd during flood tide; End-of-pipe discharge concentration of fDOM = 204.34 ppb (QSU); End of pipe salinity = 0.71 psu; Trapping level (pycnocline depth) = -26.9 m (-88.3 ft) MSL; Mean flood tide current = 0.301 m/s (0.58 kts) toward the northwest. 3-64
- Figure 3.3.16:** Full-depth contour plot (aka, heat map) of the signal to noise ratio (SNR) of fDOM during AUV surveys of SEOO during flood tide on 3 March 2022. Average SEOO discharge rate = 11.851 mgd during flood tide; End-of-pipe discharge concentration of fDOM = 204.34 ppb (QSU); End of pipe salinity = 0.71 psu; Trapping level (pycnocline depth) = -26.9 m (-88.3 ft) MSL; Mean flood tide current = 0.301 m/s (0.58 kts) toward the northwest. 3-65
- Figure 3.3.17:** Full depth contour plot (aka, heat map) of the dilution factor, (D_{fDOM}) of fDOM during AUV surveys of SEOO during AUV surveys of SEOO during flood tide on 3 March 2022. Average SEOO discharge rate = 11.851 mgd during flood tide; End-of-pipe discharge concentration of fDOM = 204.34 ppb (QSU); End of pipe salinity = 0.71 psu; Trapping level (pycnocline depth) = -26.9 m (-88.3 ft) MSL; Mean flood tide current = 0.301 m/s (0.58 kts) toward the northwest. 3-68
- Figure 3.3.18:** Storage rating function of the newly restored San Dieguito Lagoon, (cf. AECOM, 2016, “Environmental Impact Report/Environmental Impact Statement for the San Elijo Lagoon Restoration Project”). Annotations in blue designate the tidal range and tidal influx volume from the lagoon during flood tide on 3 March 2022. 3-69
- Figure 3.3.19:** CORMIX v-11 Simulation of the discharge plume from the San Elijo Lagoon during flood tide on 3 March 2022. Average SEOO discharge rate = 11.851 mgd during flood tide; End-of-pipe discharge concentration of fDOM = 204.34 ppb (QSU); End of pipe salinity = 0.71 psu; Trapping level (pycnocline depth) = -26.9 m (-88.3 ft) MSL; Mean flood tide current = 0.301 m/s (0.58 kts) toward the northwest.. 3-70
- Figure 4.1:** NPDES permit monitoring stations for SEOO, per CA0107999; Order Nos. R9-2018-0002 and R9-2018-0003. 4-2

LIST OF ACRONYMS AND ABBREVIATIONS

ADCP	Acoustic doppler current profiler
ARV	Air release valve
AUV	Autonomous underwater vehicle
CDOM	Colored dissolved organic matter
CFD	Computational fluid dynamics
CTD	Conductivity / temperature / depth
D_m	Monthly average initial dilution during minimum month conditions, as defined within the California Ocean Plan
D_{fDOM}	Dilution estimated using concentrations of fDOM
EOO	Encina Ocean Outfall
EWA	Encina Wastewater Authority
EWPCF	Encina Water Pollution Control Facility
fDOM	Fluorescence dissolved organic matter
ft	feet
HARRF	Hale Avenue Resource Recovery Facility
hr	hours
IMU	Inertial motion unit
in	Inches
kts	Knots (nautical miles per hour)
M	Meter
m/s	Meters per second
MF	Membrane Filtration
mgd	Million gallons per day
mg/L	Milligrams per liter
MLLW	Mean low low water
MSL	Mean sea level
NPDES	National Pollutant Discharge Elimination System
ppb	parts per billion
ppt	parts per trillion
psu	Practical Salinity Units
QSU	quinine sulfate equivalent units
RFU	Relative fluorescence units
RO	Reverse Osmosis
RWQCB	Regional Water Quality Control Board, San Diego Region
SCB	Southern California Bight
SEJPA	San Elijo Joint Powers Authority
SEOO	San Elijo Ocean Outfall
SEWRF	San Elijo Water Reclamation Facility
SNR	Signal to noise ratio
SWRCB	State Water Resources Control Board
ZID	Zone of initial dilution

EXECUTIVE SUMMARY

Regional Water Quality Control Board (RWQCB) Order No. R9-2018-0002 (NPDES CA0107981) regulates the discharge of wastewater from the City of Escondido to the Pacific Ocean via San Elijo Ocean Outfall (SEOO). RWQCB Order No. R9-2018-0003 (NPDES CA0107999) regulates the discharge of wastewater from the San Elijo Joint Powers Authority (SEJPA) to the Pacific Ocean via the SEOO. RWQCB Order No. R9-2018-0059 (NPDES CA0107395) regulates the discharge from the Encina Wastewater Authority (EWA) to the Pacific Ocean via Encina Ocean Outfall (EOO). In accordance with plume tracking monitoring requirements established by the RWQCB in the SEOO and EOO NPDES permits, in June 2020 the SEJPA, City of Escondido and EWA submitted a Plume Tracking Monitoring Plan (PTMP) for the SEOO and EOO. The PTMP identified plume tracking monitoring questions to be addressed and presented a monitoring plan and approach for addressing the monitoring questions. The PTMP was based on a “multiple lines of evidence” approach for assessing plume movement and included boat-based monitoring conducted by the outfall agencies in conjunction with data collected by Michael Baker International (Michael Baker) via boat-mounted sensors and sensors on remotely controlled underwater vehicles. This report presents the results of data collection efforts by Michael Baker from three deployment events per outfall.

The joint PTMP recommended similar monitoring approaches for the SEOO and EOO, as the two outfalls have similar designs, discharge characteristics and receiving water characteristics. Additionally, both outfalls feature seasonally varying flows (higher discharge flows during winter months and lower discharge flows during summer/fall months). **Table 1** summarizes outfall features and typical discharge flows for the SEOO and EOO.

Table 1: Comparison of SEOO and EOO Features

Parameter	SEOO	EOO
Total Outfall Length:	8,000 feet	7,800 feet
Approx. Diffuser Length:	1,200 feet	800 feet
Discharge Depth:	110 – 148 feet	165 – 168 feet
Approx. Avg. Annual Discharge Flow:	11 mgd	25 mgd
Assigned Initial Dilution:	237:1	144:1

In accordance with the monitoring approaches set forth in the SEOO/EOO PTMP, support field studies using autonomous underwater vehicles (AUVs) and boat-mounted sensors were conducted by Michael Baker in September 2021 (1st Deployment), December 2021 (2nd Deployment) and March 2022 (3rd Deployment). Key data gathered during these studies included salinity and colored dissolved organic matter (CDOM), and its surrogate fDOM, which is the portion of CDOM that fluoresces.

AUV deployments were selected to address typical fall conditions of maximum or near-maximum stratification, typical spring conditions of minimum or no stratification, and atypical (post storm) conditions. As shown in **Table 2**, the 1st Deployment was selected to be characteristic of typical fall conditions under maximum or near-maximum stratification, the 2nd Deployment date was selected as representative of atypical (post storm) conditions, and the 3rd Deployment was selected to be characteristic of typical spring conditions.

Table 2: Summary of Comparison of SEOO and EOO Features

Deployment	Date	Conditions to Be Assessed
1st:	September 2021	Typical Conditions: Fall conditions of maximum or near-maximum stratification
2nd:	December 2021	Atypical Conditions: Post-storm conditions with higher-than-average outfall discharge flows and runoff
3rd	March 2022	Typical Conditions: Spring conditions where strong pycnocline is absent

As part of the deployments, salinity and fDOM were tracked across 459 to 988 acres of ocean surrounding the EOO and SEOO by an Iver3 autonomous underwater vehicle (AUV) supported by 15 to 18 stationary monitoring stations using fDOM sensors, conductivity / temperature / depth (CTD) sensors and acoustic doppler current profilers (ADCPs). Advantages to sampling the EOO and SEOO with an AUV included the ability to run pre-programmed survey track lines to efficiently cover a large survey area with high density sampling that produces as many as 65,000 to 68,500 separate measurements of fDOM and salinity. These AUV survey results produce high-resolution, three-dimensional data models of the outfall plumes and receiving waters.

Signal detection theory was used to differentiate between what may be identifiable as the outfall discharge plume and the surrounding ambient water mass. Plume detectability was approached as a signal-to-noise problem which is measured by the signal to noise ratio, SNR ; where the noise is the ambient (aka, *natural ocean background*) concentrations of salinity or fDOM; and the signal is the difference between the ambient concentrations of salinity or fDOM and the measured concentrations of salinity or fDOM. Signal detection theory teaches that the lowest order significance threshold for detection arises when $SNR \geq 1$.

During the first AUV deployments, 21-23 September 2021, natural ocean background levels of fDOM were elevated in the range of 0.64 parts per billion (ppb) to 0.77 ppb. With these high ambient fDOM concentrations, the highest SNR of any fDOM feature anywhere in the 988.4 acres of ocean water mass surveyed around the SEOO was only a $SNR_{fDOM} \cong 0.68$ to 0.70, which does not meet the lowest order significance threshold for detection, namely $SNR_{fDOM} \geq 1$. Because of the high natural receiving water concentrations of fDOM during this September 2021 deployment, SNR_{fDOM} ratios were insufficient to detect or reliably discern remnants of either the SEOO discharge plumes. However, the EOO was discharging about 2.5 times more effluent than the SEOO, and SNR in the 988.4 acres of ocean water mass surveyed around the EOO reached $1.0 \leq SNR_{fDOM} \leq 1.5$ in several small plume remnants located between 33 m and 588 m of the downstream side of the EOO diffuser. Dilution factors in these plume remnants were no less than 260:1, or about 80.5% higher than the assigned minimum month dilution of $D_m = 144:1$ established in the current NPDES permit for the EOO (No. CA0107395; Order No. RS-2018-0059).

Based on fDOM patterns measured during the first AUV deployments, the resolution of the survey pattern was increased by a factor of 2.4 during subsequent deployments. This was accomplished by reducing the distance between survey track lines and increasing the number of track lines from 5 to 12. However, because the battery capacity of the Iver3 AUV limited the total distance traveled to about 20 km, the length of each track line was reduced resulting in a reduction of the total area surveyed from 998.4 acres to 494.2 acres.

The second AUV deployments 20-21 December 2021 occurred after passage of a dry cold front that brought strong onshore winds the week prior. This represented post-storm conditions that were sufficiently safe for AUV deployment. During this deployment period, natural ocean background levels of fDOM dropped to approximately 0.3 ppb. With these reduced background fDOM concentrations, singular, large fDOM features were discovered 268 meters (m) to 394 m down-drift in the shore parallel direction from both the EOO and SEOO diffusers. The signal to noise ratios of these fDOM features ranged from $SNR_{fDOM} \cong 1.2$ along the outer perimeter of the suspected plume remnants, to as high as $SNR_{fDOM} \cong 3$ in the inner core of the suspected plume remnants, thereby readily satisfying the lowest order significance threshold for detection, (i.e., $SNR_{fDOM} \geq 1$). This detection metric is indicative of the probable presence of remnants of the EOO and SEOO discharge plumes. It should be noted that this “probable” detection is based exclusively on fDOM. Due to the relatively small variation between discharge salinity and ocean background salinity, it was concluded that salinity is an unsatisfactory tracer of the plumes because it always produced signal to noise ratios several orders of magnitude less than unity.

Additionally, it should be noted that the use of fDOM as a tool for plume detection assumes that natural concentrations of fDOM in receiving waters are homogenous. In reality, receiving water fDOM can naturally vary from location to location, depending on time of year, ocean conveyance conditions, and proximity to shore-based sources or offshore sources. As a result of these factors, plume detections that rely exclusively on fDOM data are appropriately referred to herein as “probable” or “potential” detections.

The discovery of potential plume remnants during the December 2021 fDOM surveys (located several hundred meters down current from the EOO and SEOO in the shore parallel or upcoast/downcoast direction) prompts the question of whether these plume remnants had been detected subsequent to the completion of initial dilution. The initial approach to this question involved performing initial dilution simulations with Plumes 20 (UM3), the latest update to the Visual Plumes (UM3) dilution model, using actual ambient currents on 20-21 December 2021 for the EOO and SEOO. Under these modeling conditions, initial dilution was determined to be completed in the immediate vicinity of the SEOO and EOO. The EOO initial dilution was simulated in excess of 310:1, while the SEOO initial dilution was simulated in excess of 390:1. Based on collected fDOM data, the plume tracking study of the EOO and SEOO discharges on 20-21 December 2021 indicates that the discharge plume can spread several hundred meters beyond the EOO and SEOO diffusers. As would be expected, dilution would continue to increase as discharge remnants are dispersed and carried downstream. By the time the discharges are carried more than 100 meters down current, fDOM-derived dilutions at the SEOO exceeded 766:1 and dilutions at the EOO exceeded 638:1.

The third AUV deployments at SEOO and EOO on 2-3 March 2022 utilized a slightly modified AUV survey pattern having the same horizontal resolution as that used during the second deployments but included 100 m of overlap between the ebb-tide and flood-tide survey boxes in the long-shore direction in order to increase resolution of any suspected plume remnants found close to the outfall diffusers. This overlap reduced the total area surveyed during the third deployments to 459.3 acres. The third AUV deployments occurred about 32 hours prior to the arrival of an extratropical frontal cyclone, approaching from the

northwest that generated strong southward flowing wind-driven currents, which when combined with tidal currents and wave surges produced strong velocity shear across the outfall discharge area, causing the discharge to break up into small fragments. Furthermore, the water column exhibited linear, continuous, stable stratification between the sea surface and the seabed, resulting in a deep trapping level that arrested initial dilution at a relatively short distance above the seabed. Ambient fDOM background concentrations were low, ranging between 0.170 ppb and 0.279 ppb during the third deployments, favoring detection of any plume fragments that survived in the strong current shear. However, the plume was not detectable at the SEOO and only small fragments of a plume were possibly detected at the EOO that were located 332 m to 670 m down current from the EOO diffuser in the shore parallel direction. Minimum dilution ratios in these plume fragments were never less than 477:1.

While evidence of the SEOO discharge was difficult to discern during the 2 March 2022 deployment, the presence of the ebb-tide discharge from the San Elijo Lagoon was strongly evident. The fDOM feature identified as a discharge from the lagoon was substantial, comprised of 14,000 to 15,000 separate fDOM measurements with a sharp frontal boundary located 579 m to 686 m inshore of the shoreward end of the SEOO diffuser. The conclusion that the source of the fDOM front was ebb tide discharges from the San Elijo Lagoon was verified by CORMIX v-11 simulations of shoreline discharges at the location of the inlet to San Elijo Lagoon and supported by field observations of a red tide located inshore, beginning along the 60 ft depth contour.

Charge Question: Based on the June 2020 joint PTMP for the SEOO and EOO, along with plume tracking requirements in the SEOO and EOO NPDES permits (RWQCB Order Nos. R9-2018-0002, R9-2018-0003, and R9-2018-0059), the plume tracking program was intended to address, at minimum, the following questions:

(1) Are the current monitoring locations and methods adequate to determine whether the wastewater plume is encroaching on water recreational areas, including, but not limited to, areas used for swimming, scuba diving, surfing, and fishing? If not, what monitoring locations and/or methods are more appropriate?

Based on the findings of the plume tracking field studies in September 2021, December 2021 and March 2022, the wastewater plumes were never found inshore of the shoreward end of either the SEOO or the EOO diffusers. What is discharged offshore remains offshore.

The present-day monitoring stations for the SEOO (**Figure 4.1**) and EOO (**Figure 2.1.1**) are more than adequate to confirm that the outfall wastewater plume is not encroaching on water recreational areas. No additional monitoring stations are required for that purpose. Further, evidence that the outfall discharges remain offshore is sufficiently strong as to question why shore-based monitoring is required at all. The lack of need for such shore-based bacteriological monitoring as part of the SEOO and EOO NPDES outfall permits is supported by the fact that the existing near-shore SEOO and EOO receiving water monitoring stations (located between the shore and the outfall discharge point) consistently show compliance with Ocean Plan body contact recreational standards.

SEOO plume tracking measurements using an AUV never produced evidence of the discharge plume further than 329.8 m (1,082 ft) from the SEOO diffuser in a shore parallel direction. The criteria for plume detection were based on signal detection metrics that require the measurements of a plume tracer must have a signal to noise ratio of at least unity in order to identify the presence of the plume. As a result, it may be concluded that the SEOO inshore monitoring stations (T, N, and S stations) are best suited for monitoring effects caused by shoreline discharges. In support of this conclusion, the inshore AUV survey plume tracking measurements in March 2022 detected the discharge of the San Elijo Lagoon whose frontal boundary was along the 60 ft MSL depth contour in the vicinity the N-monitoring stations in **Figure 4.1**. Additionally, eliminating the offshore sampling points greater than 2,000 ft away from the outfall is warranted as no evidence of the discharge was observed further than 329.8 m (1,082 ft) from the outfall.

EOO plume tracking measurements of fDOM and salinity using AUV sensors never found evidence of the discharge plume further than 669.8 m (2,197 ft) from the EOO diffuser in a shore parallel direction. The plume was never found inshore of the shoreward end of the EOO diffuser. Based on this finding, the present disposition of the NPDES offshore monitoring stations for the EOO (blue triangles in **Figure 2.1.1**, **Figure 2.2.1**, and **Figure 2.3.1**) appear to be adequate to determine whether the wastewater plume is encroaching on water recreational areas.

(2) Is the removal of the SEOO Surf Zone monitoring location S-6 (historical) still appropriate?

Based on the findings of the plume tracking field studies in September 2021, December 2021 and March 2022, removal of the Surf Zone monitoring location S-6 (historical) remains appropriate. Further, as documented above, available evidence indicates that the SEOO and EOO discharges remain offshore (carried upcoast/downcoast), and that shore-based discharges remain near the shore (also carried upcoast/downcoast). As a result, SEOO and EOO shore stations appear to be of little use in assessing outfall discharge effects and instead the stations record effects from shore-based sources. Removal of SEOO Surf Zone Station S-6 is appropriate.

(3) How does the brine discharge from the MFRO Facility and San Elijo Water Reclamation Facility and future brine discharges (along with increased recycled water use and decreased outfall discharge flows) affect the dynamics of the wastewater plume and initial dilution?

This question is being further evaluated as part of a SEOO initial dilution study that is being performed pursuant to requirements in Order Nos. R9-2018-0002 and R9-2018-0003. Data developed as part of initial dilution modeling performed in this plume tracking study, however, indicate that brine discharges from the MFRO Facility and San Elijo Water Reclamation Facility will have not have a significant effect on the dynamics of the SEOO wastewater plume and initial dilution. Similarly, existing and proposed brine discharges to the EOO are unlikely to discernibly affect initial dilution.

(4) Does the wastewater plume have the potential to interact with wastewater plumes from other ocean outfalls or other sources of pollution, such as storm water and outflows from the San Elijo Lagoon?

Based on the findings of the plume tracking field studies in September 2021, December 2021, and March 2022, the SEOO and EOO wastewater plumes have no potential to interact with each other or with wastewater plumes from other ocean outfalls or other sources of pollution, such as storm water and outflows from the San Elijo Lagoon or Agua Hedionda Lagoon. The plume tracking measurements (over 66,000 measurement points) never found evidence of the SEOO discharge plume further than 329.8 m (1,082 ft) from the SEOO diffuser in a shore parallel direction, and no further than 669.8 m (2,197 ft) from the EOO diffuser in a shore parallel direction. At either outfall, the wastewater plumes were never found inshore of the shoreward end of either the SEOO or EOO diffusers. AUV survey plume tracking measurements of fDOM in March 2022 presented convincing evidence of the shore-based discharge from the San Elijo Lagoon whose frontal boundary was detected at a distance 685.9 m (2,250 ft) shoreward of the shoreward end of the SEOO diffuser during ebb tide near the 60 ft. MSL depth contour. The lagoon discharge, however, did not impinge on the SEOO discharge.

(5) What is the fate of the wastewater plume in typical and atypical oceanographic conditions, and when and under what conditions is the wastewater plume no longer distinguishable from ambient receiving water?

The plume tracking field studies in September 2021 were conducted under typical late summer/fall oceanographic conditions when the water column was strongly stratified, forming a two-layer water mass with a well-defined pycnocline at 8 m depth (-26.2 ft. MSL). Ambient background concentrations of fDOM were relatively high, averaging 0.639 ppb to 0.776 ppb. With the high ambient fDOM concentrations under typical summer oceanographic conditions, the discharge plumes of the SEOO and EOO could not be distinguished from the ambient receiving water. Additionally, salinity was found to be useless as a plume tracer due to its low signal to noise ratio at the point of discharge.

The plume tracking field studies in December 2021 were conducted after the passage of a dry cold front (post-storm conditions) that included high winds. At this time, a cold, nearly homogeneous surface layer, (about 6° C cooler than during the first deployment in September 2021) existed down to approximately a 25 m depth, while the bottom layer remained about the same temperature as in September 2021. Consequently, the water column during December 2021 was only weakly stratified (i.e., less stable) and the trapping level rose to within 4 m of the sea surface. However, ambient background concentrations of fDOM were relatively low, averaging 0.294 ppb to 0.310 ppb. Due to the low ambient fDOM concentrations, the discharge plumes of the SEOO and EOO could be distinguished from the ambient receiving water using fDOM, with high signal to noise ratios reaching $SNR_{fDOM} \cong 2.46$ in the inner core of the SEOO wastewater plume located 329.8 m (1,082 ft) downstream of the SEOO diffuser in a shore parallel direction; and as high as $SNR_{fDOM} = 3.39$ in the inner core of the EOO wastewater plume, located 393.9 m (1,292 ft) downstream of the EOO diffuser in a shore parallel direction.

The plume tracking field studies in March 2022 were conducted to characterize late winter/early spring conditions. The March 2022 conditions included a cold bottom layer having temperatures ranging from 11.4° C at the seabed, warming rapidly to 13° C at 3 m above the seabed, and then warming almost linearly to 14.7° C at the sea surface. The salinity reached 33.7 ppt near the seabed, declining to 33.48 ppt at approximately a depth of -27 m MSL; and then remained nearly constant between -27 m depth and the sea surface. The density profile during the third AUV deployment represented a continuously stratified water column rather than a two-layer system as prevailed during the first and second deployments in September and December 2021. Consequently, the trapping level during March 2022 was deep, at a depth of -26.9 m (-88.26 ft) MSL, which is more typical of a worst-case dilution scenario, because initial dilution is arrested relatively close to the seabed. Nonetheless, ambient background concentrations of fDOM were low averaging 0.170 ppb to 0.279 ppb due to reduced biological activity in the cold water with short daylight hours, compounded by the absence of recent rainfall. In spite of the low ambient background concentrations of fDOM, the plumes remained difficult to distinguish from the ambient receiving water because of strong currents in the presence of an approaching extratropical frontal cyclone from the northwest. Mean currents (on the order of 1 kts) were flowing shore-parallel in combination with transient wave surges as high as 1.53 kts flowing obliquely to the mean current, thereby exposing the wastewater plumes to high velocity shearing rates. This shearing by the ambient currents broke up the wastewater plumes into small fragments. Small plume fragments with signal to noise ratios of $SNR_{fDOM} \cong 2.3$ in the inner core were only detected at the EOO, located 669.8 m downstream of the EOO diffuser in a shore parallel direction. No plume fragments could be detected at the SEOO during the March 2022 AUV surveys.

(6) What parameters are most useful for assessing the presence of a wastewater plume?

The AUV deployments indicated that fDOM can be an effective parameter in indicating the possible or probable presence of remnants of the SEOO and EOO discharges. Bacteriological parameters (e.g., fecal coliform and enterococcus) can be combined with fDOM to provide additional evidence of the presence of the discharge plumes.

At present, small, low-power electronic sensors capable of being carried aboard an AUV are only capable of measuring potential plume tracers such as salinity and fDOM (the component of colored dissolved organic matter that fluoresces). Salinity was found to be useless as a plume tracer. Signal to noise ratios of salinity measurements during the plume tracking study never exceeded $SNR_S \cong 0.008$. This is due to fact that effluent salinity at the point of discharge is typically about 1 to 1.5 psu, compared with natural background ocean salinity which averages 33.5 psu; so that the signal to noise ratio of salinity at the point of discharge is on the order of $SNR_S \approx 0.96$, less than the threshold of detection by signal detection metrics. On the other hand, effluent fDOM at the point of discharge is typically in the range of 200 to 300 ppb, significantly greater than natural background ocean fDOM which is typically in the range of 1 ppb. Consequently, the signal to noise ratio of fDOM at the point of discharge is typically no less than $SNR_{fDOM} \approx 199$. Signal to noise ratios of fDOM features believed to be the wastewater plume were found to be in the range of $SNR_{fDOM} \cong 2$ to 3. This means the fDOM concentrations of features believed to be the wastewater plume were 3 - 4 times greater than the ambient background fDOM concentrations.

(7) What is the variability in the degree of initial dilution that occurs under typical and atypical oceanographic conditions?

The plume tracking field studies that were conducted in September 2021 under typical late summer oceanographic conditions were unable to detect the wastewater plumes from either the SEOO or the EOO, due to high ambient concentrations of fDOM. Therefore, no conclusion could be drawn regarding the degree of initial dilution that occurs under typical late summer oceanographic conditions.

The plume tracking field studies in December 2021 that were conducted under typical dry weather winter oceanographic conditions detected fDOM features of the SEOO wastewater plume having dilution ratios as high as 311:1 in the inner core of the plume, or a factor of 1.3 times greater than the minimum month dilution of $D_m = 237:1$ assigned in the current NPDES permits (Order Nos. R9-2018-0002 and R9-2018-0003). At the EOO, dilution ratios of the fDOM features of the wastewater plume were never less than 215:1 in the inner core of the plume, or a factor 1.5 times greater than the minimum month dilution of $D_m = 144:1$ assigned within the current EOO permit (Order No. R9-2018-0059).

The plume tracking field studies in March 2022 coincided with worst case (maximum trapping depth) oceanographic conditions. The March 2022 field studies were unable to detect the wastewater plume from the SEOO due to high ambient currents and surges that sheared the plume into small undetectable fragments. At the EOO, observed fDOM-derived dilutions of wastewater plume fragments were at least 477:1 in the core of the plume fragments, or a factor of 3.18 times greater than the minimum month dilution of $D_m = 144:1$ assigned within the EOO NPDES permit (Order No. R9-2018-0059).

1 INTRODUCTION

This is a field study to address questions established in the SEOO and EOO NPDES permits and with the joint SEOO/EOO PTMP. Many of the key PTMP questions relate to how far away from the point of discharge can the SEOO and EOO discharges be recognizable from ambient receiving water.

Two effluent properties are used to address the PTMP questions: salinity and colored dissolved organic matter (CDOM), or its surrogate fDOM, which is the portion of CDOM that fluoresces. On average, fDOM makes up between 85% and 91% of the total CDOM in ocean waters, (cf. Cobble, 2007); and so its concentrations are reasonably representative of CDOM concentrations. Effluent salinity at the point of discharge is typically about 1 to 1.5 parts per trillion (ppt), which is significantly smaller than the natural background ocean salinity, which averages 33.5 ppt over the long-term. On the other hand, effluent fDOM at the point of discharge is typically in the range of 200 to 300 ppb, significantly greater than natural background ocean fDOM which is typically in the range of 1 ppb. Consequently, as the effluent dilutes with increasing distance away from the outfall, the effluent salinity increases while the effluent fDOM decreases, until both these effluent properties become indistinguishable from the natural ocean background. The decisive question in this regard is whether the effluent is distinguishable from ambient ocean water beyond the immediate discharge zone. This question can be answered quantitatively using *signal detection theory*, which is a calculus to differentiate between information-bearing patterns (referred to as *signal*), and random patterns that distract from the information (called *noise*). Noise is the result of natural background variability, random environmental activity, or limited sensor resolution. Detectability is a signal-to-noise problem which is measured by the signal to noise ratio, SNR, (cf. Peterson, et al., 1954), where the noise is the ambient (aka, *natural ocean background*) concentrations of salinity, or fDOM; and the signal is the difference between the ambient concentrations of salinity, or fDOM and the measured concentrations of salinity or fDOM, (cf. Stanislaw & Todorov, 1999), written as:

$$SNR_S = \frac{S_\infty - S_{(x)}}{S_\infty} \text{ (for effluent salinity measurements where } S_{(x)} \leq S_\infty \text{)}$$

and,(1)

$$SNR_{fDOM} = \frac{fDOM_{(x)} - fDOM_\infty}{fDOM_\infty} \text{ (for effluent fDOM measurements)}$$

Here, S_∞ , $fDOM_\infty$ are the ambient (*natural ocean background*) concentrations of salinity and fDOM as a function of location and time, respectively; and $S_{(x)}$, $fDOM_{(x)}$ are the measured concentrations of salinity and fDOM at any arbitrary distance, x , from the point of discharge. It is important to understand that $S_{(x)}$, $fDOM_{(x)}$ are not purely signal, but rather are comprised of signal overlaid on noise. Consequently, if $SNR = 1$, the signal strength matches the strength of the background noise. Signal detection theory teaches that significance threshold for detection arises when $SNR \geq 1$, (cf. Schonhoff & Giordano, 2006). the salinity or fDOM signal from the outfall must be at least as strong as the background noise in order for that outfall signal to be considered as having been detected. In other words, the threshold for detection is achieved when $S_{(x)} \leq 1/2(S_\infty)$ and $fDOM_{(x)} \geq 2fDOM_\infty$.

Given the order of magnitude characteristic values of ambient vs. effluent salinity and fDOM cited above, the SNR at the point of discharge of salinity is on the order of $SNR_S \approx 0.96$. Therefore, the effluent salinity is probably not a good signal for tracking a treated wastewater plume since the SNR for salinity is less than unity even at the point of discharge. This assumption is studied in detail in Sections 2 & 3 by generating maps of the SNR of salinity (referred to as heat maps) derived from AUV measurements of the salinity field over areas of 500 to 1000 acres around the Encina and San Elijo Ocean Outfalls.

For the order of magnitude estimates of ambient fDOM and effluent fDOM given above, the SNR of fDOM at the point of discharge is typically no less than $SNR_{fDOM} \approx 199$. Therefore, beginning from the point of discharge and extending outward into the receiving waters, the signal of the effluent fDOM is intrinsically more detectable than the effluent salinity signal because the fDOM initiates dilution and dispersion with a SNR at least two orders of magnitude greater than that of effluent salinity.

As the effluent dilutes with increasing distance away from the outfall, the SNR decreases and the effluent is no longer detectable once the SNR becomes vanishingly small, $SNR \rightarrow 0$. The dilution factor and SNR are related. The Ocean Plan definition of dilution factor, D_m , is parts seawater per parts effluent, which is calculated as:

$$D_m = \frac{S_\infty - S_{(x=0)}}{S_\infty - S_{(x)}} - 1 \quad (\text{for effluent salinity measurements where } S_{(x)} \leq S_\infty)$$

and,(2)

$$D_{fDOM} = \frac{fDOM_{(x=0)} - fDOM_\infty}{fDOM_{(x)} - fDOM_\infty} - 1 \quad (\text{for effluent fDOM measurements})$$

where $S_{(x=0)}$, $fDOM_{(x=0)}$ are the salinity and fDOM concentrations at the point of discharge, $x = 0$. Combining equations (1) & (2) allows the dilution factor dilution factor to be calculated directly from the SNR , or:

$$D_m = \frac{S_\infty - S_{(x=0)}}{S_\infty SNR} - 1 \quad (\text{for effluent salinity measurements where } S_{(x)} \leq S_\infty)$$

and,(3)

$$D_{fDOM} = \frac{fDOM_{(x=0)} - fDOM_\infty}{fDOM_\infty SNR} - 1 \quad (\text{for effluent fDOM measurements})$$

Inspection of equation (3) indicates that as the effluent dilutes with increasingly larger distances from the outfall, that the dilution factor becomes infinite, $D_{fDOM} \rightarrow \infty$, as the SNR becomes vanishingly small, $SNR \rightarrow 0$.

To determine the natural background values of salinity and fDOM on the day of the field measurements reported in this study, vertical profiles across the entire water column of salinity and fDOM are conducted at fixed-point monitoring locations positioned up and down coast and on and offshore of outfall diffuser locations. To determine the signal strength of the effluent salinity and fDOM, an autonomous underwater

vehicle (AUV) equipped with conductivity/temperature/depth (CTD) sensors and an fDOM sensor was deployed to navigate search patterns that extend several kilometers away from the outfalls.

1.1 FLUID MECHANICS AND REGULATORY STANDARDS OF EFFLUENT DILUTION

Because treated wastewater is buoyant in seawater, discharges from the SEOO and EOO are regulated under Provisions III.C.4(b-d) of the California Ocean Plan (cf. SWRCB, 2019). In particular, the present-day NPDES permits were drafted for consistency with Requirement III.C.4(b) as it would apply to a Zone of Initial Dilution (ZID). The California Ocean Plan defines the ZID as the zone in which the process of initial dilution is completed. Initial dilution is defined in Appendix I of the CA Ocean Plan as follows:

“Initial Dilution is the process which results in the rapid and irreversible turbulent mixing of wastewater with ocean water around the point of discharge. For a submerged buoyant discharge, characteristic of most municipal and industrial wastes that are released from the submarine outfalls, the momentum of the discharge and its initial buoyancy act together to produce turbulent mixing”

Provision III.C.4(d) of the Ocean Plan requires that minimum initial dilution be determined in a specific manner:

“For the purpose of this Plan, minimum initial dilution is the lowest average initial dilution within any single month of the year. Dilution estimates shall be based on observed waste characteristics, observed receiving water density structure, and the assumption that no currents, of sufficient strength to influence the initial dilution process, flow across the discharge structure”.

The current NPDES permit for the EOO (No. CA 0107395, Order No. R9-2018-0059) assigns a minimum initial dilution ratio of 144:1 at 43.3 million gallons per day (mgd) during dry weather and 52.6 mgd during wet weather. On the other hand, the current NPDES permits for the SEOO (Order Nos. R9-2018-0002 and R9-2018-0003) assign a minimum initial dilution ratio of 237:1 at 25.5 mgd of secondary effluent plus brine wastes from its Membrane Filtration (MF) / Reverse Osmosis (RO) Facility. These minimum initial dilution ratios are calculated at the *“trapping level”* during *worst-month conditions*, per Provision III.C.4(b) & (d) of the Ocean Plan. The trapping level refers to the height in the water column above the point of discharge where the buoyant discharge plume ceases to rise further, (cf. [Figure 1.1.1](#)). The trapping level may become the sea surface during winter conditions when the water column is well-mixed from the sea surface down to the seabed. To understand the dynamics of trapping layers, consider a buoyant plume as shown schematically in [Figure 1.1.1](#). The effluent is initially discharged at high velocity from many small diameter discharge ports, creating the same number of turbulent jets. Upon discharge, the momentum flux of these turbulent jets dominates over the buoyancy of the treated wastewater effluent, and the jets follow an initial trajectory along the axis of the diffuser discharge ports.

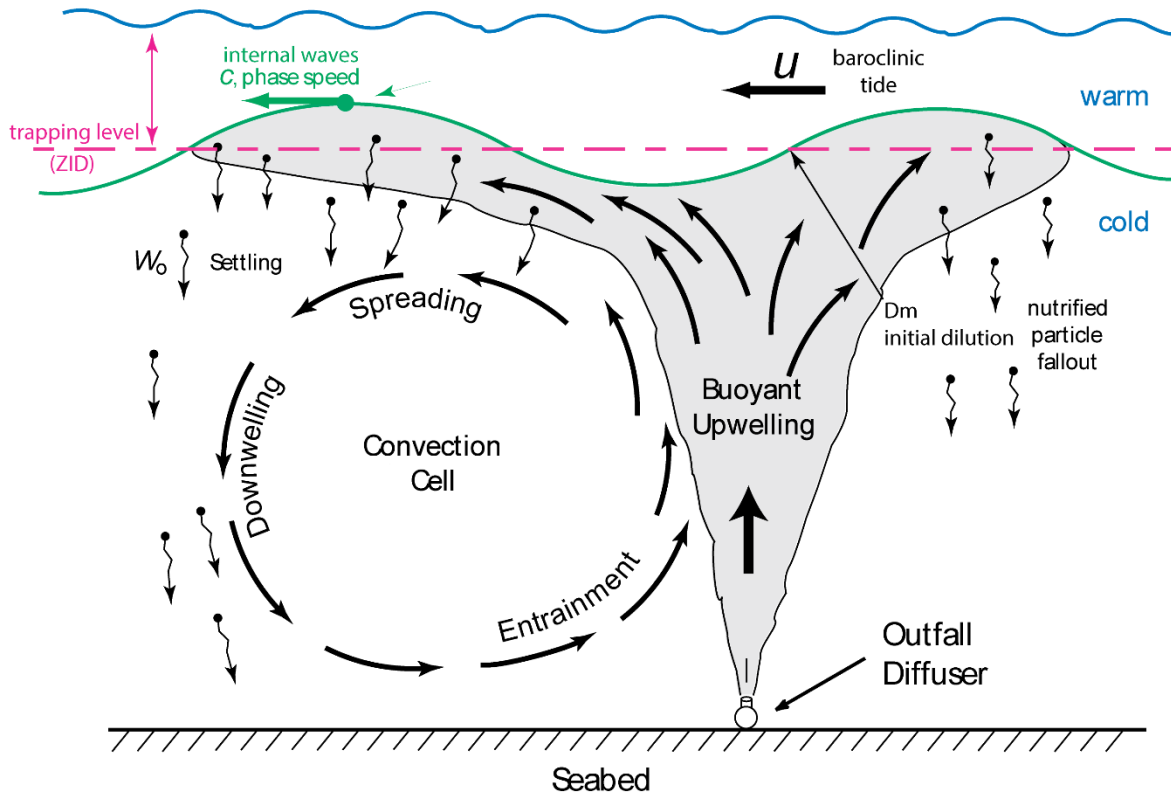


Figure 1.1.1: Schematic diagram of the rising wastewater plume pancaking at the pycnocline (trapping level) and spreading laterally along the base of the pycnocline under the influence of its residual momentum and internal wave mass transport.

As the trajectory of the jets extends outward from the diffuser ports, the diameter of each jet expands until merging with its neighbor, as shown schematically in [Figure 1.1.2](#). The large turbulent eddies are produced as these turbulent jets undergo axial expansion during the initial phase of discharge. These turbulent eddies dilute the jet momentum, until the momentum flux is diminished to less than the effluent buoyancy, typically at the point of jet merging. Once the effluent buoyancy exceeds the momentum flux during the jet merging, the discharge becomes a *convective plume* that rises in the water column. As the eddies and convective circulation of the plume entrain more and more of the surrounding water mass, the plume becomes diluted, and the buoyancy declines until the plume no longer rises further in the water column. This typically occurs at a density interface in the water column referred to as the *pycnocline*, usually formed between two water masses, the warm surface mixed layer and the colder bottom water. The pycnocline forms a *trapping layer*, and the residual turbulent momentum of the plume causes it to spread out horizontally. At the discharge depths of the SEOO and EOO, the pycnocline (sometimes referred to as a thermocline, since temperature is typically a dominant factor affecting density) exists throughout almost all of the year. Upon rising to the pycnocline, the discharge will spread out horizontally along the trapping layer interface until all of its turbulent kinetic energy and buoyant potential energy is dissipated, at which dilution ceases to change. The dilution at this point is referred to as initial dilution.

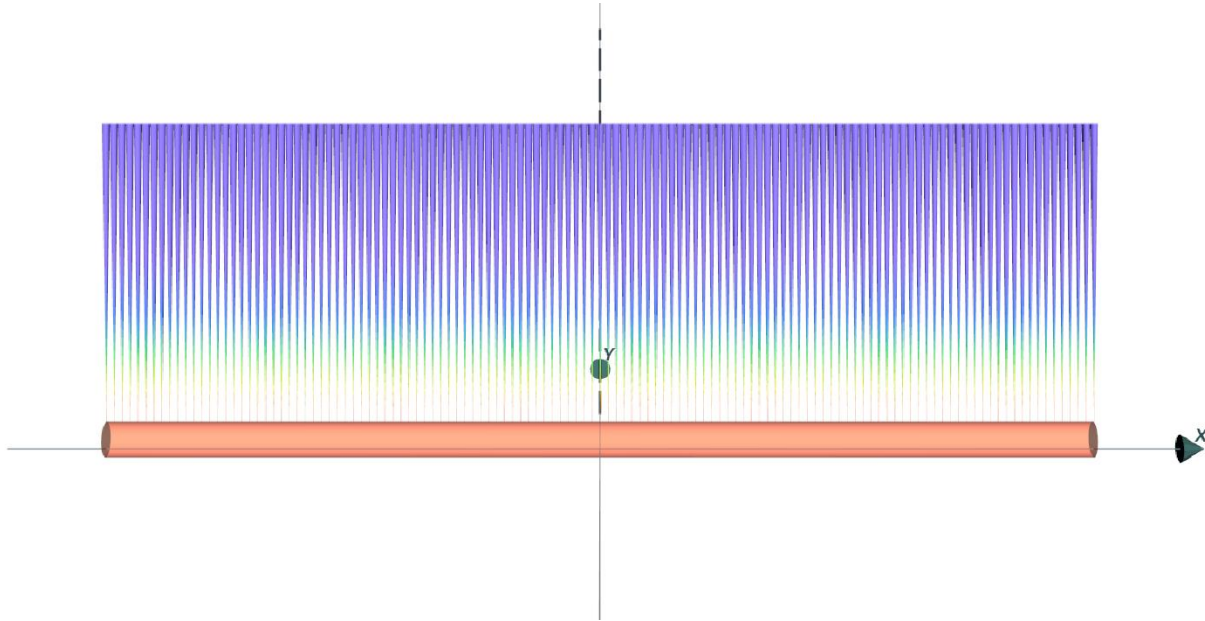


Figure 1.1.2: Schematic of jet merging due to axial expansion of each of the 200 jets during the initial phase of discharge from the SEOO diffuser, when the momentum flux of each jet exceeds the buoyancy of the effluent. Image from CORMIX v-12 near-field simulation of the SEOO diffuser.

In the natural ocean environment, the pycnocline (or trapping layer) is dynamic, rising and falling in the water column with the seasons, and with internal (baroclinic) tides that propagate along the pycnocline interface. While seasonal effects on pycnocline heights and trapping levels were included in the previous dilution studies for the EOO and SEOO (RWQCB, 2005), the effects of baroclinic tides and the currents they create across the diffuser are excluded from the hydrodynamic modeling under Provision III.C.4(d) of the Ocean Plan. The present study will present both field data from AUV surveys, and plume modeling results that reveal the effects that ambient currents can have on initial dilution and subsequent dilution or dispersion.

1.2 OUTFALL SURVEY METHODS

Advantages to sampling the EOO and SEOO with an AUV include the ability to run pre-programmed mission track lines to efficiently cover a large survey area with high density sampling at 4 Hz sampling rate that produces as many as 64,000 to 68,000 separate measurements per survey of plume observables (fDOM and salinity). These AUV survey results produce a high-resolution, three-dimensional data model as shown in [Figure 1.2.1](#). In accordance with the approach set forth in the SEOO/EOO PTMP, the plume tracking monitoring with the AUV occurred over a one-day period for each of three seasonal deployment scenarios (summer-fall, winter-spring, and post-storm) over the course of the data collection schedule (2021/2022). A specific AUV survey plan was developed for each survey, and mission parameters remained constant for each of the AUV surveys (i.e., AUV speed over ground was held constant at 2.5 kts).

The Iver3 AUV (cf. [Figure 1.2.3](#)) was used for all AUV surveys of the EOO and SEOO.

The Iver3 AUV has exceptionally precise navigation and depth control due to a high-end inertial motion unit (IMU) with GPS set points that work in a control loop in conjunction with a Doppler velocity logger and bottom-locking sonar that provides constant speed over ground throughout the survey flight path. Refer to [Table 3](#) through [Table 5](#) for listings of Iver3 specifications and on-board equipment.

The Iver3 AUV was deployed for one full day over each outfall to survey a full tidal cycle during each of the 3 seasonal deployments selected to capture the envelope of variability of oceanographic conditions. Total survey track length was held constant at the longest possible track length that could be safely achieved within the limited battery life of the AUV. Survey depth was variable, dependent on CTD data collection results during the pre-deployment site characterization data sampling operations which determined pycnocline depth in the water column. Each track-line in the AUV survey was flown out and return, proceeding outbound with the current along a dolphin style dive profile between the seabed and a couple of meters above the pycnocline (trapping level) as shown in [Figure 1.2.2](#). On the return leg of the track-line, the AUV proceeded at constant depth a couple of meters below the pycnocline (trapping level).

In addition, 15 water column monitoring stations in the far-field of each outfall were sampled during the AUV deployments to establish natural ocean background conditions and ambient currents. The monitoring stations were sampled twice during each tide, evenly spaced before and after mid-tide, for a total of four grid set control samples during each survey. These monitoring stations utilized the Sea-bird SBE 19*plus*V2 CTD ([Figure 1.2.4](#)) and the 2 MHz Nortek acoustic Doppler current profiler (ADCP, cf. [Figure 1.2.5](#)). The ADCP was deployed at the far-field monitoring station from the R/V Benthic Cat ([Figure 1.2.6](#)). The R/V Benthic Cat is equipped with a station keeping system that allows the boat to automatically stay on a fixed location for the time needed to acquire CTD and ADCP current data.

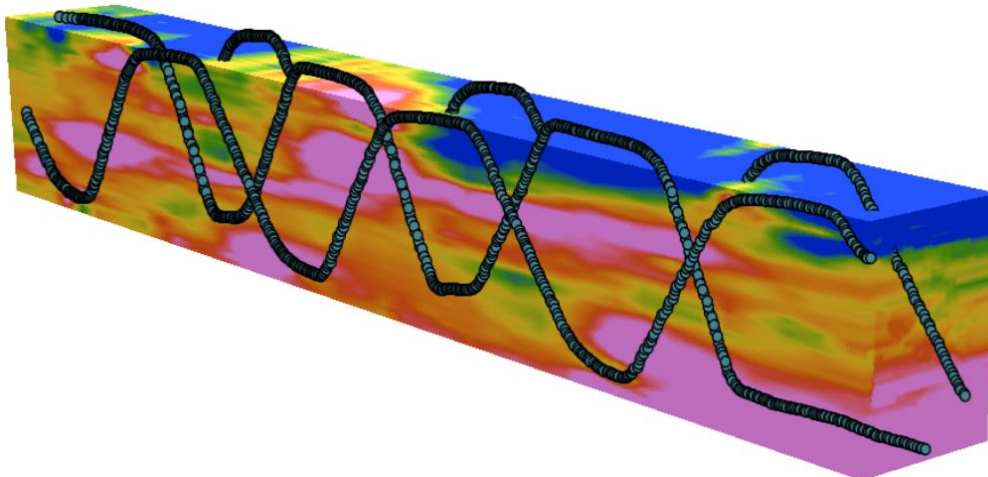


Figure 1.2.1: Three-Dimensional Data Model of fDOM collected with the Iver3 AUV. AUV track lines are shown in black.

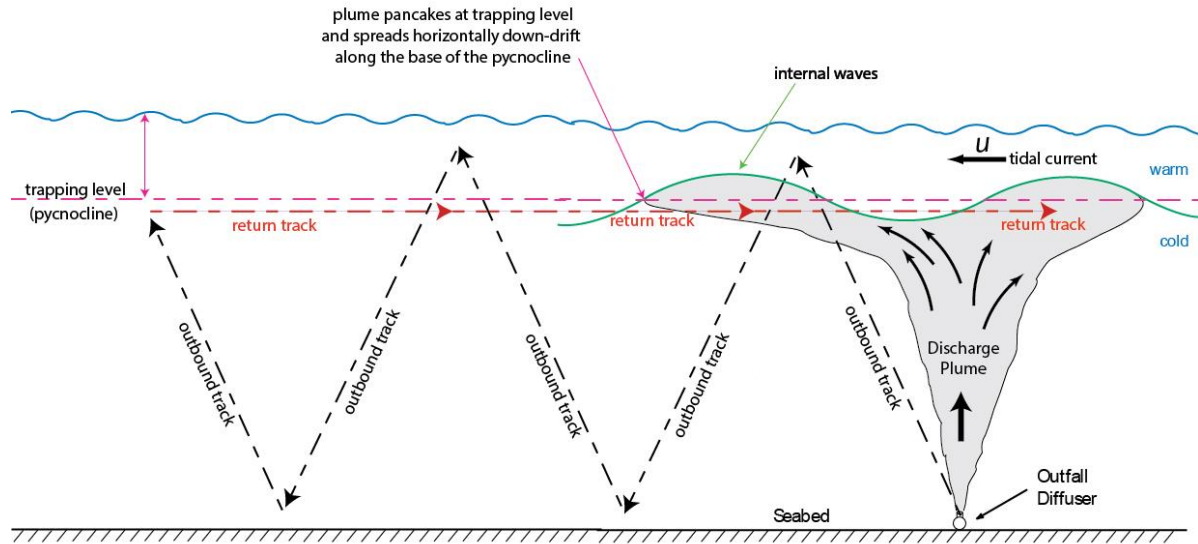


Figure 1.2.2: Schematic of AUV out and return legs along any given track line in the AUV survey pattern, in order to capture the vertical structure of the plume while maximizing transit time in regions of maximum horizontal spreading.

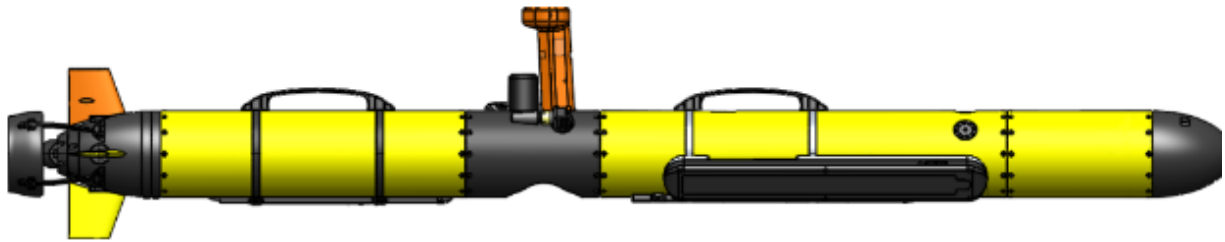


Figure 1.2.3: Iver3 Autonomous Underwater Vehicle (AUV)

Table 3: Iver3 AUV Specifications

Specification	Value
Manufacturer:	L3
Max Operating Depth:	200 meters
Diameter:	5.8 inches (15 cm)
Length:	86 inches (218 cm)
In-Air Weight:	85 pounds (39kg)
Speed:	2 to 3 knots
DVL bottom lock:	80 meters
Estimated Endurance:	5.5 hours at 2.5 knots

Table 4: Iver3 AUV Subsystems

Specification	Value
Internal Navigation System	iXBlue PHINS C3 fiber-optic gyro
Doppler Velocity Log	Teledyne RDI Explorer (600khz)
Depth Sensor:	200 meters
GPS:	WASS GPS
Sound Velocity Sensor:	AML
Acoustic Modem:	Teledyne Benthos
Radio Frequency:	2.4 GHz telemetry radio
Iridium	Tracking and status updates
Wi-Fi	Remote access
USB	USB 2.0 data download
Power	Lithium Ion Batteries – 780 Watt hours

Table 5: Iver3 AUV fDOM Sensor Specifications

Specification	Value
Manufacturer:	YSI / Xylem EXO fDOM Sensor
Sensor Type:	Optical, fluorescence
Range	0 – 300 ppb QSU
Sensitivity	0.01 ppb QSU
Limit	0.07 ppb QSU



Figure 1.2.4: Sea-Bird SBE 19plusV2 CTD and typical shipboard casting equipment



Figure 1.2.5: The 2 MHz Nortek ADCP with rigid mount for deployment from the R/V Benthic Cat.



Figure 1.2.6: Research Vessel (R/V) Benthic Cat (Source: Orca Maritime)

In addition to the offshore work, mixed discharge samples were collected on an hourly basis by autosamplers during the period of the offshore sampling. The autosamplers were provided and setup by the client. The fDOM concentrations of these samples were read using a Eureka Manta Sub3 hand-held analyzer (cf. [Figure 1.2.7](#)) to provide real-time effluent fDOM values to be utilized during the plume data analysis. SEJPA and City of Escondido discharge treated wastewater to the SEOO. SEJPA flows are treated at the San Elijo Water Reclamation Facility (SEWRF) and City of Escondido flows are treated at the City of Escondido Hale Avenue Resource Recovery Facility (HARRF). A common monitoring point exists at Cardiff Beach where the co-mingled wastewater from both the SEWRF and HARRF can be sampled, the onshore sampling location is an air release valve (ARV), located near Cardiff State Beach, as shown in [Figure 1.2.8](#). During the trial sample collection run, the ARV location did not produce water samples, and therefore SEJPA used a different location onsite at the SEWRF to collect samples for both the SEJPA effluent and City of Escondido effluent.

EWA discharges treated wastewater to the EOO from three facilities, including the Encina Water Pollution Control Facility (EWPCF), the Meadowlark Water Reclamation Plant, and the Carlsbad Water Reclamation Facility. A common monitoring point exists at the EWPCF (near the parking lot) where co-mingled wastewater from all three (3) facilities can be sampled, as shown in [Figure 1.2.9](#).



Figure 1.2.7: Eureka Handheld fDOM Probe with iPad data recorder for onshore sampling of the treated wastewater effluent prior to discharge and typical autosampler provided by EWA.



Figure 1.2.8: Onshore SEOO Sampling Site at Cardiff State Beach (not used) (Source: SEJPA)

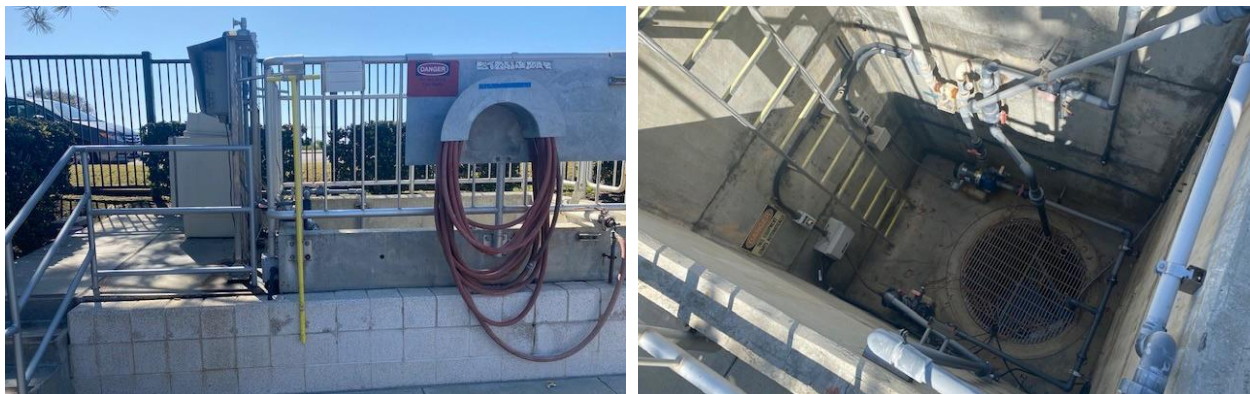


Figure 1.2.9: Onshore EOO Sampling Site at EWPCF (Source: EWA)

1.3 CDOM/FDOM CALIBRATION

A surrogate for CDOM is referred to as *fDOM*, which is the portion of CDOM that fluoresces and on average, makes up between 85% and 91% of the total CDOM in ocean waters, (cf. Cobble, 2007). Hence, *fDOM* concentrations are reasonably representative of CDOM concentrations., (cf. Cobble, 2007). Concentrations of *fDOM* are measured in parts per billion (ppb) of quinine sulfate, which, in acid solution, fluoresces similarly to colored dissolved organic matter.

The units of *fDOM* are quinine sulfate equivalent units (QSU) where 1 QSU = 1 ppb quinine sulfate. Thus, quinine sulfate is really an indirect surrogate for the desired *fDOM* concentrations. The EXO *fDOM* sensor carried by the Iver3 AUV shows virtually perfect linearity ($R^2=1.0000$) on serial dilution of a colorless solution of quinine sulfate. However, on serial dilution of stained water field samples, the sensor shows some under-linearity. The point of under-linearity in field samples varies and is affected by the UV absorbance of the dissolved organic matter in the water. Testing shows that under-linearity can occur at *fDOM* concentrations as low as 50 QSU. This factor means that a field sample with an *fDOM* reading of 140 QSU will contain significantly more than double the *fDOM* of a sample that reads 70 QSU. From our plume tracking experience at the EOO and the SEOO, excellent fidelity has been found between the *fDOM* sensor in the AUV which measures *fDOM* in QSU vs. the *fDOM* sensor in the Sea-bird SBE 19*plus*V2 CTD which measures *fDOM* in *relative fluorescence units* (RFU). **Figure 1.3.1** shows the two sensor types are well correlated by a second-degree polynomial which gives a coefficient of determination of R-squared = 0.9991. The polynomial in **Figure 1.3.1** was used to convert the Seabird SBE measurements in RFU *fDOM* units at the farfield monitoring stations to QSU *fDOM* units that were measured along the survey track lines by the AUV.

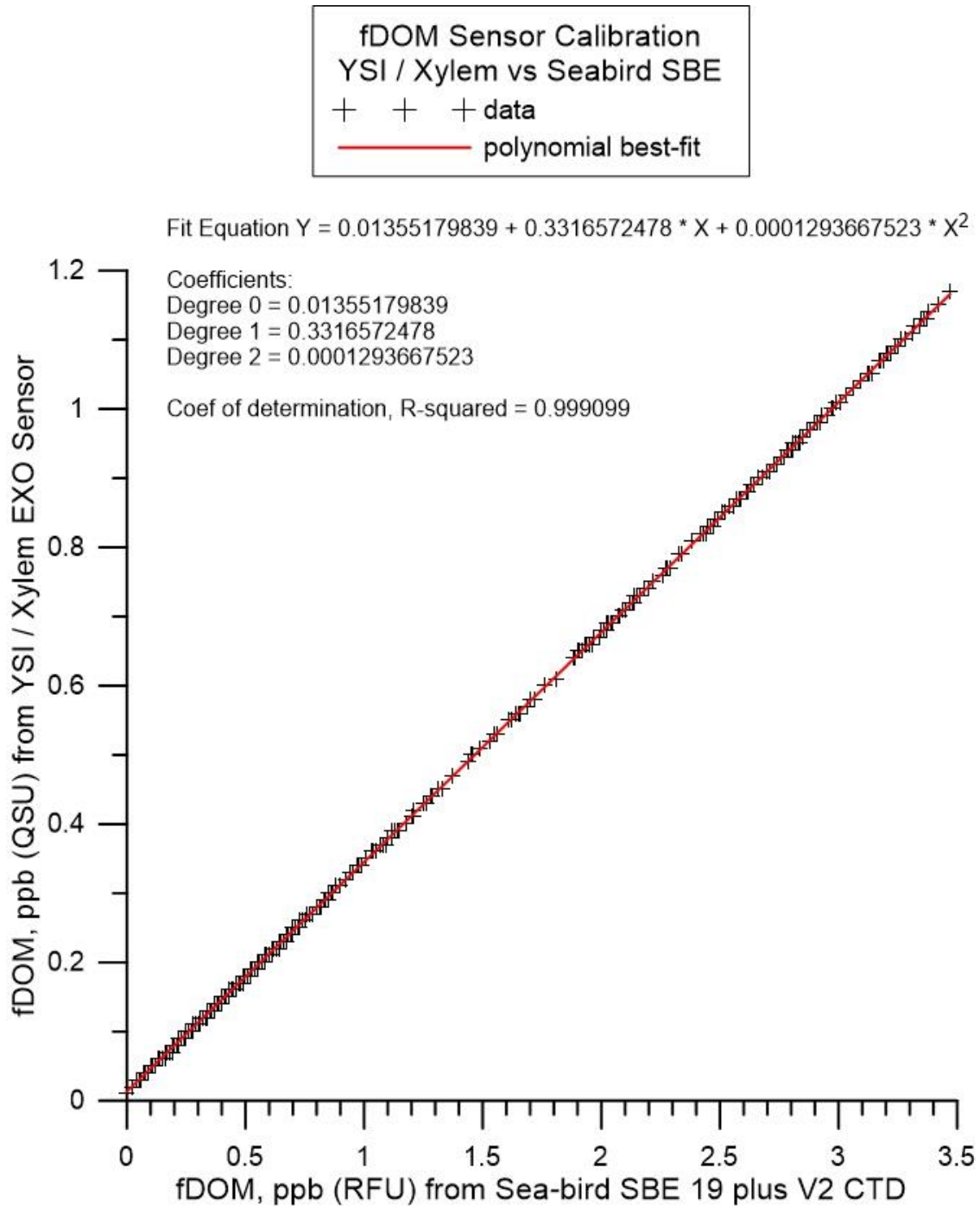


Figure 1.3.1: Correlation function between the YSI / Xylem EXO f/DOM sensor in the AUV which measures fDOM in QSU vs. the Sea-bird BE 19plusV2 CTD which measures fDOM in relative fluorescence units (RFU) at the stationary monitoring stations.

2 PLUME TRACKING RESULTS FOR ENCINA OCEAN OUTFALL (EOO)

During both the first and second deployments of the AUV at the EOO, the same basic strategy was used to fly the AUV along the track lines of the survey search pattern. The AUV is flown along a dolphin-style dive path when transiting outbound with the current along a given track line, i.e., a succession of yo-yo dive cycles, whereby the AUV dives and ascends through the water column between the seabed and an apex halfway between the sea surface and the pycnocline, as illustrated in [Figure 1.2.2](#). On the return legs of each track line, (against the current) the AUV is flown at a constant depth immediately beneath the pycnocline (trapping level) where the maximum horizontal dispersion of the plume is expected per [Figure 1.1.1](#), (cf. Baumgartner, 1994; Frick et al., 2003). The battery capacity of the Iver3 AUV limits the total distance traveled during any given ebb or flood tide survey to about 21 kilometers during a survey period of approximately 5 hours. The survey period is centered within each ebb or flood tide interval of 6.2 hrs. The AUV batteries are changed during the 1.2 hour interval around slack water between ebb and flood tide interval, allowing for AUV surveys of the EOO over a complete semi-diurnal tide cycle. The 15 stationary water column monitoring stations (shown as green circles in [Figure 2.1.1](#)) are distributed between the 160 ft and 60 ft depth contours around the EOO, and provide vertical profiles of salinity, temperature, and fDOM water mass properties immediately prior to and during the AUV surveys. Measurements from the control stations EOO-Ebb and EOO-Flood (shown as yellow and orange circles, respectively, in [Figure 2.1.1](#)) provide far-field measurements of natural background (ambient) water-mass properties (salinity, temperature, and fDOM). The measurements of the fDOM at the 15 stationary monitoring stations were in units of RFU which were converted to QSU fDOM units using the second order polynomial in [Figure 1.3.1](#). [Figure 2.1.1](#) also shows a group of blue triangles around the EOO diffuser, indicating the locations of the offshore regulatory discharge monitoring stations used for NPDES permit compliance determination.

2.1 FIRST EOO DEPLOYMENT - 21 SEPTEMBER 2021

The initial EOO deployment of 21 September 2022 addressed oceanic and outfall discharge conditions under typical fall conditions of strong stratification as shown in [Table 6](#).

Table 6: Summary of Comparison of SEOO and EOO Features

Deployment	Date	Conditions to Be Assessed
1st:	September 2021	Typical Conditions: Fall conditions of maximum or near-maximum stratification
2nd:	December 2021	Atypical Conditions: Post-storm conditions with higher-than-average outfall discharge flows and runoff
3rd	March 2022	Typical Conditions: Spring conditions where strong pycnocline is absent

These highly stratified conditions also typically coincide with periods of high recycled water demands, which result in discharge flows that are lower than the annual average. During the 21 September 2021 deployment, the AUV was flown along five (5) track lines around the EOO outfall diffuser within survey boxes shown in [Figure 2.1.1](#). Two separate survey boxes were flown, one during ebb tide as diagramed in yellow in [Figure 2.1.1](#), the other flown during flood tide as diagramed in orange in [Figure 2.1.1](#). The track lines surveyed on ebb tide are shown in [Figure 2.1.8](#) as actually flown by the AUV, while those track lines as flown on flood tide appear in [Figure 2.1.15](#). The track lines were biased in the down current direction,

with 1500 m long tracks flown south of the outfall with the southward flowing current on an ebbing tide, as indicated by the yellow survey box in [Figure 2.1.1](#). Track lines extended 500 m north of the outfall during ebb tide. On flood tide, the tidal current direction reverses and flows toward the north. Hence the track lines were biased northward with the flood tide current direction, so that 1500 m long tracks extended north of the outfall and 500 m south of the outfall. The total dimension of the AUV surveyed area on either ebb or flood tide was 2000 m in the along shore direction and 1000 m in the cross-shore direction. Thus, the total area surveyed during both ebb and flood tide is approximately 988.4 acres. Note the natural background (ambient) water-mass properties of salinity, temperature, and fDOM were obtained by CTD casts at the far-field monitoring stations EOO-Ebb and EOO-Flood, indicated by the yellow dots and orange dots, respectively, in [Figure 2.1.1](#). These far-field measurements were performed twice during each ebb or flood tide survey of the EOO, one at the beginning of the AUV surveys and the other at the completion of each AUV survey.

The vertical ascent of the EOO outfall plume is typically arrested at the pycnocline (thermocline) interface, (referred to as the trapping level), where it then spreads out laterally along the pycnocline interface as illustrated in [Figure 1.1.1](#). Lateral spreading of the plume can be augmented by the mass transport caused by the tidal currents that flow toward the north on a flood tide and to the south on an ebbing tide; and by internal waves which propagate along the pycnocline interface, (propagating shoreward on a rising tide and seaward on a falling tide). Immediately after completion of initial dilution, the plume will laterally spread along the pycnocline interface, augmented by advection from tidal currents and internal waves. Immediately upon completion of initial dilution, the outfall plume will make its greatest excursions (beyond the ZID) directly beneath the pycnocline, (cf. [Figure 1.1.1](#)). Therefore, it was critical to the plume tracking effort to program the AUV to fly directly beneath the pycnocline during the return leg (against the current) along each track line, as shown in [Figure 1.2.2](#). To locate the depth of the pycnocline, the CTD casts were performed prior to the AUV survey on 19 September 2021 and quickly processed to determine the salinity changes and temperature changes with depth, (cf. [Figure 2.1.2](#)). These CTD data indicated the water column was strongly stratified, forming a two-layer water mass with a well-defined pycnocline at 8 m depth (-26.2 ft. MSL), per [Figure 2.1.2](#). Based on this finding, the AUV was programed on its outbound dolphin- style legs (with the current) for dive cycle apex points set above the pycnocline at a depth of 4m depth (-13.1 ft. MSL) and dive cycle bottoming points set at 2 m (-6.6 ft) above the seabed. The Iver3 AUV uses its bottom-locking sonar to determine the distance above the local seabed at any location within the survey box. Along the return leg of each track line (flown against the current), the AUV was programmed to fly at a constant depth of 9 m depth (-29.5 ft. MSL).

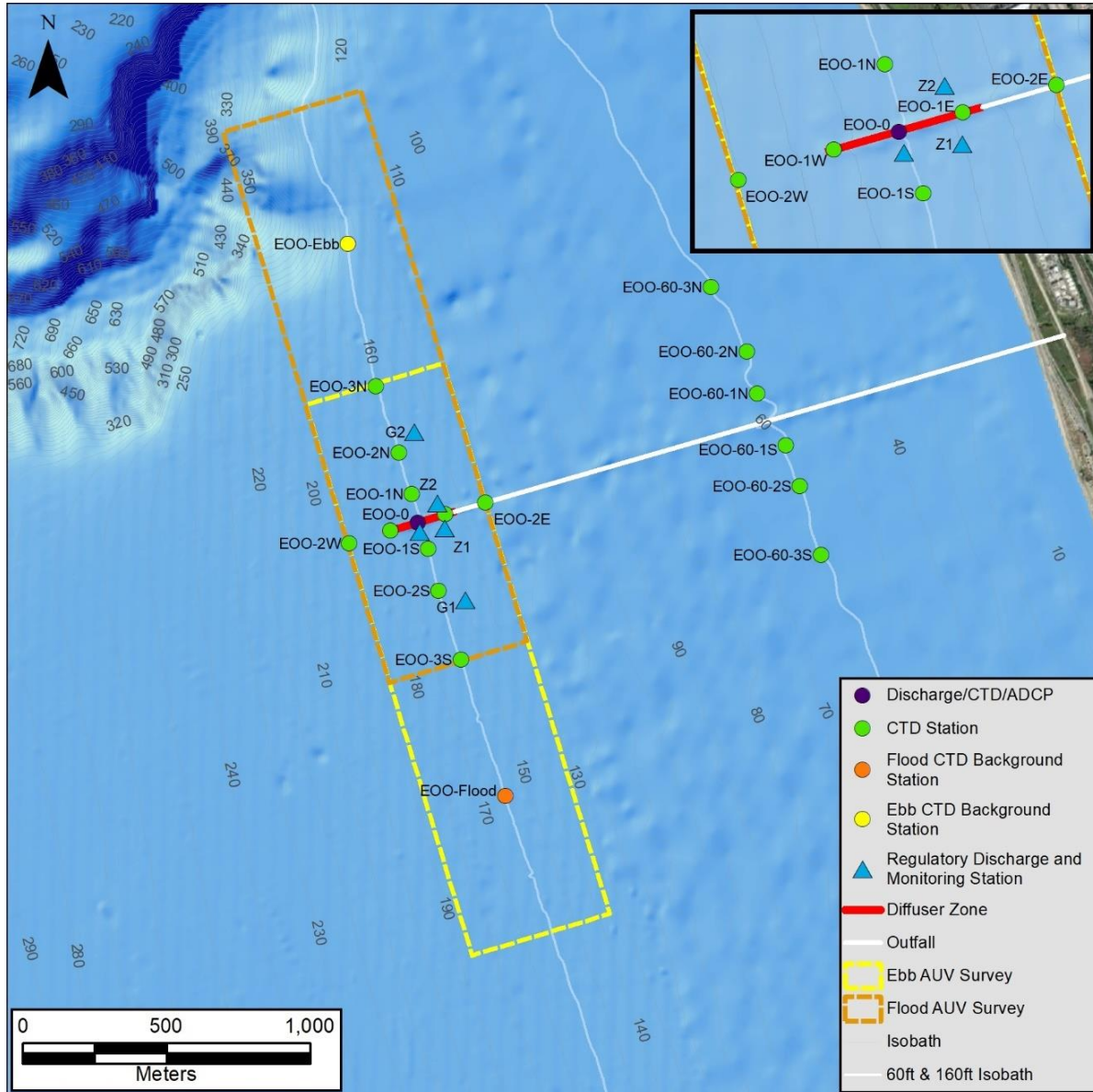


Figure 2.1.1: EOO Survey boxes and sampling stations for the first AUV deployment, 21 September 2021

At the time of the ebb tide AUV survey on 21 September 2021, the EOO was discharging 24.17 mgd of wastewater having an average discharge salinity of 0.85 psu and an average fDOM discharge concentration of 248.71 ppb (QSU), based on shoreside monitoring of the EOO effluent, (see tabulations of EOO shoreside monitoring data in Appendix-A). Later in the day during flood tide, the EOO discharge rates increased slightly to 26.318 mgd, while average discharge salinity and fDOM concentrations remained unchanged, (cf. Appendix-A). Assuming that receiving water fDOM concentrations are homogeneous, the average EOO discharge concentrations of fDOM are significantly higher (by more than 2 orders of magnitude) than the natural ocean background concentrations of fDOM measured at far-field control stations, EOO-Ebb and EOO-Flood. Vertical profiles of natural background fDOM measured during ebb tide at EOO-Ebb (cf. Figure 2.1.3) exhibited depth-averaged concentrations ranging between 0.636 ppb and 0.639 ppb. Natural background fDOM measured later during flood tide on 21 September 2021 at

EOO-Flood (cf. **Figure 2.1.4**) produced depth-averaged concentrations ranging between 0.578 ppb and 0.582 ppb. Consequently, the signal to noise ratio of the fDOM plume observable at any point of discharge along the EOO diffuser ranges between $SNR_{fDOM} = 388.2$ and $SNR_{fDOM} = 429.3$, based on the depth averaged concentrations of natural background fDOM measured at far-field control stations, EOO-Ebb and EOO-Flood (**Figure 2.1.3** and **Figure 2.1.4**), applied to equation (1). While profiles of natural background fDOM concentrations measured during both ebb and flood tide showed both random variations (noise) with some general vertical structure (with higher concentration near the bottom, declining near the surface), the standard deviations around the depth averaged fDOM concentrations were small, ranging between $\sigma = 0.11$ ppb and $\sigma = 0.16$ ppb, (cf. **Figure 2.1.3** and **Figure 2.1.4**).

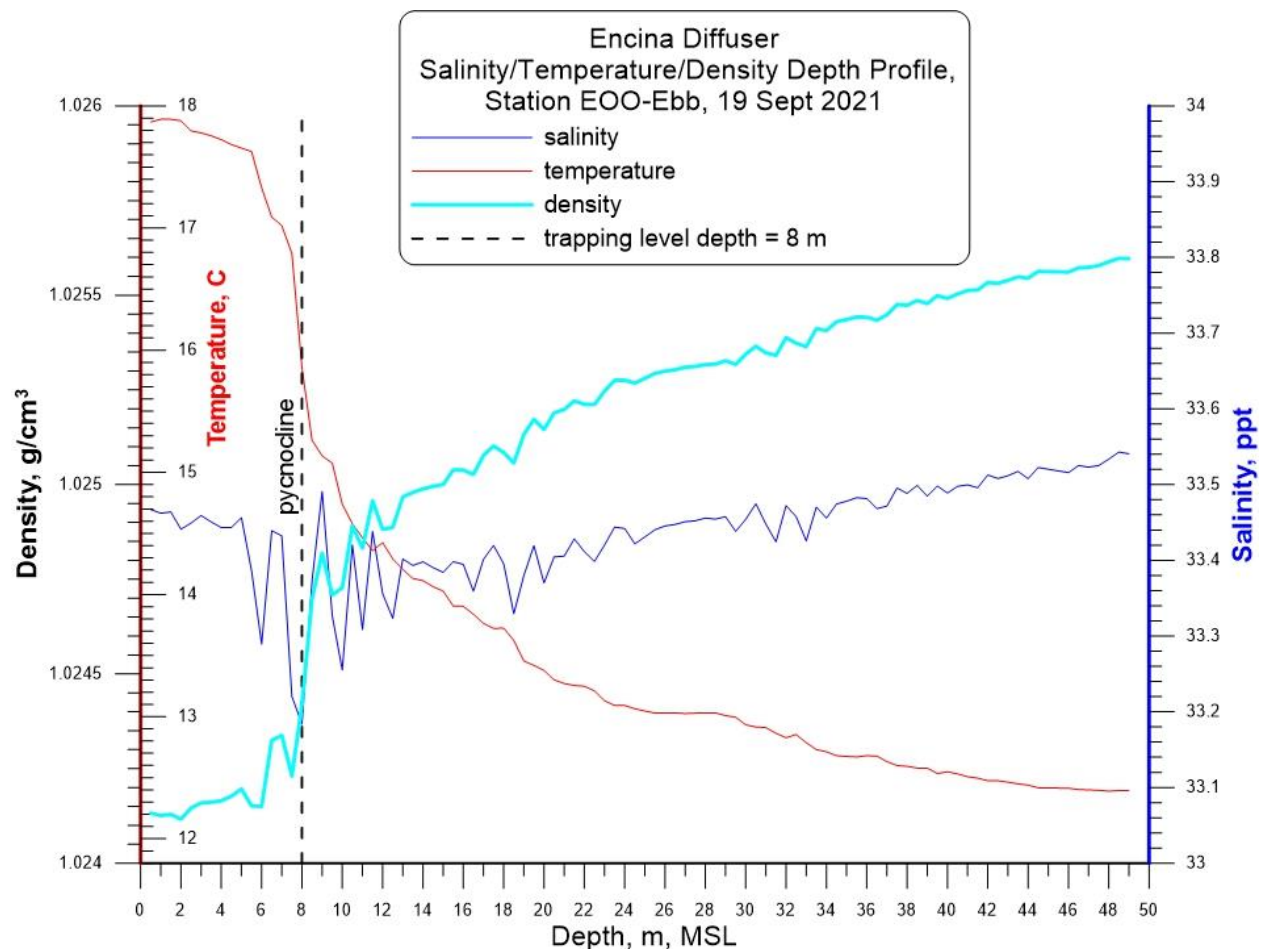


Figure 2.1.2: Salinity/Temperature/Density depth profiles derived from CTD casts on 19 September 2021 at Station EOO-Ebb, prior to the AUV survey of the plume dispersion from EOO on 21 September 2021 during ebb tide.

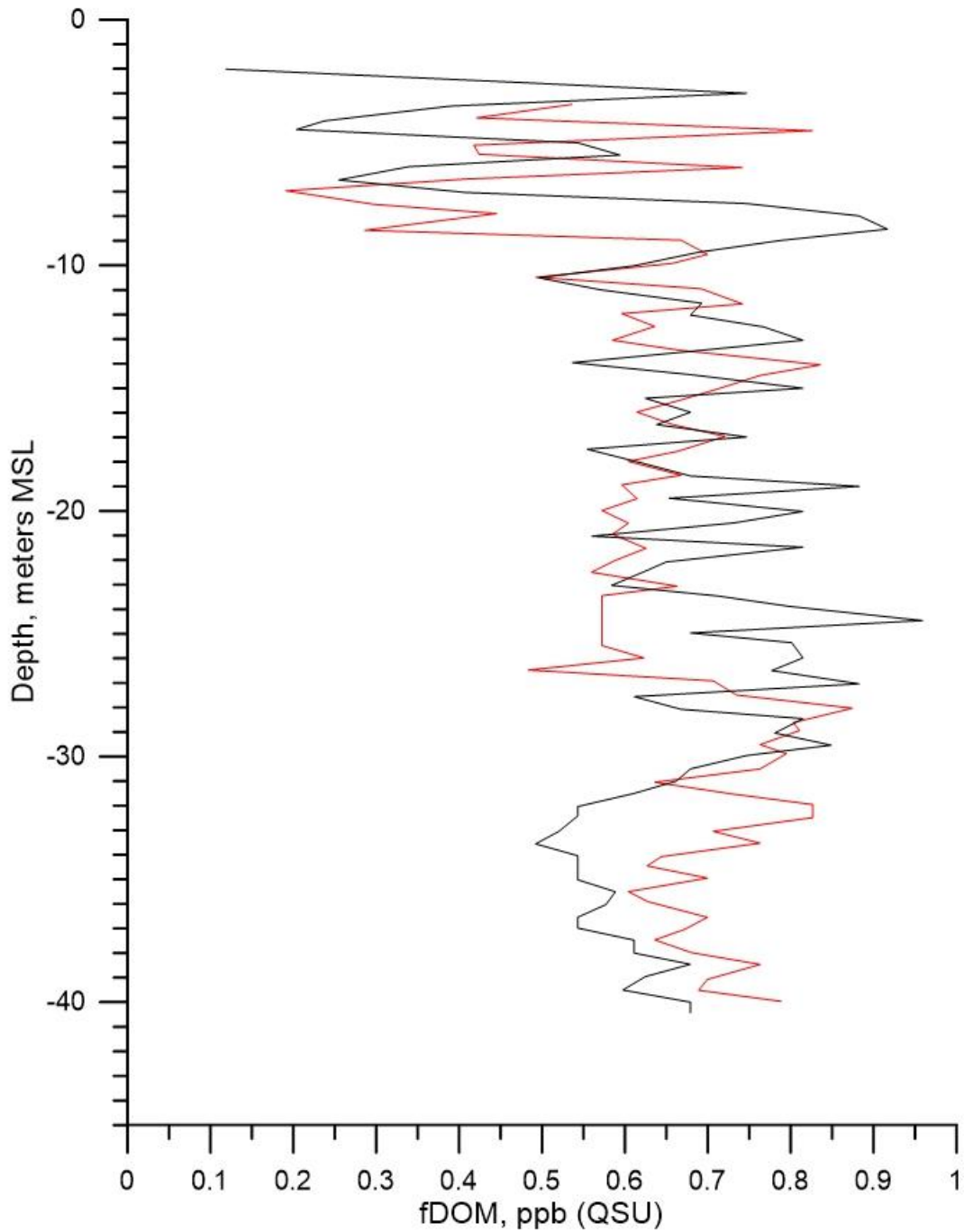
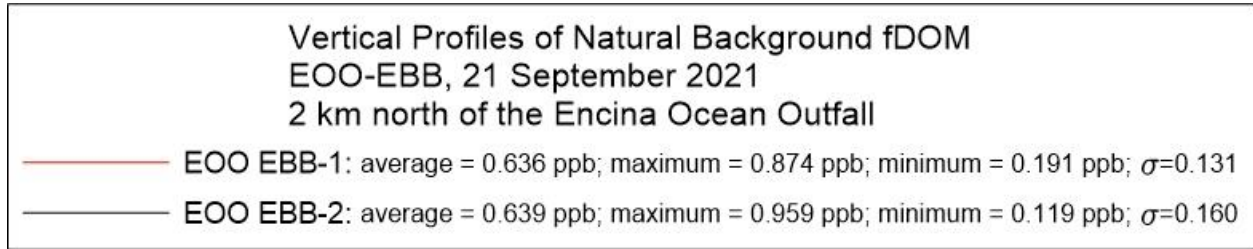


Figure 2.1.3: Vertical profiles of natural background fDOM concentrations measured during the first deployment at the far-field ebb tide monitoring station "EOO-EBB," located 2 kilometers northwest of EOO along the -160 ft. MLLW depth contour, cf. yellow dot in Figure 2.1.1.

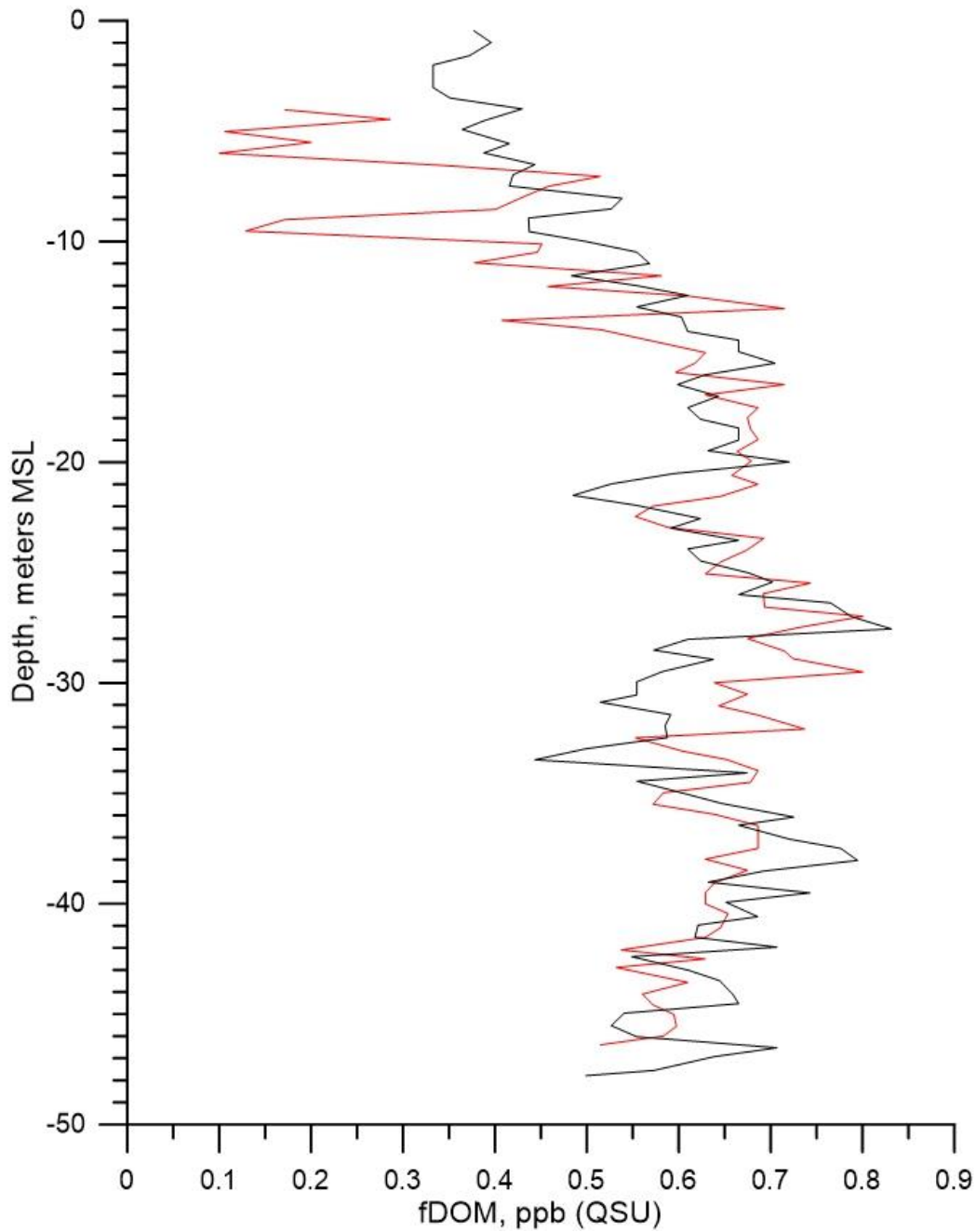
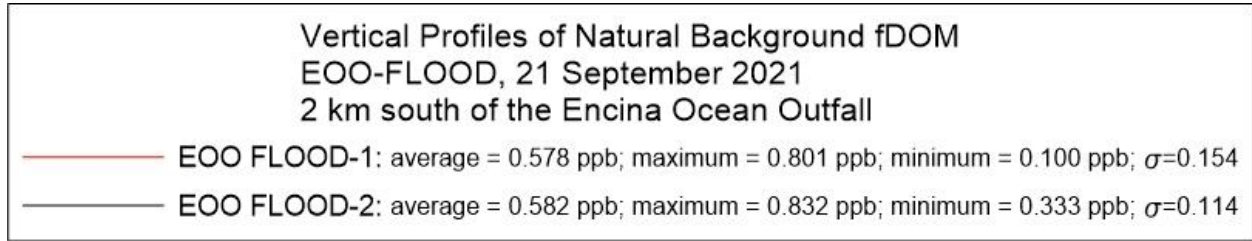


Figure 2.1.4: Vertical profiles of natural background fDOM concentrations measured during the first deployment at the far-field flood tide monitoring station “EOO-Flood,” located 2 km southeast of EOO along the -160 ft. MLLW depth contour, cf. orange dot in Figure 2.1.1.

Mean ebb tide currents on 21 September 2021 at the far-field control station, EOO-Ebb, were 0.288 m/s (0.56 kts) toward the southeast, based on ADCP readings at far field monitoring station, EOO-Ebb, (cf. [Figure 2.1.5](#)) located up-drift of the yellow AUV survey box shown in [Figure 2.1.1](#). These mean currents convey a net shore-parallel drift of the EOO discharge plume. However, there are other transient short-lived current oscillations reaching 0.809 m/s (1.57 kts) in the ebb tide ADCP time series record on 21 September 2021. The current direction data in the ADCP record indicates these spikes of higher oscillatory currents were directed cross-shore, indicating they were due to shoaling internal waves. Because of the oscillatory nature of these current spikes, they produce no net drift of the EOO discharge plume, but merely serve to smear the plume or break off pieces from the main body of the plume and smear or disperse those pieces in the cross-shore direction. ADCP measurements of currents at far field monitoring station, EOO-Flood, (cf. [Figure 2.1.6](#)) find that mean flood tide currents on 21 September 2021 were slightly less than the mean ebb tide currents, reaching only 0.265 m/s (0.52 kts) directed toward the northwest. This is due to the fact that tidal currents along the coastline of the lower Southern California Bight do not reverse symmetrically between ebb and flood tide, but rather are *ebb-tide dominant*, imparting a net southeasterly drift to the EOO discharge plume over a complete tidal day of 24.83 hours. Transient oscillatory current spikes in the flood tide ADCP current record on 21 September 2021 reached 0.905 m/s (1.76 kts) in the cross-shore direction, again indicating the presence of internal wave activity. These internal waves are excited by the extreme bathymetric depression of the head of the Carlsbad Submarine Canyon, (cf. [Figure 2.1.7](#)). The Carlsbad Submarine Canyon encroaches on the northern end of the EOO flood tide survey box. As tidal currents flow across the Carlsbad Submarine Canyon, this bathymetric depression excites internal waves that radiate outward from the canyon much like lee waves do in the atmosphere when storm winds blow over canyons and mountainous topography. The cross-shore oscillations of the internal waves that radiate from the Carlsbad Submarine Canyon produce the high current spikes in the ADCP records on 21 September 2021 (cf. [Figure 2.1.5](#) and [Figure 2.1.6](#)).

[Figure 2.1.8](#) reveals accurate repeatability of the outbound and return legs along each of the five track lines as flown by the AUV during ebb tide surveys of the EOO on 21 September 2021. During this survey, the AUV collected 68,644 separate measurements of salinity and fDOM. Originally, 29,605 measurements of fDOM taken along the return legs of each of the 5 track lines at a constant depth of 9 m depth (-29.5 ft. MSL) were parsed from the original 68,644 measurements to create a map of fDOM just below the pycnocline (trapping layer, as shown in [Figure 2.1.9](#)).

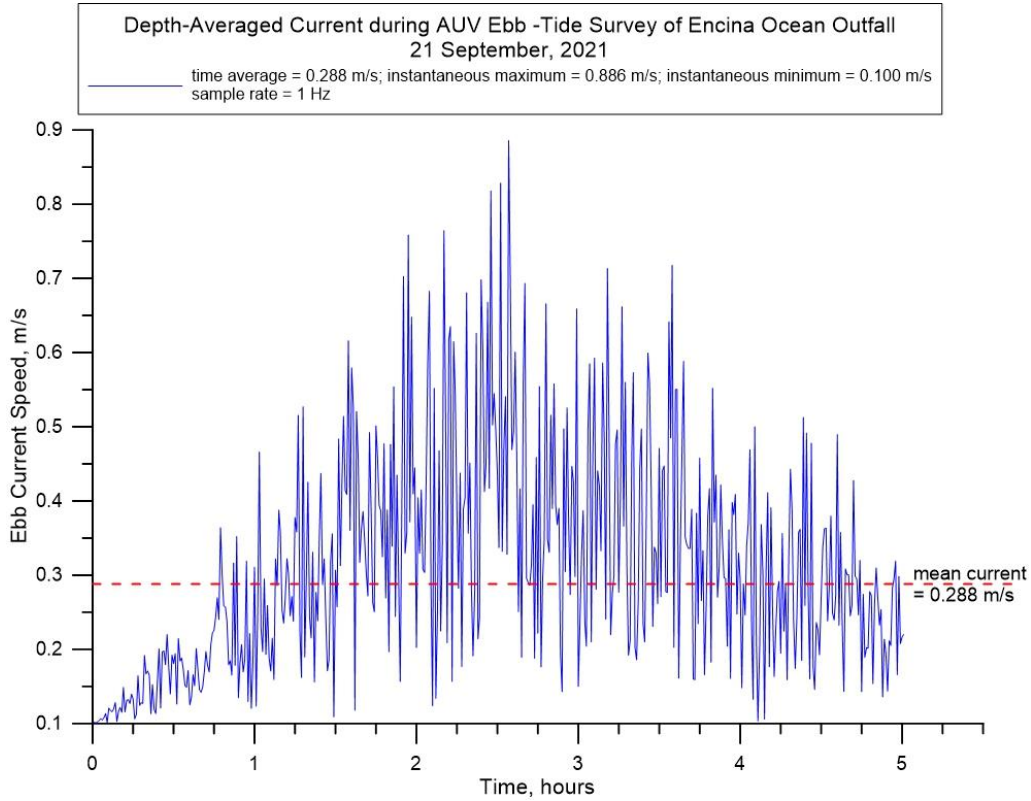


Figure 2.1.5: Time series of depth averaged current derived from ADCP measurements at EOO during ebb-tide AUV survey on 21 September 2021.

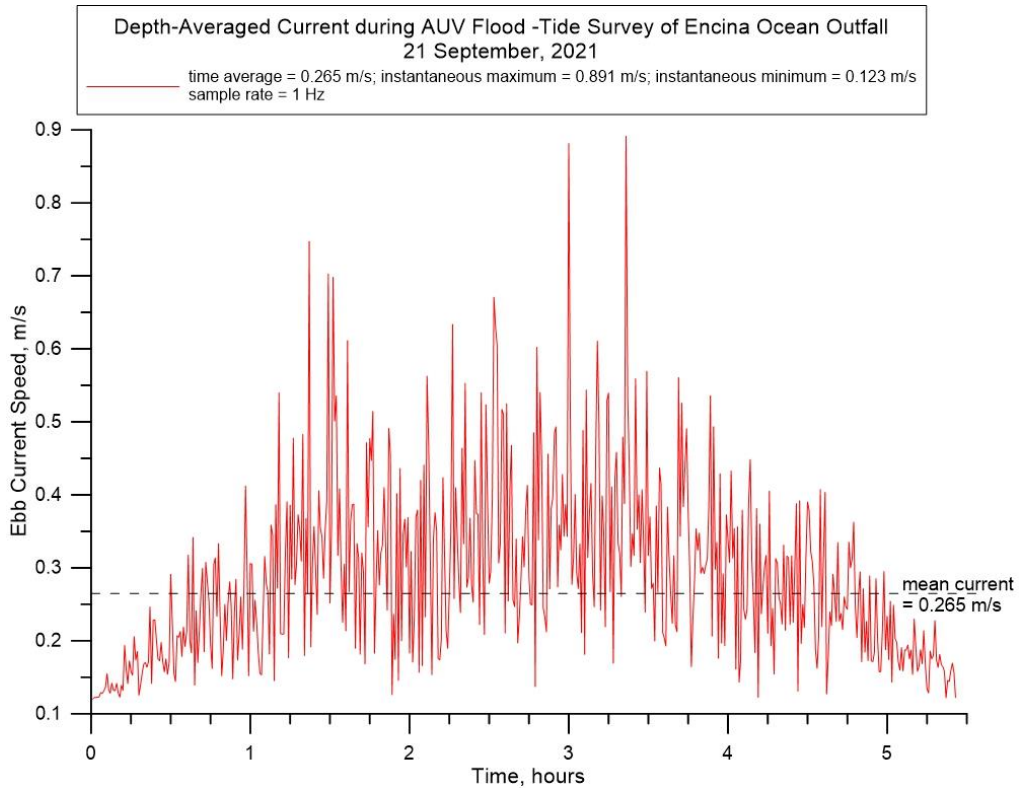


Figure 2.1.6: Time series of depth averaged current derived from ADCP measurements at EOO during flood-tide AUV survey on 21 September 2021.

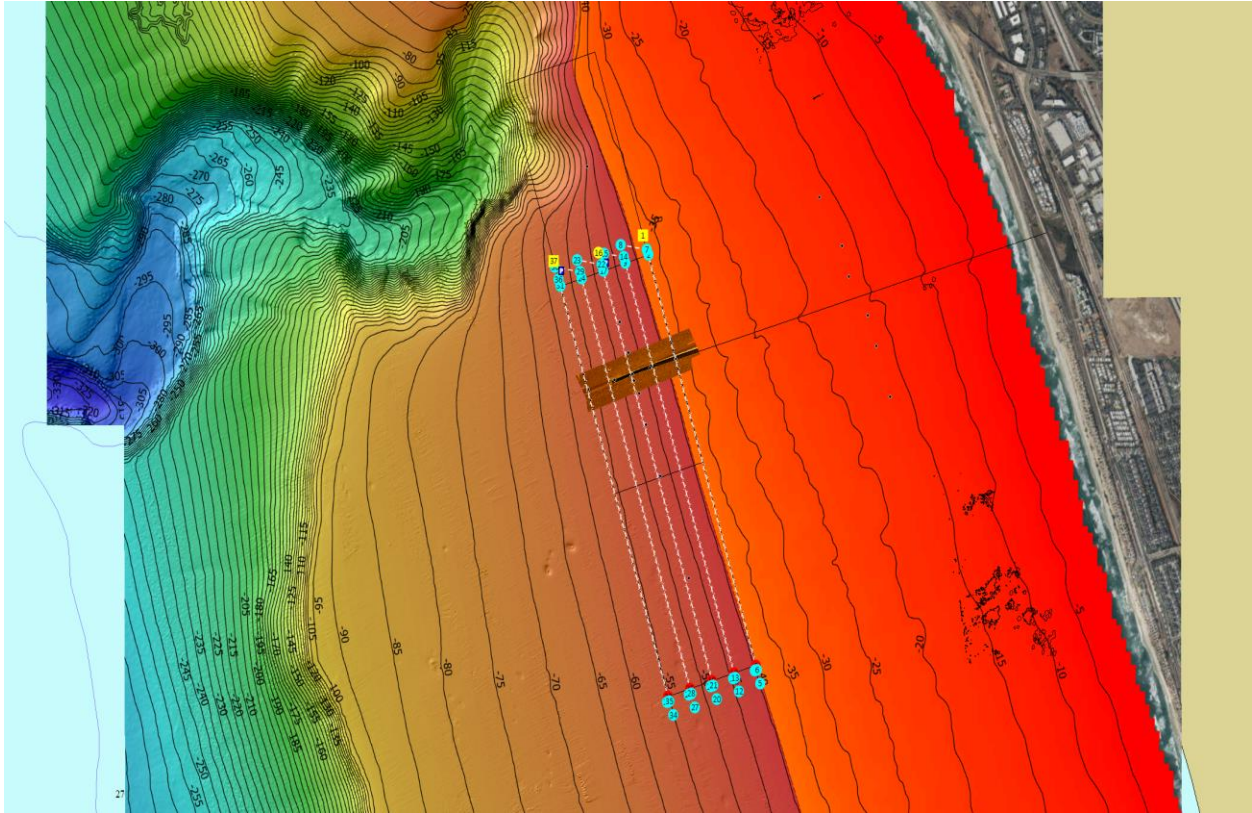


Figure 2.1.7: Bathymetric contour map overlaid onto the EOO survey boxes (solid black lines) and the EOO ebb-tide AUV survey track lines (dotted white lines). Note the extreme bathymetric depression of the head of the Carlsbad Submarine Canyon that encroaches on the northern end of the EOO flood tide survey box. As tidal currents flow across the Carlsbad Submarine Canyon, this bathymetric depression excites internal waves whose cross-shore oscillations produce the high current spikes in the ADCP records on 21 September 2021 (cf. [Figure 2.1.5](#) and [Figure 2.1.6](#)).

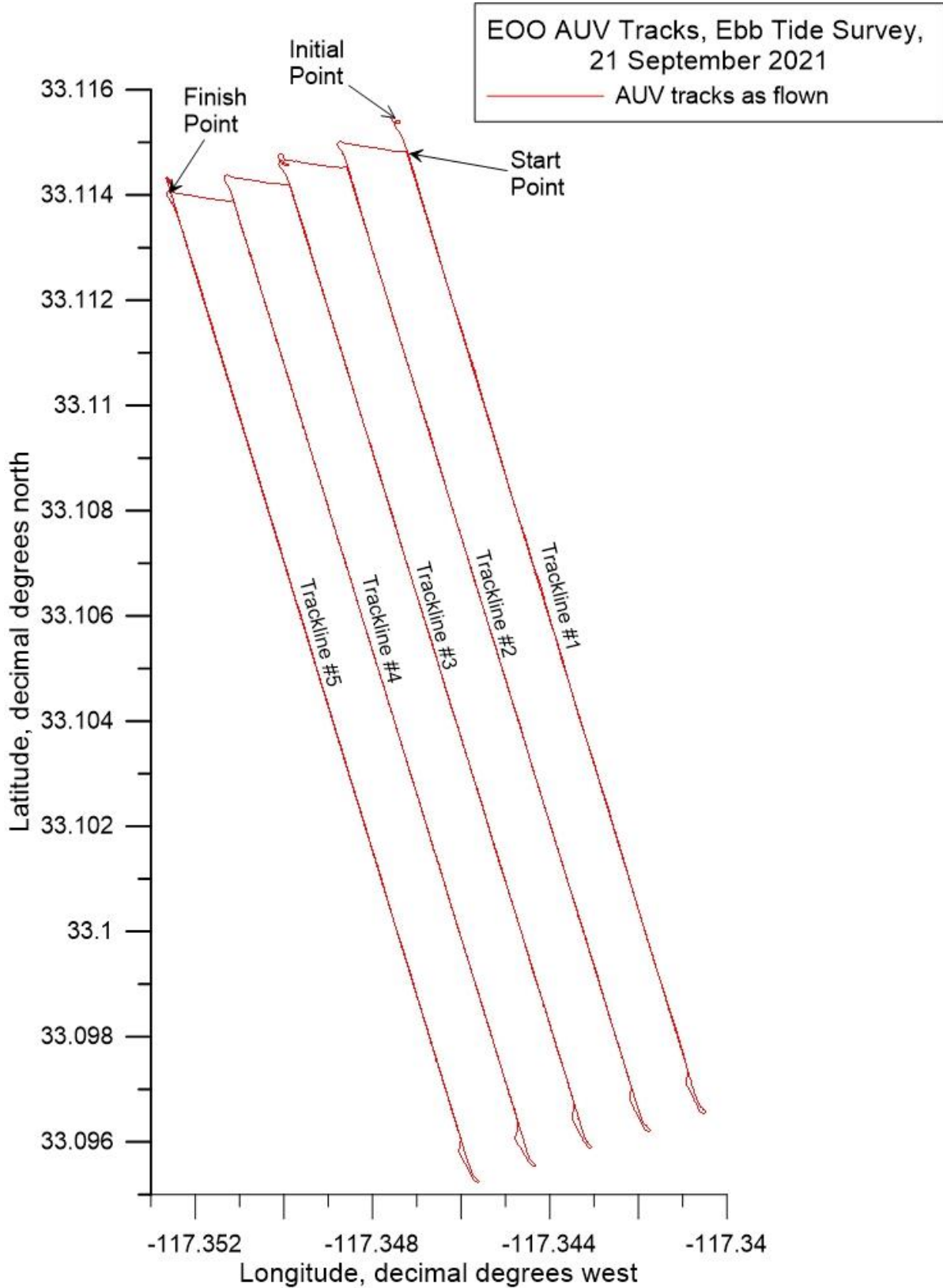


Figure 2.1.8: AUV track lines as flown during ebb tide surveys of the discharge plume from EOO during the first deployment, 21 September 2021. The total dimension of the AUV surveyed area on ebb tide was 2000 m in the along shore direction and 1000 m in the cross-shore direction or a total surveyed area of approximately 494.3 acres. Note, at 30° N latitude, 1° longitude = 93,453.2 m, while 1° latitude = 110,904.4 m.

Dispersion of fDOM at the Trapping Level, (depth = - 8m MSL)
 Encina Ocean Outfall, Ebb Tide, 21 September 2021
 average discharge concentration end-of-pipe = 248.7 ppb

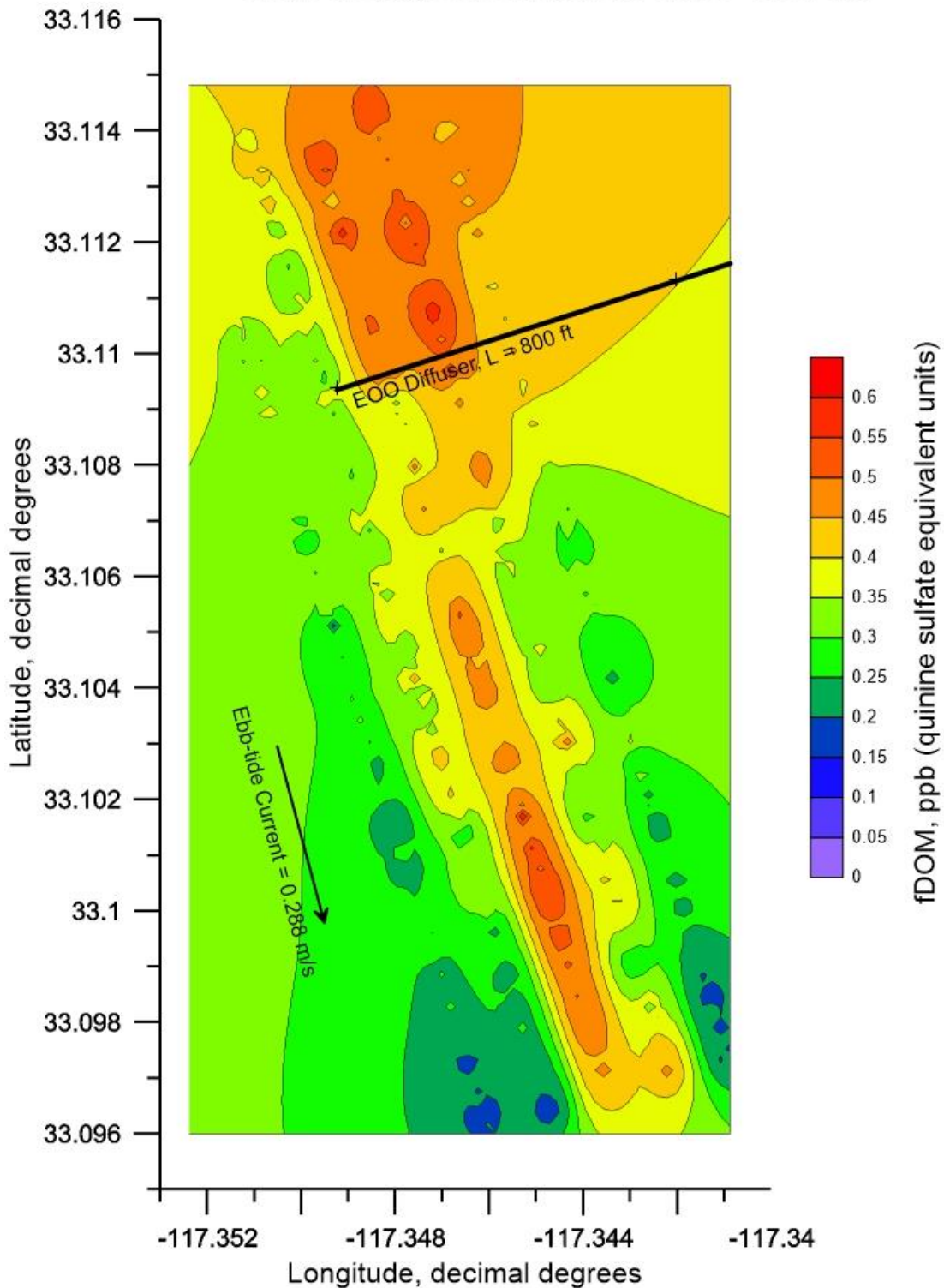


Figure 2.1.9: Contour plot of AUV measurements of fDOM at the trapping level during ebb tide surveys of the discharge plume from EOO. EOO discharge rate = 24.17 mgd; End-of-pipe discharge concentration of fDOM = 248.71 ppb (QSU); End of pipe discharge salinity = 0.85 psu; Trapping level (pycnocline depth) = 26.24 ft MSL; Mean ebb tide current = 0.288 m/s (0.56 kts) toward the southeast.

It was anticipated that such a map would capture the maximum dispersion of the EOO discharge plume since the State Water Board approved dilution models (CORMIX v-11, Visual Plumes UM3 and Plumes 20 UM3) all show that discharge trajectories reach maximum horizontal excursions at or near the trapping level, (cf. Frick et al., 2010). Unfortunately, the highest concentrations of fDOM found anywhere along the trapping level in [Figure 2.1.9](#) only reach $fDOM_{(x)} = 0.65$ ppb, only slightly greater than the depth averaged natural background fDOM concentration of $fDOM_{\infty} = 0.639$ ppb measured at the far-field control station, EOO-Ebb, (cf. [Figure 2.1.3](#)). Inserting these values into equation (1), the largest signal to noise ratio of any feature in the fDOM map along the trapping level in [Figure 2.1.9](#) is only $SNR_{fDOM} = 0.017$. This SNR result is significantly beneath even the lowest order significance threshold for detection that requires $SNR_{fDOM} \geq 1$. Therefore, nothing can be concluded about any fDOM feature along the trapping level in [Figure 2.1.9](#).

To explore possible reasons for the failure to discover evidence of the EOO plume at the trapping level during ebb tide, a calibrated computational fluid dynamics (CFD) simulation was prepared using the AUV measurements of fDOM along the track line #3 (cf. [Figure 2.1.8](#)) to examine vertical dispersion of the plume through the water column. The calibrated CFD simulation in [Figure 2.1.10](#) indicates that the EOO plume drifts a significant distance horizontally near the seabed in the 0.288 m/s (0.56 kts) ebb current, before it rises and pancakes on the base of the trapping layer. As the plume drifts horizontally with the ebb currents, it undergoes significant dilution before rising to the trapping level. As a result, fDOM concentrations at the trapping level are no more than $fDOM_{(x)} = 0.634$ ppb. [Figure 2.1.3](#) indicates that natural background concentrations of fDOM at the trapping level (8 m depth) during ebb tide are $fDOM_{\infty} = 0.55$ ppb. Therefore, the signal to noise ratio of the fDOM at the trapping level in this CFD simulation was found to be only $SNR_{fDOM} = 0.15$, again below the lowest order significance threshold for detection (i.e., $SNR_{fDOM} \geq 1$). From this result, it was concluded that the strongly stratified water column portrayed in the temperature/salinity profiles in [Figure 2.1.2](#) retarded the immediate upward movement of the EOO plume. The plume, however, underwent sufficient dilution while it drifted horizontally in the ebb current to allow fDOM concentrations to drop below the significance threshold detection limit by the time the plume fully rose to the trapping level. Consequently, an alternative method was developed for mapping fDOM data from the AUV surveys of the EOO.

The new fDOM mapping method involved displaying all 68,644 fDOM measurements simultaneously across all depths, including even those measured along the cross-shore tracks that connect with each of the 5 survey track lines, (cf. [Figure 2.1.8](#)). It was anticipated that detectable portions of the EOO plume could be found at certain depths and locations beneath the trapping level. [Figure 2.1.11](#) employs the new fDOM mapping technique with a full depth contour plot of AUV measurements of fDOM during ebb tide surveys of the EOO on 21 September 2021. These types of plots are referred to as *heat maps* in signal detection theory, (Schonhoff & Giordano, 2006). Inspection of [Figure 2.1.11](#) reveals that variations in fDOM concentrations across all depths surveyed by the AUV range from 0.2 ppb to 1.6 ppb. However, these fDOM variations exhibit horizontal structure, being arranged in a repeated banding pattern that does not appear to be spatially coherent with the alignment of the EOO pipeline and diffuser but appears to align with the 5 track lines in the ebb tide survey pattern, (cf. [Figure 2.1.8](#)).

It is likely that the repeated banding patterns in the fDOM heat map in **Figure 2.1.11** is a result of insufficient spatial resolution in fDOM sampling between the track lines, referred to as *spatial aliasing*, (Peterson, et al, 1954). The mechanism producing the blue bands in the fDOM heat map result from the AUV measurements near the apex of the dolphin style dive cycles, when the AUV is in the shallow water above the trapping layer where ambient fDOM concentrations are lower (**Figure 2.1.3**). Yellow, orange and red banding features in the fDOM heat map could be remnants of the EOO plume at deeper depths along each track line. To sort out potential plume remnants from among the highly variable and banded fDOM measurements, the fDOM heat map in **Figure 2.1.11** is converted into a signal to noise ratio heat map in **Figure 2.1.12** by invoking equation (1) to convert the fDOM concentrations in **Figure 2.1.11** into corresponding SNR_{fDOM} patterns. Since only fDOM features having signal to noise ratios of unity or greater are possible remnants of the plume, **Figure 2.1.12** has been scaled to filter out features having $SNR_{fDOM} < 0.8$, where features having $0.8 \leq SNR_{fDOM} < 1.0$ are potentially diluted fragments or diluted outer edges of a plume remnants. Inspection of **Figure 2.1.12** reveals that two small potential plume remnants having $1.0 \leq SNR_{fDOM} \leq 1.5$ are found 192 m to 588 m downstream of the EOO diffuser, while several other more diluted fragments having $0.8 \leq SNR_{fDOM} < 1.0$ are found further downstream. Therefore, at least two of the elevated (yellow, orange or red) features in the fDOM heat map in **Figure 2.1.11** can be regarded as remnants of the EOO ebb-tide plume. To verify this conclusion, the SNR_{fDOM} heat map in **Figure 2.1.12** was transposed into a dilution heat map in **Figure 2.1.13** using equation (2) under the assumption that the initial fDOM discharge concentration is $fDOM_{(x=0)} = 248.17$ ppb. From that assumption, **Figure 2.1.13** indicates that the dilution factor (D_{fDOM}) for the fDOM features in **Figure 2.1.11** would range from as little as 260:1 within 192 m of the EOO diffuser to as high as 10,000:1 to 45,000:1 further downstream, where any regulated or unregulated toxic EOO effluent constituents would be well below quantifiable detection limits.

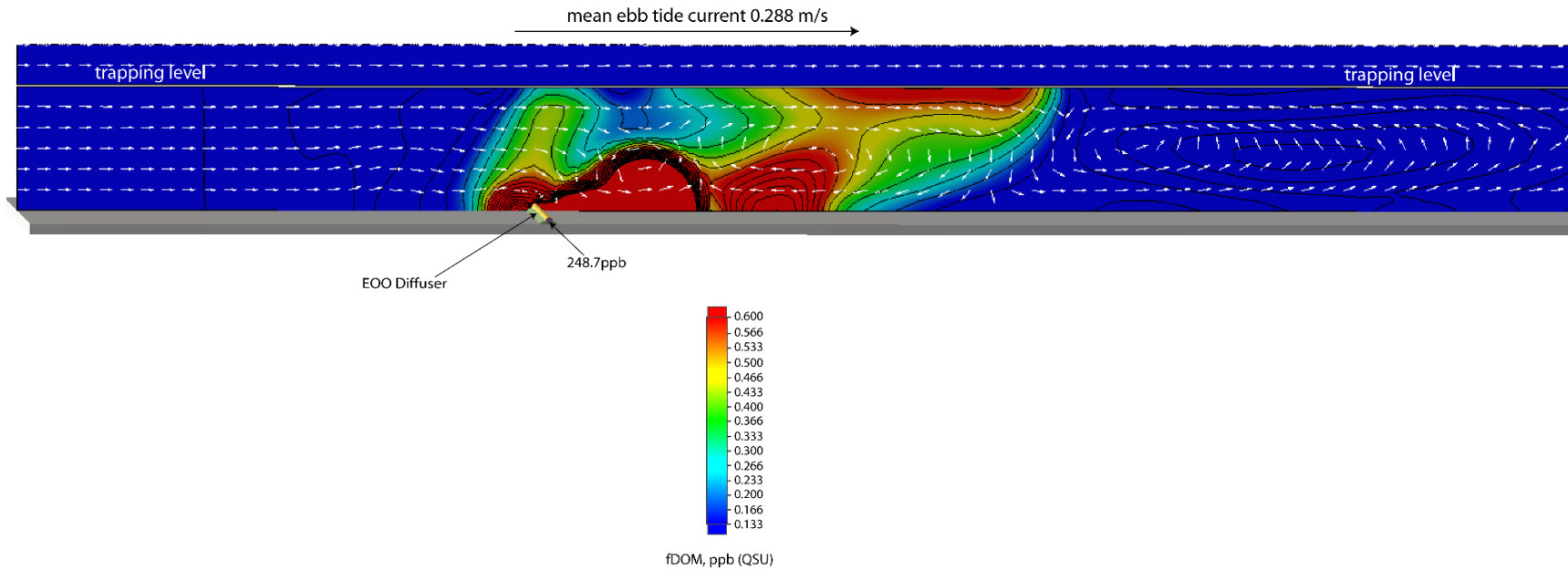


Figure 2.1.10: Calibrated CFD simulation of the plume dispersion through the water column from EOO. CFD simulation calibrated to AUV measurements of fDOM along the track line #3 during ebb tide on 21 September 2021. CFD simulation based on EOO discharge rate = 26.318 mgd; End-of-pipe discharge concentration of $fDOM_{(x=0)} = 248.71$ ppb (QSU); Trapping level (pycnocline depth) = 26.24 ft MSL; Mean ebb tide current = 0.288 m/s (0.56 kts) toward the southeast.

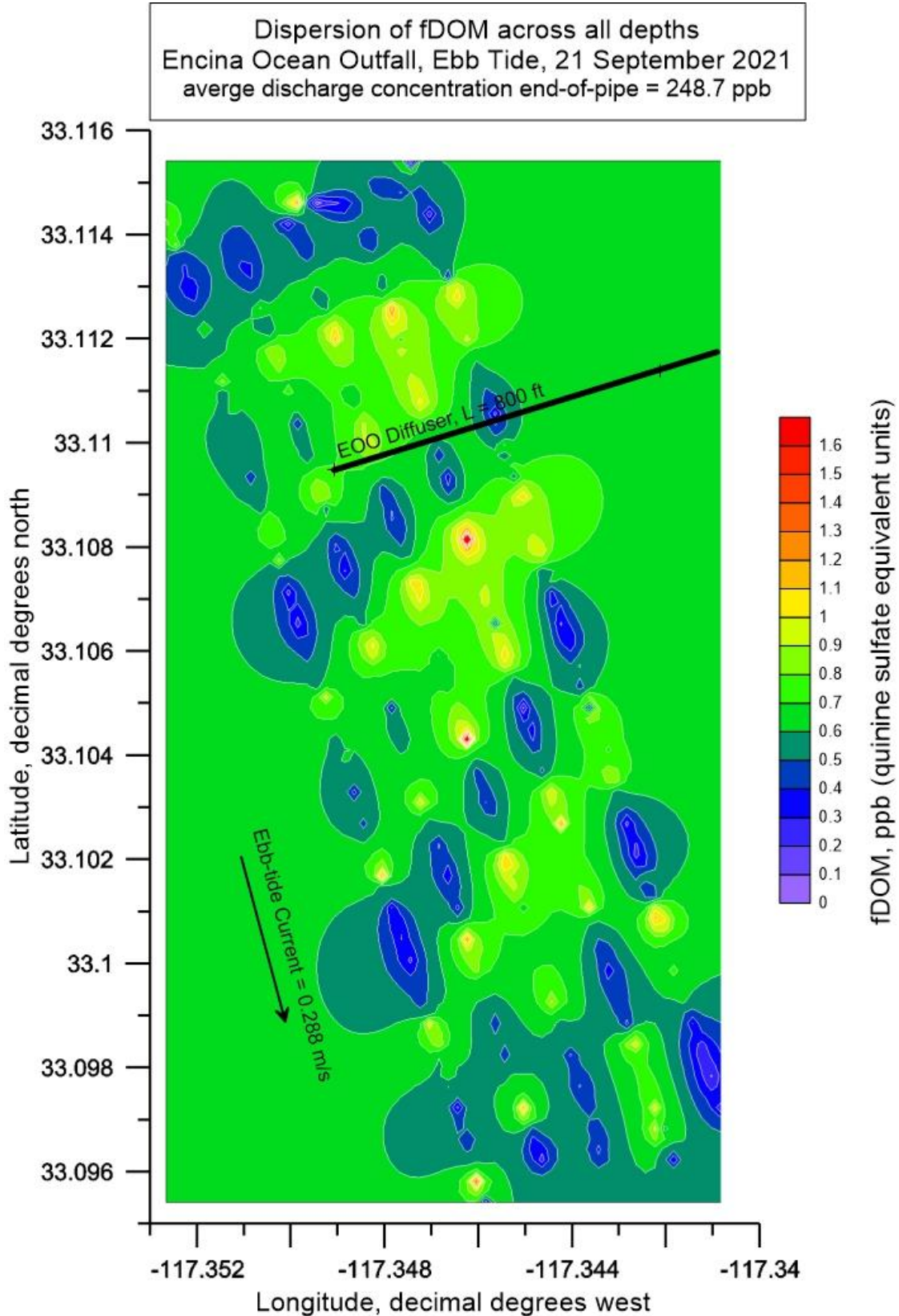


Figure 2.1.11: Full depth contour plot (aka, heat map) of AUV measurements of fDOM during ebb tide surveys of the discharge plume from the EOO. EOO discharge rate = 24.17 mgd; End-of-pipe discharge concentration of fDOM = 248.71 ppb (QSU); End of pipe salinity = 0.85 psu; Mean ebb tide current = 0.288 m/s (0.56 kts) toward the southeast.

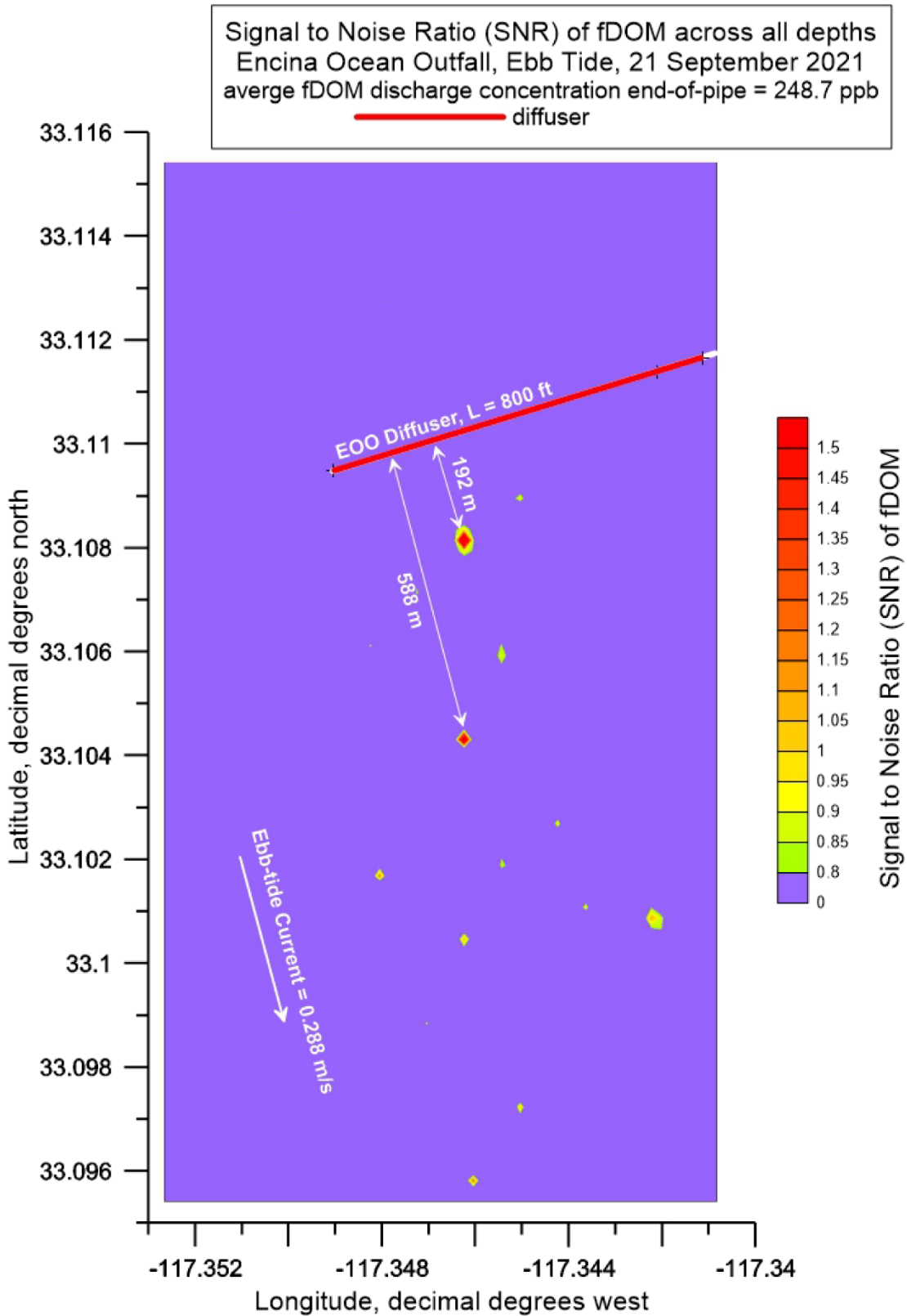


Figure 2.1.12: Full depth contour plot (aka, heat map) of the signal to noise ratio (SNR) of fDOM during the AUV ebb tide surveys of the discharge plume from the EOO. EOO discharge rate = 24.17 mgd; End-of-pipe discharge concentration of fDOM = 248.71 ppb (QSU); End of pipe salinity = 0.85 psu; Mean ebb tide current = 0.288 m/s (0.56 kts) toward the southeast.

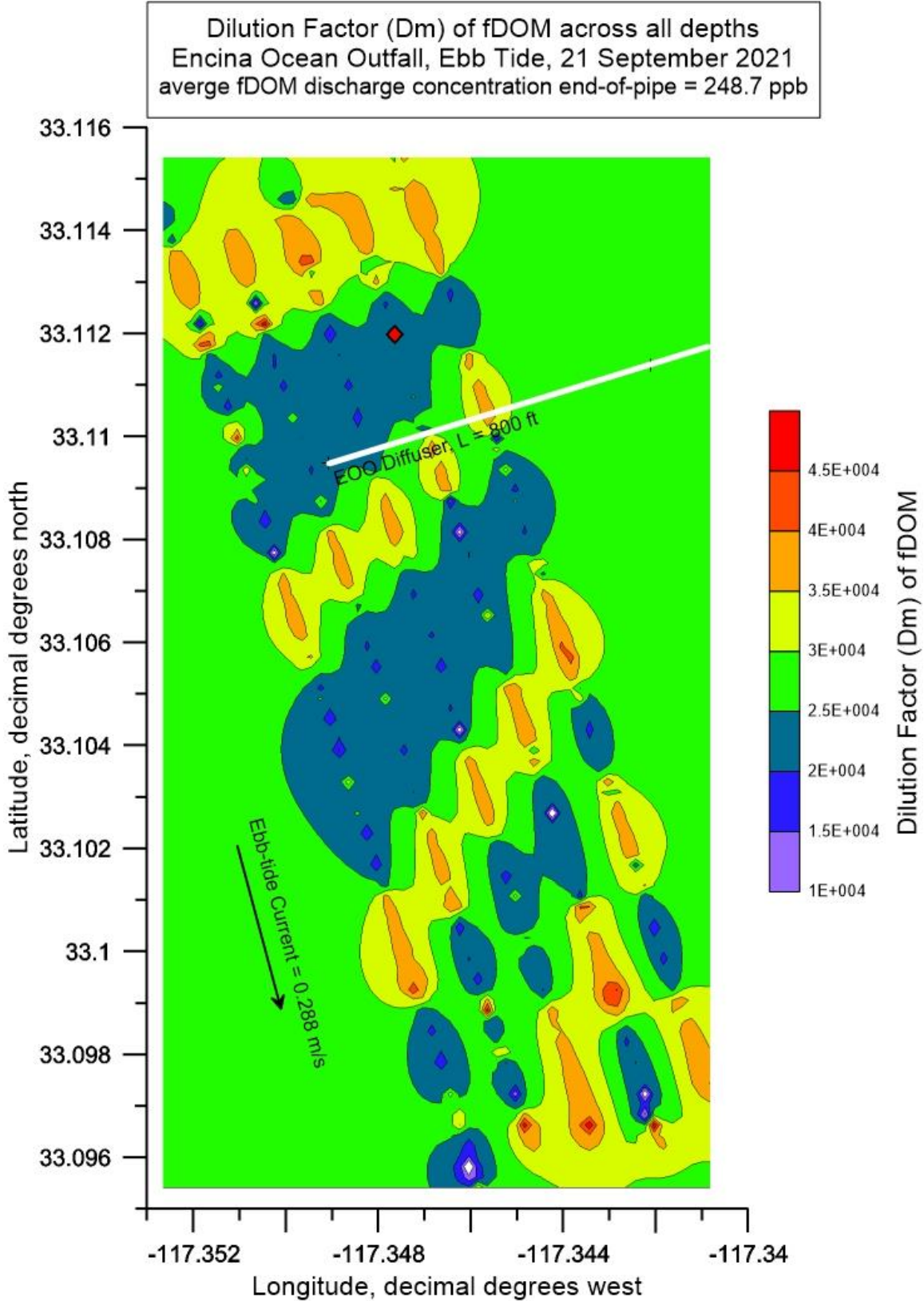


Figure 2.1.13: Full depth contour plot (aka, heat map) of the dilution factor (D_{fDOM}) of fDOM during the AUV ebb tide surveys of the discharge plume from the EOO. EOO discharge rate = 24.17 mgd; End-of-pipe discharge concentration of fDOM = 248.71 ppb (QSU); End of pipe salinity = 0.85 psu; Mean ebb tide current = 0.288 m/s (0.56 kts) toward the southeast

Salinity was considered a potentially useful alternative to CDOM for plume observation. **Figure 2.1.14** provides the salinity heat map generated from the AUV salinity measurements during the EOO ebb tide survey. Most of the features in the salinity heat map range from $S_{(x)} = 33.5$ psu to $S_{(x)} = 33.55$ psu with some small random heat bubbles offshore of the outfall reaching as low as $S_{(x)} = 33.25$ psu and as high as $S_{(x)} = 33.65$ psu. None of these salinity features in **Figure 2.1.14** appear to be spatially coherent with the EOO pipeline or diffuser. The far-field depth averaged salinity in **Figure 2.1.2** indicates that natural background salinity is $S_{\infty} = 33.44$ psu with a standard deviation of $\sigma = 0.066$ psu. Inserting these values into equation (1) indicates that the signal to noise ratio of the predominant salinity features in **Figure 2.1.14** range from $SNR_S = 0.0018$ to $SNR_S = 0.0033$, while the signal to noise ratio of the small scale salinity heat bubbles in **Figure 2.1.14** range from $SNR_S = 0.0054$ to $SNR_S = 0.0063$. Regardless, all the salinity features in **Figure 2.1.14** have signal to noise ratios significantly below the lowest order significance threshold for detection (i.e., $SNR_S \geq 1$) and consequently cannot be associated with plume fragments by any statistically meaningful measure. The conclusion that salinity is not a useful observable for tracking the EOO plume was anticipated at the outset since the signal to noise ratio of the salinity signal at the point of discharge is only $SNR_{S(x=0)} = 0.97$, or less than lowest order significance threshold for detection.

The AUV survey tracks at the EOO are reversed with bias toward the northwest (cf. **Figure 2.1.15**) to maximize the search area in the down-drift region of the flood tide currents flowing toward the northwest. Again, accurate repeatability of the outbound and return legs is found along each of the five track lines as flown by the AUV during flood tide surveys of the EOO on 21 September 2021. During the flood tide survey, the AUV collected 66,269 separate measurements of salinity and fDOM. The fDOM heat map generated from these 66,269 measurements of fDOM concentrations is plotted in **Figure 2.1.16**. Inspection of **Figure 2.1.16** reveals that variations in fDOM concentrations across all depths surveyed by the AUV range again from 0.2 ppb to 1.6 ppb. These fDOM variations during flood tide also exhibit horizontal banding structures along each track line, likely due to spatial aliasing due to insufficient fDOM sampling resolution between the track lines, (cf. Peterson et al., 1954). However, there are several small elevated fDOM immediately downstream side of the diffuser where fDOM concentrations are in the range of 1.3 ppb to 1.6 ppb as well as additional smaller scattered spots of elevated fDOM at 0.8 ppb to 1.1 ppb trailing away from the EOO toward the northwest with the flood tide current that appear to be spatially coherent with the alignment of the EOO pipeline and diffuser, but also align with the 5 track lines in the flood tide survey pattern due to spatial aliasing, (cf. **Figure 2.1.15**). To ascertain whether these scattered spots of elevated fDOM downstream of the EOO are in fact remnants of the EOO plume, the fDOM heat map in **Figure 2.1.16** is converted into a SNR heat map in **Figure 2.1.17** by invoking equation (1) to convert the fDOM concentrations in **Figure 2.1.16** into corresponding SNR_{fDOM} patterns. Again, to help sort out potential plume remnants from among the highly variable and banded fDOM measurements, **Figure 2.1.17** has been scaled to filter out features having $SNR_{fDOM} < 0.8$, where features having $0.8 \leq SNR_{fDOM} < 1.0$ are potentially diluted fragments or diluted outer edges of a plume remnants. Inspection of **Figure 2.1.17** reveals that two small plume remnants having $1.3 \leq SNR_{fDOM} \leq 1.5$ are found directly adjacent the EOO diffuser along its northwest side, (within 33 m), while an additional potential plume remnant having $1.0 \leq SNR_{fDOM} \leq 1.5$ is found 526 m downstream of the EOO diffuser. Several other more diluted fragments having $0.8 \leq SNR_{fDOM} < 1.0$ are found scattered around the downstream side of the EOO

diffuser. To further verify this conclusion, the SNR_{fDOM} heat map in **Figure 2.1.17** was transposed into a dilution heat map in **Figure 2.1.18** using equation (2) under the assumption that the initial fDOM discharge concentration is $fDOM_{(x=0)} = 248.17$ ppb. **Figure 2.1.18** indicates that the dilution factor (D_{fDOM}) for the fDOM features in **Figure 2.1.16** would range from as little as 260:1 within 33 m of the EOO diffuser to as high as 5,000:1 to 40,000:1 further downstream, where any regulated or unregulated toxic EOO effluent constituents would be well below quantifiable detection limits.

Figure 2.1.19 provides the salinity heat map generated from the AUV salinity measurements during the EOO flood tide survey. Most of the features in the flood tide salinity heat map range from $S_{(x)} = 33.4$ psu to $S_{(x)} = 33.65$ psu arranged in lines of elevated salinity heat bubbles that trail away to the northwest along the AUV survey track lines, (cf. **Figure 2.1.15**). All of these salinity features in **Figure 2.1.19** show higher spatial coherence with the AUV track lines than with the EOO diffuser and pipeline. The far-field depth averaged salinity from the salinity depth profile in **Figure 2.1.2** indicates that natural background salinity is $S_{\infty} = 33.44$ psu with a standard deviation of $\sigma = 0.066$ psu. Inserting these values into equation (1) indicates that the signal to noise ratio of the elevated salinity features in **Figure 2.1.19** range from $SNR_S = 0.0012$ to $SNR_S = 0.0063$. Therefore, all the salinity features in **Figure 2.1.19** have signal to noise ratios significantly below the lowest order significance threshold for detection (i.e., $SNR_S \geq 1$) and consequently cannot be associated with plume fragments by any statistically meaningful measure. Again, the conclusion that salinity is not a useful observable for tracking the EOO plume was anticipated at the outset since the SNR of the salinity signal at the point of discharge is only $SNR_{S(x=0)} = 0.97$, i.e., less than lowest order significance threshold for detection.

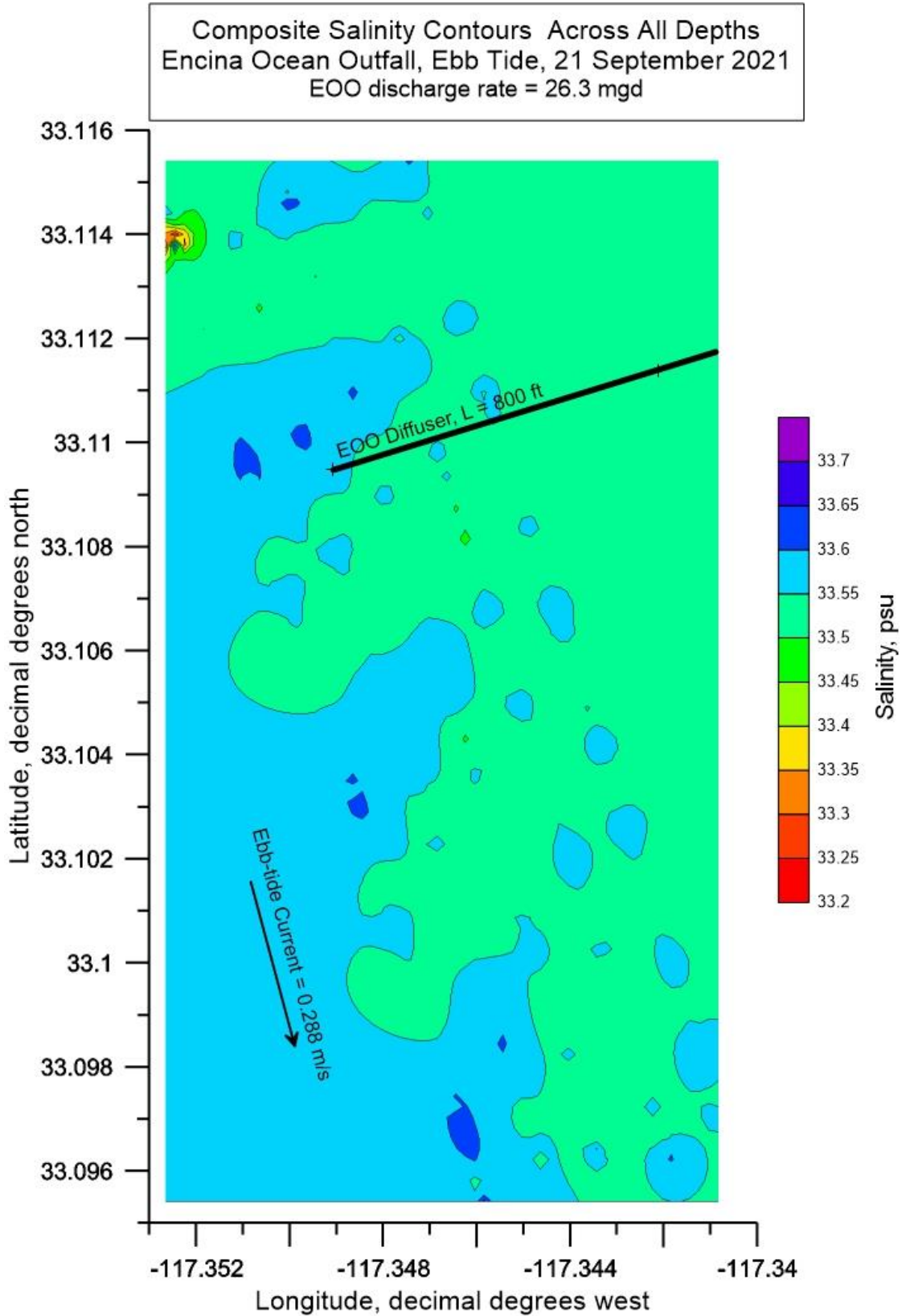


Figure 2.1.14: Full depth composite contour plot (aka, heat map) of AUV measurements of salinity during ebb tide surveys of the discharge plume from EOO. EOO discharge rate = 24.17 mgd; End-of-pipe discharge salinity = 0.85 psu; Mean ebb tide current = 0.288 m/s (0.56 kts) toward the southeast.

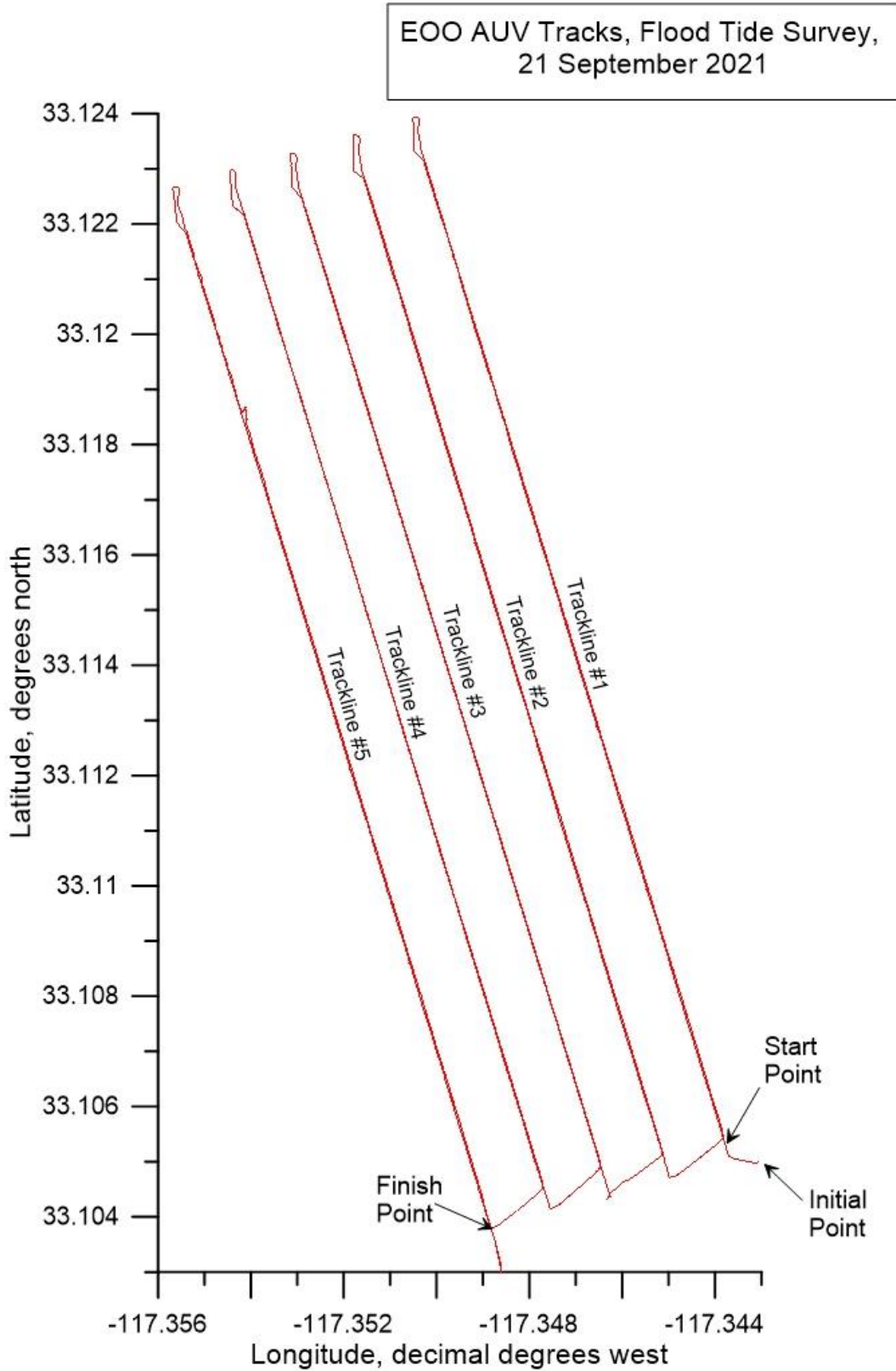


Figure 2.1.15: AUV track lines as flown during flood tide surveys of the discharge plume from EOO during the first deployment, 21 September 2021. The total dimension of the AUV surveyed area on flood tide was 2000 m in the along shore direction and 1000 m in the cross-shore direction or a total surveyed area of approx. 494.3 acres. Note, at 30° N latitude, 1° longitude = 93,453.2 m, while 1° latitude = 110,904.4 m.

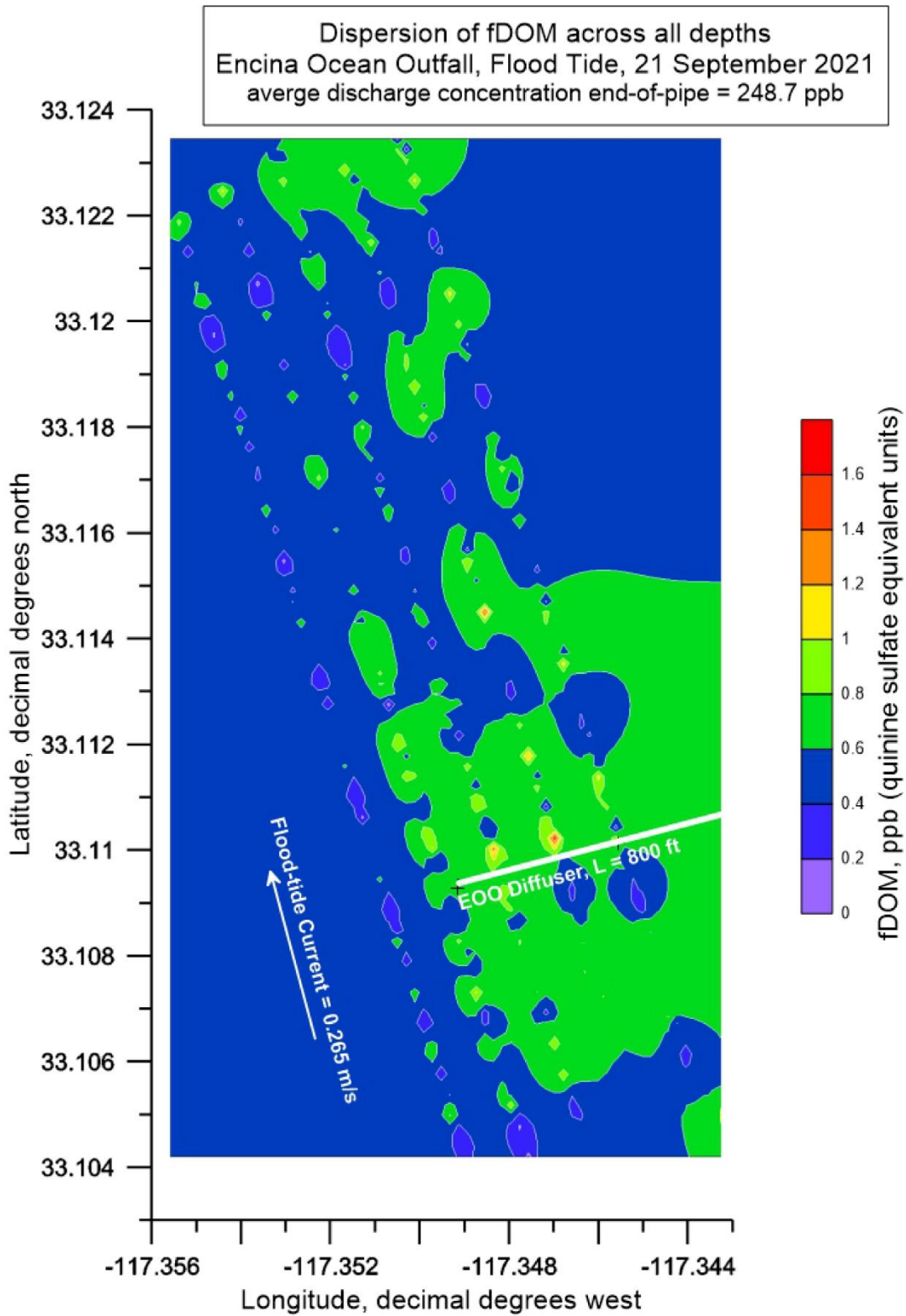


Figure 2.1.16: Full depth contour plot (aka, heat map) of AUV measurements of fDOM during flood tide surveys of the discharge plume from EOO. EOO discharge rate = 26.318 mgd; End-of-pipe discharge concentration of fDOM = 248.71 ppb (QSU); End of pipe salinity = 0.85 psu; Mean ebb tide current = 0.265 m/s (0.52 kts) toward the northwest.

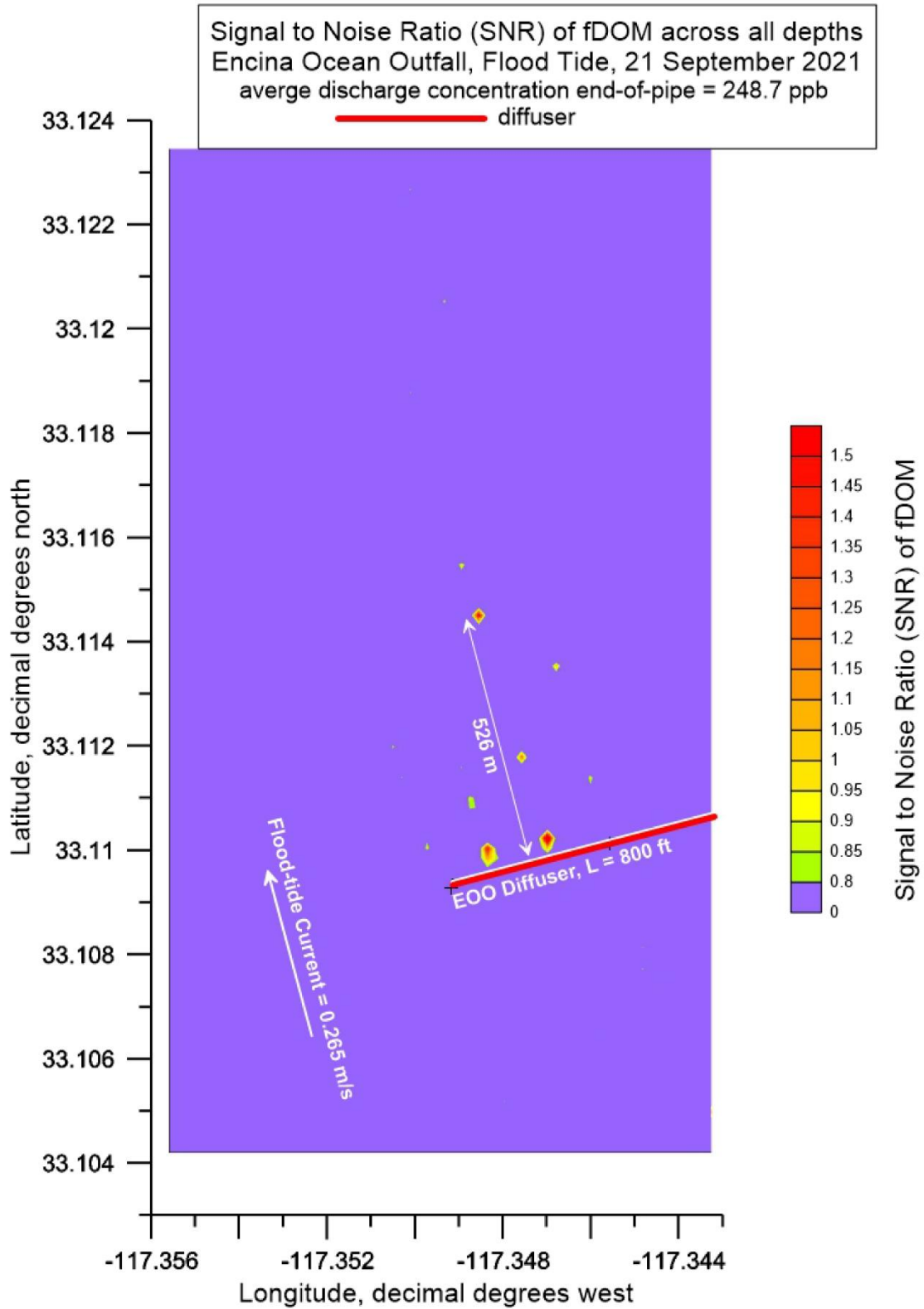


Figure 2.1.17: Full depth contour plot (aka, heat map) of the signal to noise ratio (SNR) of fDOM during flood tide AUV surveys of the discharge plume from EOO. EOO discharge rate = 26.318 mgd; End-of-pipe discharge concentration of fDOM = 248.71 ppb (QSU); End of pipe salinity = 0.85 psu; Mean ebb tide current = 0.265 m/s (0.52 kts) toward the northwest.

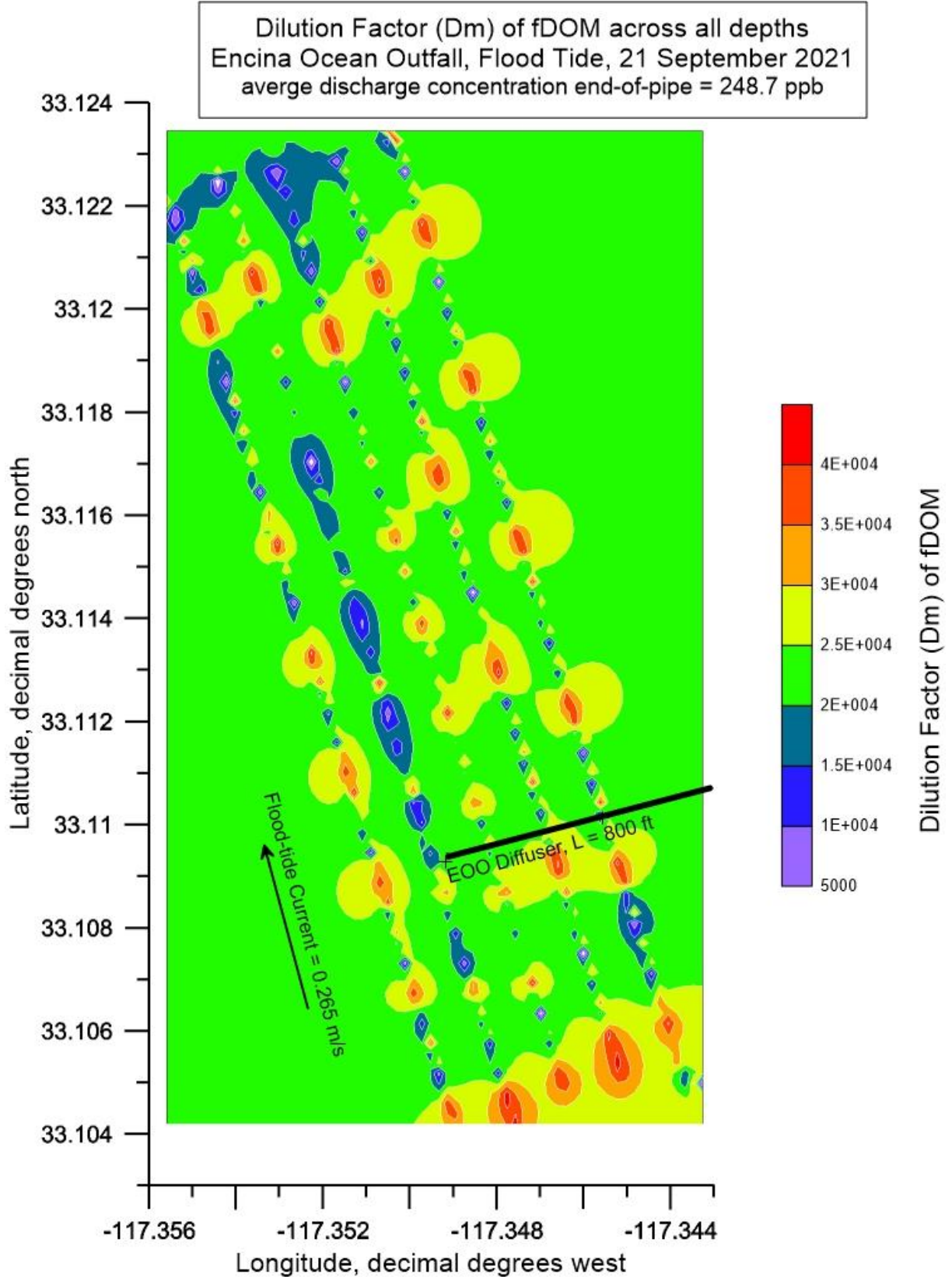


Figure 2.1.18: Full depth contour plot (aka, heat map) of the dilution factor (D_{fDOM}) of fDOM during flood tide AUV surveys of the discharge plume from EOO. EOO discharge rate = 26.318 mgd; End-of-pipe discharge concentration of fDOM = 248.71 ppb (QSU); End of pipe salinity = 0.85 psu; Mean ebb tide current = 0.265 m/s (0.52 kts) toward the northwest.

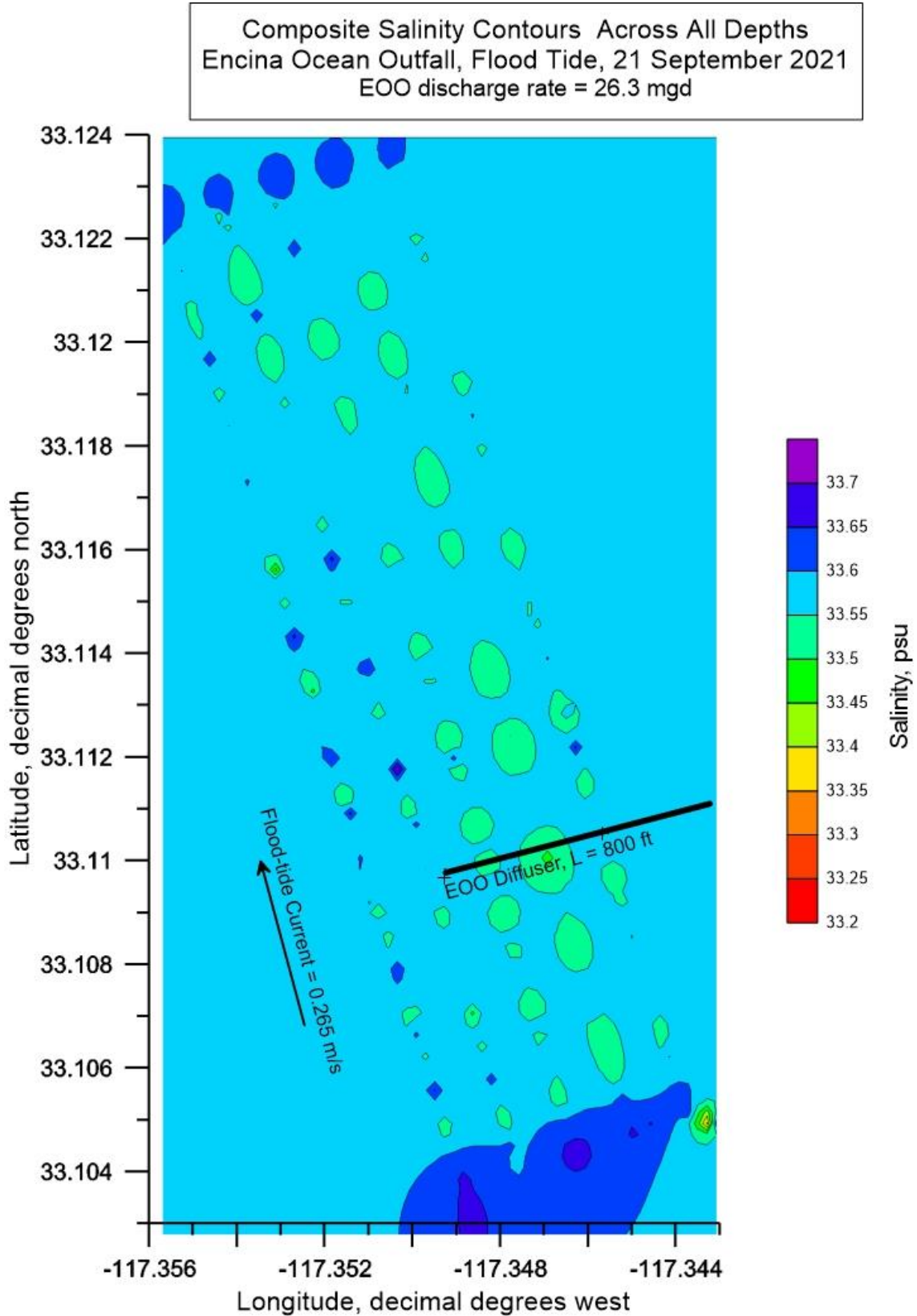


Figure 2.1.19: Full depth composite contour plot (aka, heat map) of AUV measurements of salinity during flood tide surveys of the discharge plume from EOO. EOO discharge rate = 26.318 mgd; End-of-pipe discharge concentration of salinity = 0.85 psu; Mean ebb tide current 0.265 m/s (0.52 kts) toward the northwest.

2.2 SECOND EOO DEPLOYMENT - 20 DECEMBER 2021

The design of the EOO survey boxes and the AUV track lines within those boxes was modified for the second AUV deployment on 20 December 2021. Based on the patterns of fDOM features found in the fDOM heat maps of the first deployments, it was determined that the distance surveyed in the long-shore direction could be reduced since no evidence of plume dispersion beyond 1,000 m from the EOO had been found. By reducing the long-shore search range, additional survey area could be added to the inshore region to determine if there was any evidence of the plume drifting shoreward due to mass transport by shoaling internal waves. The modified survey plan still includes 2 separate AUV survey boxes (a flood tide box shown in orange in [Figure 2.2.1](#) and an ebb tide box shown in yellow) while the numbers of stationary water column monitoring stations (where CTD casts and ADCP velocity profiles are taken) was increased from 15 to 18 stations. The 18 stationary water column monitoring stations (shown as green circles in [Figure 2.2.1](#)) are distributed between the 160 ft and 60 ft depth contours around the EOO, and provide vertical profiles of salinity, temperature, and fDOM water mass properties immediately prior to and during the AUV surveys. [Figure 2.2.1](#) also shows a group of blue triangles around the EOO diffuser, indicating the locations of the offshore regulatory discharge monitoring stations used for NPDES permit compliance determination. The total dimension of the AUV surveyed area on either ebb or flood tide was 707.1 m in the longshore (shore parallel) direction and 1,414.2 m on the cross-shore (on/off shore) direction. Thus, the total area surveyed during both ebb and flood tide is approximately 494.2 acres. While this is only half the size of the ebb and flood tide survey boxes used during the first deployment in September 2021, it allows for increasing the numbers of track lines from 5 to 12 shore parallel AUV track lines at 108.8 m spacings within each survey box. This increase in numbers of track lines increases the horizontal resolution within each ebb and flood survey box by a factor of 2.4, thereby reducing or eliminating the spurious fDOM features that aligned with sparse track lines during the September 2021 deployments (cf. [Figure 2.1.11](#) and [Figure 2.1.16](#)). Those spurious features in the fDOM heat maps of the September 2021 deployments were the result of *spatial aliasing* which arises from insufficient sampling density in the spatial domain. To eliminate spatial aliasing, the AUV track line spacing must be no more than $\frac{1}{2}$ the length scale of the finest scale features in the fDOM spatial distribution. By increasing the horizontal resolution of the second deployment survey boxes by a factor of 2.4, it was anticipated that the spatial aliasing fDOM features encountered during the first deployment could be eliminated, or at least significantly muted.

As practiced during the first AUV deployment in September 2021 the new survey boxes in [Figure 2.2.1](#), were searched twice for the presence of the EOO plume, (i.e., out and return). As before, the AUV is flown along a dolphin-style flight path when transiting outbound with the current, i.e., a yo-yo flight path diving and ascending through the water column between the seabed and an apex halfway between the sea surface and the pycnocline. On the return legs of each track line, (against the current) the AUV is flown at a constant depth immediately beneath the pycnocline (trapping level) where the maximum horizontal dispersion of the plume is expected, (cf. Baumgartner, 1994; Frick et al., 2003). Altogether, the AUV covers a distance of about 20.0 kilometers in about 5 hours within each survey box which is roughly the endurance limit of the AUV with fully charged batteries. The survey period is centered within each ebb or flood tide interval of 6.2 hours. The AUV batteries are changed during the 1.2-hour interval around slack

water between ebb and flood tide intervals, allowing for AUV surveys of the EOO over a complete semi-diurnal tide cycle.

The 18 stationary water column monitoring stations are distributed between the 160 ft and 60 ft depth contours around the EOO, and provide vertical profiles of salinity, temperature, and fDOM water mass properties immediately prior to and during the AUV surveys. Measurements from the control stations EOO-Ebb and EOO-Flood provide far-field measurements of natural background (ambient) water-mass properties (salinity, temperature, and fDOM). The measurements of the fDOM at the 18 stationary monitoring stations were in units of RFU which were converted to QSU fDOM units using the second order polynomial in **Figure 1.3.1**.

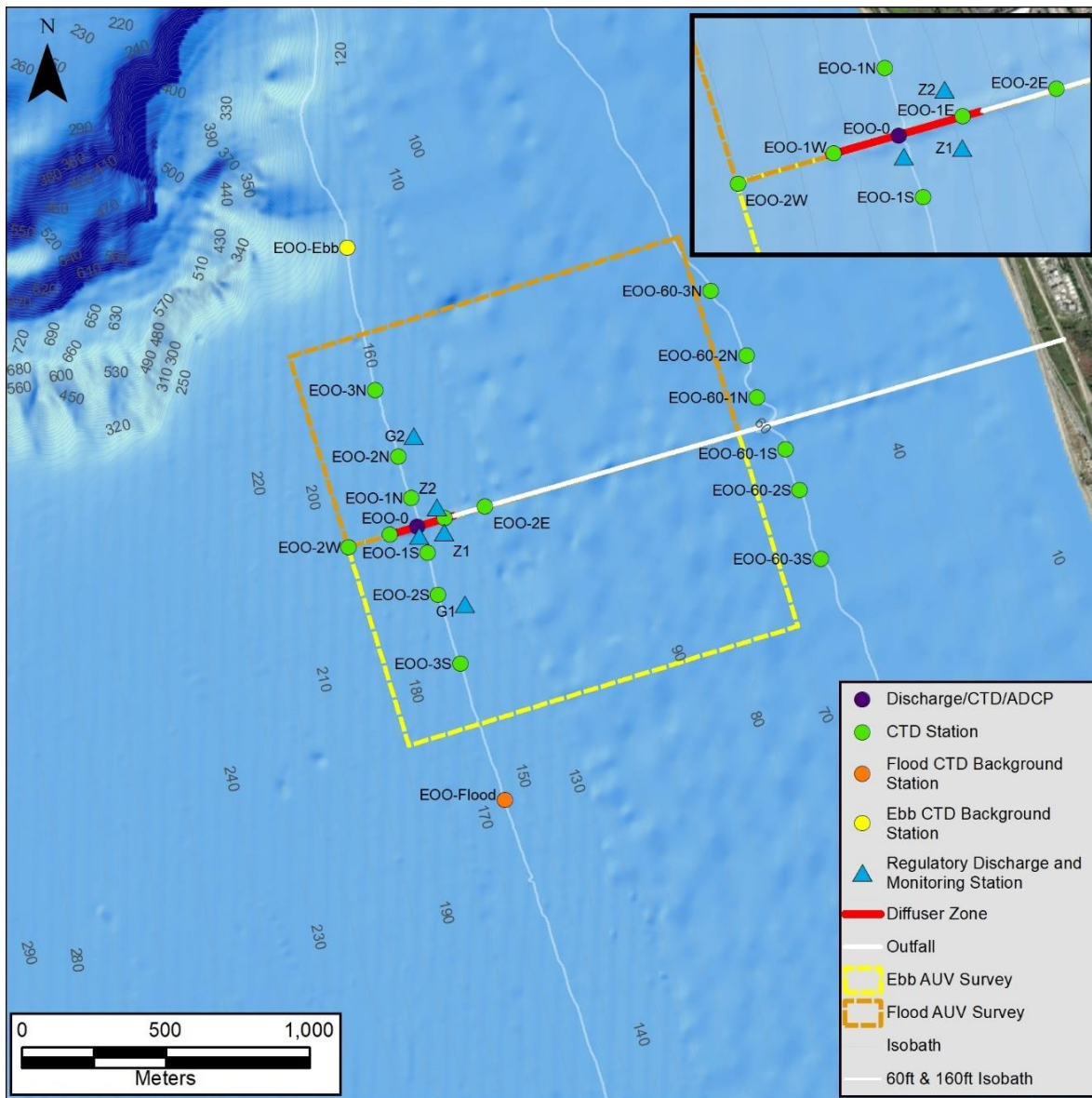


Figure 2.2.1: EOO Survey boxes and sampling stations for second AUV deployment, 19-21 December 2021

To establish the precise location of the Encina Ocean Outfall, a side-scan sonar survey of the outfall was performed prior to the AUV deployments on 19 December 2021 to obtain precision geo-referenced coordinates along the length of the pipeline and diffuser, (cf. [Figure 2.2.2](#)).

It was critical to the plume tracking effort to program the AUV to fly directly beneath the pycnocline during the return leg (against the current) along each of the 12 track lines within the ebb and flood survey boxes shown in [Figure 2.2.1](#). To locate the depth of the pycnocline, the CTD casts were performed prior to the AUV survey on 19 December 2021 and quickly processed to determine the salinity changes and temperature changes with depth, (cf. [Figure 2.2.3](#)). These CTD data showed a cold, nearly homogeneous surface layer, (about 6° C cooler than during the first deployment in September 2021) that mixed down to about 25 m depth, while the bottom layer remained about the same temperature as in September 2021. Consequently, the water column during the second deployments on 21 December 2021 was only weakly stratified (i.e., less stable than in September 2021) and the trapping level rose to only 4 m depth. Based on this finding, the AUV was programed on its outbound dolphin-style legs (with the current) for dive cycle apex points set above the pycnocline at a depth of 2 m depth (-6.6 ft. MSL) and dive cycle bottoming points set at 2 m (-6.6 ft) above the seabed. The Iver3 AUV uses its bottom-locking sonar to determine the distance above the local seabed at any location within the survey box. Along the return leg of each track line (flown against the current), the AUV was programmed to fly at a constant depth of 6 m depth (-19.7 ft. MSL).

At the time of the ebb tide AUV survey on 20 December 2021, the EOO was discharging 31.2 mgd of wastewater having an average discharge salinity of 0.96 psu and an average fDOM discharge concentration of 217.5 ppb (QSU), based on shoreside monitoring of the EOO effluent, (see tabulations of EOO shoreside monitoring data in Appendix-A). Later in the day during flood tide the EOO discharge rates decreased slightly to 29.7 mgd, while average discharge salinity and fDOM concentrations remained unchanged, (cf. Appendix-A). The average EOO discharge concentrations of fDOM are significantly higher (by more than 2 orders of magnitude) than the natural ocean background concentrations of fDOM measured at far-field control stations, EOO-Ebb and EOO-Flood, which were profiled twice during each ebb and flood tide event on 20 December 2021. Vertical profiles of natural background fDOM measured during ebb tide at EOO-Ebb (cf. [Figure 2.2.4](#)) exhibited depth-averaged concentrations ranging between 0.294 ppb and 0.298 ppb. Natural background fDOM measured later during flood tide on 20 December 2021 at EOO-Flood (cf. [Figure 2.2.5](#)) produced depth-averaged concentrations ranging between 0.308 ppb and 0.310 ppb. Consequently, the signal to noise ratio of the fDOM plume observable at any point of discharge along the EOO diffuser ranges between $SNR_{fDOM} = 700.6$ and $SNR_{fDOM} = 738.8$, based on the depth averaged concentrations of natural background fDOM measured at far-field control stations, EOO-Ebb and EOO-Flood ([Figure 2.2.4](#) and [Figure 2.2.5](#)), applied to equation (1). While profiles of natural background fDOM concentrations measured during both ebb and flood tide showed both random variations (noise) with some general vertical structure (with higher concentration near the bottom, declining near the surface), the standard deviations around the depth averaged fDOM concentrations were small, ranging between $\sigma = 0.027$ ppb and $\sigma = 0.045$ ppb, (cf. [Figure 2.2.4](#) and [Figure 2.2.5](#)).



Figure 2.2.2: Side-scan sonar survey image of EOO used to obtain precision geo-referenced coordinates along the length of the pipeline and diffuser.

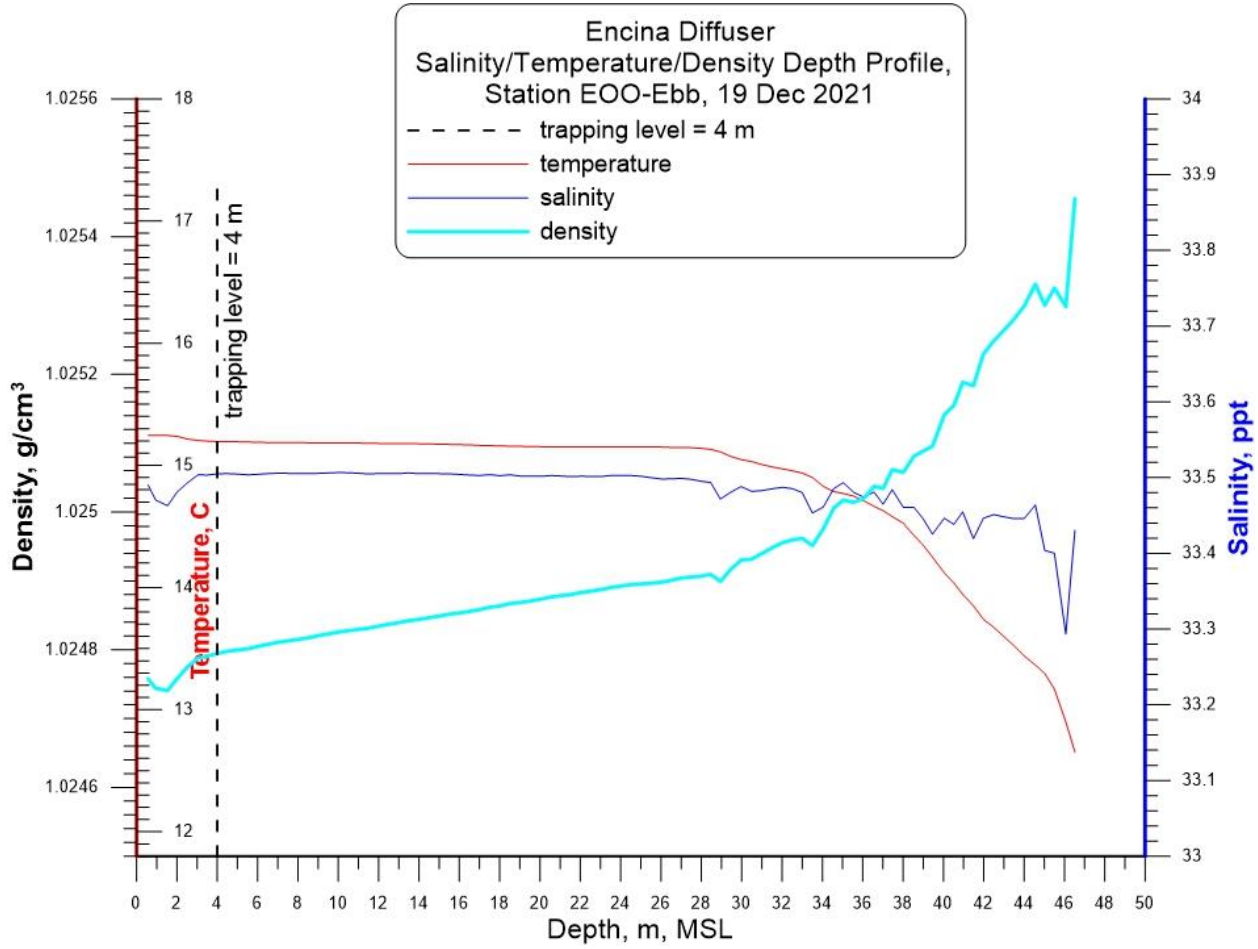


Figure 2.2.3: Salinity/Temperature/Density depth profiles derived from CTD casts on 19 December 2021 used to program the AUV surveys of the plume dispersion from EOO on 20 December 2021.

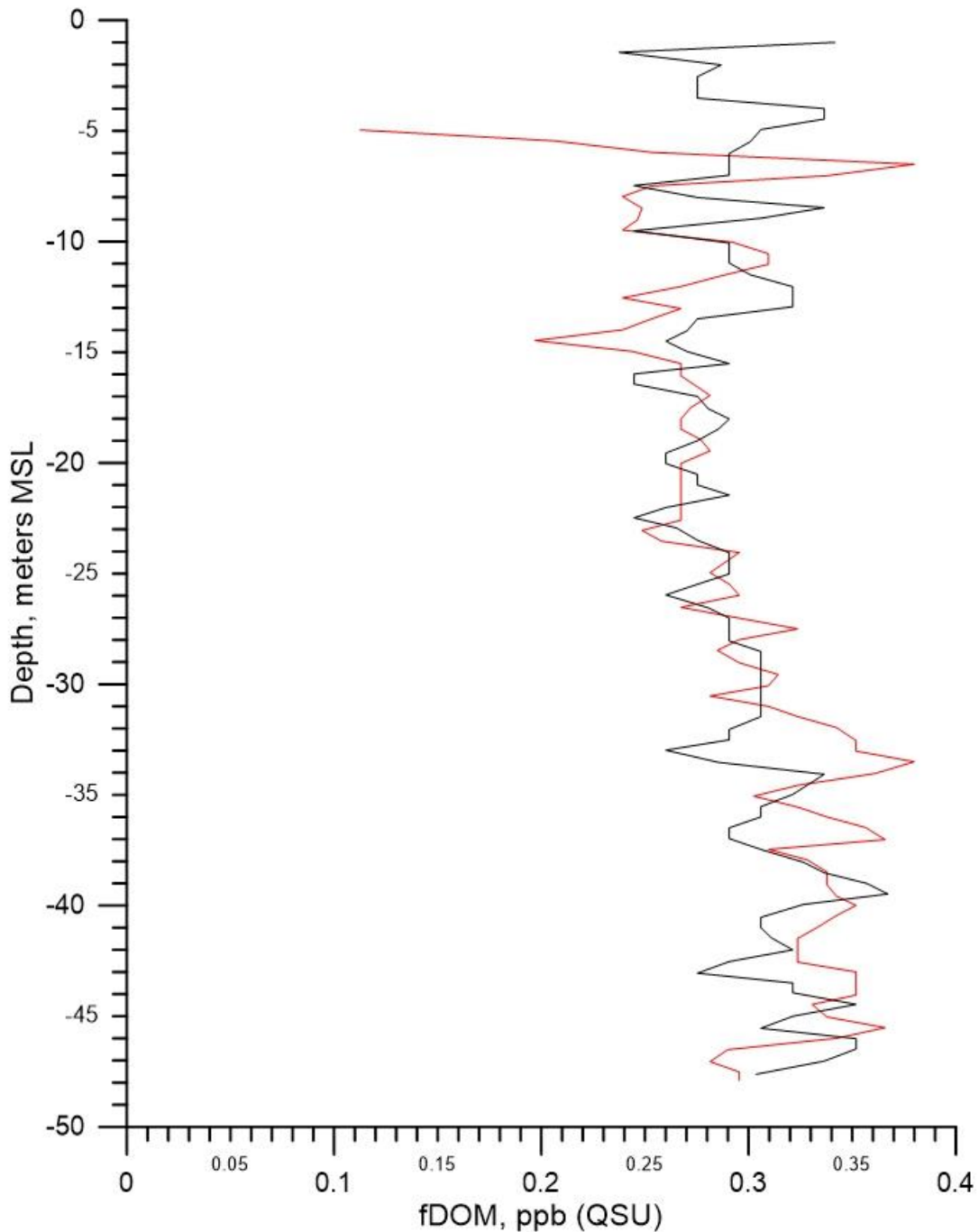
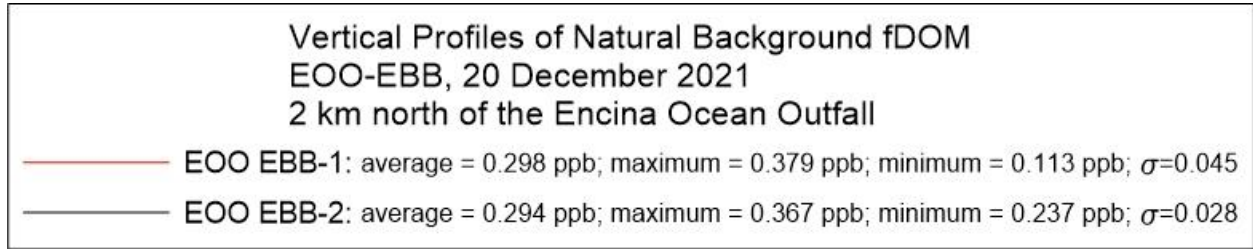


Figure 2.2.4: Vertical profiles of natural background fDOM concentrations measured during the second deployment at the far-field ebb tide monitoring station “EOO-EBB,” located 2 km northwest of EOO along the -160 ft. MLLW depth contour, cf. yellow dot in Figure 2.2.1.

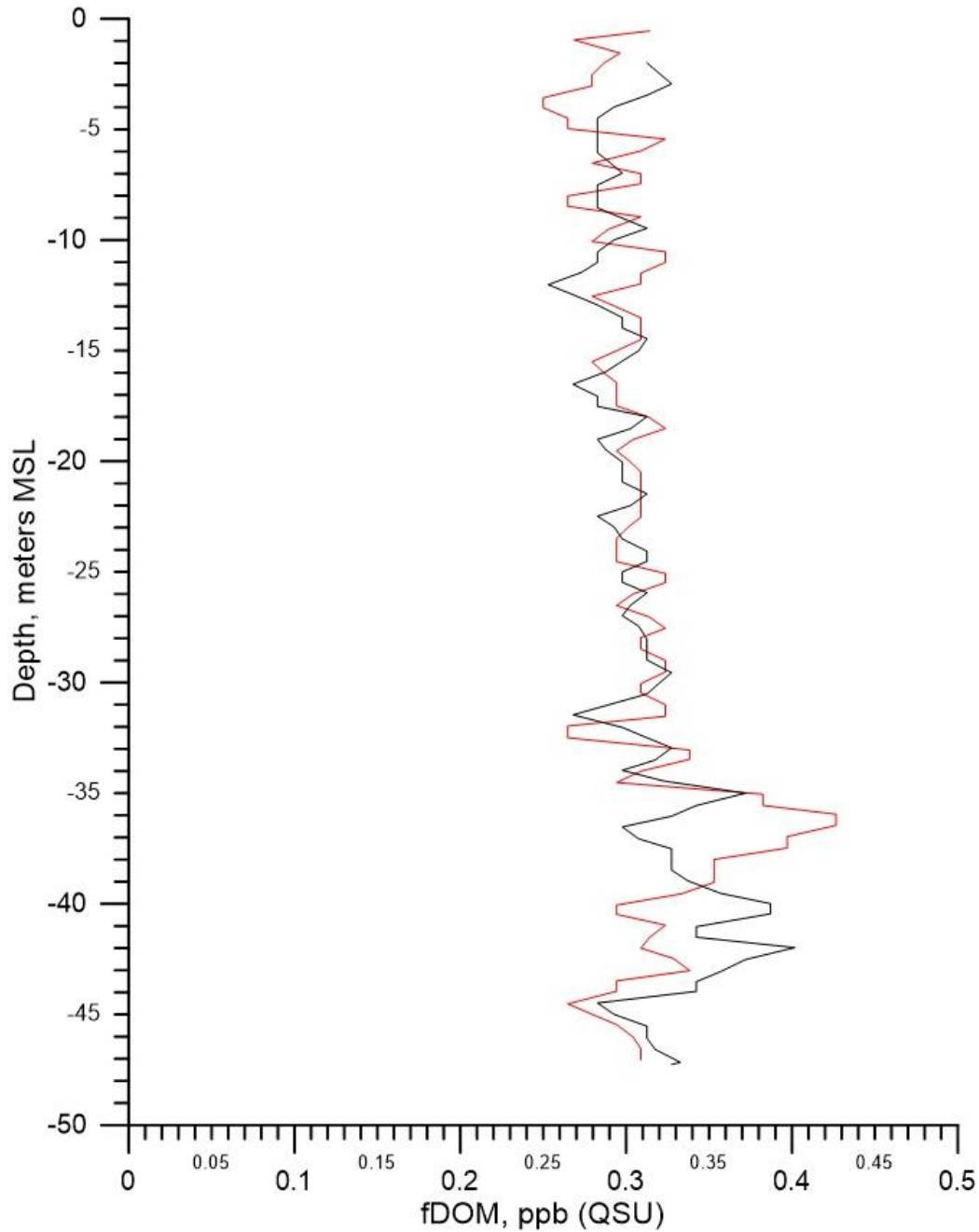
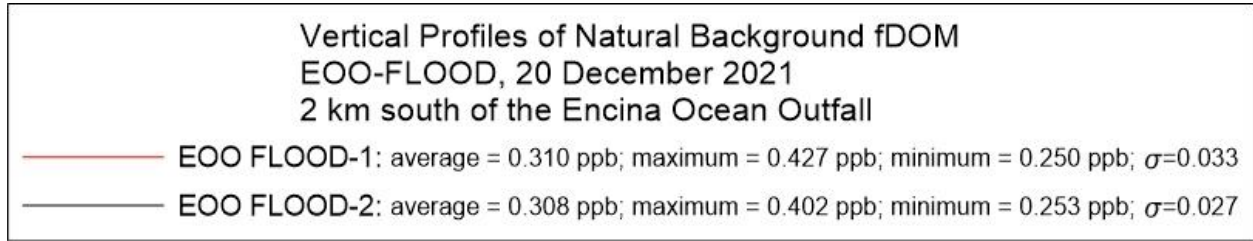


Figure 2.2.5: Vertical profiles of natural background fDOM concentrations measured during the second deployment at the far-field flood tide monitoring station “EOO-FLOOD,” located 2 kilometers southeast of EOO along the -160 ft. MLLW depth contour, cf. orange dot in Figure 2.2.1.

Mean ebb tide currents on 20 December 2021 at the far-field control station, EOO-Ebb, were 0.304 m/s (0.59 kts) toward the southeast, based on acoustic Doppler profiling (ADCP) at far field monitoring station, EOO-Ebb, (cf. [Figure 2.2.6](#)) located up-drift of the yellow AUV survey box shown in [Figure 2.2.1](#). These mean currents impart a net shore-parallel drift of the EOO discharge plume. However, there are other transient short-lived current oscillations reaching 0.979 m/s (1.90 kts) in the ebb tide ADCP time series record on 20 December 2021. The current direction data in the ADCP record indicates these spikes of higher oscillatory currents were directed cross-shore, indicating they were due to shoaling internal waves. Because of the oscillatory nature of these current spikes, they produce no net drift of the EOO discharge plume, but merely serve to smear the plume or break off pieces from the main body of the plume and smear or disperse those pieces in the cross-shore direction. ADCP measurements of currents at far field monitoring station, EOO-Flood, (cf. [Figure 2.2.7](#)) find that mean flood tide currents on 21 September 2021 were slightly less than the mean ebb tide currents, reaching only 0.211 m/s (0.41 kts) directed toward the northwest. This is due to the fact that tidal currents along the coastline of the lower Southern California Bight do not reverse symmetrically between ebb and flood tide, but rather are *ebb-tide dominant*, imparting a net southeasterly drift to the EOO discharge plume over a complete tidal day of 24.83 hrs. Transient oscillatory current spikes in the flood tide ADCP current record on 20 December 2021 again reached 0.979 m/s (1.90 kts) in the cross-shore direction, indicating the presence of internal wave activity of the same strength as occurred earlier on ebb tide. These internal waves are excited by the extreme bathymetric depression of the head of the Carlsbad Submarine Canyon, (cf. [Figure 2.1.7](#)). The Carlsbad Submarine Canyon borders the northern end of the EOO flood tide survey box in [Figure 2.2.1](#). As tidal currents flow across the Carlsbad Submarine Canyon, this bathymetric depression excites internal waves that radiate outward from the canyon much like lee waves do in the atmosphere when storm winds blow over canyons and mountainous topography. The cross-shore oscillations of the internal waves that radiate from the Carlsbad Submarine Canyon produce the high current spikes in the ADCP records on 20 December 2021 (cf. [Figure 2.2.6](#) and [Figure 2.2.7](#)).

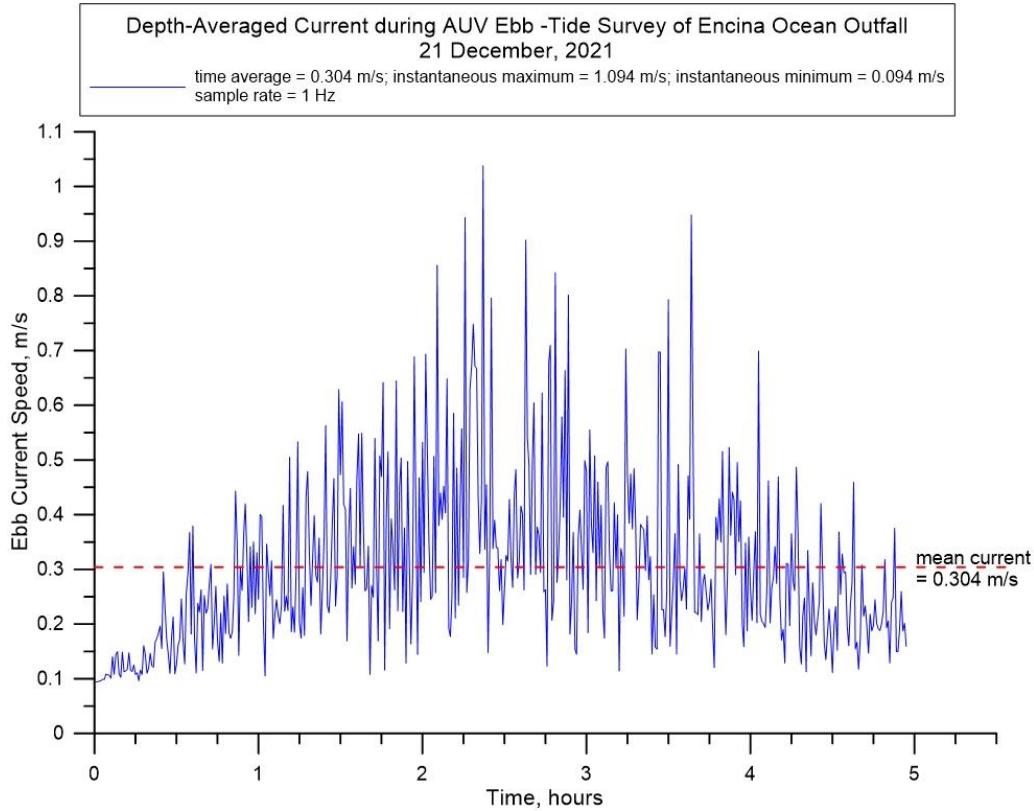


Figure 2.2.6: Time series of depth averaged current derived from ADCP measurements at EOO during ebb-tide AUV survey on 20 December 2021.

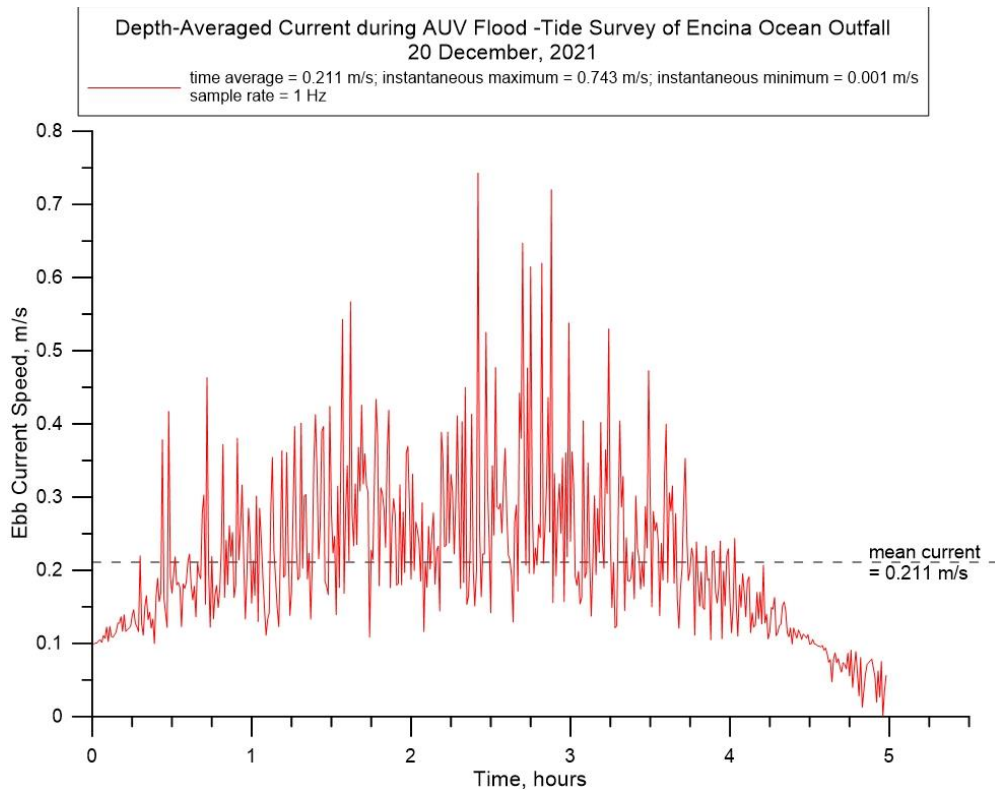


Figure 2.2.7: Time series of depth averaged current derived from ADCP measurements at EOO during flood-tide AUV survey on 20 December 2021.

Figure 2.2.8 reveals accurate repeatability of the outbound and return legs along each of 12 track lines as flown by the AUV during ebb tide surveys of the EOO on 20 December 2021. During this survey, the AUV collected 68,538 separate measurements of salinity and fDOM along a total distance surveyed of 21.2 km. The fDOM heat map generated from these 68,538 measurements of fDOM concentrations is plotted in **Figure 2.2.9**. Inspection of **Figure 2.2.9** reveals that variations in fDOM concentrations across all depths surveyed by the AUV range from $fDOM_{(x)} = 0.2$ ppb to 1.3 ppb. These fDOM variations during ebb tide exhibit horizontal structures having high spatial coherence with the EOO diffuser, with a singular, large fDOM feature centered 393.9 m down-drift (south) of the EOO diffuser in which elevated fDOM are in the range of $fDOM_{(x)} = 0.7$ ppb to 1.3 ppb, or 136% to 339% higher than the depth-averaged natural background fDOM concentration $fDOM_{(\infty)} = 0.296$ ppb (cf. **Figure 2.2.4**). Furthermore, with the increased horizontal resolution afforded by the 12 closely spaced track lines in **Figure 2.2.8**, repeating banded patterns due to spatial aliasing are significantly diminished relative to the heat maps derived from the first EOO deployment in September 2021. Moreover, the fDOM concentrations in the remainder of the surveyed area outside of this singular elevated fDOM feature are on the order of $fDOM_{\infty} \cong 0.3$ ppb, consistent with the depth-averaged natural background fDOM concentration. Therefore, the primary elevated fDOM feature in **Figure 2.2.9** that is centered 393.9 m downstream of the EOO diffuser in the ebb tide current has the spatial coherence, structure, and contrast against natural background to possibly be a remnant of the EOO discharge plume.

To verify this hypothesis, the fDOM heat map in **Figure 2.2.9** is converted into a signal to noise ratio heat map in **Figure 2.2.10** by invoking equation (1) to convert the fDOM concentrations in **Figure 2.2.9** into corresponding SNR_{fDOM} patterns. Again, since only fDOM features having signal to noise ratios of unity or greater are possible remnants of the plume, **Figure 2.2.10** has been scaled to filter out features having $SNR_{fDOM} < 0.8$, where features having $0.8 \leq SNR_{fDOM} < 1.0$ are potentially diluted fragments or diluted outer edges of a plume remnants. Inspection of **Figure 2.2.10** reveals that the signal to noise ratio of the suspected plume remnant ranges from $0.8 \leq SNR_{fDOM} \leq 1.1$ along its outer perimeter, to as high as $SNR_{fDOM} = 3.39$ in its inner core 393.9 m downstream of the EOO diffuser. Therefore, the elevated fDOM concentrations found in this feature satisfy the lowest order significance threshold for detection, (i.e., $SNR_{fDOM} \geq 1$). Based on this detection metric, we conclude the EOO discharge plume has likely detected 393.9 m downstream of the EOO diffuser during ebb tide on 20 December 2021.

To assess minimum dilution levels in the EOO plume remnant, the SNR_{fDOM} heat map in **Figure 2.2.10** was transposed into a dilution heat map in **Figure 2.2.11** using equation (2) on the basis that the initial fDOM concentration at the point of discharge is $fDOM_{(x=0)} = 217.5$ ppb. Equation (2) teaches that regions of high SNR will correspond to regions of low values of D_{fDOM} relative to the dilution elsewhere within the AUV survey area. **Figure 2.2.11** indicates that the dilution factor (D_{fDOM}) for the fDOM features would be no less than as $D_{fDOM} = 215:1$ in the inner core of the plume remnant, or a factor of 1.5 times greater than the assigned minimum month dilution of $D_m = 144:1$ established in the current NPDES permit (No. CA0107395; Order No. RS-2018-0059). The dilution along the outer perimeter of the plume remnant ranges from $D_{fDOM} = 666:1$ to as much as 15,000:1. Elsewhere in the wake of the EOO diffuser dilution ranges from $D_{fDOM} = 35,000:1$ to 75,000:1 so that any regulated or unregulated toxic constituents in the

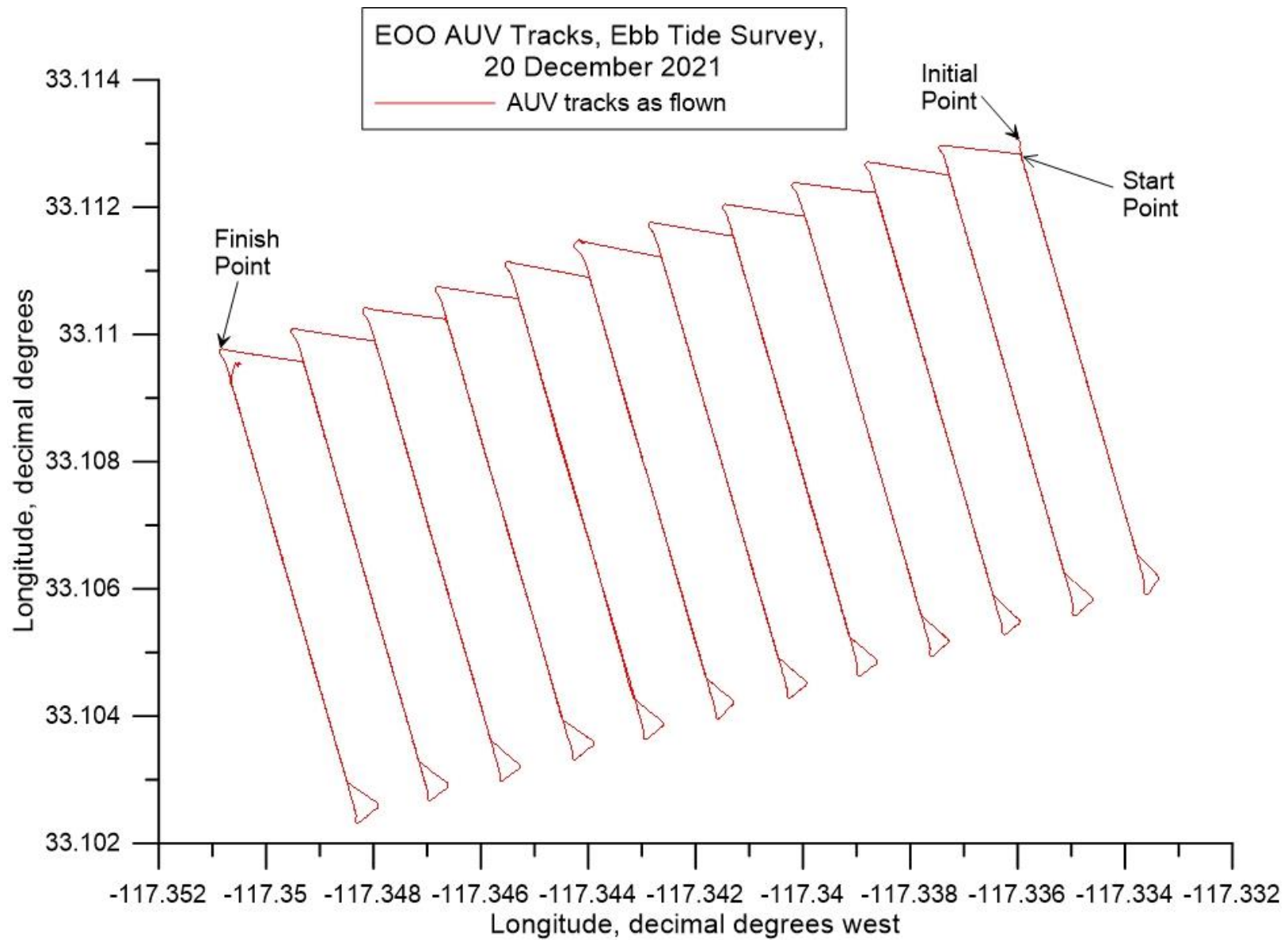


Figure 2.2.8: AUV track lines as flown during ebb tide surveys of the discharge plume from EOO during the second deployment, 20 December 2021. The total dimension of the AUV surveyed area on ebb tide was 707.1 m in the longshore (shore parallel) direction and 1,414.2 m on the cross-shore (on/off shore) direction or a total surveyed area of approximately 247.1 acres. Note, at 30° N latitude, 1° longitude = 93,453.2 m, while 1° latitude = 110,904.4 m.

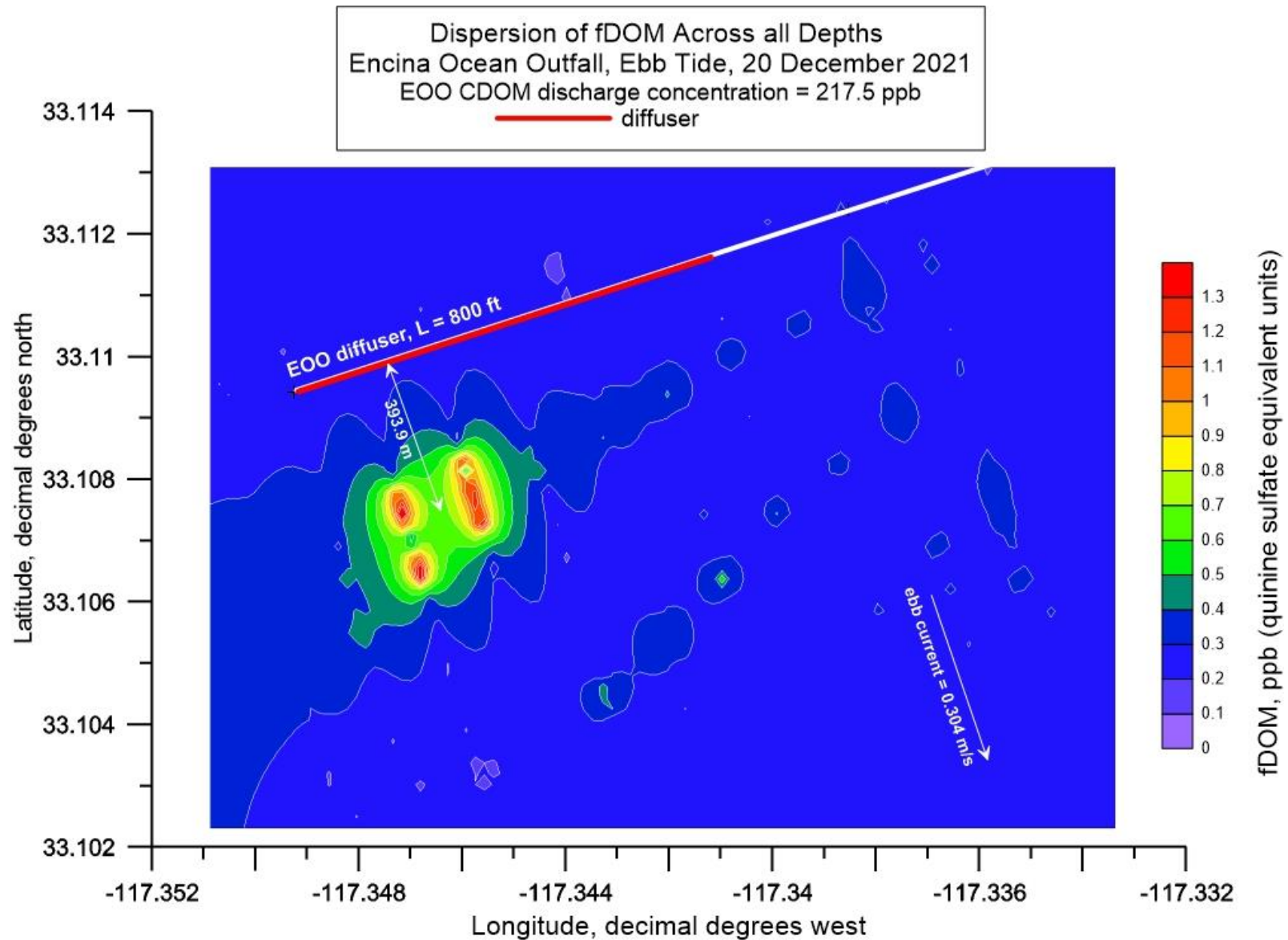


Figure 2.2.9: Full depth contour plot (aka, heat map) of AUV measurements of fDOM during surveys of the discharge plume from EOO during ebb tide on 20 December 2021. Average EOO discharge rate = 31.20 mgd during ebb tide; End-of-pipe discharge concentration of fDOM = 217.5 ppb (QSU); End of pipe salinity = 0.96 psu; Trapping level (pycnocline depth) = -13.1 ft MSL; Mean ebb tide current = 0.304 m/s (0.59 kts) toward the southeast.

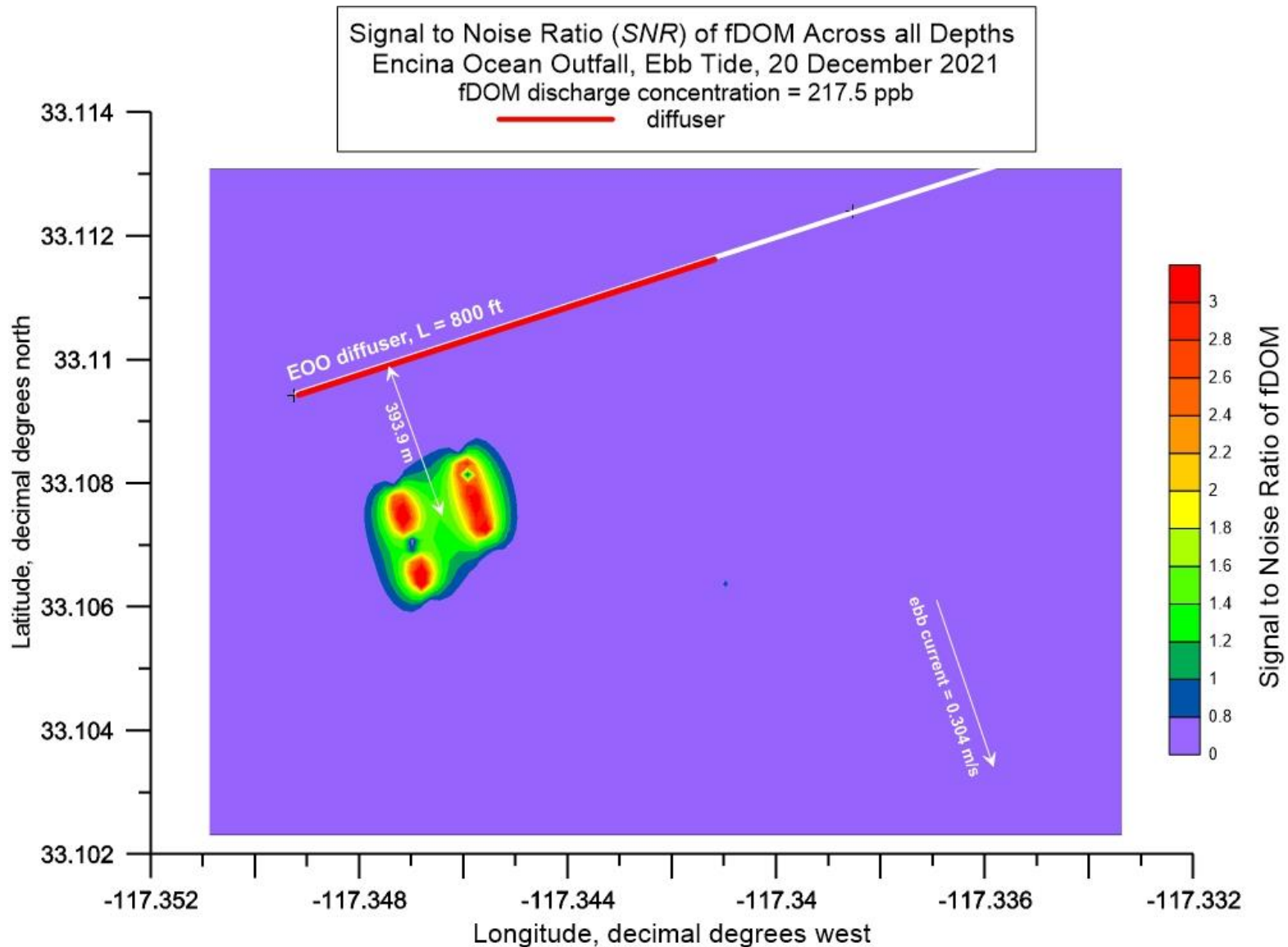


Figure 2.2.10: Full depth contour plot (aka, heat map) of the Signal to Noise Ratio (SNR) of fDOM during AUV surveys of the discharge plume from EOO during ebb tide on 20 December 2021. Average EOO discharge rate = 31.20 mgd during ebb tide; End-of-pipe discharge concentration of fDOM = 217.5 ppb (QSU); End of pipe salinity = 0.96 psu; Trapping level (pycnocline depth) = -13.1 ft MSL; Mean ebb tide current = 0.304 m/s (0.59 kts) toward the southeast.

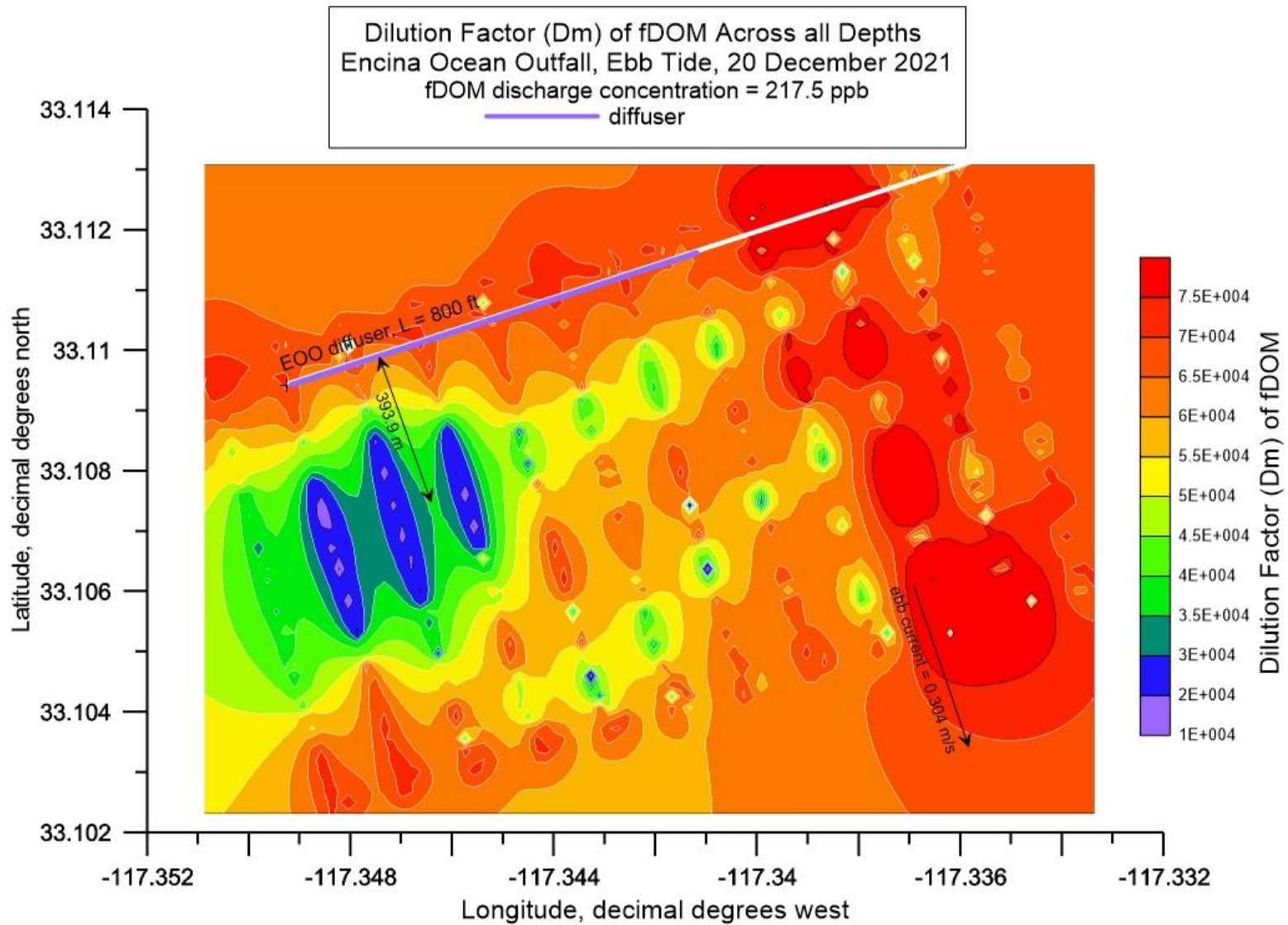


Figure 2.2.11: Full depth contour plot of the (aka, *heat map*) dilution factor (D_{fDOM}) of fDOM during AUV surveys of the discharge plume from EOO during ebb tide on 20 December 2021. Average EOO discharge rate = 31.20 mgd during ebb tide; End-of-pipe discharge concentration of fDOM = 217.5 ppb (QSU); End of pipe salinity = 0.96 psu; Trapping level (pycnocline depth) = -13.1 ft MSL; Mean ebb tide current = 0.304 m/s (0.59 kts) toward the southeast.

EOO effluent would be below quantifiable detection limits for any plume remnants beyond 400 m from the outfall.

Figure 2.2.12 provides the salinity heat map generated from the AUV salinity measurements during the EOO ebb tide survey. Most of the features in the ebb tide salinity heat map range from $S_{(x)} = 33.4$ psu in the core of the plume remnant to as high as $S_{(x)} = 33.55$ psu in the far-field of the EOO diffuser. The far-field depth-averaged salinity from the salinity profile in **Figure 2.2.3** indicates that natural background salinity is $S_{\infty} = 33.48$ psu with a standard deviation of $\sigma = 0.032$ psu. While it seems possible that the $S_{(x)} = 33.4$ psu salinity minimum could be due to salinity depression within the EOO plume remnant, the signal to noise ratio of the salinity features in **Figure 2.2.12** range from only $SNR_S = 0.0020$ to $SNR_S = 0.0021$. Therefore, all the salinity features in **Figure 2.2.12** have signal to noise ratios significantly below the lowest order significance threshold for detection (i.e., $SNR_S \geq 1$) and consequently cannot be associated with suspected plume remnants.

Despite the low signal to noise ratios in the salinity heat map in **Figure 2.2.12**, the fDOM heat map data in **Figure 2.2.9** and the corresponding signal to noise ratio data in **Figure 2.2.10** represent probable evidence of an EOO plume remnant centered 393.9 m downstream of the EOO diffuser in the 0.304 m/s (0.59 kts) ebb tide current. This prompts the question of whether the EOO plume has been detected beyond the point where initial dilution had been completed under the ebb tide current and water column stratification that persisted on 21 December 2021.

We approach this question by performing a Plumes 20 (UM3) initial dilution simulations (see **Table 7**) using actual ebb tide currents of 0.304 m/s (0.59 kts) on 21 December 2021. The solution file listed in **Table 8** indicates that the EOO initial dilution was 439.4:1 at 31.2 mgd.

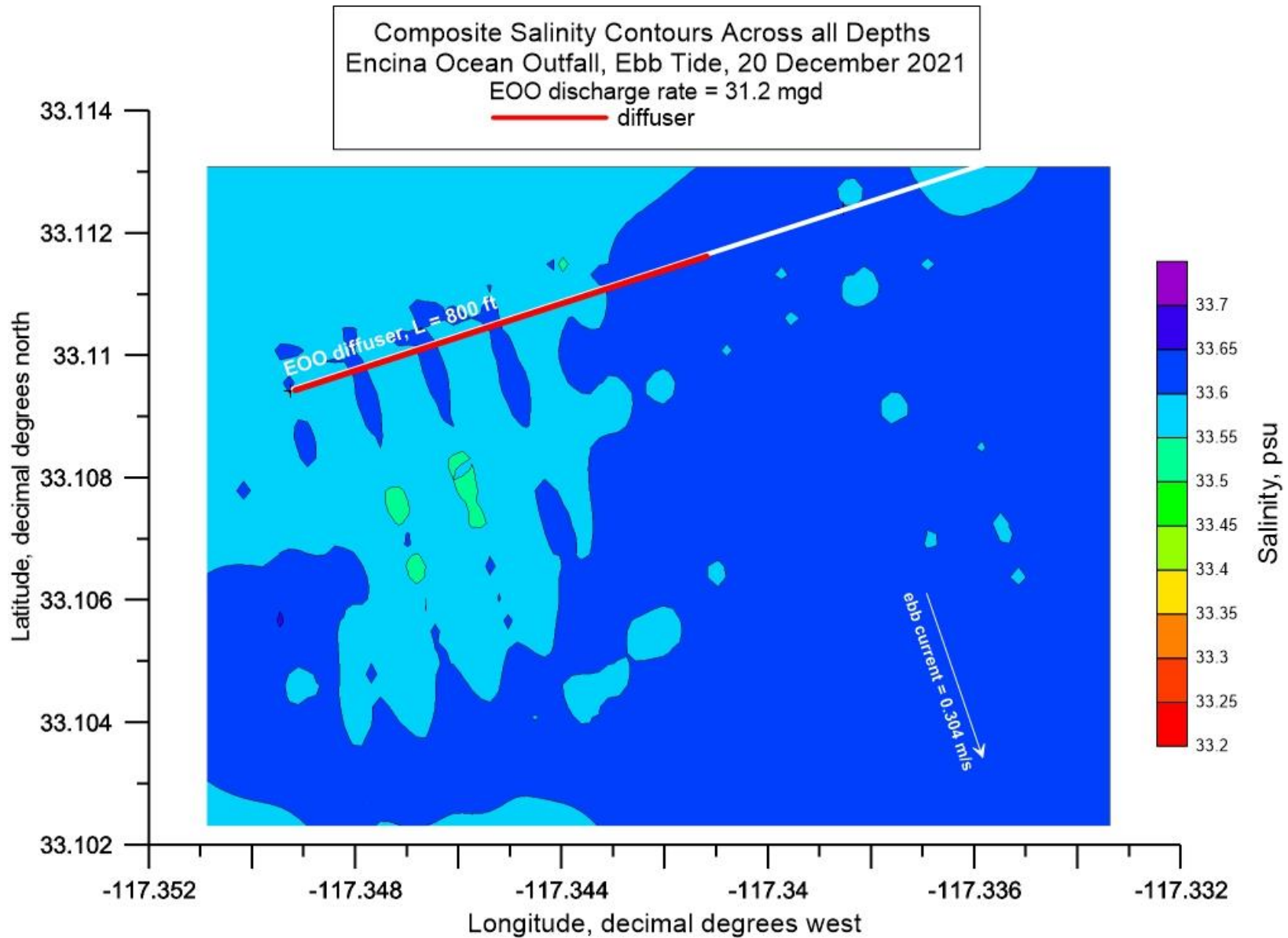


Figure 2.2.12: Full depth composite contour plot (aka, heat map) of AUV measurements of salinity during surveys of the discharge plume from EOO during ebb tide on 20 December 2021. Average EOO discharge rate = 31.20 mgd during ebb tide; End of pipe salinity = 0.96 psu; Trapping level (pycnocline depth) = -13.1 ft MSL; Mean ebb tide current = 0.304 m/s (0.59 kts) toward the southeast.

The Plumes 20 (UM3) solution also indicates that initial dilution under the 21 December 2021 conditions was completed within 197 m of the EOO diffuser. Data presented in the fDOM heat map in [Figure 2.2.9](#) during ebb tide shows the probable presence of an EOO plume remnant approximately 400 m beyond the EOO. This suggests that the EOO plume (under December 2021 conditions) can be detected approximately 200 m beyond the point where initial dilution is complete. Consistent with this hypothesis, fDOM data indicate a dilution ratio in excess of 215:1 in the core of the plume remnant, which is approximately 50% greater than the minimum initial dilution of $D_m = 144:1$ assigned within the current NPDES permit for the EOO (No. CA 0107395, Order No. R9-2018-0059).

On the following flood tide on 20 December 2021, the orange survey box in [Figure 2.2.1](#) was flown by the AUV with accurate repeatability of the outbound and return legs along each of 12 track lines, (cf. [Figure 2.2.14](#)). During this survey, the AUV collected 64,923 separate measurements of salinity and fDOM along a total distance surveyed of 21.2 km. The fDOM heat map generated from these measurements of fDOM concentrations is plotted in [Figure 2.2.15](#), which do not exhibit the banding patterns during the first AUV deployment in September 2021 that were associated with spatial aliasing; displaying instead fDOM features that are similar to those that were mapped during the preceding ebb-tide, (cf. [Figure 2.2.9](#)). The fDOM heat map during flood tide in [Figure 2.2.15](#) displays variations in fDOM concentrations across all depths that range from $fDOM_{(x)} = 0.2$ ppb to 1.3 ppb. These fDOM variations during flood tide also exhibit horizontal structure having high spatial coherence with the EOO diffuser, with a singular, large fDOM feature centered 268.6 m down-drift (north) of the EOO diffuser in which elevated fDOM are in the range of $fDOM_{(x)} = 0.7$ ppb to 1.3 ppb, or 126% to 321% higher than the depth-averaged natural background fDOM concentration, $fDOM_{\infty} = 0.309$ ppb, at control station EOO-Flood (cf. [Figure 2.2.5](#)). Furthermore, with the increased horizontal resolution afforded by the 12 closely spaced track lines in [Figure 2.2.14](#), there is little evidence of spatial aliasing like the repeating banded patterns in the flood tide heat map of [Figure 2.2.15](#). Moreover, the fDOM concentrations in the remainder of the surveyed area outside of this singular elevated fDOM feature are on the order of $fDOM_{\infty} \cong 0.3$ ppb, consistent with the depth-averaged natural background fDOM concentration of $fDOM_{\infty} \cong 0.309$ ppb. Therefore, the primary elevated fDOM feature in [Figure 2.2.15](#) that is centered 268.6 m downstream (north) of the EOO diffuser in the 0.211 m/s (0.41 kt) flood tide current has the spatial coherence, structure, and contrast against natural background to possibly be a remnant of the EOO discharge plume.

Table 7: Plumes 20 (UM3) Initialization of EOO Ebb tide Ambient Conditions on 20 December 2021 with Ambient Current

Project "C:\Plumes20\EOO_Ebb_21Dec2021_1_with-current"	
Model configuration items checked:	
Channel width (m)	100
Start case for graphs	1
Max detailed graphs	10 (limits plots that can overflow memory)
Elevation Projection Plane (deg)	0
Shore vector (m,deg)	not checked
Bacteria model:	Mancini (1978) coliform model
PDS sfc. model heat transfer	Medium
Equation of State	S, T
Similarity Profile	Default profile (k=2.0, ...)
Diffuser port contraction coefficient	1
Light absorption coefficient	0.16
Farfield increment (m)	200
UM3 aspiration coefficient	0.1
Output file:	text output tab
Output each ?? steps	25
Maximum dilution reported	10000
Text output format	Standard
Max vertical reversals	to max rise or fall

/ UM3. 4/19/2022 1:09:10 PM

Case 1; ambient file C:\Plumes20\EOO_Ebb_21Dec2021_1_with-current.001.db; Diffuser table record 1:

Ambient Table:

Depth m	Amb-cur m/s	Amb-dir deg	Amb-sal psu	Amb-tem C	Amb-pol kg/kg	Decay s-1	Far-spnd m/s	Far-dir deg	Disprsn m0.67/s2	Density sigma-T
0.0	0.304	0.0	33.51	15.34	3.0000E-10	0.0	0.0	0.0	0.0	24.76877
3.465	0.304	0.0	33.51	15.34	2.9000E-10	0.0	0.0	0.0	0.0	24.77234
6.389	0.304	0.0	33.51	15.33	2.5000E-10	0.0	0.0	0.0	0.0	24.77418
9.479	0.304	0.0	33.51	15.30	2.8000E-10	0.0	0.0	0.0	0.0	24.78128
12.52	0.304	0.0	33.51	15.28	2.8000E-10	0.0	0.0	0.0	0.0	24.78438
15.53	0.304	0.0	33.51	15.28	2.1000E-10	0.0	0.0	0.0	0.0	24.78515
18.50	0.304	0.0	33.51	15.25	2.5000E-10	0.0	0.0	0.0	0.0	24.79055
21.44	0.304	0.0	33.50	15.23	2.6000E-10	0.0	0.0	0.0	0.0	24.79126
24.48	0.304	0.0	33.41	15.04	2.5000E-10	0.0	0.0	0.0	0.0	24.76392
27.48	0.304	0.0	33.48	14.50	3.0000E-10	0.0	0.0	0.0	0.0	24.93144
30.52	0.304	0.0	33.32	13.82	3.1000E-10	0.0	0.0	0.0	0.0	24.94873
33.47	0.304	0.0	33.12	12.61	2.9000E-10	0.0	0.0	0.0	0.0	25.03897
36.47	0.304	0.0	33.31	12.15	3.1000E-10	0.0	0.0	0.0	0.0	25.26924
39.47	0.304	0.0	33.55	12.42	3.2000E-10	0.0	0.0	0.0	0.0	25.40460
42.55	0.304	0.0	33.53	12.19	3.4000E-10	0.0	0.0	0.0	0.0	25.43855
45.55	0.304	0.0	33.53	12.19	3.7000E-10	0.0	0.0	0.0	0.0	25.43780
48.68	0.304	0.0	33.55	12.08	3.7300E-10	0.0	0.0	0.0	0.0	25.46989

Diffuser Table:

P-dia (in)	Ver angl (deg)	H-Angle (deg)	SourceX (ft)	SourceY (ft)	Ports ()	MZ-dis (m)	Isopth (concent)	P-depth (ft)	Ttl-flo (MGD)	Eff-sal (psu)	Temp (C)	Polutnt (ppb)
2.7750	0.0	0.0	0.0	0.0	138.00	2000.0	0.0	155.75	31.200	0.9600	19.380	217.50

Table 8: Plumes 20 (UM3) Output of EOO Dilution Factor ($D_{F_{DOM}}$) during Ebb Tide on 20 December 2021 with Ambient Current (Final $D_{F_{DOM}}$ solution highlighted in yellow)

Simulation: Froude No: 18.81; Strat No: 3.88E-5; Spcg No: 7.909; k: 8.351; eff den (sigmaT) -0.874719; eff vel 2.539(m/s);

Depth Step	Amb-cur (ft)	Amb-sal (m/s)	P-dia (psu)	Eff-sal (in)	Polutnt (psu)	Dilutn (ppb)	CL-diln (l)	x-posn (l)	y-posn (ft)	Iso (ft)	dia (m)
0	155.8	0.304	33.54	2.775	0.960	217.5	1.000	1.000	0.0	0.0	0.0;
25	155.7	0.304	33.54	4.403	14.05	131.7	1.654	1.000	0.376	0.0	0.1118;
50	155.7	0.304	33.54	6.814	21.66	80.89	2.697	1.348	0.958	0.0	0.1731;
75	155.7	0.304	33.54	10.31	26.30	49.64	4.408	2.204	1.893	0.0	0.2618;
100	155.6	0.304	33.54	15.15	29.13	30.47	7.216	3.608	3.412	0.0	0.3849;
125	155.4	0.304	33.54	21.60	30.85	18.75	11.82	5.911	5.878	0.0	0.5487;
127	155.4	0.304	33.54	22.19	30.96	18.04	12.30	6.149	6.114	0.0	0.5638; merging
150	154.8	0.304	33.54	30.49	31.90	11.59	19.38	10.73	9.943	0.0	0.7744;
175	153.6	0.304	33.54	43.63	32.54	7.214	31.78	21.10	16.17	0.0	1.1083;
200	151.5	0.304	33.54	64.44	32.93	4.547	52.12	34.75	25.26	0.0	1.6369;
225	148.0	0.304	33.53	99.36	33.17	2.920	85.49	56.99	38.83	0.0	2.5239;
250	142.4	0.304	33.53	159.0	33.31	1.924	140.2	93.49	59.72	0.0	4.0388;
275	133.4	0.304	33.54	259.9	33.40	1.308	230.1	153.4	92.82	0.0	6.6016;
293	123.8	0.304	33.42	374.3	33.43	1.015	328.6	219.0	129.9	0.0	9.5075; trap level
300	120.5	0.304	33.33	425.0	33.43	0.941	367.5	245.0	145.5	0.0	10.795;
325	115.9	0.304	33.24	512.6	33.41	0.850	430.1	286.7	179.6	0.0	13.021;
339	115.4	0.304	33.23	526.6	33.40	0.839	439.4	292.9	194.6	0.0	13.376; local maximum rise or fall;

Horiz plane projections in effluent direction: radius(m): 0.0; CL(m): 59.330

Lmz(m): 59.330

forced entrain 1 210.4 12.30 13.38 1.000

Rate sec-1 0.0 dy-1 0.0 kt: 0.0 Amb Sal 33.2259; 1:09:16 PM. amb fills: 4

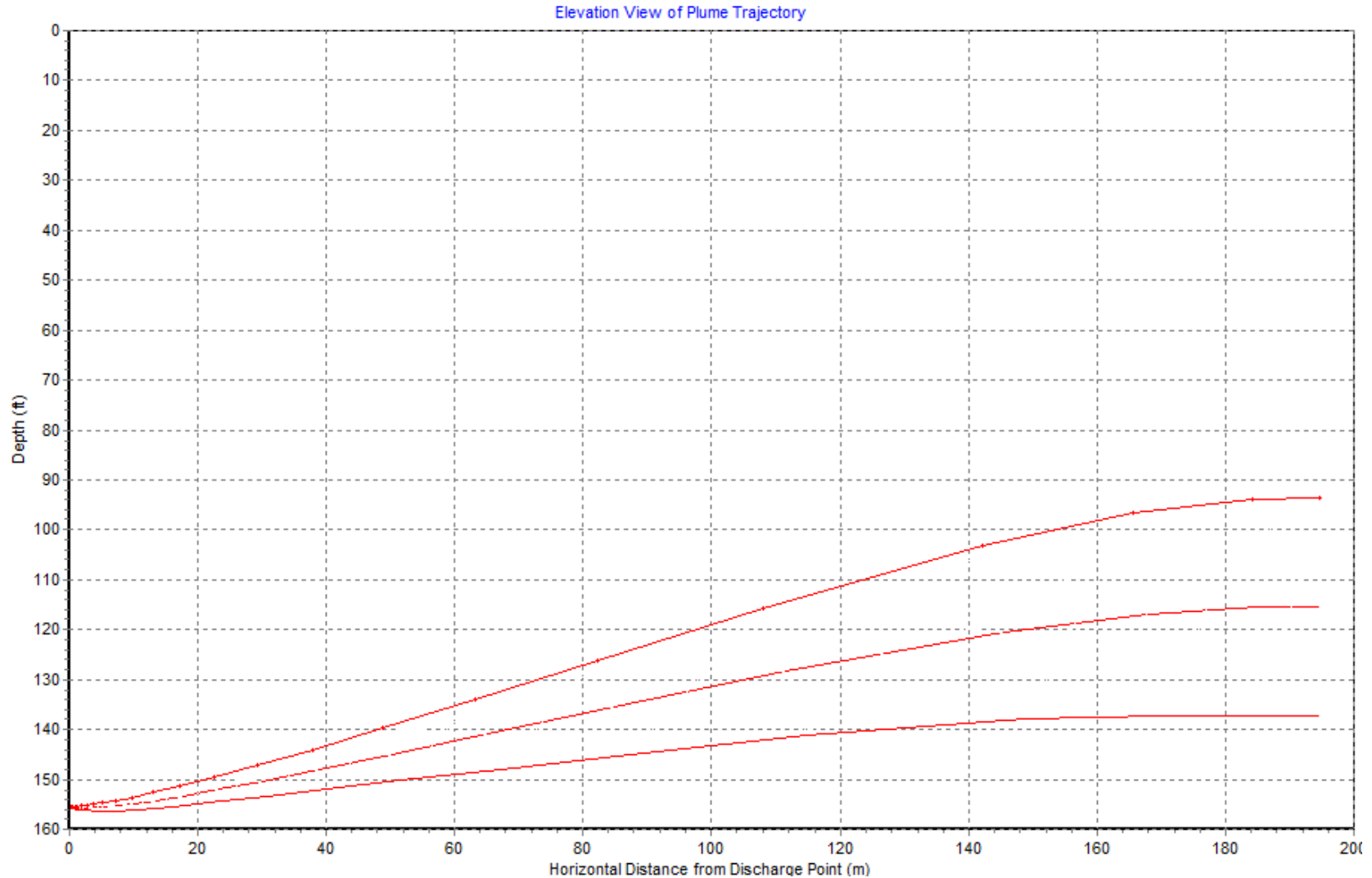


Figure 2.2.13: Plumes 20 solution of discharge plume trajectories for discharges of 31.2 mgd of EOO effluent at a discharge salinity of $S_{(x=0)} = 0.96$ psu, per operating conditions and water mass temperature/salinity profiles during ebb tide on 20 December 2021. Plumes 20 simulation performed based on ambient current = 0.304 m/s per ADCP measurements. For the 20 December 2021 conditions, the ZID (completion of initial dilution) is defined by the maximum horizontal excursion of trajectories from the origin. From the maximum horizontal spreading of the plume, the ZID extends from $X = 0.0$ m to $X = 197$ m so that ZID = 197 m.

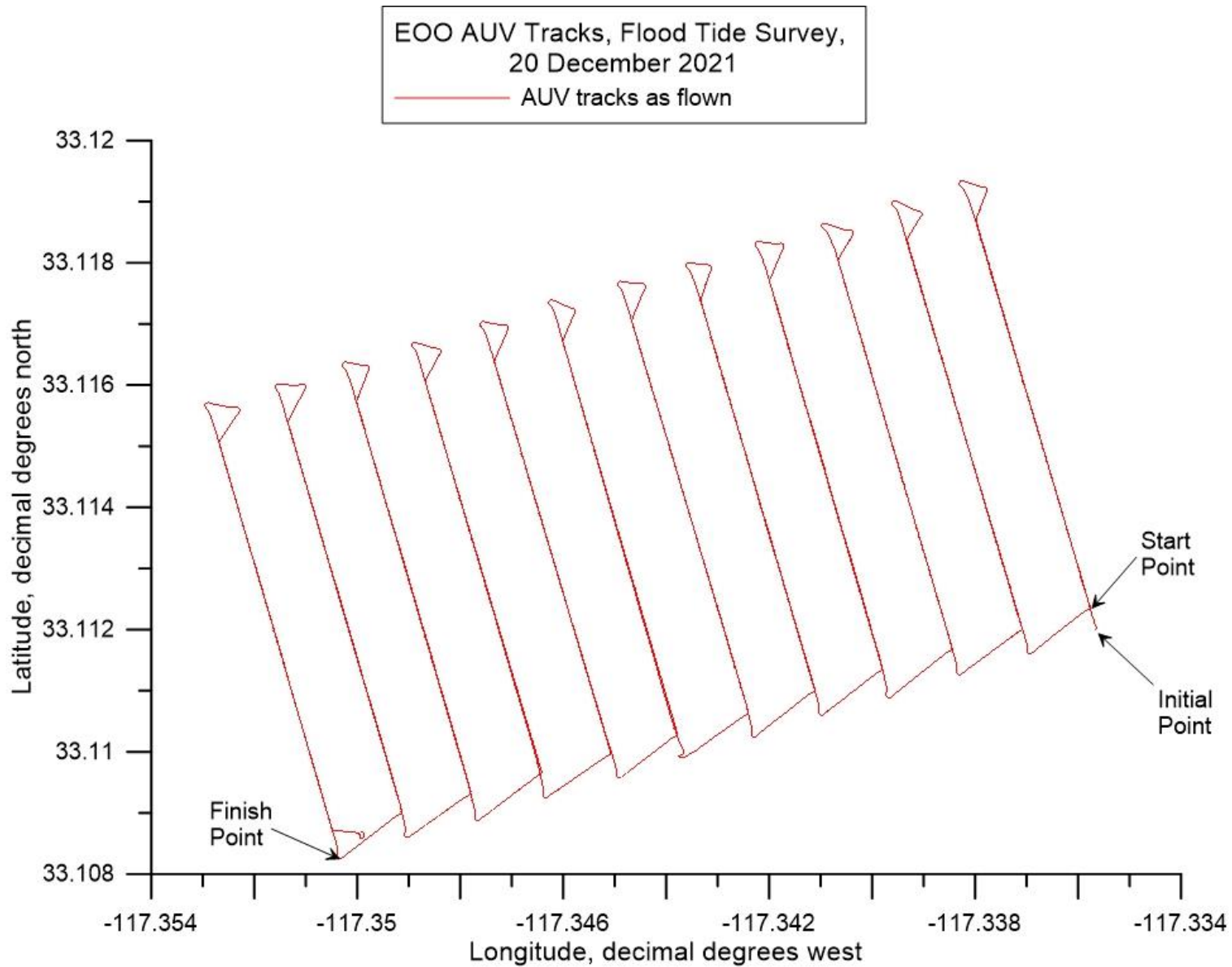


Figure 2.2.14: AUV track lines as flown during flood tide surveys of the discharge plume from EOO during the second deployment, 20 December 2021. The total dimension of the AUV surveyed area on flood tide was 707.1 m in the longshore (shore parallel) direction and 1,414.2 m on the cross-shore (on/off shore) direction or a total surveyed area of approximately 247.1 acres. Note, at 30° N latitude, 1° longitude = 93,453.2 m, while 1° latitude = 110,904.4 m.

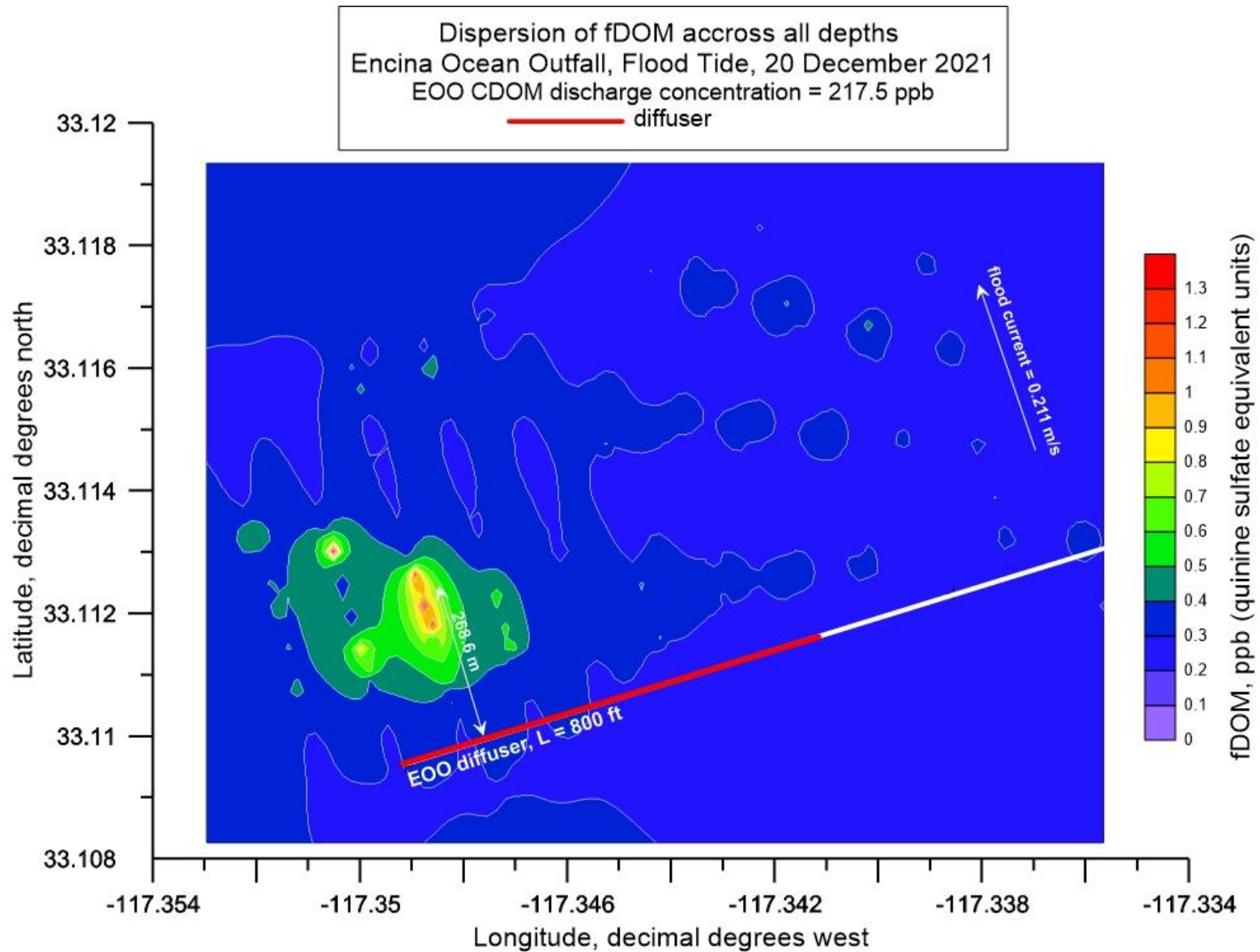


Figure 2.2.15: Full depth contour plot (aka, heat map) of AUV measurements of fDOM during surveys of the discharge plume from EOO during flood tide on 20 December 2021. Average EOO discharge rate =29.70 mgd during flood tide; End-of-pipe discharge concentration of fDOM = 217.5 ppb (QSU); End of pipe salinity = 0.96 psu; Trapping level (pycnocline depth) = -13.1 ft MSL; Mean flood tide current = 0.211 m/s (0.41 kts) toward the northwest.

To verify this hypothesis, the fDOM heat map in **Figure 2.2.15** is converted into a signal to noise ratio heat map in **Figure 2.2.16** by invoking equation (1) to convert the fDOM concentrations in **Figure 2.2.15** into corresponding SNR_{fDOM} patterns. Again, since only fDOM features having signal to noise ratios of unity or greater are possible remnants of the plume, **Figure 2.2.16** has been scaled to filter out features having $SNR_{fDOM} < 0.8$, where features having $0.8 \leq SNR_{fDOM} < 1.0$ are potentially diluted fragments or diluted outer edges of a plume remnants. Inspection of **Figure 2.2.16** reveals that the signal to noise ratio of this suspected plume remnant ranges from $SNR_{fDOM} \cong 1.1$ along its outer perimeter, to as high as $SNR_{fDOM} \cong 2.6$ in its inner core 268.6 m downstream (north) of the EOO diffuser. Therefore, the elevated fDOM concentrations found centered 268.6 m downstream of the EOO diffuser satisfy the lowest order significance threshold for detection, (i.e., $SNR_{fDOM} \geq 1$). Based on this detection metric, we conclude the EOO discharge plume has been located 268.6 m downstream (north) of the EOO diffuser during flood tide on 20 December 2021.

To assess minimum dilution levels in the EOO plume remnant, the SNR_{fDOM} heat map in **Figure 2.1.16** was transposed into a dilution heat map in **Figure 2.2.17** using equation (2) on the basis that the initial fDOM concentration is $fDOM_{(x=0)} = 217.5$ ppb. Equation (2) teaches that the regions of high SNR will correspond to regions of low values of D_{fDOM} relative to the dilution elsewhere within the AUV survey area. **Figure 2.2.17** indicates that the dilution factor (D_{fDOM}) for the fDOM features would be no less than $D_{fDOM} = 269:1$ in the core of the plume remnant, or a factor of 1.9 times greater than the initial dilution of $D_m = 144:1$ assigned within the current NPDES permit (No. CA0107395; Order No. RS-2018-0059). The dilution along the outer perimeter of the plume remnant ranges from 638:1 to as much as 10,000:1. Elsewhere in the wake of the EOO diffuser, dilutions range from $D_{fDOM} = 30,000:1$ to 70,000:1 so that any regulated or unregulated toxic EOO effluent constituents would be below quantifiable detection limits within any plume remnants beyond 330 m from the outfall.

Figure 2.2.18 provides the salinity heat map generated from the AUV salinity measurements during the EOO flood tide survey. Most of the features in the ebb tide salinity heat map range from $S_{(x)} = 33.45$ psu in the core of the plume remnant to as high as $S_{(x)} = 33.6$ psu in the far-field of the EOO diffuser. The far-field depth-averaged salinity in **Figure 2.2.3** indicates that natural background salinity is $S_{\infty} = 33.48$ psu with a standard deviation of $\sigma = 0.032$ psu. While it seems possible that the $S_{(x)} = 33.45$ psu salinity minimum could be due to salinity depression within the EOO plume remnant, the signal to noise ratio of the salinity features in **Figure 2.2.19** range from only $SNR_S = 0.0009$ to $SNR_S = 0.0036$. Therefore, all the salinity features in **Figure 2.2.18** have signal to noise ratios significantly below the lowest order significance threshold for detection (i.e., $SNR_S \geq 1$) and consequently cannot be associated with suspected plume remnants.

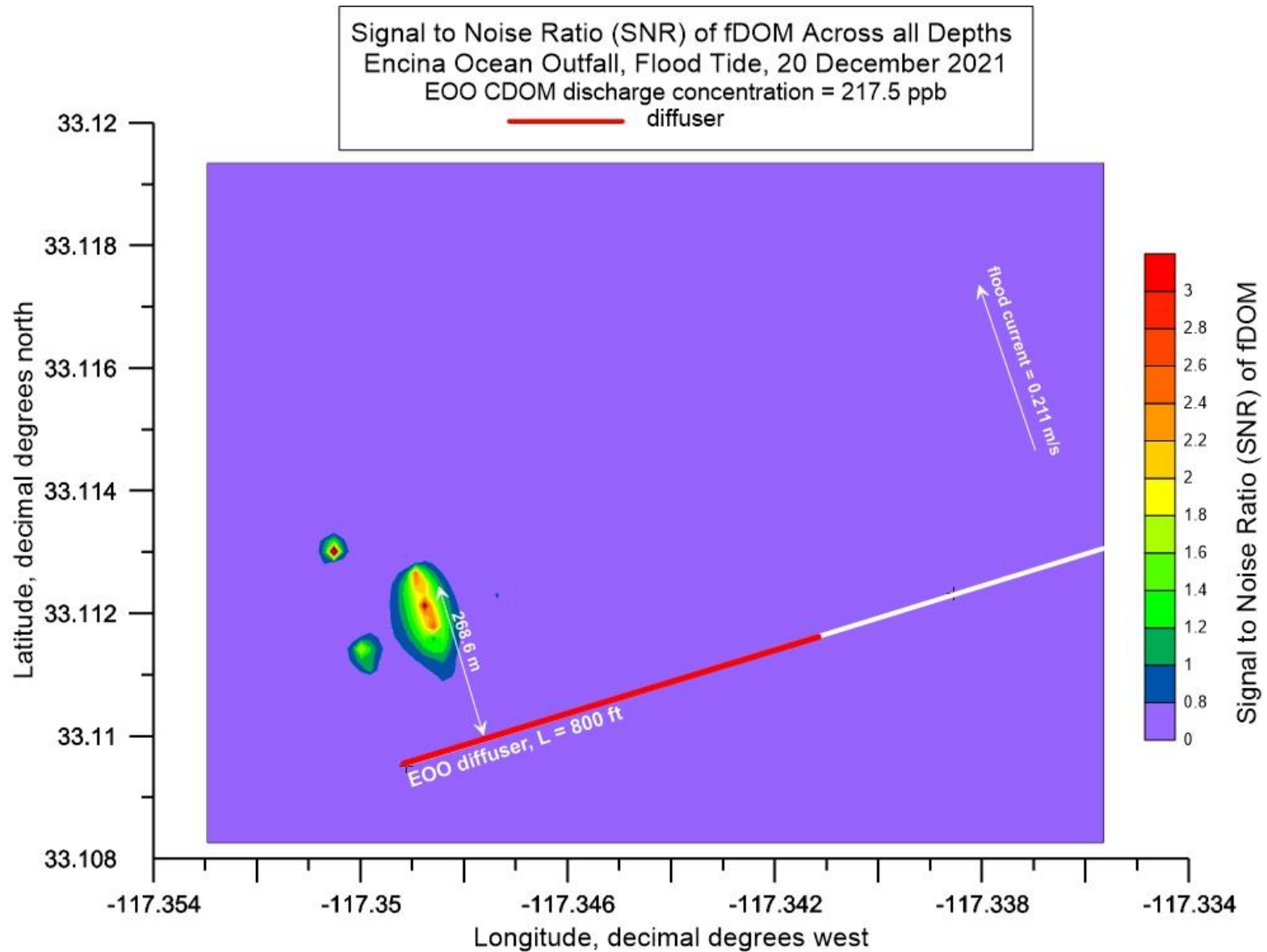


Figure 2.2.16: Full depth contour plot (aka, heat map) of the Signal to Noise Ratio (SNR) of fDOM during AUV surveys of the discharge plume from EOO during flood tide on 20 December 2021. Average EOO discharge rate = 29.70 mgd during flood tide; End-of-pipe discharge concentration of fDOM = 217.5 ppb (QSU); End of pipe salinity = 0.96 psu; Trapping level (pycnocline depth) = -13.1 ft MSL; Mean flood tide current = 0.211 m/s (0.41 kts) toward the northwest.

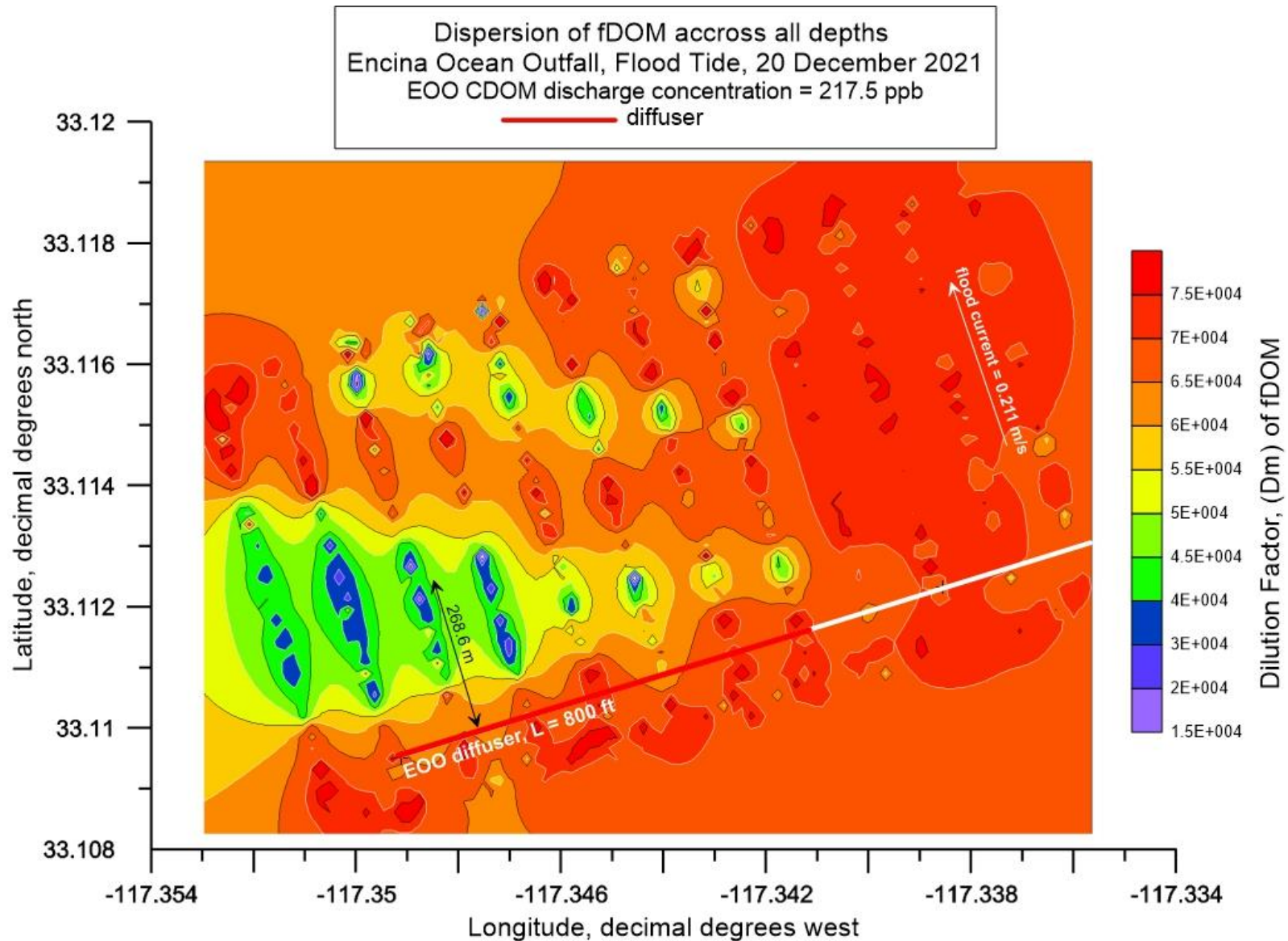


Figure 2.2.17: Full depth contour plot (aka, heat map) of the Dilution Factor (D_{fDOM}) of fDOM during AUV surveys of the discharge plume from EOO during flood tide on 20 December 2021. Average EOO discharge rate = 29.70 mgd during flood tide; End-of-pipe discharge concentration of fDOM = 217.5 ppb (QSU); End of pipe salinity = 0.96 psu; Trapping level (pycnocline depth) = -13.1 ft MSL; Mean flood tide current = 0.211 m/s (0.41 kts) toward the northwest.

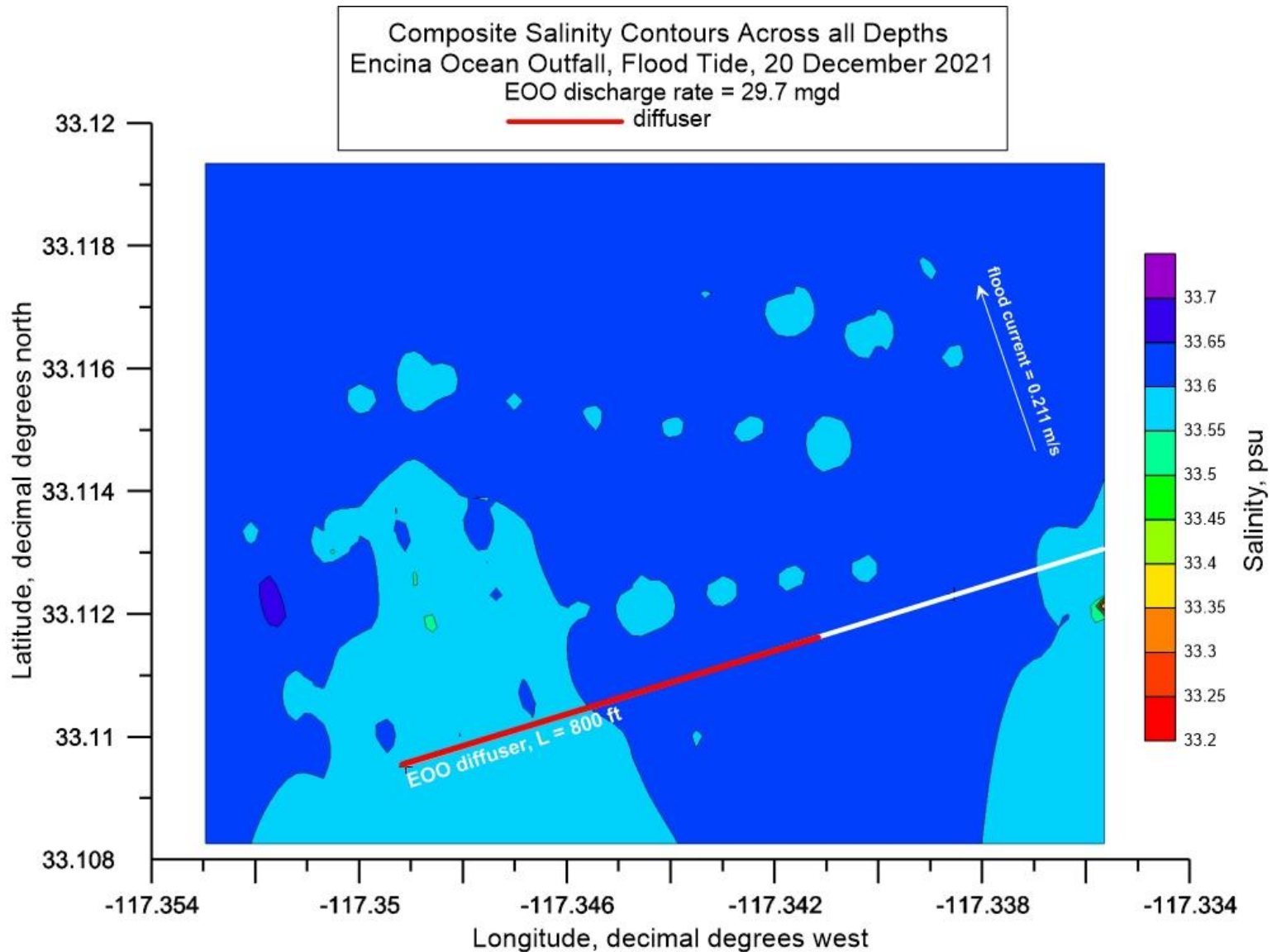


Figure 2.2.18: Full depth composite contour plot (aka, heat map) of salinity during AUV surveys of the discharge plume from EOO during flood tide on 20 December 2021. Average EOO discharge rate =29.70 mgd during flood tide; End of pipe salinity = 0.96 psu; Trapping level (pycnocline depth) = -13.1 ft MSL; Mean ebb tide current = 0.211 m/s (0.41 kts) toward the northwest.

Despite the low SNR in the salinity heat map in **Figure 2.2.18**, the fDOM heat map data in **Figure 2.2.15** and the corresponding SNR data in **Figure 2.2.16** represent probable evidence of an EOO plume remnant centered 268.6 m downstream of the EOO diffuser in the 0.211 m/s (0.41 kt) flood tide current. This prompts the question of whether the EOO plume is detected before or after initial dilution is complete. This question was initially addressed by performing a Plumes 20 (UM3) initial dilution simulation (see **Table 9**) based on the actual flood tide currents of 0.211 m/s (0.41 kt) on 20 December 2021. As shown in the solution file listed in **Table 10**, the EOO initial dilution for this case was simulated at 273.8:1 at a discharge flow of 29.7 mgd.. The simulation also demonstrates that initial dilution under these conditions was completed within approximately 120 m of the EOO diffuser, or about 45% of the horizontal excursion of the EOO plume remnant found in the fDOM heat map in **Figure 2.2.15** during flood tide. Therefore, the plume tracking study of the EOO discharge during flood tide on 20 December 2021 indicates that after initial dilution, the discharge plume may be detectable several hundred meters beyond the outfall diffuser, but at this distance dilution ratios are in excess of 638:1 and can exceed 10,000:1.

Table 9: Plumes 20 (UM3) Initialization of EOO Flood tide Ambient Conditions on 20 December 2021 with Ambient Current

Project "C:\Plumes20\EOO_Flood_21Dec2021_1_with-curr"nt"	
Model configuration items checked:	
Channel width (m)	100
Start case for graphs	1
Max detailed graphs	10 (limits plots that can overflow memory)
Elevation Projection Plane (deg)	0
Shore vector (m,deg)	not checked
Bacteria model:	Mancini (1978) coliform model
PDS sfc. model heat transfer	Medium
Equation of State	S, T
Similarity Profile	Default profile (k=2.0, ...)
Diffuser port contraction coefficient	1
Light absorption coefficient	0.16
Farfield increment (m)	200
UM3 aspiration coefficient	0.1
Output file:	text output tab
Output each ?? steps	25
Maximum dilution reported	10000
Text output format	Standard
Max vertical reversals	to max rise or fall

/ UM3. 4/18/2022 3:59:52 PM

Case 1; ambient file C:\Plumes20\EOO_Flood_21Dec2021_1_with-current.001.db; Diffuser table record 1:

Ambient Table:

Depth m	Amb-cur m/s	Amb-dir deg	Amb-sal Psu	Amb-tem C	Amb-pol kg/kg	Decay s-1	Far-spd m/s	Far-dir deg	Disprsn m0.67/s2	Density sigma-T
0.0	0.211	0.0	33.50	15.19	3.4000E-10	0.0	0.0	0.0	0.0	24.79668
3.490	0.211	0.0	33.51	15.17	3.2000E-10	0.0	0.0	0.0	0.0	24.80573
6.487	0.211	0.0	33.51	15.17	3.1000E-10	0.0	0.0	0.0	0.0	24.80744
9.540	0.211	0.0	33.51	15.16	3.1000E-10	0.0	0.0	0.0	0.0	24.80995
12.54	0.211	0.0	33.51	15.16	3.0000E-10	0.0	0.0	0.0	0.0	24.81068
15.56	0.211	0.0	33.51	15.15	3.3000E-10	0.0	0.0	0.0	0.0	24.81273
18.48	0.211	0.0	33.50	15.13	3.2000E-10	0.0	0.0	0.0	0.0	24.81177

Depth m	Amb-cur m/s	Amb-dir deg	Amb-sal Psu	Amb-tem C	Amb-pol kg/kg	Decay s-1	Far-spd m/s	Far-dir deg	Disprsn m0.67/s2	Density sigma-T
21.48	0.211	0.0	33.50	15.11	3.1000E-10	0.0	0.0	0.0	0.0	24.81839
24.44	0.211	0.0	33.48	14.99	3.2000E-10	0.0	0.0	0.0	0.0	24.82382
27.50	0.211	0.0	33.49	14.69	3.0900E-10	0.0	0.0	0.0	0.0	24.89472
30.57	0.211	0.0	33.46	14.35	3.3000E-10	0.0	0.0	0.0	0.0	24.94822
33.46	0.211	0.0	33.36	14.04	3.1000E-10	0.0	0.0	0.0	0.0	24.93718
36.47	0.211	0.0	33.37	13.02	3.5000E-10	0.0	0.0	0.0	0.0	25.15306
39.44	0.211	0.0	33.43	12.53	3.3000E-10	0.0	0.0	0.0	0.0	25.29416
42.53	0.211	0.0	33.53	12.19	3.2000E-10	0.0	0.0	0.0	0.0	25.43855
45.46	0.211	0.0	33.57	11.83	2.8000E-10	0.0	0.0	0.0	0.0	25.53567
48.68	0.211	0.0	33.58	11.80	3.2000E-10	0.0	0.0	0.0	0.0	25.55021

Diffuser Table:

P-dia (in)	Ver angl (deg)	H-Angle (deg)	SourceX (ft)	SourceY (ft)	Ports ()	MZ-dis (m)	Isoplth (concent)	P-depth (ft)	Ttl-flo (MGD)	Eff-sal (psu)	Temp (C)	Polutnt (ppb)
2.7750	0.0	0.0	0.0	0.0	138.00	2000.0	0.0	155.75	29.700	0.9600	19.380	217.50

Table 10: Plumes 20 (UM3) Output of EOO Dilution Factor (D_{fDOM}) during Flood Tide on 20 December 2021 with Ambient Current (Final D_{fDOM} solution highlighted in yellow)

Simulation: Froude No: 17.87; Strat No: 4.20E-5; Spcg No: 7.909; k: 11.45; eff den (sigmaT) -0.874719; eff vel 2.417(m/s);

Depth Step	Amb-cur (ft)	Amb-sal (m/s)	P-dia (psu)	Eff-sal (in)	Polutnt (psu)	Dilutn (ppb)	CL- ()	diln ()	x- posn (ft)	y- posn (ft)	Iso dia (m)
0	155.8	0.211	33.58	2.775	0.960	217.5	1.000	1.000	0.0	0.0	0.07049;
25	155.7	0.211	33.58	4.444	14.05	131.7	1.653	1.000	0.374	0.0	0.1129;
50	155.7	0.211	33.58	6.971	21.68	80.89	2.695	1.348	0.957	0.0	0.1771;
75	155.7	0.211	33.58	10.73	26.32	49.61	4.406	2.203	1.889	0.0	0.2726;
100	155.6	0.211	33.58	16.10	29.16	30.43	7.212	3.606	3.386	0.0	0.4088;
121	155.4	0.211	33.58	22.08	30.66	20.21	10.92	5.459	5.316	0.0	0.5609; merging;
125	155.3	0.211	33.58	23.42	30.88	18.69	11.82	6.008	5.784	0.0	0.5948;
150	154.4	0.211	33.58	33.93	31.94	11.53	19.37	11.22	9.781	0.0	0.8619;
175	152.7	0.211	33.58	49.96	32.58	7.148	31.76	21.17	15.43	0.0	1.2689;
200	149.7	0.211	33.57	76.20	32.97	4.474	52.09	34.73	23.37	0.0	1.9355;
225	144.7	0.211	33.56	121.4	33.20	2.842	85.44	56.96	35.00	0.0	3.0837;
250	136.9	0.211	33.51	201.3	33.33	1.858	140.2	93.44	53.26	0.0	5.1126;
265	130.7	0.211	33.45	277.3	33.37	1.473	187.5	125.0	69.76	0.0	7.0433; trap level;
275	127.7	0.211	33.42	324.0	33.38	1.336	213.3	142.2	79.26	0.0	8.2287;
300	123.4	0.211	33.40	402.1	33.38	1.176	254.3	169.5	98.79	0.0	10.214;
325	121.8	0.211	33.39	438.7	33.38	1.121	272.4	181.6	116.2	0.0	11.143;
331	121.8	0.211	33.39	441.5	33.38	1.118	273.8	182.5	120.3	0.0	11.215; local maximum rise or fall;

Horiz plane projections in effluent direction: radius(m): 0.0; CL(m): 36.666

Lmz(m): 36.666

forced entrain 1 129.2 10.36 11.21 1.000

Rate sec-1 0.0 dy-1 0.0 kt: 0.0 Amb Sal 33.3863;

3:59:52 PM. amb fills: 4

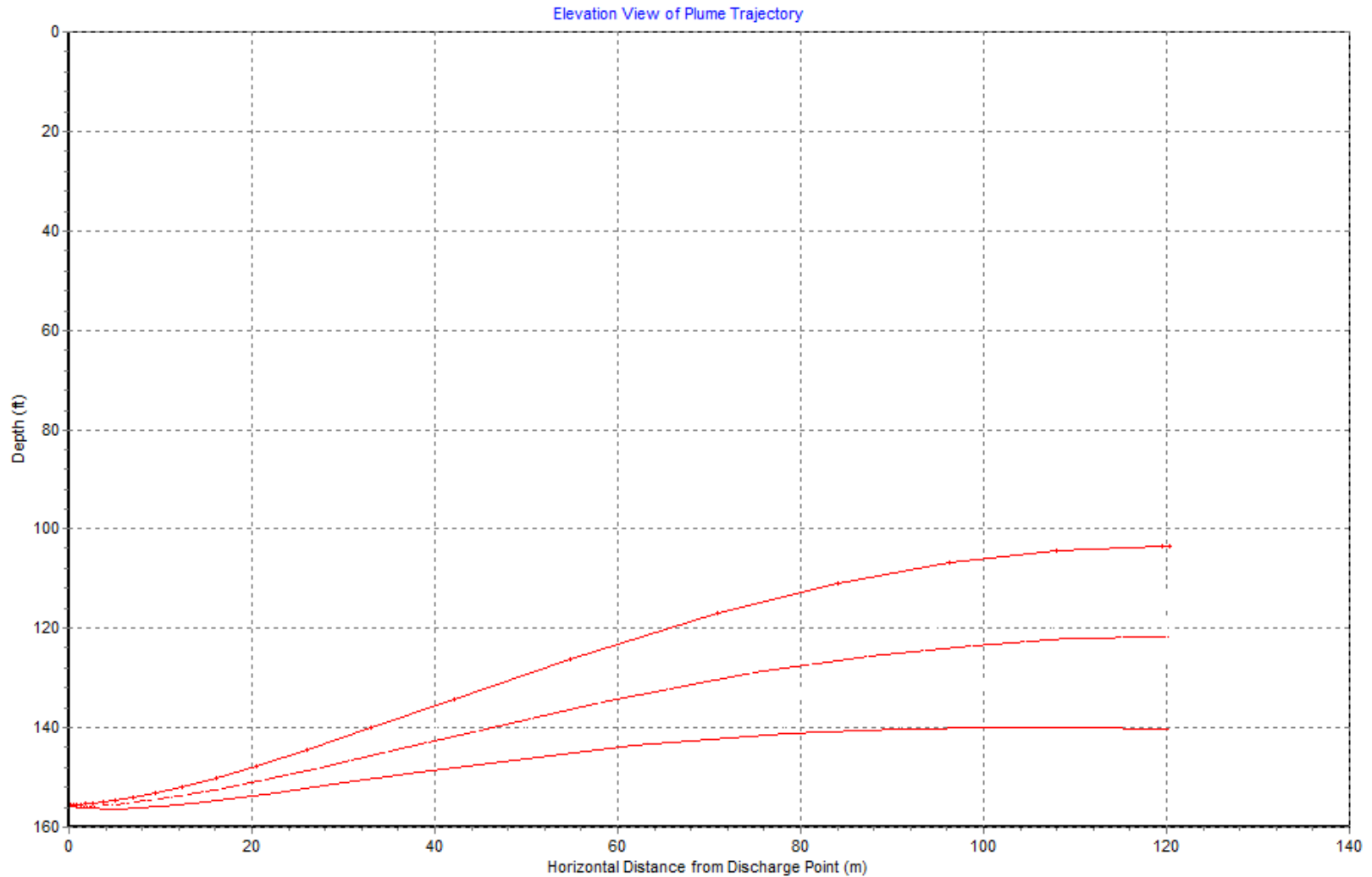


Figure 2.2.19: Plumes 20 solution of discharge plume trajectories for discharges of 29.7 mgd of EOO effluent at a discharge salinity of $S_{(x=0)} = 0.96$ psu, per operating conditions and water mass temperature/salinity profiles during flood tide on 20 December 2021. Plumes 20 simulation performed based on ambient current = 0.211 m/s per ADCP measurements. For the 20 December 2021 conditions, the ZID (zone within which initial dilution is completed) is defined by the maximum horizontal excursion of trajectories from the origin. From the maximum horizontal spreading of the plume, the ZID extends from $X = 0.0$ m to $X = 120$ m so that $ZID = 120$

2.3 THIRD EOO DEPLOYMENT - 2 MARCH 2022

The design of the EOO survey boxes was slightly modified for the third AUV deployment on 2 March 2022. The patterns of the fDOM features were spatially coherent with the EOO diffuser. Because of this and the fact that the patterns of the fDOM features that had SNR's exceeding unity did not extend beyond 300 to 400 m from the diffuser in the heat maps of the second deployments, it was decided to create 100 m of overlap between the ebb-tide and flood-tide survey boxes in the long-shore direction in order to increase resolution of suspected plume remnants. Within each overlapping ebb-tide and flood-tide survey box, the same track line pattern used during the second AUV deployments in December 2021 were retained, with 12 shore parallel track lines at 108.8 m spacings spread across 1,414.2 m in the cross-shore (on/off shore) direction with each track line measuring 707.1 m in length along the longshore (shore parallel) direction. This arrangement was found in the second EOO deployment to provide sufficient horizontal resolution to suppress spatial aliasing of the fDOM sampling. The modified survey plan with overlapping ebb and flood tide survey boxes over the EOO outfall is shown in [Figure 2.3.1](#), where again the flood tide box shown in orange and the ebb tide box is shown in yellow. The numbers of stationary water column monitoring stations (where CTD casts and ADCP velocity profiles are taken) remained the same as during the second deployment on 20 December 2021, with 18 stations distributed along the 160 ft and 60 ft depth contours (shown as green circles in [Figure 2.3.1](#)). The total dimension of the AUV surveyed area on either ebb or flood tide was 707.1 m in the longshore (shore parallel) direction and 1,414.2 m on the cross-shore (on/off shore) direction. However, the total area surveyed during both ebb and flood tide is reduced from 494.2 acres during the second deployment to 459.3 acres during the third deployment due to the 100 m of overlap between the ebb-tide and flood-tide survey boxes.

As practiced during the first and second AUV deployments in September and December 2021, the new survey boxes in [Figure 2.3.1](#), were searched twice for the presence of the EOO plume, (i.e., out and return). As before, the AUV is flown along a dolphin-style flight path when transiting outbound with the current, i.e., a yo-yo flight path diving and ascending through the water column between the seabed and an apex halfway between the sea surface and the pycnocline, (cf. [Figure 1.2.2](#)) On the return legs of each track line, (against the current) the AUV is flown at a constant depth immediately beneath the pycnocline (trapping level) where the maximum horizontal dispersion of the plume is expected, (cf. Baumgartner, 1994; Frick et al., 2003). Altogether, the AUV covers a distance of about 20.0 kilometers in about 5 hours within each survey box which is roughly the endurance limit of the AUV with fully charged batteries. The survey period is centered within each ebb or flood tide interval of 6.2 hours. The AUV batteries are changed during the 1.2 hour interval around slack water between ebb and flood tide intervals, allowing for AUV surveys of the EOO over a complete semi-diurnal tide cycle.

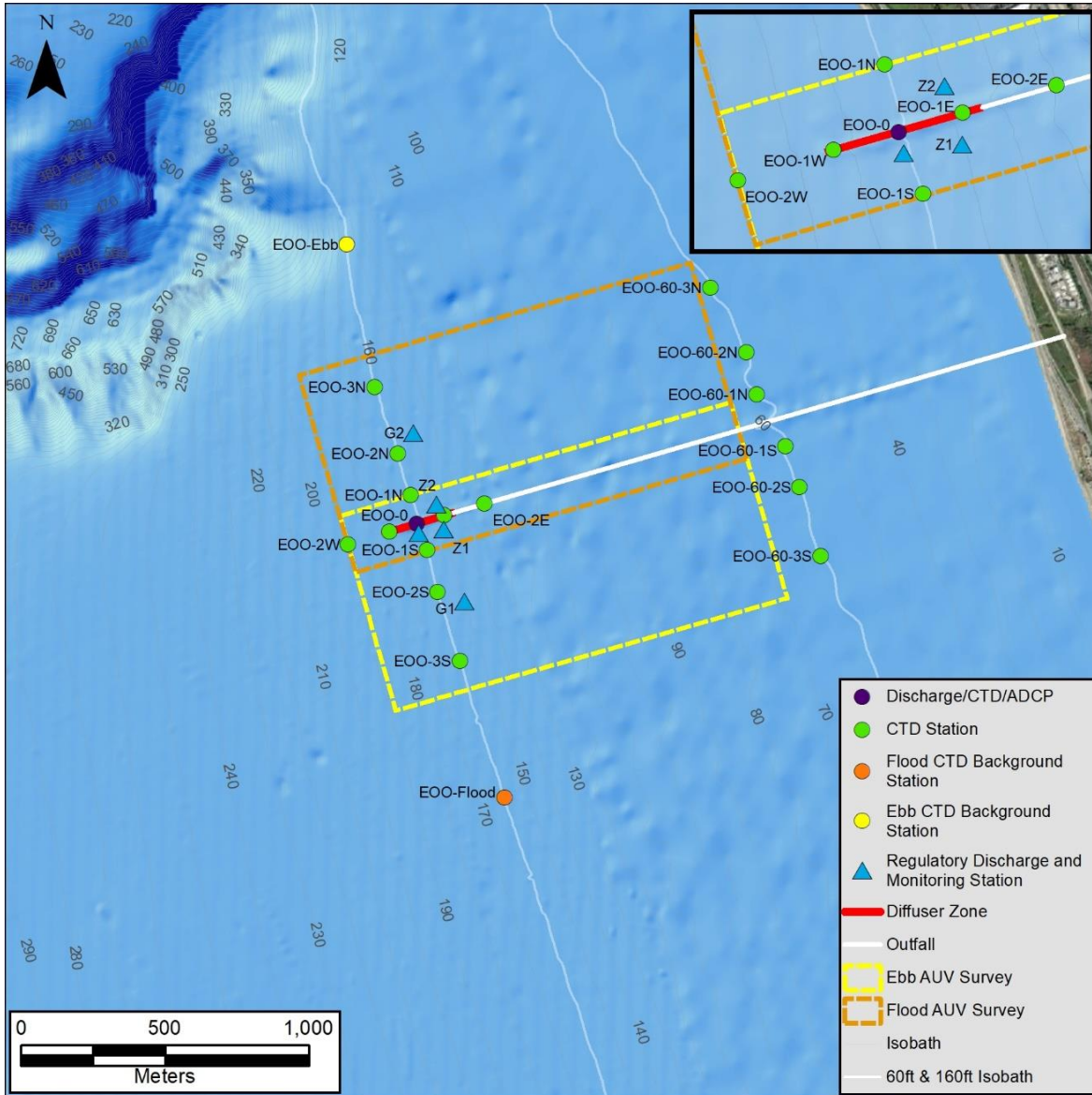


Figure 2.3.1: EOO Survey boxes and sampling stations for the third AUV deployment, 1-2 March 2022

The 18 stationary water column monitoring stations are distributed between the 160 ft and 60 ft depth contours around the EOO, and provide vertical profiles of salinity, temperature, and fDOM water mass properties immediately prior to and during the AUV surveys. Measurements from the control stations EOO-Ebb and EOO-Flood provide far-field measurements of natural background (ambient) water-mass properties (salinity, temperature, and fDOM). The measurements of the fDOM at the 18 stationary monitoring stations were in units of RFU which were converted to QSU fDOM units using the second order polynomial in [Figure 1.3.1](#).

It was critical to the plume tracking effort to program the AUV to fly directly beneath the pycnocline during the return leg (against the current) along each of the 12 track lines within the ebb and flood survey boxes shown in [Figure 2.3.1](#). To locate the depth of the pycnocline, the CTD casts were performed prior to the

AUV survey on 1 March 2022 at monitoring stations EOO-Ebb and EOO-Flood and quickly processed to determine the salinity and temperature changes with depth, (cf. [Figure 2.3.2](#)). These CTD data showed a cold bottom layer with temperatures ranging from 11.4° C at the seabed, warming rapidly to 13° C at 3 m above the seabed, and then warming almost linearly to 14.7° C at the sea surface. The salinity reached 33.7 ppt near the seabed, declining to 33.48 ppt at about a depth of -27m MSL and then remained nearly constant between -27 m depth and the sea surface. Consequently, the density profile during the third AUV deployment was more typical of a continuously stratified water column rather than a two layer system as prevailed during the first and second deployments with a cold bottom layer and warm surface mixed layer. Consequently, the trapping level was deep, at a depth of -26.9 m (-88.26 ft) MSL, which is more typical of a worst-case dilution scenario, because initial dilution is arrested relatively close to the seabed. Based on this finding, the AUV was programmed on its outbound dolphin-style legs (with the current) for dive cycle apex points set halfway between the trapping level and the sea surface at a depth of the pycnocline at a depth of -13.45 m (-44.1 ft) MSL and dive cycle bottoming points set at 2 m (-6.6 ft) above the seabed. The Iver3 AUV uses its bottom-locking sonar to determine the distance above the local seabed at any location within the survey box. Along the return leg of each track line (flown against the current), the AUV was programmed to fly at a constant depth of -15.5 m depth (-50.8 ft) MSL.

At the time of the ebb tide AUV survey on 2 March 2022, the EOO was discharging 27.6 mgd of wastewater during ebb tide with an average daily discharge salinity of 0.82 psu and an average daily fDOM discharge concentration of 261.8 ppb (QSU), based on shoreside monitoring of the EOO effluent, (see tabulations of EOO shoreside monitoring data in Appendix-A). Later in the day during flood tide the EOO discharge rates decreased slightly to 24.2 mgd, while average discharge salinity and fDOM concentrations remained unchanged, (cf. Appendix-A). The average EOO discharge concentrations of fDOM are significantly higher (by more than 2 orders of magnitude) than the natural ocean background concentrations of fDOM measured at far-field control stations, EOO-Ebb and EOO-Flood, which were profiled twice during each ebb and flood tide event on 2 March 2022. Vertical profiles of natural background fDOM measured during ebb tide at EOO-Ebb (cf. [Figure 2.3.3](#)) exhibited depth-averaged concentrations ranging between 0.237 ppb and 0.239 ppb. Natural background fDOM measured later during flood tide on 2 March 2022 at EOO-Flood (cf. [Figure 2.3.4](#)) declined to depth-averaged concentrations ranging between 0.171 ppb and 0.170 ppb. These are relatively low natural background fDOM concentrations, likely due to the absence of winter rains prior to the third deployment, and reduced biological activity during short winter daylight conditions. Consequently, the signal to noise ratio of the fDOM plume observable at any point of discharge along the EOO diffuser ranges between $SNR_{fDOM} = 1,094$ and $SNR_{fDOM} = 1,539$, based on the depth averaged concentrations of natural background fDOM measured at far-field control stations, EOO-Ebb and EOO-Flood ([Figure 2.3.3](#) and [Figure 2.3.4](#)), applied to equation (1). While profiles of natural background fDOM concentrations measured during both ebb and flood tide showed both random variations (noise) with some general vertical structure (with higher concentration near the surface during ebb tide, and declining near the surface during flood tide), the standard deviations around the depth averaged fDOM concentrations were small, ranging between $\sigma = 0.019$ ppb and $\sigma = 0.061$ ppb, (cf. [Figure 2.3.3](#) and [Figure 2.3.4](#)).

Mean ebb tide currents on 2 March 2022 at the far-field control station, EOO-Ebb, were strong, 0.526 m/s (1.02 kts) toward the southeast, based on acoustic Doppler profiling (ADCP) at far field monitoring station, EOO-Ebb, (cf. [Figure 2.3.5](#)) located up-drift of the yellow AUV survey box shown in [Figure 2.3.1](#). Mean current speeds reaching 1 knot are not typical of tidal currents in the Southern California Bight. An approaching extratropical frontal cyclone from the northwest on 2 March 2022 imparted a considerable wind-driven component to the local coastal currents, which when combined with the ebb tidal component induced a large net shore-parallel drift to the EOO discharge plume directed toward the southeast. However, there are other transient short-lived current oscillations in the ebb tide ADCP time series record on 2 March 2022 that reached 1.3 m/s (1.53 kts), cf. [Figure 2.3.5](#). The current direction data in the ADCP record indicates these spikes of higher oscillatory currents were directed cross-shore, indicating they were due to shoaling surface gravity waves from the approaching storm, possibly combined with internal waves. Because of the oscillatory nature of these current spikes, they produce no net drift of the EOO discharge plume, but merely serve to smear the plume or break off pieces from the main body of the plume and smear or disperse those pieces in the cross-shore direction. ADCP measurements of currents at far field monitoring station, EOO-Flood, (cf. [Figure 2.3.6](#)) find that mean flood tide currents on 2 March 2022 were considerably less than the mean ebb tide currents, reaching only 0.261 m/s (0.51 kts) directed toward the northwest. This sharp decline in the flood tide current ADCP record relative to the ebb tide current record earlier in the day is due to combination of factors. One of these factors is the flood tidal current component directed toward the northwest is flowing against the wind driven current component directed toward the southeast. The other factor is the fact that tidal currents along the coastline of the lower Southern California Bight do not reverse symmetrically between ebb and flood tide, but rather are *ebb-tide dominant*, imparting a net southeasterly drift to the EOO discharge plume over a complete tidal day of 24.83 hrs. Transient oscillatory current spikes in the flood tide ADCP current record on 2 March 2022 were non the less significant, reaching 1.05 m/s (2.04 kts) in the cross-shore direction, again due to shoaling surface gravity waves from the approaching storm, in combination with internal waves. The internal waves are excited by the extreme bathymetric depression of the head of the Carlsbad Submarine Canyon, (cf. [Figure 2.1.7](#)). The Carlsbad Submarine Canyon borders the northern end of the EOO flood tide survey box in [Figure 2.3.1](#). As tidal currents flow across the Carlsbad Submarine Canyon, this bathymetric depression excites internal waves that radiate outward from the canyon much like lee waves do in the atmosphere when storm winds blow over canyons and mountainous topography. The cross-shore oscillations of the internal waves that radiate from the Carlsbad Submarine Canyon would contribute to the high current spikes in the ADCP records 2 March 2022 (cf. [Figure 2.3.5](#) and [Figure 2.3.6](#)).

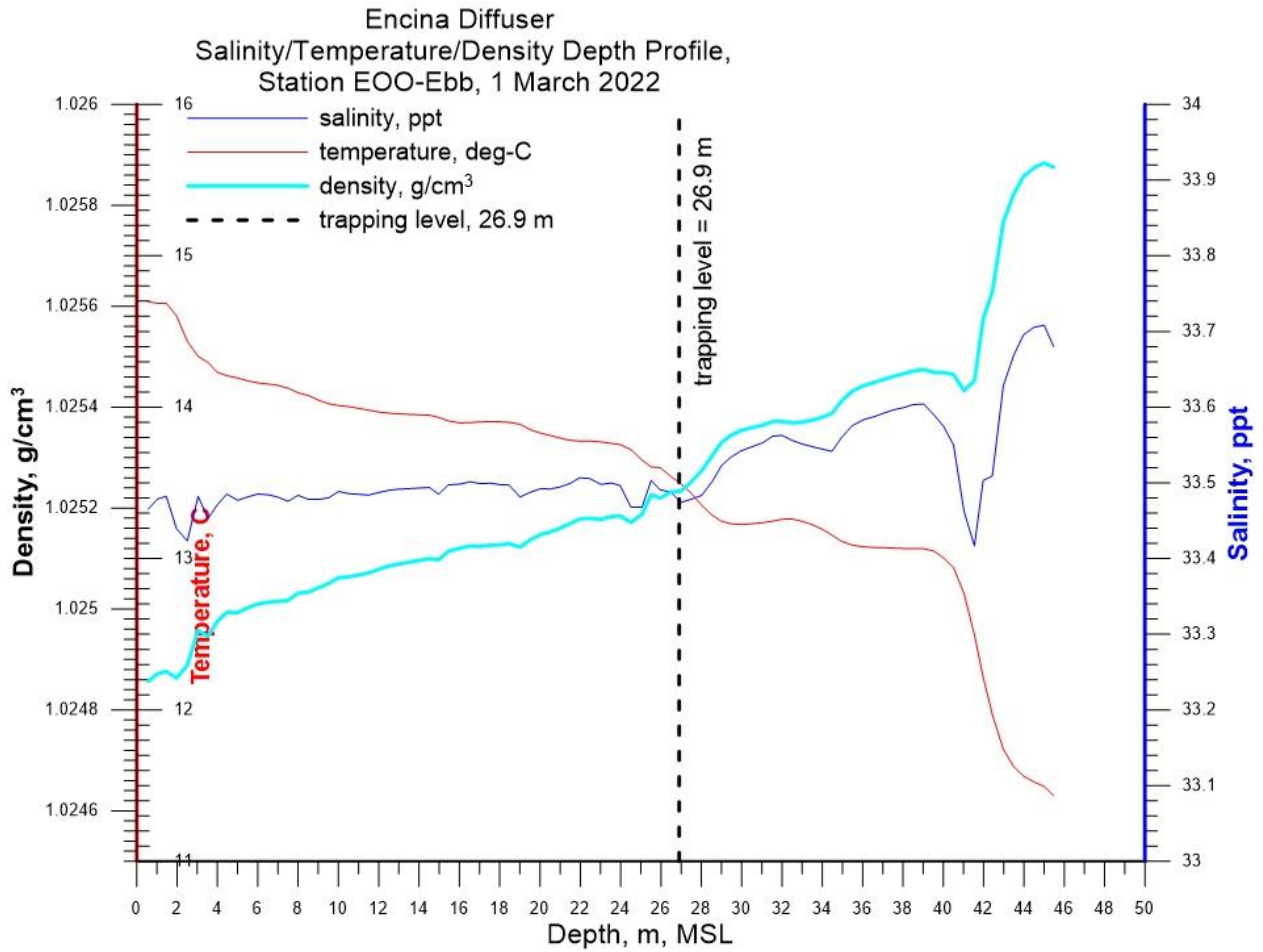


Figure 2.3.2: Salinity/Temperature/Density depth profiles derived from CTD casts on 1 March 2022 used to program the AUV surveys of the plume dispersion from the Encina Ocean Outfall during ebb and flood tides on 2 March 2022.

**Vertical Profiles of Natural Background fDOM
 EOO-EBB, 2 March 2022
 2 km north of the Encina Ocean Outfall**

— EOO EBB-1: average = 0.237 ppb; maximum = 0.510 ppb; minimum = 0.157 ppb; $\sigma=0.053$
 — EOO EBB-2: average = 0.239 ppb; maximum = 0.591 ppb; minimum = 0.063 ppb; $\sigma=0.061$

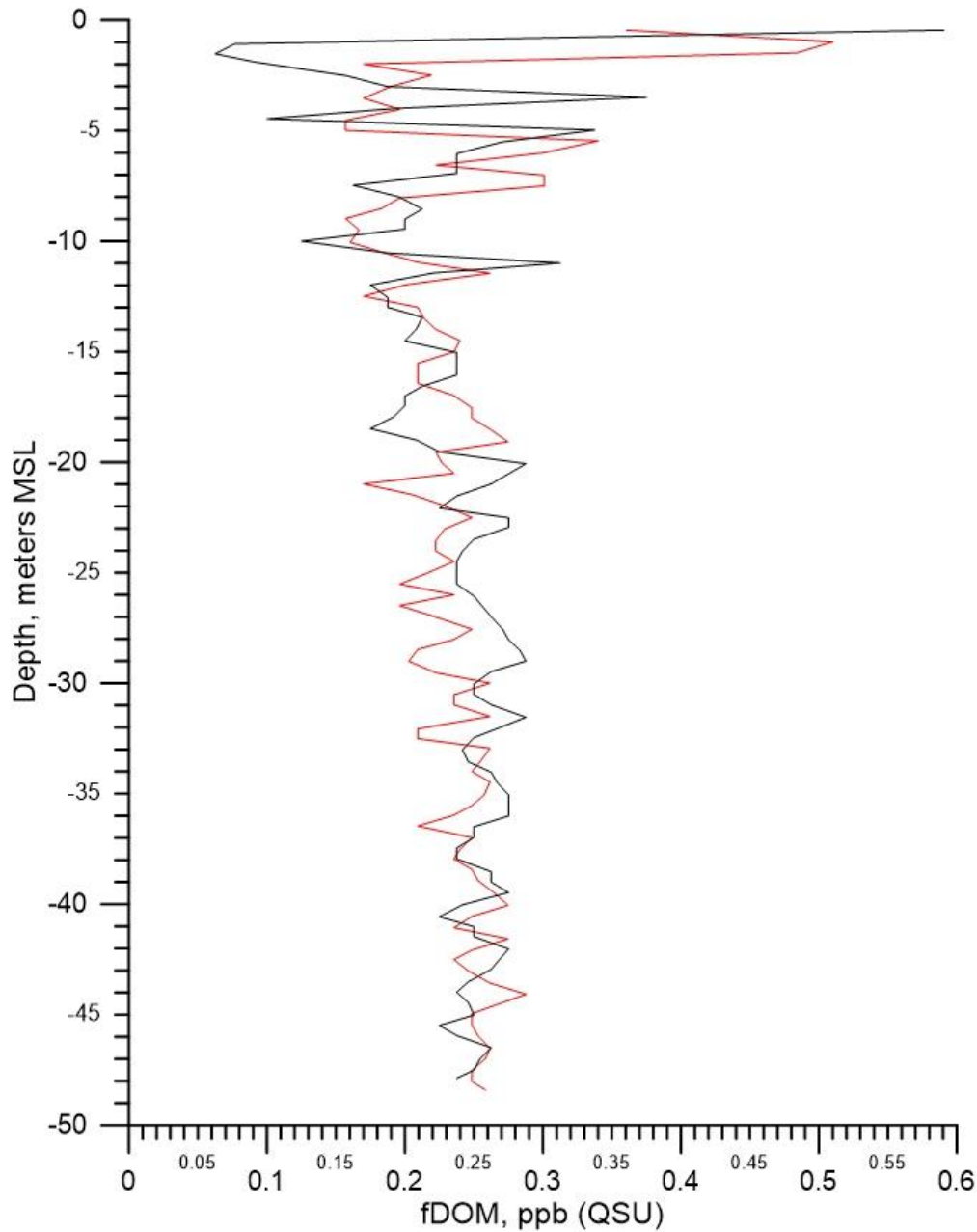


Figure 2.3.3: Vertical profiles of natural background fDOM concentrations measured during the third deployment at the far-field flood tide monitoring station “EOO-Ebb,” located 2 kilometers southeast of EOO along the -160 ft. MLLW depth contour, cf. orange dot in Figure 2.3.1

Vertical Profiles of Natural Background fDOM
EEO-Flood, 2 March 2022
2 km south of the Encina Ocean Outfall

— EEO Flood-1: average = 0.171 ppb; maximum = 0.213 ppb; minimum = 0.102 ppb; $\sigma=0.021$
 — EEO Flood-2: average = 0.170 ppb; maximum = 0.211 ppb; minimum = 0.125 ppb; $\sigma=0.019$

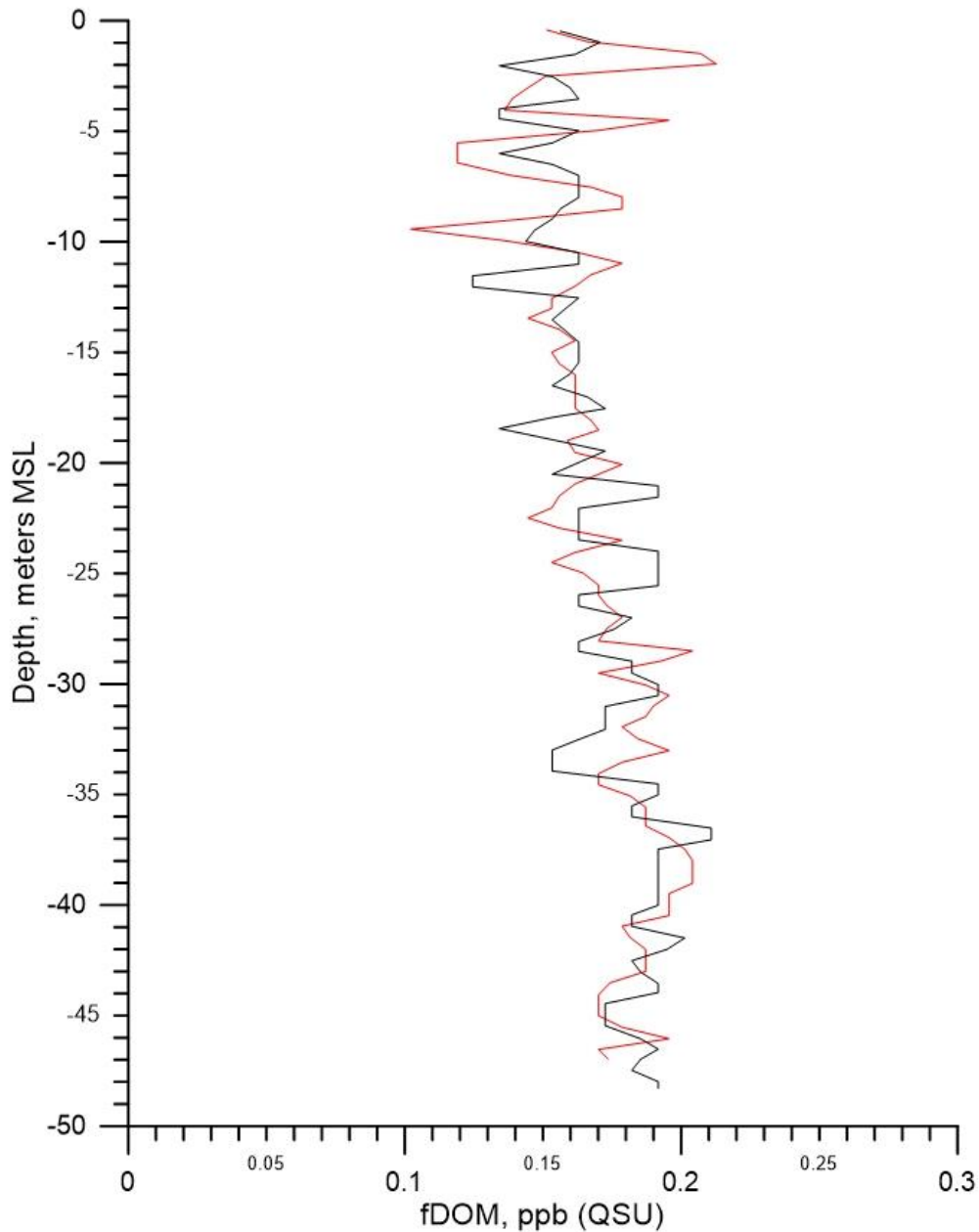


Figure 2.3.4: Vertical profiles of natural background fDOM concentrations measured during the third deployment at the far-field flood tide monitoring station “EEO-Flood,” located 2 kilometers southeast of EEO along the -160 ft. MLLW depth contour, cf. orange dot in [Figure 2.3.1](#)

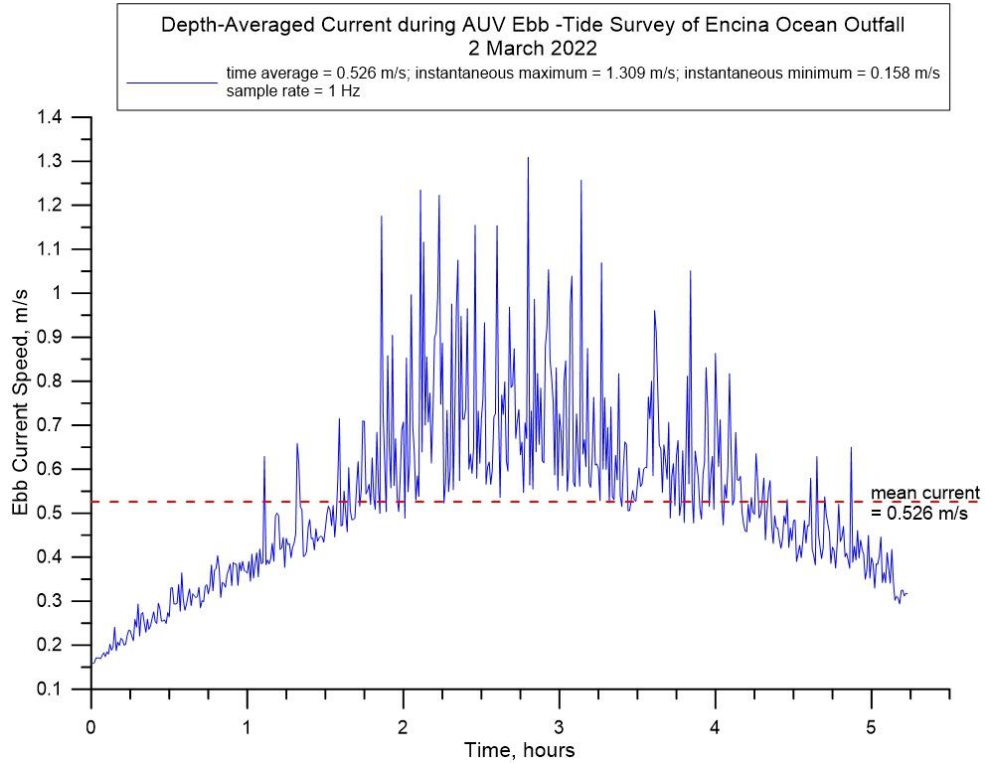


Figure 2.3.5: Time series of depth averaged current derived from ADCP measurements at EOO during ebb-tide AUV survey on 2 March 2022.

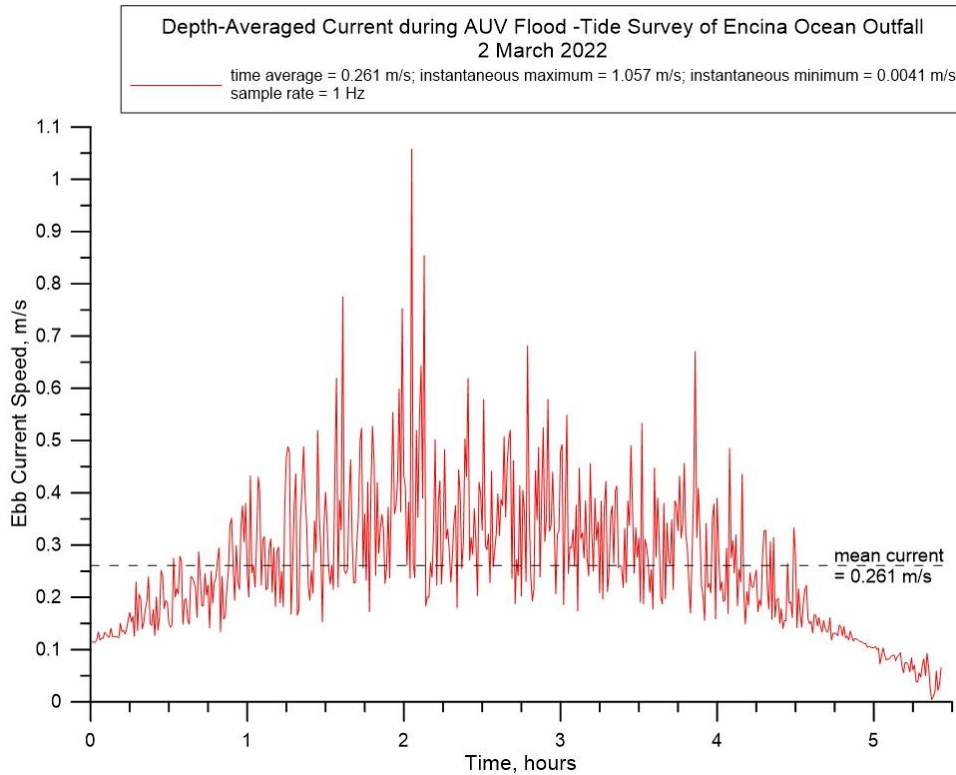


Figure 2.3.6: Time series of depth averaged current derived from ADCP measurements at EOO during flood-tide AUV survey on 2 March 2022

Figure 2.3.7 shows the 12 track lines flown by the AUV during ebb tide surveys of the EOO on 2 March 2022. Again, the navigation precision of the AUV is excellent with accurate repeatability of the outbound and return legs of each track line. During this survey, the AUV collected 65,700 separate measurements of salinity and fDOM along a total distance surveyed of 21.2 km. The fDOM heat map generated from these 65,700 measurements of fDOM concentrations is plotted in **Figure 2.3.8**. **Figure 2.3.8** exhibits a small degree of banding in the fDOM distribution along the 12 track lines due to mild spatial aliasing. However, the fDOM heat map also exhibits certain horizontal structures having high spatial coherence with the EOO diffuser. The fDOM concentrations across all depths in **Figure 2.3.8** range from $fDOM_{(x)} = 0.02$ ppb to 0.53 ppb in the center of a relatively small, singular feature believed to be a plume fragment found 669.8 m downstream from the EOO diffuser. The fDOM concentrations in this fDOM feature are as much as 229% higher than the depth-averaged natural background fDOM concentration $fDOM_{\infty} = 0.238$ ppb (cf. **Figure 2.3.3**). Moreover, this fDOM feature is not a sampling anomaly as it is defined by 668 separate fDOM measurements having concentrations ranging between 0.5 ppb and 0.78 ppb. No other fDOM features having this high a concentration can be found anywhere else in the EOO ebb-tide heat map in **Figure 2.3.8**., where the fDOM concentrations in the remainder of the surveyed area are on the order of $fDOM_{\infty} \cong 0.1$ to 0.35 ppb, consistent with the depth variation of natural background fDOM concentration plotted in **Figure 2.3.3**.

The probable reason for finding only a small remnant of the plume is the extremely high mean currents (1.02 kts) flowing shore-parallel in combination with transient wave surges as high as 1.53 kts flowing obliquely to the mean current, thereby exposing the EOO plume to high velocity shearing rates. This shearing by the ambient currents breaks up the plume into fragments and greatly accelerates dilution rates. Therefore, the singular elevated fDOM feature in **Figure 2.3.8** that is centered 669.8 m downstream of the EOO diffuser in the ebb tide current has the spatial coherence, structure, and contrast against natural background to possibly be a remnant of the EOO discharge plume. To verify this hypothesis, the fDOM heat map in **Figure 2.3.8** is converted into a signal to noise ratio heat map in **Figure 2.3.9** by invoking equation (1) to convert the fDOM concentrations into corresponding SNR_{fDOM} patterns. Again, since only fDOM features having signal to noise ratios of unity or greater are possible remnants of the plume **Figure 2.3.9** has been scaled to filter out features having $SNR_{fDOM} < 0.8$, where features having $0.8 \leq SNR_{fDOM} < 1.0$ are potentially diluted fragments or diluted outer edges of a plume remnants. Inspection of **Figure 2.3.9** reveals that the signal to noise ratio of the suspected plume remnant reaches $SNR_{fDOM} \cong 1.1$ in its inner core 669.8 m downstream of the EOO diffuser. Therefore, the elevated fDOM concentrations found centered in this feature satisfy the lowest order significance threshold for detection, (i.e., $SNR_{fDOM} \geq 1$). Based on this detection metric, we conclude that at least a fragment of the EOO discharge plume has been located 669.8 m downstream of the EOO diffuser during ebb tide on 2 March 2022.

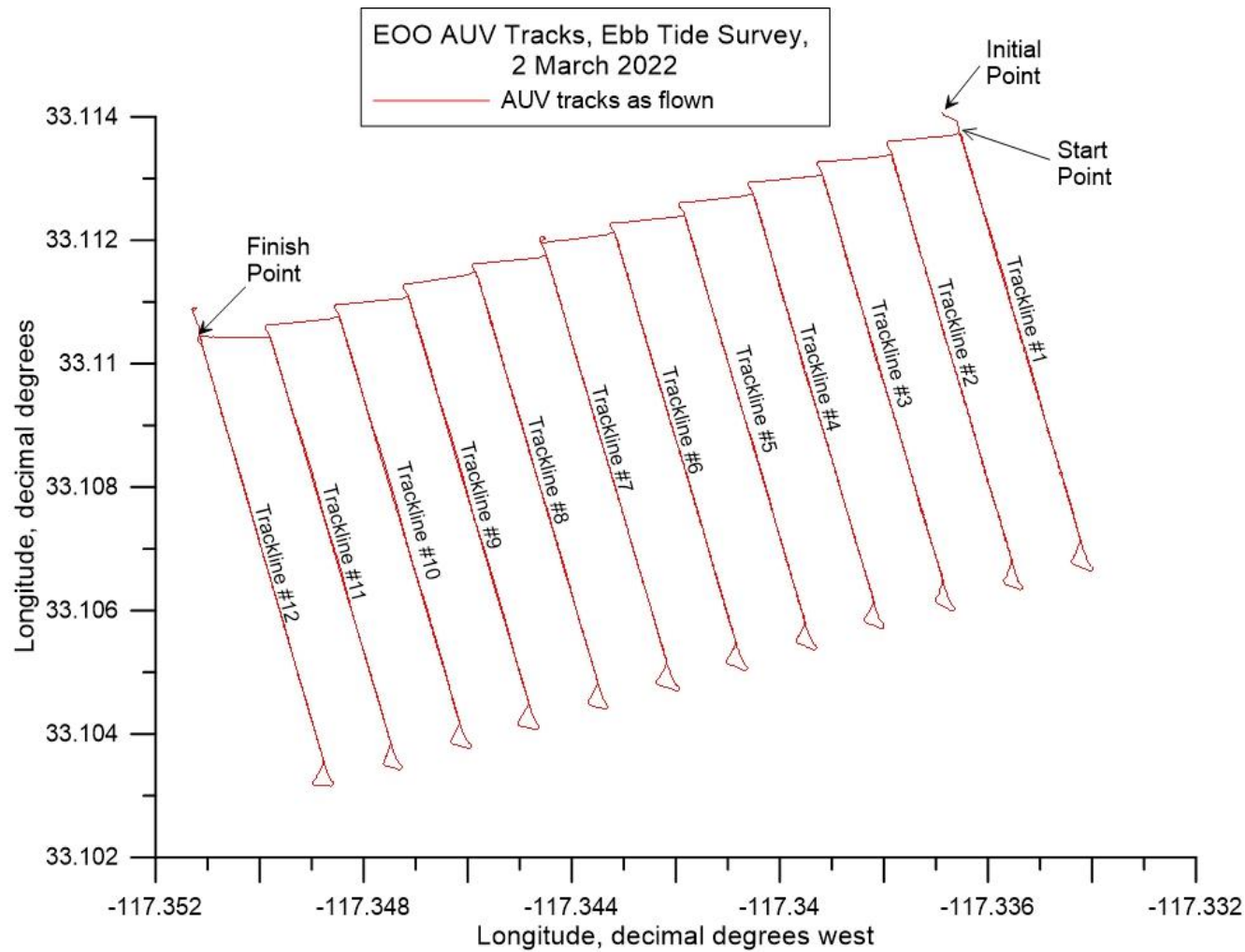


Figure 2.3.7: AUV track lines as flown during ebb tide surveys of the discharge plume from EOO during the second deployment, 2 March 2022. The total dimension of the AUV surveyed area on ebb tide was 707.1 m in the longshore (shore parallel) direction and 1,414.2 m on the cross-shore (on/off shore) direction or a total surveyed area of approximately 247.1 acres. Note, at 30° N latitude, 1° longitude = 93,453.2 m, while 1° latitude = 110,904.4 m.

Dispersion of fDOM Across all Depths
 Encina Ocean Outfall, Ebb Tide, 2 March 2022
 EOO fDOM discharge concentration = 261.8 ppb
 ——— diffuser

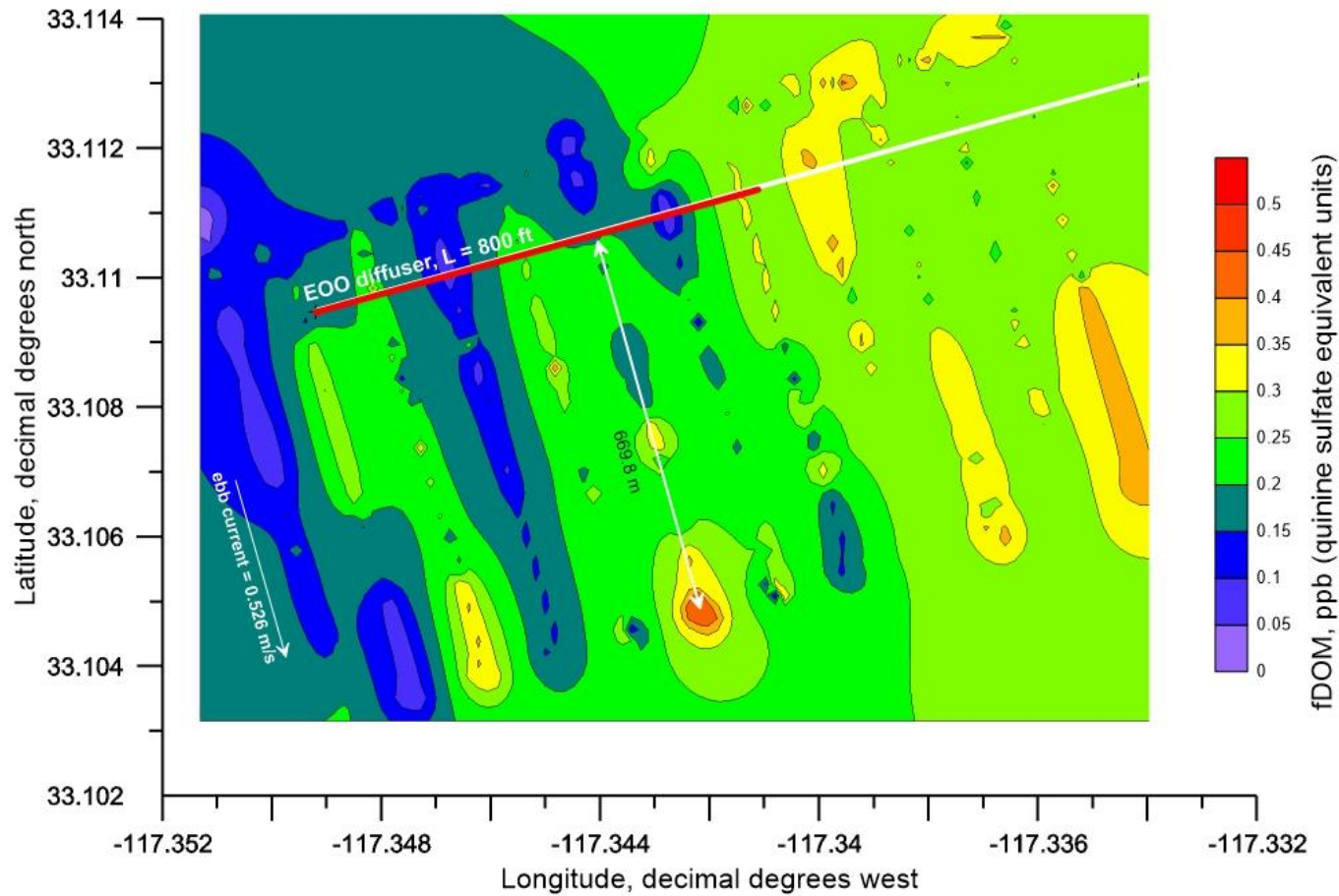


Figure 2.3.8: Full depth contour plot (aka, heat map) of AUV measurements of fDOM during surveys of the discharge plume from EOO during ebb tide on 2 March 2021. Average EOO discharge rate = 27.6 mgd during ebb tide; End-of-pipe discharge concentration of fDOM = 261.8 ppb (QSU); End of pipe salinity = 0.82 psu; Trapping level (pycnocline depth) = -26.9 m (-88.3 ft) MSL; Mean ebb tide current = 0.526 m/s (1.02 kts) toward the southeast.

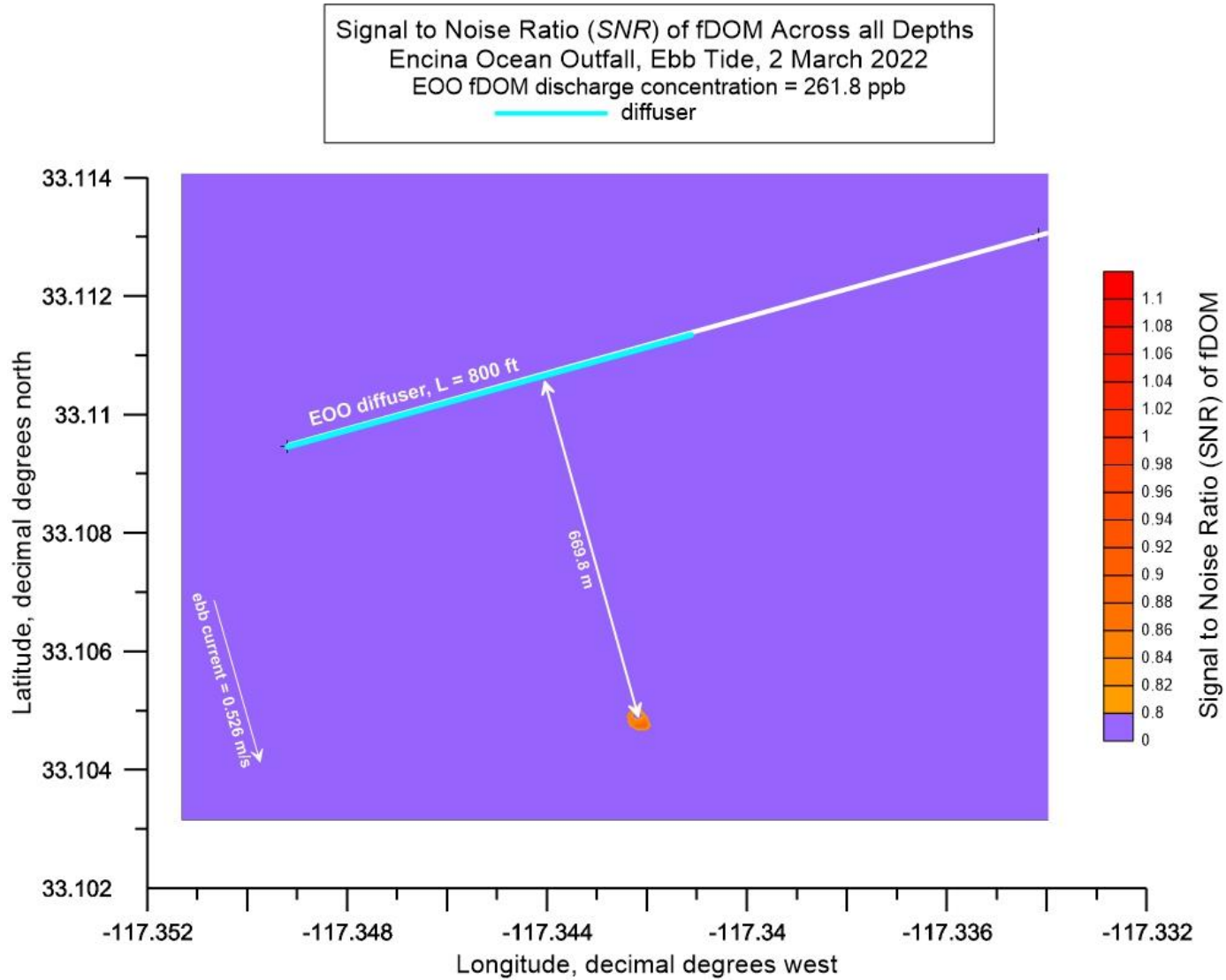


Figure 2.3.9: Full depth contour plot (aka, *heat map*) of the Signal to Noise Ratio (SNR) of fDOM during AUV surveys of the discharge plume from EOO during ebb tide on 2 March 2021. Average EOO discharge rate = 27.6 mgd during ebb tide; End-of-pipe discharge concentration of fDOM = 261.8 ppb (QSU); End of pipe salinity = 0.82 psu; Trapping level (pycnocline depth) = -26.9 m (-88.3 ft) MSL; Mean ebb tide current = 0.526 m/s (1.02 kts) toward the southeast.

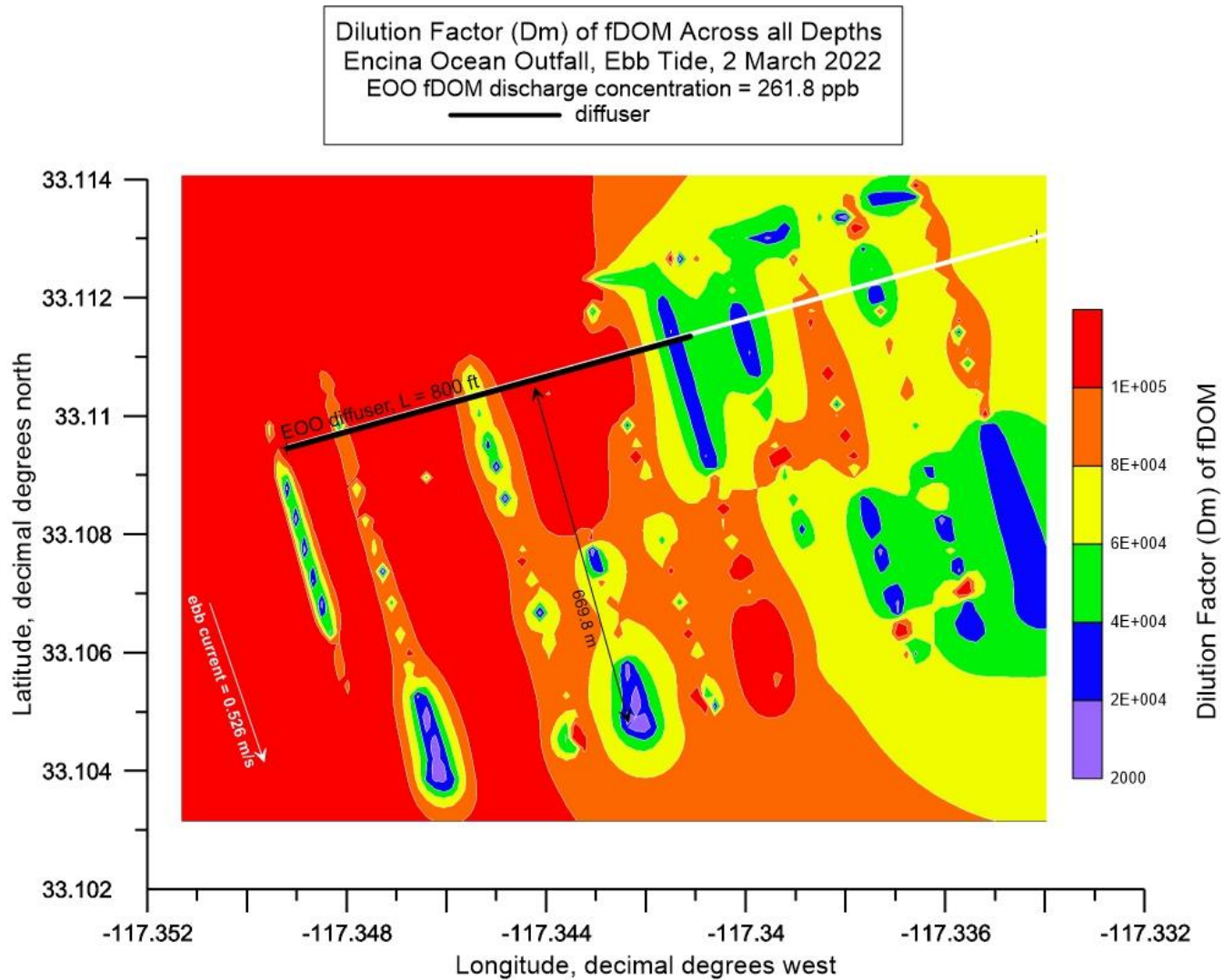


Figure 2.3.10: Full depth contour plot of the (aka, *heat map*) dilution factor (D_{fDOM}) of fDOM during AUV surveys of the discharge plume from EOO during ebb tide on 2 March 2021. Average EOO discharge rate = 27.6 mgd during ebb tide; End-of-pipe discharge concentration of fDOM = 261.8 ppb (QSU); End of pipe salinity = 0.82 psu; Trapping level (pycnocline depth) = -26.9 m (-88.3 ft) MSL; Mean ebb tide current = 0.526 m/s (1.02 kts) toward the southeast.

To assess minimum dilution levels in the EOO plume fragment, the SNR_{fDOM} heat map in **Figure 2.3.9** was transposed into a dilution heat map in **Figure 2.3.10** using equation (2) on the basis that the initial fDOM concentration is $fDOM_{(x=0)} = 261.8$ ppb. Note that regions of high SNR will correspond to regions of low values of D_{fDOM} relative to the dilution elsewhere within the AUV survey area. **Figure 2.3.10** indicates that the dilution factor (D_{fDOM}) for the fDOM in the core of the plume remnant is at least $D_{fDOM} = 999:1$, or a factor of 6.94 times greater than the 144:1 initial dilution assigned within the current EOO NPDES permit (No. CA0107395; Order No. RS-2018-0059). The fDOM-derived dilution along the outer perimeter of the plume fragment ranged from $D_{fDOM} = 1100:1$ to 20,000:1. Elsewhere down current from the EOO diffuser, dilution ranged from $D_{fDOM} = 30,000:1$ to 100,000:1. As a result of these high dilutions, any regulated or unregulated toxic constituents in the EEO discharge would be below quantifiable detection limits in any plume remnants beyond 700 m from the outfall.

Figure 2.3.11 provides the salinity heat map generated from the AUV salinity measurements during the EOO ebb tide survey. Most of the features in the ebb tide salinity heat map range from $S_{(x)} = 33.33$ psu in the core of the plume fragment to as high as $S_{(x)} = 33.6$ psu in the far-field of the EOO diffuser. The far-field depth-averaged salinity in **Figure 2.3.11** indicates that the natural background salinity is $S_{\infty} = 33.52$ psu with a standard deviation of $\sigma = 0.059$ psu. While it seems possible that the $S_{(x)} = 33.4$ psu salinity minimum could be due to salinity depression within the EOO plume remnant, the signal to noise ratio of the salinity features in **Figure 2.3.12** range from only $SNR_S = 0.004$ to $SNR_S = 0.008$. Therefore, all the salinity features in **Figure 2.3.12** have signal to noise ratios significantly below the lowest order significance threshold for detection (i.e., $SNR_S \geq 1$) and consequently cannot be associated with suspected plume remnants.

Despite the low signal to noise ratios in the salinity heat map in **Figure 2.3.12**, the fDOM heat map data in **Figure 2.3.8** and the corresponding signal to noise ratio data in **Figure 2.3.9** represent probable evidence of an EOO plume fragment centered 669.8 m downstream of the EOO diffuser in the 0.526 m/s (1.02 kts) ebb tide current. This prompts the question of whether the EOO plume fragment has been transported beyond the point where initial dilution had been completed under the discharge and oceanic conditions that persisted on 2 March 2022.

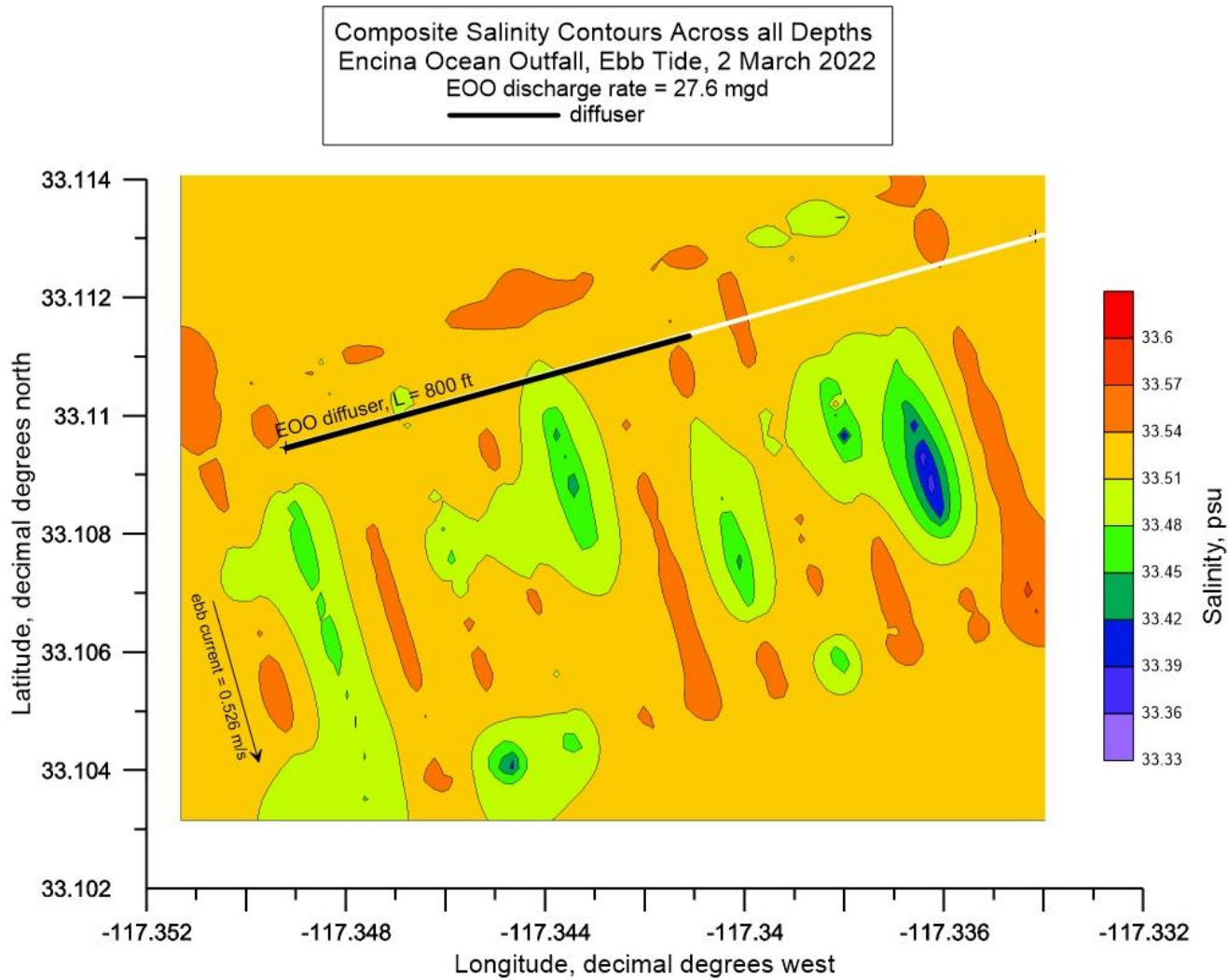


Figure 2.3.11: Full depth composite contour plot (aka, *heat map*) of AUV measurements of salinity during surveys of the discharge plume from EOO during ebb tide on 2 March 2021. Average EOO discharge rate = 27.6 mgd during ebb tide; End-of-pipe discharge concentration of fDOM = 261.8 ppb (QSU); End of pipe salinity = 0.82 psu; Trapping level (pycnocline depth) = -26.9 m (-88.3 ft) MSL; Mean ebb tide current = 0.526 m/s toward the southeast.

Signal to Noise Ratio (SNR) of Salinity Across all Depths
 Encina Ocean Outfall, Ebb Tide, 2 March 2022
 EOO discharge rate = 27.6 mgd
 _____ diffuser

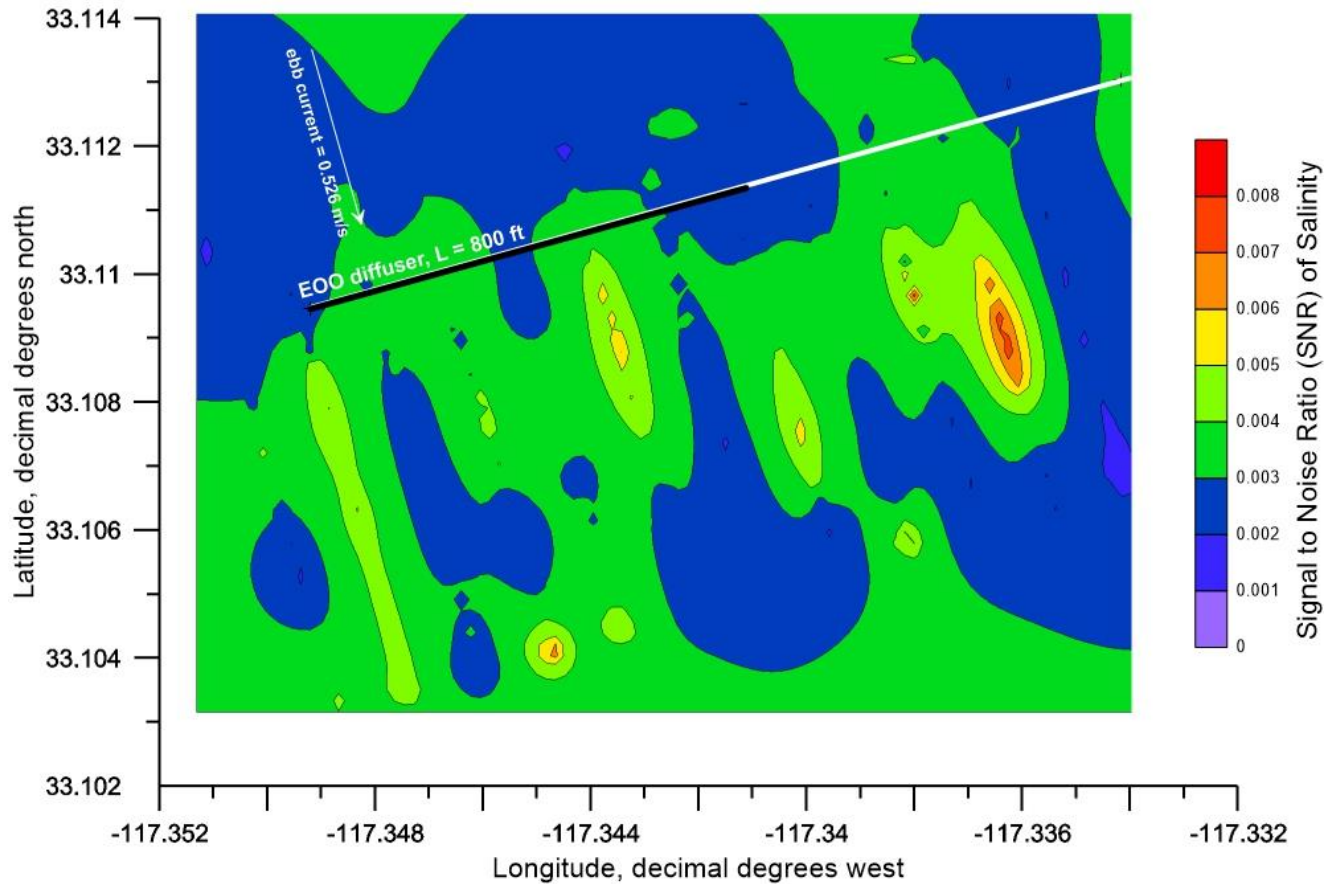


Figure 2.3.12: Full depth contour plot (aka, *heat map*) of the Signal to Noise Ratio (SNR) of salinity during AUV surveys of the discharge plume from EOO during ebb tide on 2 March 2021. Average EOO discharge rate = 27.6 mgd during ebb tide; End-of-pipe discharge concentration of fDOM = 261.8 ppb (QSU); End of pipe salinity = 0.82 psu; Trapping level (pycnocline depth) = -26.9 m (-88.3 ft) MSL; Mean ebb tide current = 0.526 m/s toward the southeast.

This issue was further investigated by applying the Plumes 20 (UM3) dilution model (See [Table 11](#)) using actual ebb tide currents of 0.526 m/s (1.02 kts) on 2 March 2022. Under these conditions, the solution file listed in [Table 12](#) indicates that an EOO initial dilution of 359:1 at a discharge flow of 27.6 mgd. Meanwhile, [Figure 2.3.13](#) demonstrates at a 0.526 m/s (1.02 kts) ambient current, the Plumes 20 model indicates that initial dilution is completed within approximately 224 m of the EOO diffuser, or about half the distance of the horizontal excursion of the EOO plume fragment found in the fDOM heat map in [Figure 2.3.8](#) during ebb tide. Demonstrating that significant additional dilution can occur after initial dilution, the plume tracking study during ebb tide on 2 March 2022 indicates that the discharge plume was detectable (using fDOM data) approximately 450 meters beyond the point where initial dilution was completed, albeit at high dilution ratios of at least 477:1. This dilution is approximately 3.3 times greater than the minimum month initial dilution ratio of 144:1 assigned within the current NPDES permit for the EOO (No. CA 0107395, Order No. R9-2018-0059).

On the following flood tide on 2 March 2021, the orange survey box in [Figure 2.3.1](#) was flown by the AUV with accurate repeatability of the outbound and return legs along each of 12 track lines, (cf. [Figure 2.3.14](#)). During this survey, the AUV collected 64,330 separate measurements of salinity and fDOM along a total distance surveyed of 21.2 km. The fDOM heat map generated from these measurements of fDOM concentrations is plotted in [Figure 2.3.15](#), which show occasional banding patterns associated with spatial aliasing, but display fDOM features that are similar to those that were mapped during the preceding ebb-tide, (cf. [Figure 2.3.10](#)) that exhibit certain horizontal structures having high spatial coherence with the EOO diffuser. The fDOM concentrations across all depths in [Figure 2.3.15](#) range from $fDOM_{(x)} = 0.02$ ppb to 0.40 ppb in various spots along of a relatively narrow elongated, singular feature believed to be a plume fragment found 332.4 m downstream from the EOO diffuser. The fDOM concentrations in this fDOM feature are as much as 271% higher than the depth-averaged natural background fDOM concentration $fDOM_{\infty} = 0.170$ ppb (cf. [Figure 2.3.4](#)). Moreover, this fDOM feature is not a sampling anomaly as it is defined by 1,121 separate fDOM measurements having concentrations ranging between 0.5 ppb and 0.63 ppb. No other fDOM features having this high a concentration can be found anywhere else in the EOO flood-tide heat map in [Figure 2.3.15](#), where the fDOM concentrations in the remainder of the surveyed area are on the order of $fDOM_{\infty} \cong 0.1$ to 0.35 ppb, consistent with the depth variation of natural background fDOM concentration plotted in [Figure 2.3.4](#).

As during ebb tide, probable reason for finding only a small remnant of the plume during the ensuing flood tide is the fairly high mean currents 0.261 m/s (0.51 kts) flowing shore-parallel in combination with transient wave surges as high as 1.05 m/s (2.04 kts) flowed obliquely to the mean current, thereby exposing the EOO plume to high velocity shearing rates. This shearing by the ambient currents breaks up the plume into fragments and greatly accelerates dilution rates.

Table 11: Plumes 20 (UM3) Initialization of EOO Ebb tide Ambient Conditions on 2 March with Ambient Current

Project "C:\Plumes20\EOO_Ebb_With-Current_2Mar2022"

Model configuration items checked:

Channel width (m)	100
Start case for graphs	1
Max detailed graphs	10 (limits plots that can overflow memory)
Elevation Projection Plane (deg)	0
Shore vector (m,deg)	not checked
Bacteria model:	Mancini (1978) coliform model
PDS sfc. Model heat transfer	Medium
Equation of State	S, T
Similarity Profile	Default profile (k=2.0, ...)
Diffuser port contraction coefficient	1
Light absorption coefficient	0.16
Farfield increment (m)	200
UM3 aspiration coefficient	0.1
Output file:	text output tab
Output each ?? steps	10
Maximum dilution reported	10000
Text output format	Standard
Max vertical reversals	to max rise or fall

Ambient Table:

Depth m	Amb-cur m/s	Amb-dir deg	Amb-sal Psu	Amb-tem C	Amb-pol kg/kg	Decay s-1	Far-spd m/s	Far-dir deg	Disprsn m0.67/s2	Density sigma-T
0.0	0.526	0.0	33.47	14.70	3.6000E-10	0.0	0.0	0.0	0.0	24.87799
3.534	0.526	0.0	33.45	14.30	1.7000E-10	0.0	0.0	0.0	0.0	24.95378
6.535	0.526	0.0	33.48	14.15	2.2200E-10	0.0	0.0	0.0	0.0	25.00789
9.510	0.526	0.0	33.48	14.02	1.6700E-10	0.0	0.0	0.0	0.0	25.03189
12.55	0.526	0.0	33.49	13.96	1.7000E-10	0.0	0.0	0.0	0.0	25.05283
15.45	0.526	0.0	33.50	13.91	2.0900E-10	0.0	0.0	0.0	0.0	25.06862
18.47	0.526	0.0	33.50	13.90	2.6200E-10	0.0	0.0	0.0	0.0	25.07033
21.49	0.526	0.0	33.50	13.78	2.0500E-10	0.0	0.0	0.0	0.0	25.09644
24.51	0.526	0.0	33.49	13.72	2.3500E-10	0.0	0.0	0.0	0.0	25.10051
27.47	0.526	0.0	33.48	13.43	2.4800E-10	0.0	0.0	0.0	0.0	25.15101
30.51	0.526	0.0	33.55	13.23	2.3500E-10	0.0	0.0	0.0	0.0	25.24583
33.47	0.526	0.0	33.55	13.23	2.5500E-10	0.0	0.0	0.0	0.0	25.24688
36.54	0.526	0.0	33.59	13.07	2.0900E-10	0.0	0.0	0.0	0.0	25.30754
39.54	0.526	0.0	33.59	13.05	2.6500E-10	0.0	0.0	0.0	0.0	25.31448
42.43	0.526	0.0	33.51	11.97	2.3500E-10	0.0	0.0	0.0	0.0	25.46085
45.47	0.526	0.0	33.68	11.43	2.4900E-10	0.0	0.0	0.0	0.0	25.69300
48.41	0.526	0.0	33.66	11.04	2.5800E-10	0.0	0.0	0.0	0.0	25.75193

Diffuser Table:

P-dia (in)	Ver angl (deg)	H-Angle (deg)	SourceX (ft)	SourceY (ft)	Ports ()	MZ-dis (m)	Isoplth (concent)	P-depth (ft)	Ttl-flo (MGD)	Eff-sal (psu)	Temp (C)	Polutnt (ppb)
2.7750	0.0	0.0	0.0	0.0	138.00	2000.0	0.0	155.75	27.600	0.8200	20.420	261.80

Table 12: Plumes 20 (UM3) Output of EOO Dilution Factor (D_{fDOM}) during Ebb Tide on 2 March 2022 with Ambient Current (Final D_{fDOM} solution highlighted in yellow)

Simulation: Froude No: 16.45; Strat No: 4.72E-5; Spcg No: 7.909; k: 4.269; eff den (sigmaT) -1.196681; eff vel 2.246(m/s)

Depth Step	Amb-cur (ft)	Amb-sal (m/s)	P-dia (psu)	Eff-sal (in)	Polutnt (psu)	Dilutn (ppb)	CL- (')	diln (')	x-posn (ft)	y-posn (ft)	Iso dia (m)
0	155.8	0.526	33.67	2.775	0.820	261.8	1.000	1.000	0.0	0.0	0.07049;
10	155.7	0.526	33.67	3.295	6.985	213.8	1.225	1.000	0.138	0.0	0.08369;
20	155.7	0.526	33.67	3.895	11.78	176.1	1.487	1.000	0.292	0.0	0.09894;
30	155.7	0.526	33.67	4.588	15.71	145.0	1.807	1.000	0.478	0.0	0.1165;
40	155.7	0.526	33.67	5.380	18.94	119.3	2.197	1.099	0.703	0.0	0.1367;
50	155.7	0.526	33.67	6.281	21.58	98.12	2.673	1.336	0.978	0.0	0.1595;
60	155.7	0.526	33.67	7.299	23.75	80.68	3.252	1.626	1.315	0.0	0.1854;
70	155.7	0.526	33.67	8.442	25.54	66.33	3.959	1.979	1.729	0.0	0.2144;
80	155.7	0.526	33.67	9.717	27.00	54.52	4.820	2.410	2.243	0.0	0.2468;
90	155.7	0.526	33.67	11.13	28.20	44.82	5.870	2.935	2.886	0.0	0.2828;
100	155.6	0.526	33.67	12.70	29.18	36.84	7.150	3.575	3.694	0.0	0.3225;
110	155.6	0.526	33.67	14.42	29.99	30.29	8.710	4.355	4.670	0.0	0.3663;
120	155.5	0.526	33.67	16.32	30.65	24.91	10.61	5.306	5.786	0.0	0.4145;
130	155.4	0.526	33.67	18.40	31.19	20.49	12.93	6.465	7.032	0.0	0.4674;
140	155.3	0.526	33.67	20.69	31.64	16.86	15.76	7.878	8.414	0.0	0.5254;
146	155.2	0.526	33.67	22.16	31.86	15.00	17.74	8.870	9.313	0.0	0.5629; merging;
150	155.2	0.526	33.67	23.21	32.00	13.88	19.20	9.741	9.993	0.0	0.5896;
160	155.0	0.526	33.67	26.11	32.30	11.44	23.40	12.28	12.07	0.0	0.6631;
170	154.7	0.526	33.67	29.43	32.55	9.432	28.52	15.59	14.67	0.0	0.7474;
180	154.4	0.526	33.67	33.26	32.75	7.786	34.76	19.95	17.83	0.0	0.8448;
190	154.0	0.526	33.67	37.73	32.91	6.435	42.37	25.83	21.66	0.0	0.9584;
200	153.5	0.526	33.67	43.01	33.05	5.326	51.64	33.97	26.26	0.0	1.0924;
210	152.9	0.526	33.67	49.30	33.16	4.416	62.94	41.96	31.78	0.0	1.2523;
220	152.1	0.526	33.67	56.89	33.25	3.670	76.72	51.15	38.39	0.0	1.4449;
230	151.2	0.526	33.68	66.12	33.33	3.057	93.51	62.34	46.33	0.0	1.6794;
240	150.1	0.526	33.68	77.44	33.39	2.554	114.0	75.99	55.85	0.0	1.9671;
250	148.8	0.526	33.68	91.40	33.44	2.141	138.9	92.63	67.34	0.0	2.3217;
260	147.2	0.526	33.65	108.7	33.48	1.802	169.4	112.9	81.32	0.0	2.7603;
270	145.3	0.526	33.62	130.1	33.51	1.524	206.5	137.6	98.88	0.0	3.3040;
279	143.3	0.526	33.58	153.7	33.53	1.316	246.7	164.5	119.5	0.0	3.9036; trap level;
280	143.0	0.526	33.58	156.6	33.53	1.295	251.7	167.8	122.2	0.0	3.9777;
290	140.5	0.526	33.53	189.4	33.53	1.106	306.8	204.5	157.3	0.0	4.8116;
300	138.7	0.526	33.51	220.1	33.53	0.991	353.9	236.0	208.5	0.0	5.5897;
303	138.7	0.526	33.51	224.0	33.53	0.981	359.0	239.3	223.6	0.0	5.6900; local maximum rise or fall;

Horiz plane projections in effluent direction: radius(m): 0.0; CL(m): 68.152

Lmz(m): 68.152

forced entrain 1 173.6 5.188 5.690 1.000

Rate sec-1 0.0 dy-1 0.0 kt: 0.0 Amb Sal 33.5134;

3:38:38 Pm. Amb fills: 4

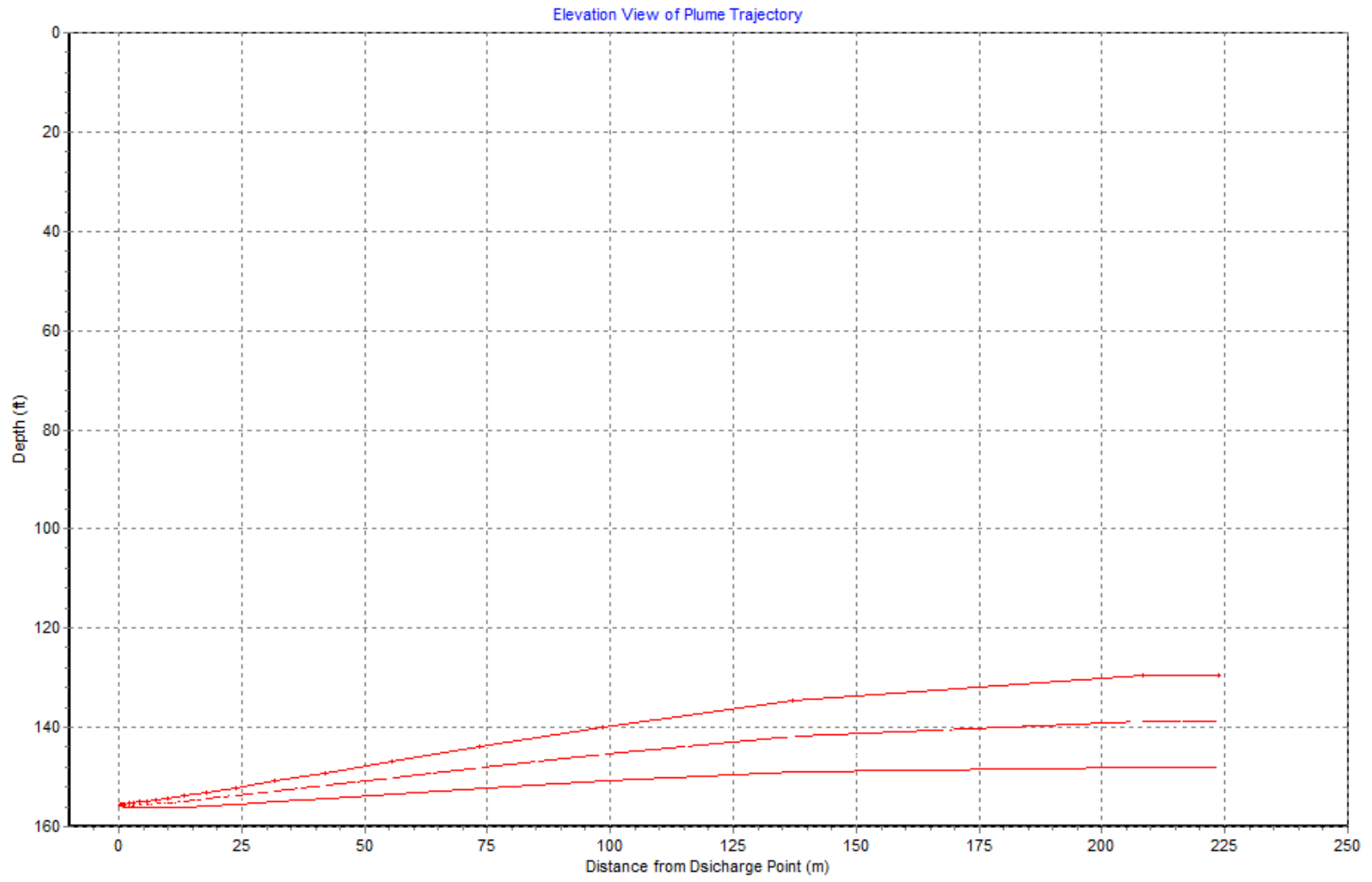


Figure 2.3.13: Plumes 20 solution of discharge plume trajectories for discharges of 27.6 mgd of EOO effluent at a discharge salinity of $S_{(x=0)} = 0.82$ psu, per operating conditions and water mass temperature/salinity profiles during ebb tide on 2 March 2022. Plumes 20 simulation performed based on ambient current = 0.526 m/s per ADCP measurements. For the 2 March 2022 conditions, the ZID (zone within which initial dilution is completed) is defined by the maximum horizontal excursion of trajectories from the origin. From the maximum horizontal spreading of the plume, the ZID extends from $X = 0.0$ m to $X = 224$ m so that $ZID = 224$ m.

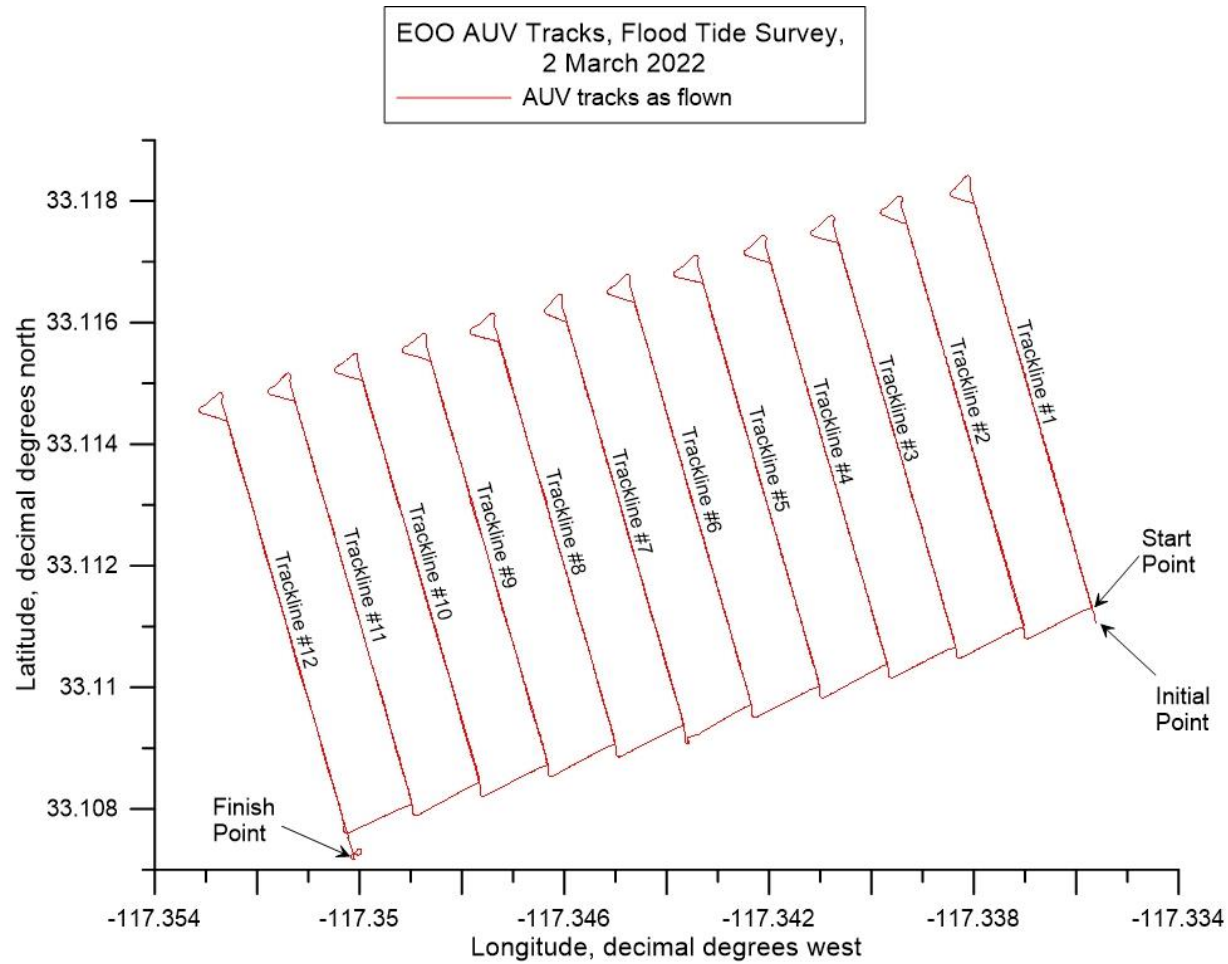


Figure 2.3.14: AUV track lines as flown during flood tide surveys of the discharge plume from EOO during the second deployment, 2 March 2022. The total dimension of the AUV surveyed area on flood tide was 707.1 m in the longshore (shore parallel) direction and 1,414.2 m on the cross-shore (on/off shore) direction or a total surveyed area of approximately 247.1 acres. Note, at 30° N latitude, 1° longitude = 93,453.2 m, while 1° latitude = 110,904.4 m.

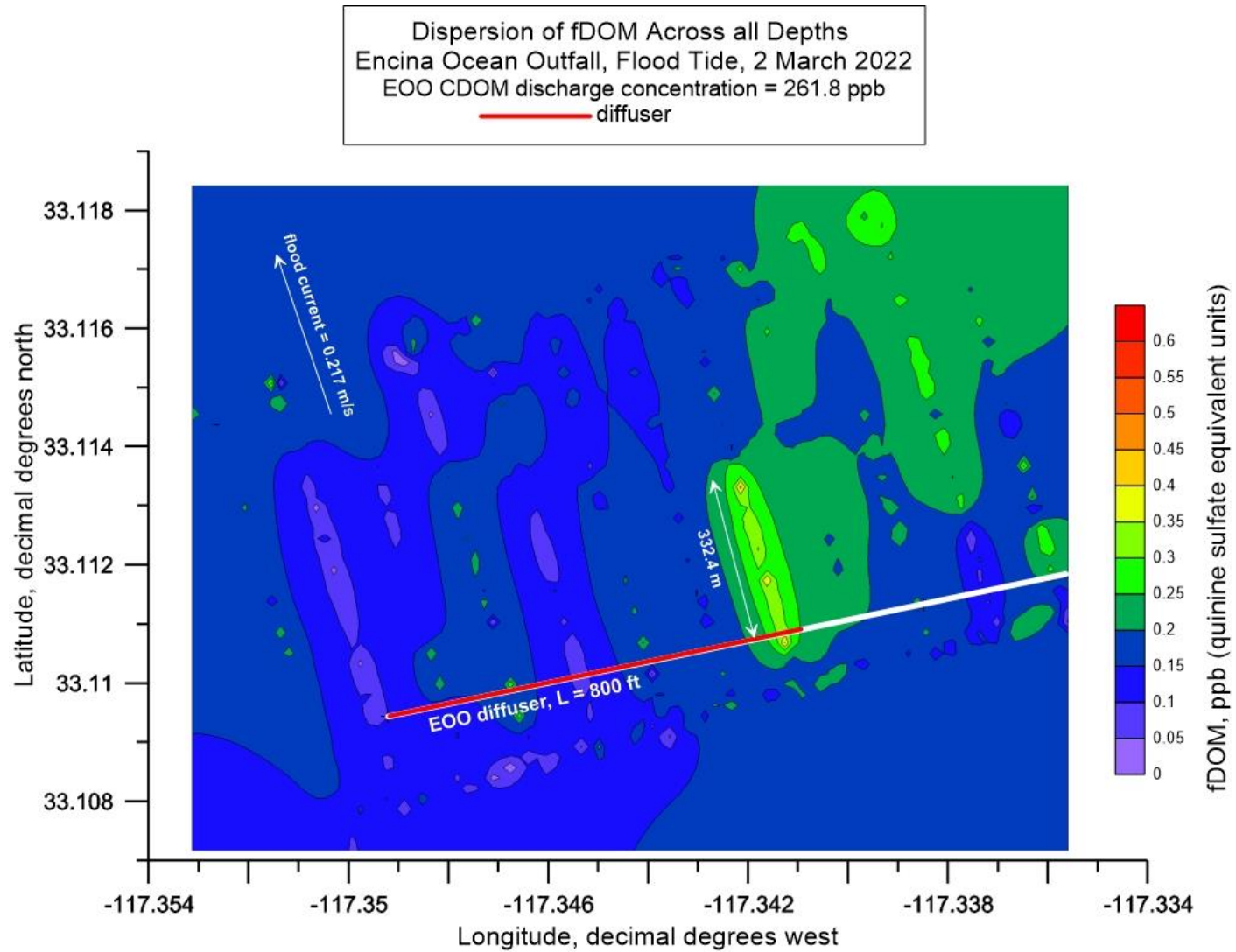


Figure 2.3.15: Full depth contour plot (aka, *heat map*) of AUV measurements of fDOM during surveys of the discharge plume from EOO during flood tide on 2 March 2021. Average EOO discharge rate = 24.2 mgd during flood tide; End-of-pipe discharge concentration of fDOM = 261.8 ppb (QSU); End of pipe salinity = 0.82 psu; Trapping level (pycnocline depth) = -26.9 m (-88.3 ft) MSL; Mean flood tide current = 0.261 m/s (0.51 kts) toward the northwest.

Therefore, the singular elevated fDOM feature in **Figure 2.3.15** that extends 332.4 m downstream from the EOO diffuser in the flood tide current has the spatial coherence, structure, and contrast against natural background to possibly be a remnant of the EOO discharge plume. To verify this hypothesis, the fDOM heat map in **Figure 2.3.15** is converted into a signal to noise ratio heat map in **Figure 2.3.16** by invoking equation (1) to convert the fDOM concentrations into corresponding SNR_{fDOM} patterns. Again, since only fDOM features having signal to noise ratios of unity or greater are possible remnants of the plume, **Figure 2.3.16** has been scaled to filter out features having $SNR_{fDOM} < 0.8$, where features having $0.8 \leq SNR_{fDOM} < 1.0$ are potentially diluted fragments or diluted outer edges of a plume remnants. Inspection of **Figure 2.3.16** reveals that the signal to noise ratio of the suspected plume remnant ranges from $SNR_{fDOM} \cong 1.0$ to 1.3 in its inner core 332.4 m downstream of the EOO diffuser. Therefore, the elevated fDOM concentrations in this feature satisfy the lowest order significance threshold for detection, (i.e., $SNR_{fDOM} \geq 1$). Based on this detection metric, it is concluded that at least a fragment of the EOO discharge plume has been located stretching from the EOO diffuser northwestward 332.4 m downstream of the EOO diffuser during flood tide on 2 March 2022.

To assess minimum dilution levels, the SNR_{fDOM} heat map in **Figure 2.3.16** was transposed into a dilution heat map in **Figure 2.3.17** using equation (2) on the basis that the initial fDOM concentration at the point of discharge is $fDOM_{(x=0)} = 261.8$ ppb. Again, regions of high SNR will correspond to regions of low values of D_{fDOM} relative to the dilution elsewhere within the AUV survey area. **Figure 2.3.17** indicates that the dilution factor (D_{fDOM}) for the fDOM features is 1,180:1 in the inner core of the plume remnant, or a factor of 8.2 times greater than the minimum month initial dilution of $D_m = 144:1$ assigned within the current NPDES permit (No. CA0107395; Order No. RS-2018-0059). The dilution along the outer perimeter of the plume fragment ranges from $D_{fDOM} = 1,539:1$ to 20,000:1. Elsewhere in the wake of the EOO diffuser dilution ranges from $D_{fDOM} = 20,000:1$ to 80,000:1. At these dilutions, any regulated or unregulated toxic constituents in the EEO discharge would be below quantifiable detection limits.

Figure 2.3.18 provides the salinity heat map generated from the AUV salinity measurements during the EOO flood tide survey. The AUV salinity measurements range from $S_{(x)} = 33.37$ psu to $S_{(x)} = 33.67$ psu standard deviation of $\sigma = 0.027$ psu throughout the flood tide survey area; but most of the features in the wake of the EOO diffuser range from $S_{(x)} = 33.50$ psu to $S_{(x)} = 33.54$ psu and there is no evidence of the plume fragment found in the fDOM heat map in **Figure 2.3.15**. The signal to noise ratio of the salinity features in **Figure 2.3.19** range from only $SNR_S = 0.0$ to only $SNR_S = 0.008$. Therefore, all the salinity features in **Figure 2.3.18** have signal to noise ratios significantly below the lowest order significance threshold for detection (i.e., $SNR_S \geq 1$) and consequently cannot be associated with suspected plume fragments. Again, this supports the initial hypothesis that salinity is not a useful tracer of an outfall plume.

Despite the absence of evidence of any plume fragment in the salinity heat map in **Figure 2.3.18**, the fDOM heat map data in **Figure 2.3.15** and the corresponding signal to noise ratio data in **Figure 2.3.16** represent probable evidence of an EOO plume fragment extending from the EOO diffuser to 332.4 m downstream in the 0.261 m/s (0.51 kts) flood tide current. This prompts the question of whether the EOO

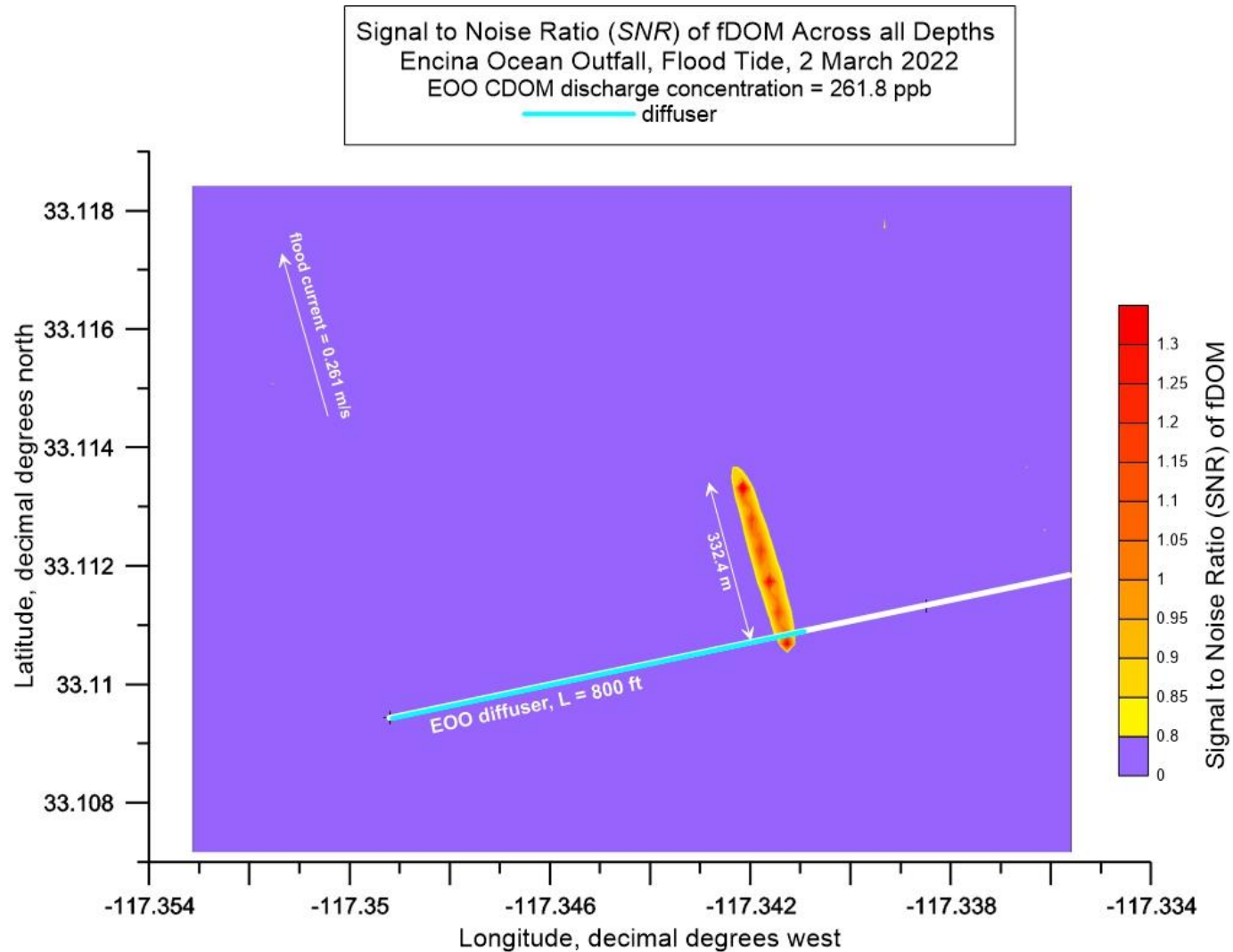


Figure 2.3.16: Full depth contour plot (aka, *heat map*) of Signal to Noise Ratio (SNR) of fDOM during AUV surveys of the discharge plume from EOO during flood tide on 2 March 2021. Average EOO discharge rate = 24.2 mgd during flood tide; End-of-pipe discharge concentration of fDOM = 261.8 ppb (QSU); End of pipe salinity = 0.82 psu; Trapping level (pycnocline depth) = -26.9 m (-88.3 ft) MSL; Mean flood tide current = 0.261 m/s (0.51 kts) toward the northwest.

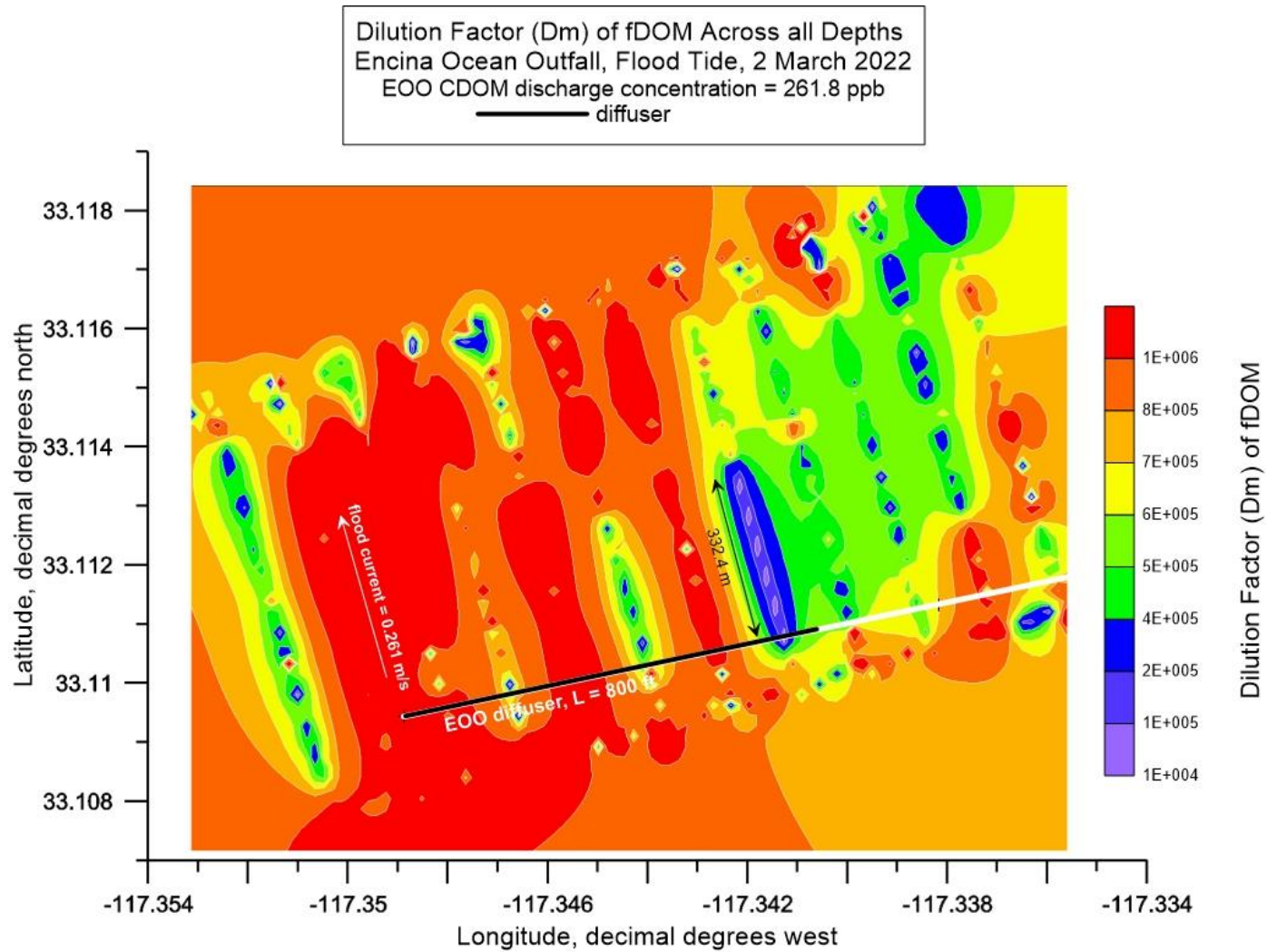


Figure 2.3.17: Full depth contour plot (aka, *heat map*) of Dilution Factor (D_{fDOM}) of fDOM during AUV surveys of the discharge plume from EOO during flood tide on 2 March 2021. Average EOO discharge rate = 24.2 mgd during flood tide; End-of-pipe discharge concentration of fDOM = 261.8 ppb (QSU); End of pipe salinity = 0.82 psu; Trapping level (pycnocline depth) = -26.9 m (-88.3 ft) MSL; Mean flood tide current = 0.261 m/s (0.51 kts) toward the northwest.

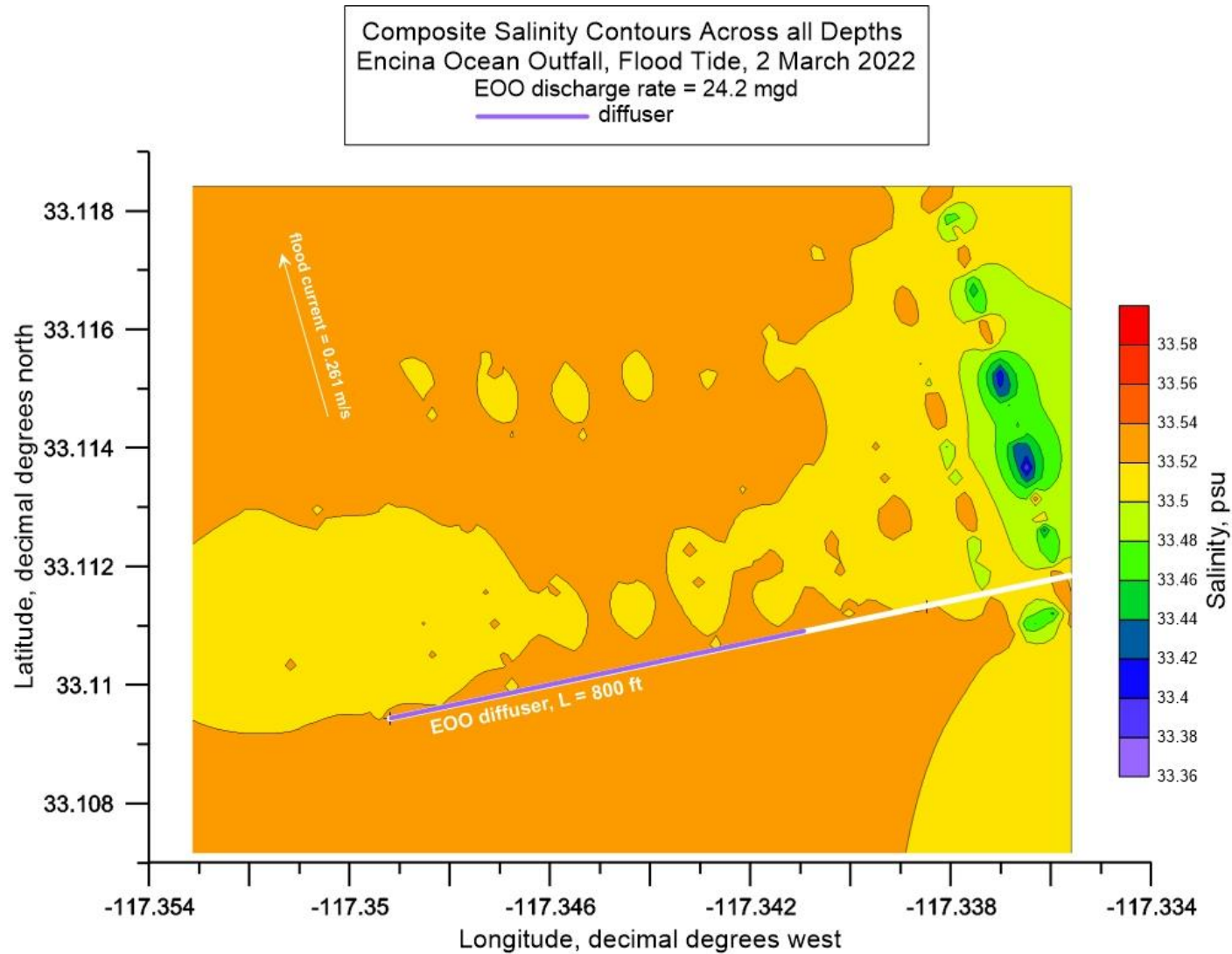


Figure 2.3.18: Full depth composite contour plot (aka, *heat map*) of AUV measurements of salinity during surveys of the discharge plume from EOO during flood tide on 2 March 2021. Average EOO discharge rate = 24.2 mgd during flood tide; End-of-pipe discharge concentration of fDOM = 261.8 ppb (QSU); End of pipe salinity = 0.82 psu; Trapping level (pycnocline depth) = -26.9 m (-88.3 ft) MSL; Mean flood tide current = 0.261 m/s (0.51 kts) toward the northwest.

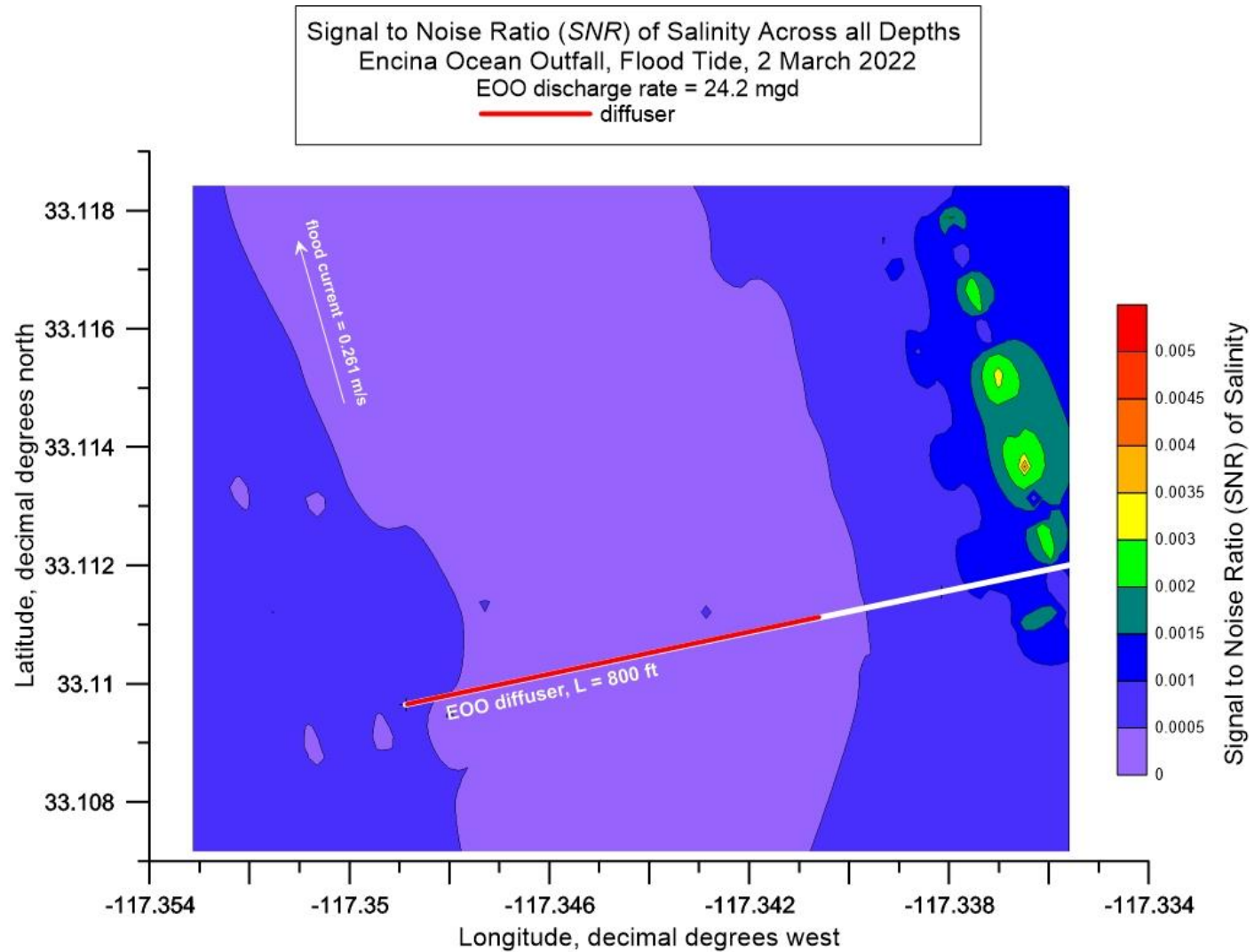


Figure 2.3.19: Full depth contour plot (aka, *heat map*) of the Signal to Noise Ratio (SNR) of salinity during AUV surveys of the discharge plume from EOO during flood tide on 2 March 2021. Average EOO discharge rate = 24.2 mgd during flood tide; End-of-pipe discharge concentration of fDOM = 261.8 ppb (QSU); End of pipe salinity = 0.82 psu; Trapping level (pycnocline depth) = -26.9 m (-88.3 ft) MSL; Mean flood tide current = 0.261 m/s (0.51 kts) toward the northwest.

plume fragment has been transported beyond the point at which initial dilution has been completed under the oceanic and discharge conditions of 2 March 2022.

To further investigate, a Plumes 20 (UM3) initial dilution simulation (see [Table 13](#)) was performed using the actual flood tide currents of 0.261 m/s (0.51 kts) on 2 March 2022. The solution file listed in [Table 14](#) indicates that the EOO initial dilution under these conditions was 268:1 at a discharge flow of 24.2 mgd. The simulation also indicates that, under the 2 March 2022 conditions, initial dilution (see [Figure 2.3.20](#)) was completed within approximately 120 meters of the outfall diffuser, or about a third the horizontal excursion of the EOO plume fragment depicted in the fDOM heat map in [Figure 2.3.15](#) during flood tide. Comparing these model predictions to what the plume tracking study actually observed during flood tide on 2 March 2022 indicates that the discharge plume may be detectable at least 212 meters beyond the point where initial dilution is completed, albeit at high dilution ratios of at least $D_{fDOM} = 1,180:1$ which is 8.2 times greater than the minimum month initial dilution of 144:1 assigned within the current NPDES permit for the EOO (No. CA 0107395, Order No. R9-2018-0059).

Table 13: Plumes 20 (UM3) Initialization of EOO flood tide Ambient Conditions on 2 March with Ambient Current

Project"C:\Plumes20\EOO_Flood_With-Current_2Mar2022" memo

Model configuration items checked:	
Channel width (m)	100
Start case for graphs	1
Max detailed graphs	10 (limits plots that can overflow memory)
Elevation Projection Plane (deg)	0
Shore vector (m,deg)	not checked
Bacteria model:	Mancini (1978) coliform model
PDS sfc. model heat transfer	Medium
Equation of State	S, T
Similarity Profile	Default profile (k=2.0, ...)
Diffuser port contraction coefficient	1
Light absorption coefficient	0.16
Farfield increment (m)	200
UM3 aspiration coefficient	0.1
Output file:	text output tab
Output each ?? steps	10
Maximum dilution reported	10000
Text output format	Standard
Max vertical reversals	to max rise or fall

Ambient Table:										
Depth m	Amb-cur m/s	Amb-dir deg	Amb-sal Psu	Amb-tem C	Amb-pol kg/kg	Decay s-1	Far-spd m/s	Far-dir deg	Disprsn m0.67/s2	Density sigma-T
0.0	0.261	0.0	33.47	14.70	3.6000E-10	0.0	0.0	0.0	0.0	24.87799
3.534	0.261	0.0	33.45	14.30	1.7000E-10	0.0	0.0	0.0	0.0	24.95378
6.535	0.261	0.0	33.48	14.15	2.2200E-10	0.0	0.0	0.0	0.0	25.00789
9.510	0.261	0.0	33.48	14.02	1.6700E-10	0.0	0.0	0.0	0.0	25.03189
12.55	0.261	0.0	33.49	13.96	1.7000E-10	0.0	0.0	0.0	0.0	25.05283
15.45	0.261	0.0	33.50	13.91	2.0900E-10	0.0	0.0	0.0	0.0	25.06862
18.47	0.261	0.0	33.50	13.90	2.6200E-10	0.0	0.0	0.0	0.0	25.07033
21.49	0.261	0.0	33.50	13.78	2.0500E-10	0.0	0.0	0.0	0.0	25.09644
24.51	0.261	0.0	33.49	13.72	2.3500E-10	0.0	0.0	0.0	0.0	25.10051

Depth m	Amb-cur m/s	Amb-dir deg	Amb-sal Psu	Amb-tem C	Amb-pol kg/kg	Decay s-1	Far-spd m/s	Far-dir deg	Disprsn m0.67/s2	Density sigma-T
27.47	0.261	0.0	33.48	13.43	2.4800E-10	0.0	0.0	0.0	0.0	25.15101
30.51	0.261	0.0	33.55	13.23	2.3500E-10	0.0	0.0	0.0	0.0	25.24583
33.47	0.261	0.0	33.55	13.23	2.5500E-10	0.0	0.0	0.0	0.0	25.24688
36.54	0.261	0.0	33.59	13.07	2.0900E-10	0.0	0.0	0.0	0.0	25.30754
39.54	0.261	0.0	33.59	13.05	2.6500E-10	0.0	0.0	0.0	0.0	25.31448
42.43	0.261	0.0	33.51	11.97	2.3500E-10	0.0	0.0	0.0	0.0	25.46085
45.47	0.261	0.0	33.68	11.43	2.4900E-10	0.0	0.0	0.0	0.0	25.69300
48.41	0.261	0.0	33.66	11.04	2.5800E-10	0.0	0.0	0.0	0.0	25.75193

Diffuser Table:

P-dia (in)	Ver angl (deg)	H-Angle (deg)	SourceX (ft)	SourceY (ft)	Ports ()	MZ-dis (m)	Isoplth (concent)	P-depth (ft)	Ttl-flo (MGD)	Eff-sal (psu)	Temp (C)	Polutnt (ppb)
2.7750	0.0	0.0	0.0	0.0	138.00	2000.0	0.0	155.75	24.200	0.8200	20.420	261.80

Table 14: Plumes 20 (UM3) Output of EOO Dilution Factor (D_{fDOM}) during Flood Tide on 2 March 2022 with Ambient Current (Final D_{fDOM} solution highlighted in yellow)

Simulation: Froude No: 14.42; Strat No: 4.72E-5; Spcg No: 7.909; k: 7.544; eff den (sigmaT) -1.196681; eff vel 1.969(m/s)

Depth Step	Amb-cur (ft)	Amb-sal (m/s)	P-dia (psu)	Eff-sal (in)	Polutnt (psu)	Dilutn (ppb)	CL- (m)	diln (m)	x-posn (ft)	y-posn (ft)	Iso dia (m)
0	155.8	0.261	33.67	2.775	0.820	261.8	1.000	1.000	0.0	0.0	0.07049; Ambient species greater than plume isopleth value, physical boundary graphed
10	155.7	0.261	33.67	3.328	6.979	213.8	1.225	1.000	0.132	0.0	0.08453;
20	155.7	0.261	33.67	3.982	11.77	176.1	1.487	1.000	0.282	0.0	0.1011;
30	155.7	0.261	33.67	4.751	15.71	145.0	1.807	1.000	0.463	0.0	0.1207;
40	155.7	0.261	33.67	5.652	18.93	119.3	2.197	1.098	0.682	0.0	0.1436;
50	155.7	0.261	33.67	6.701	21.58	98.14	2.672	1.336	0.946	0.0	0.1702;
60	155.7	0.261	33.67	7.913	23.75	80.69	3.252	1.626	1.265	0.0	0.2010;
70	155.7	0.261	33.67	9.305	25.53	66.34	3.958	1.979	1.651	0.0	0.2363;
80	155.7	0.261	33.67	10.89	27.00	54.53	4.819	2.410	2.120	0.0	0.2766;
90	155.6	0.261	33.67	12.68	28.19	44.83	5.869	2.934	2.691	0.0	0.3222;
100	155.6	0.261	33.67	14.70	29.18	36.85	7.148	3.574	3.388	0.0	0.3733;
110	155.5	0.261	33.67	16.94	29.98	30.30	8.708	4.354	4.205	0.0	0.4303;
120	155.4	0.261	33.67	19.44	30.65	24.91	10.61	5.305	5.099	0.0	0.4937;
130	155.2	0.261	33.67	22.19	31.19	20.49	12.93	6.464	6.054	0.0	0.5637; merging;
140	155.0	0.261	33.67	25.35	31.63	16.86	15.75	8.194	7.219	0.0	0.6439;
150	154.7	0.261	33.67	28.99	32.00	13.89	19.20	10.44	8.651	0.0	0.7363;
160	154.3	0.261	33.67	33.20	32.30	11.44	23.40	13.42	10.35	0.0	0.8433;
170	153.8	0.261	33.67	38.14	32.55	9.434	28.51	17.48	12.34	0.0	0.9688;
180	153.2	0.261	33.67	43.99	32.75	7.787	34.75	23.17	14.68	0.0	1.1173;
190	152.5	0.261	33.67	51.01	32.91	6.435	42.36	28.24	17.42	0.0	1.2956;
200	151.6	0.261	33.68	59.52	33.05	5.326	51.63	34.42	20.65	0.0	1.5118;
210	150.5	0.261	33.68	69.95	33.16	4.416	62.93	41.95	24.45	0.0	1.7768;
220	149.2	0.261	33.68	82.83	33.26	3.669	76.70	51.14	28.96	0.0	2.1038;
230	147.5	0.261	33.66	98.82	33.33	3.056	93.50	62.33	34.33	0.0	2.5099;
240	145.6	0.261	33.62	118.8	33.39	2.552	114.0	75.98	40.83	0.0	3.0182;
250	143.4	0.261	33.58	143.9	33.43	2.139	138.9	92.61	48.88	0.0	3.6563;
260	140.7	0.261	33.54	175.6	33.45	1.799	169.3	112.9	59.26	0.0	4.4598;
262	140.1	0.261	33.53	182.8	33.45	1.738	176.2	117.5	61.74	0.0	4.6442; trap level;
270	137.9	0.261	33.52	213.2	33.46	1.537	203.5	135.7	72.32	0.0	5.4150;
280	135.8	0.261	33.54	245.2	33.47	1.383	231.2	154.1	85.12	0.0	6.2286;
290	134.4	0.261	33.55	269.2	33.48	1.293	251.3	167.5	97.78	0.0	6.8377;
300	133.7	0.261	33.56	284.3	33.48	1.244	263.6	175.8	110.2	0.0	7.2219;
308	133.5	0.261	33.56	290.0	33.48	1.228	268.0	178.6	120.1	0.0	7.3655; local maximum rise or fall;

Horiz plane projections in effluent direction: radius(m): 0.0; CL(m): 36.603

Lmz(m): 36.603| forced entrain 1 128.4 6.782 7.366 1.000

Rate sec-1 0.0 dy-1 0.0 kt: 0.0 Amb Sal 33.5577; 4:50:50 PM. amb fills: 4

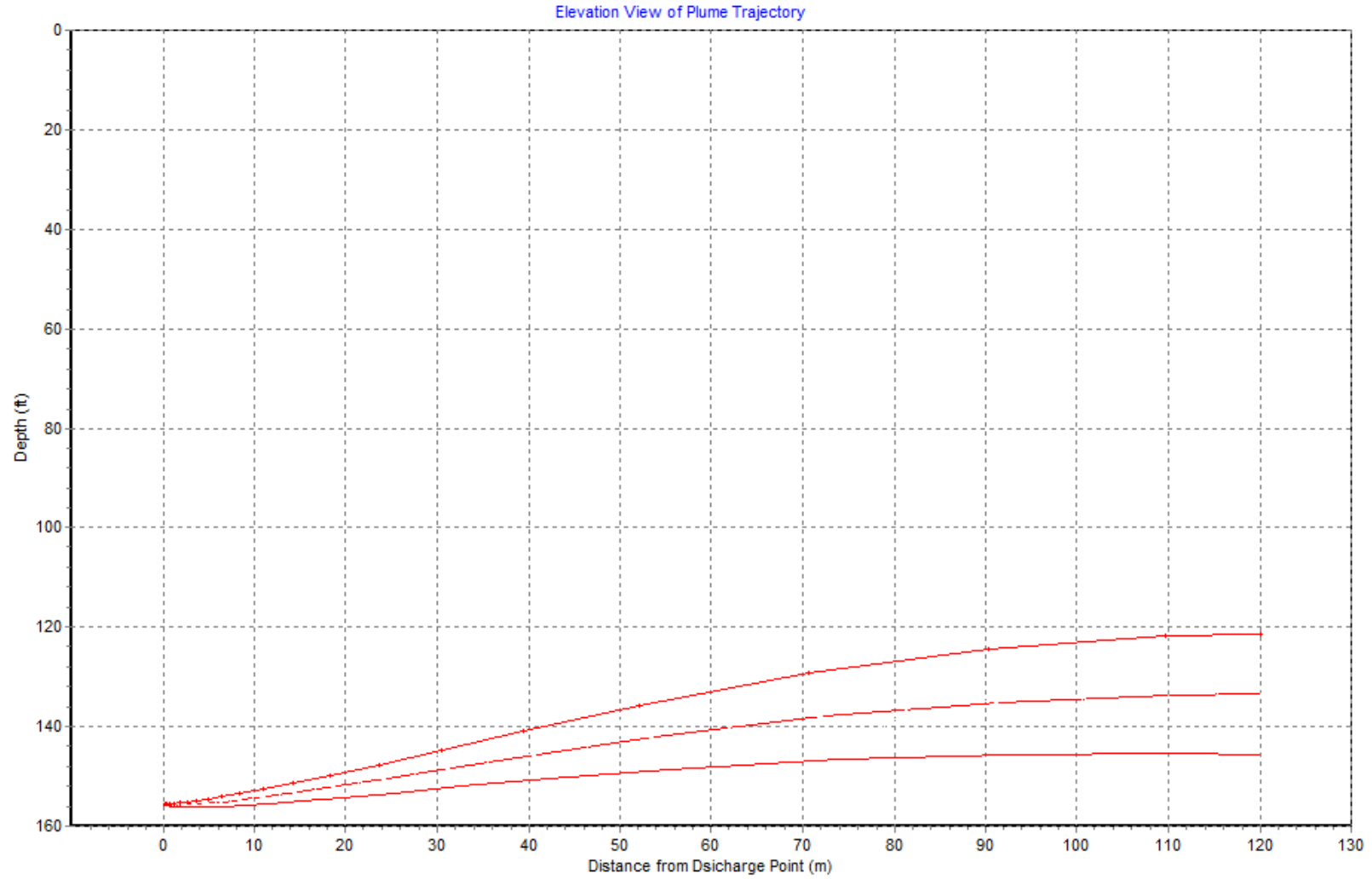


Figure 2.3.20: Plumes 20 solution of discharge plume trajectories for discharges of 24.2 mgd of EOO effluent at a discharge salinity of $S_{(x=0)} = 0.82$ psu, per operating conditions and water mass temperature/salinity profiles during ebb tide on 2 March 2022. Plumes 20 simulation performed based on ambient current = 0.261 m/s per ADCP measurements. For the March 2022 conditions, the ZID (zone within which initial dilution is completed) is defined by the maximum horizontal excursion of trajectories from the origin. From the maximum horizontal spreading of the plume, the ZID extends from $X = 0.0$ m to $X = 120$ m so that $ZID = 120$ m.

THIS PAGE INTENTIONALLY LEFT BLANK

3 PLUME TRACKING RESULTS FOR SAN ELIJO OCEAN OUTFALL (SEOO)

During both the first and second deployments of the AUV at the San Elijo Ocean Outfall (SEOO), the same basic strategy was used to fly the AUV along the track lines of a survey search pattern. The AUV is flown along a dolphin-style dive path when transiting outbound with the current along a given track line, i.e., a succession of yo-yo dive cycles, whereby the AUV dives and ascends through the water column between the seabed and an apex halfway between the sea surface and the pycnocline, as illustrated in [Figure 1.2.2](#). On the return legs of each track line, (against the current) the AUV is flown at a constant depth immediately beneath the pycnocline (trapping level) where the maximum horizontal dispersion of the plume is expected per [Figure 1.1.1](#), (cf. Baumgartner, 1994; Frick et al., 2003). The battery capacity of the Iver3 AUV limits the total distance traveled during any given ebb or flood tide survey to about 21 kilometers during survey period of about 5 hrs. The survey period is centered within each ebb or flood tide interval of 6.2 hrs. The AUV batteries are changed during the 1.2 hour interval around slack water between ebb and flood tide interval, allowing for AUV surveys of the SEOO over a complete semi-diurnal tide cycle. The 15 stationary water column monitoring stations (shown as green circles in [Figure 3.1.1](#) are distributed between the 140 ft. and 60 ft depth contours around the SEOO, and provide vertical profiles of salinity, temperature, and fDOM water mass properties immediately prior to and during the AUV surveys. Measurements from the control stations SEOO-Ebb and SEOO-Flood (shown as yellow and orange circles, respectively, in [Figure 3.1.1](#)) provide far-field measurements of natural background (ambient) water-mass properties (salinity, temperature, and fDOM). The measurements of the fDOM at the 15 stationary monitoring stations were in units of RFU which were converted to QSU fDOM units using the second order polynomial in [Figure 1.3.1](#). [Figure 3.1.1](#) also shows a group of blue triangles around the SEOO diffuser, indicating the locations of the offshore regulatory discharge monitoring stations used for NPDES permit compliance determination.

3.1 FIRST SEOO DEPLOYMENT – 23 SEPTEMBER 2021

On flood tide, the AUV was flown along five (5) track lines around the SEOO outfall diffuser within survey boxes shown in [Figure 3.1.1](#). Two separate survey boxes were planned: one during ebb tide as diagrammed in yellow in [Figure 3.1.1](#), the other flown during flood tide as diagrammed in yellow in [Figure 3.1.1](#). The track lines surveyed on flood tide are shown in [Figure 3.1.8](#) as actually flown by the AUV, while those track lines as flown on ebb tide appear in [Figure 3.1.15](#). The track lines were biased in the down current direction, with 1500 m long tracks flown south of the outfall with the southward flowing current on an ebbing tide, as indicated by the yellow survey box in [Figure 3.1.1](#). Track lines extended 500 m north of the outfall during ebb tide. On flood tide, the tidal current direction reverses and flows toward the north. Hence the track lines were biased northward with the flood tide current direction, so that 1500 m long tracks extended north of the outfall and 500 m south of the outfall. The total dimension of the AUV surveyed area on flood tide was 2000 m in the along shore direction and 1000 m in the cross-shore direction. Thus, the total area surveyed during both ebb and flood tide is approximately 988.4 acres. However, the ebb tide survey was truncated to only 3 track lines due to issues with water in the fuel tank of the R/V Benthic Cat. The total dimension of the AUV surveyed area on ebb tide was 2000 m in the along shore direction and 500 m in the cross-shore direction or a total surveyed area of approximately 247.2

acres. Note the natural background (ambient) water-mass properties of salinity, temperature, and fDOM were obtained by CTD casts at the far-field monitoring stations SEOO-Ebb and SEOO-Flood, indicated by the yellow dots and orange dots, respectively, in **Figure 3.1.1**. These far-field measurements were performed twice during each ebb or flood tide survey of the SEOO, one at the beginning of the AUV surveys and the other at the completion of each AUV survey.

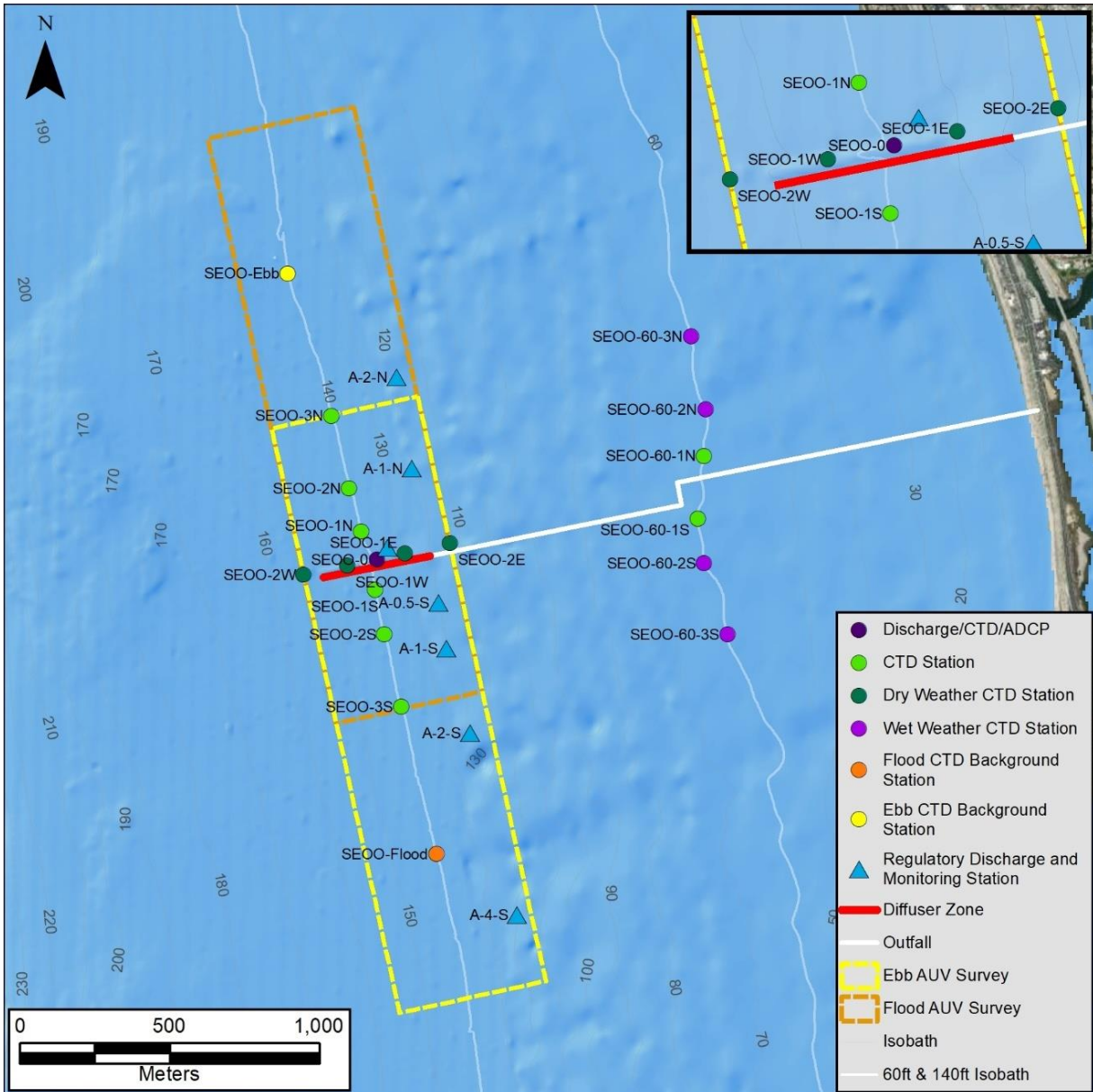


Figure 3.1.1: SEOO Survey boxes and sampling stations for the first AUV deployment, 23 September 2021

The vertical ascent of the SEOO outfall plume is typically arrested at the pycnocline (thermocline) interface, (referred to as the trapping level), where it then spreads out laterally along the pycnocline interface as illustrated in **Figure 1.1.1**. Lateral spreading of the plume can be augmented by the mass transport caused by the tidal currents that flow toward the north on a flood tide and toward the south on an ebbing tide; and by internal waves which propagate along the pycnocline interface, (propagating

shoreward on a rising tide and seaward on a falling tide). Because of plume spreading along the pycnocline interface, augmented by advection from tidal currents and internal waves, the outfall plume will make its greatest excursions (beyond the ZID) directly beneath the pycnocline, (**Figure 1.1.1**). Therefore, it was critical to the plume tracking effort to program the AUV to fly directly beneath the pycnocline during the return leg (against the current) along each track line, as shown in **Figure 1.2.2**. To locate the depth of the pycnocline, the CTD casts were performed prior to the AUV survey flood tide on 19 September 2021 and quickly processed to determine the salinity changes and temperature changes with depth, (cf. **Figure 3.1.2**). These CTD data indicated the water column was strongly stratified, forming a two-layer water mass with a well-defined pycnocline at 11.8 m depth (-38.7 ft. MSL), per **Figure 3.1.2**. Based on this finding, the AUV was programmed on its outbound dolphin-style legs (with the current) for dive cycle apex points set above the pycnocline at a depth of 5.9 m depth (-19.3 ft. MSL) and dive cycle bottoming points set at 2 m (-6.6 ft) above the seabed. The Iver3 AUV uses its bottom-locking sonar to determine the distance above the local seabed at any location within the survey box. Along the return leg of each track line (flown against the current), the AUV was programmed to fly at a constant depth of 12.8 m depth (-42.0 ft. MSL).

At the time of the flood tide AUV survey on 23 September 2021, the SEOO was discharging 9.47 mgd of wastewater having an average discharge salinity of 1.92 psu and an average fDOM discharge concentration of 206.04 ppb (QSU), based on shoreside monitoring of the SEOO effluent, (see tabulations of SEOO shoreside monitoring data in Appendix B). Earlier in the day during ebb tide the SEOO discharge rates were slightly higher at 10.44 mgd, while average discharge salinity were slightly lower at 1.87 psu and fDOM concentrations remained unchanged, (cf. Appendix B). The average SEOO discharge concentrations of fDOM are significantly higher (by more than 2 orders of magnitude) than the natural ocean background concentrations of fDOM measured at far-field control stations, SEOO-Ebb and SEOO-Flood. Natural background fDOM measured later during flood tide on 23 September 2021 at SEOO-Flood (cf. **Figure 3.1.3**) produced depth-averaged concentrations ranging between 0.770 ppb and 0.776 ppb. Vertical profiles of natural background fDOM measured earlier during ebb tide at SEOO-Ebb (cf. **Figure 3.1.4**) exhibited depth-averaged concentrations ranging between 0.0665 ppb and 0.673 ppb. Consequently, the signal to noise ratio of the fDOM plume observable at any point of discharge along the SEOO diffuser ranges between $SNR_{fDOM} = 264.5$ and $SNR_{fDOM} = 308.8$, based on the depth averaged concentrations of natural background fDOM measured at far-field control stations, SEOO-Flood and SEOO-Ebb and (**Figure 3.1.3** and **Figure 3.1.4**), applied to equation (1). While profiles of natural background fDOM concentrations measured during both ebb and flood tide showed both random variations (noise) with some general vertical structure (with higher concentration near the bottom, declining near the surface), the standard deviations around the depth averaged fDOM concentrations were small, ranging between $\sigma = 0.11$ ppb and $\sigma = 0.15$ ppb, (cf. **Figure 3.1.3** and **Figure 3.1.4**).

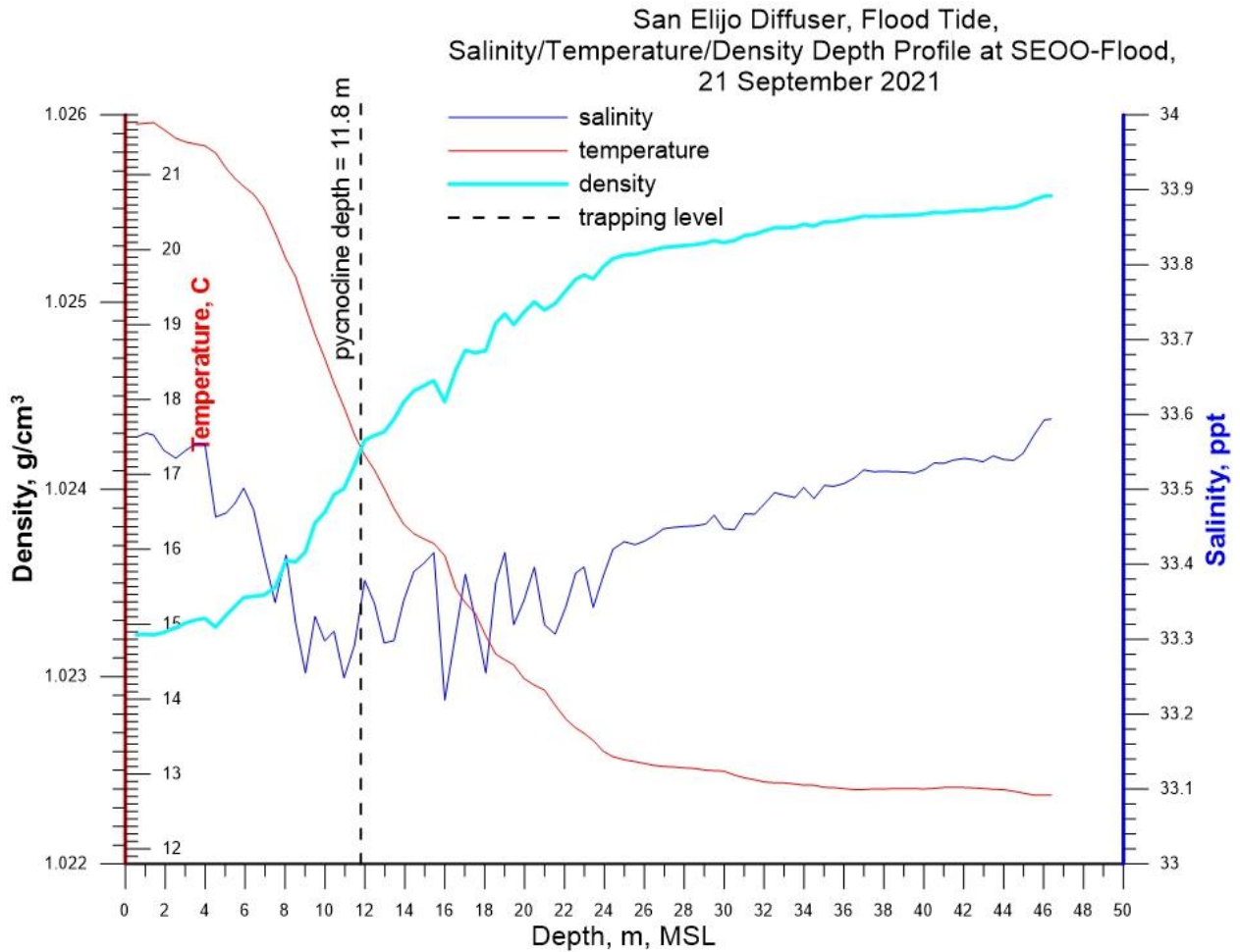


Figure 3.1.2: Salinity/Temperature/Density depth profiles derived from CTD casts on 19 September 2021 used to program the AUV survey of the plume dispersion from SEOO on 23 September 2021 during flood tide.

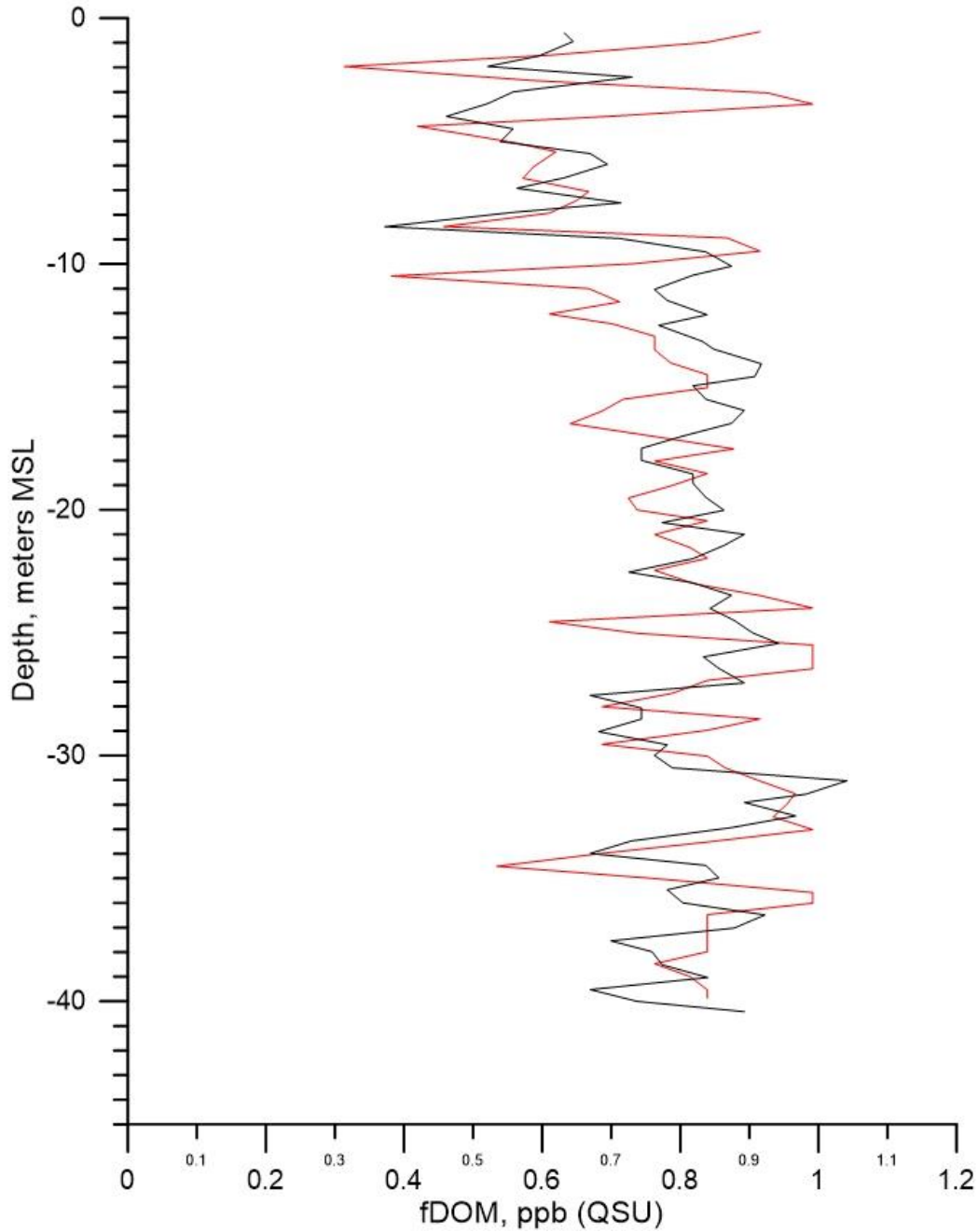
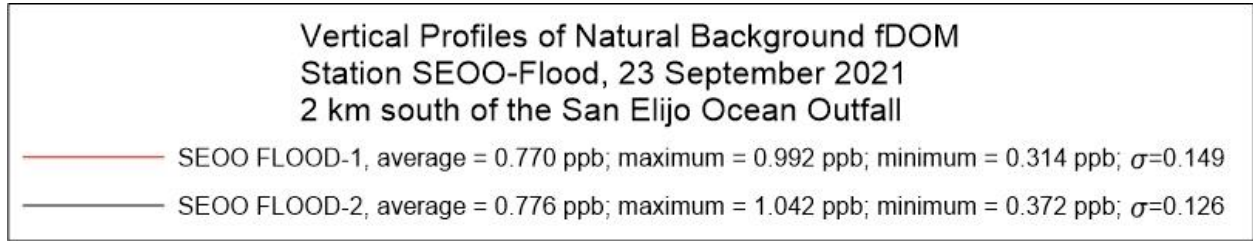


Figure 3.1.3: Vertical profiles of natural background fDOM concentrations measured during the first deployment at the far-field flood tide monitoring station “SEOO-FLOOD”, located 2 km southeast of SEOO along the -140 ft. MLLW depth contour, cf. orange dot in Figure 3.1.1.

Vertical Profiles of Natural Background fDOM
Station SEOO-EBB, 23 September 2021
2 km north of the San Elijo Ocean Outfall

— SEOO EBB-1, average = 0.673 ppb; maximum = 0.968 ppb; minimum = 0.322 ppb; $\sigma=0.113$
 — SEOO EBB-2, average = 0.665 ppb; maximum = 1.016 ppb; minimum = 0.339 ppb; $\sigma=0.121$

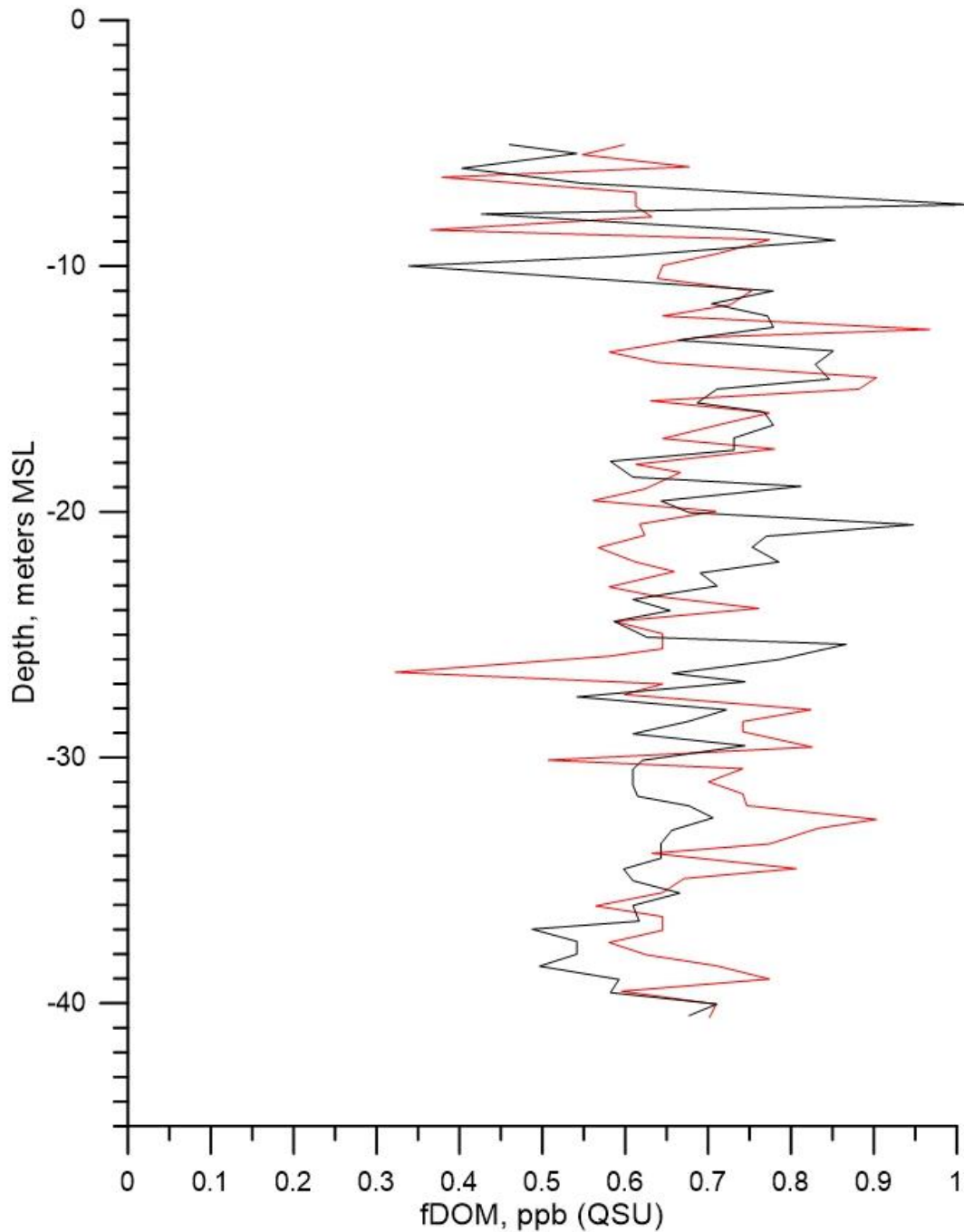


Figure 3.1.4: Vertical profiles of natural background fDOM concentrations measured during the first deployment at the far-field ebb tide monitoring station “SEOO-EBB”, located 2 km northwest of SEOO along the -140 ft. MLLW depth contour, cf. yellow dot in Figure 3.1.1

Mean flood tide currents on 23 September 2021 at the far-field control station, SEOO-Flood, were 0.326 m/s (0.63 kts) toward the northwest, based on ADCP data at far field monitoring station, SEOO-Flood, (cf. [Figure 3.1.5](#)) located up-drift of the orange AUV survey box shown in [Figure 3.1.1](#). These mean currents convey a net shore-parallel (upcoast/downcoast) drift of the SEOO discharge. However, there are other transient short-lived current oscillations reaching 0.889 m/s (1.75 kts) in the flood tide ADCP time series record on 23 September 2021. The current direction data in the ADCP record indicates these spikes of higher oscillatory currents were directed cross-shore, indicating they were due to shoaling internal waves. Because of the oscillatory nature of these current spikes, they produce no net drift of the SEOO discharge plume, but merely serve to smear the plume or break off pieces from the main body of the plume and smear or disperse those pieces in the cross-shore direction. ADCP measurements of currents at far field monitoring station, SEOO-Ebb, (cf. [Figure 3.1.6](#)) find that mean ebb tide currents on 23 September 2021 were slightly greater than the mean flood tide currents, reaching 0.373 m/s (0.72 kts) directed toward the southeast. This is due to the fact that tidal currents along the coastline of the lower SCB do not reverse symmetrically between ebb and flood tide, but rather are *ebb-tide dominant*, imparting a net southeasterly drift to the SEOO discharge plume over a complete tidal day of 24.83 hrs. Transient oscillatory current spikes in the ebb tide ADCP current record on 23 September 2021 reached 1.019 m/s (1.98 kts) in the cross-shore direction, again indicating the presence of internal wave activity. These internal waves are excited by another extreme bathymetric feature that resulted in an abrupt narrowing of the continental shelf directly offshore of the SEOO diffuser, (cf. [Figure 3.1.7](#)). This abrupt narrowing of the shelf creates a cliff that is perpendicular to the shoreline along the shelf break and excites internal waves as the tidal currents flow across the escarpment formed by this cross-shore cliff, much like lee waves do in the atmosphere when storm winds blow over mountainous topography. The cross-shore oscillations of the internal waves that radiate outward from the shelf break producing high current spikes in the ADCP records on 23 September 2021 (cf. [Figure 3.1.5](#) and [Figure 3.1.6](#)).

[Figure 3.1.8](#) reveals accurate repeatability of the outbound and return legs along each of five track lines as flown by the AUV during the flood tide survey of the SEOO on 23 September 2021. During this survey, the AUV collected 65,920 separate measurements of salinity and fDOM. Originally, 29,604 measurements of fDOM taken along the return legs of each of the 5 track lines at a constant depth of 12.8 m depth (-42.0 ft. MSL) were parsed from the original 65,920 measurements to create a map of fDOM just below the pycnocline (trapping layer, as shown in [Figure 3.1.9](#)). It was anticipated that such a map would capture the maximum dispersion of the SEOO discharge plume since the dilution models approved for use by the State Water Resources Control Board (CORMIX v-11, Visual Plumes Um3 and Plumes 20 UM3) all show that discharge trajectories reach maximum horizontal excursions at or near the trapping level, (cf. Frick et al., 2010). The highest concentrations of fDOM found anywhere along the trapping level in [Figure 3.1.9](#) reach $fDOM_{(x)} = 1.3$ ppb, almost twice the depth averaged natural background fDOM concentration of $fDOM_{\infty} = 0.773$ ppb measured at the far-field control station, SEOO-Flood, (cf. [Figure 3.1.3](#)). Inserting these values into equation (1), the largest signal to noise ratio of any feature in the fDOM map along the trapping level in [Figure 3.1.9](#) is only $SNR_{fDOM} = 0.68$. This SNR result is less than the lowest order significance threshold for detection, that requires $SNR_{fDOM} \geq 1$. Therefore, nothing can be concluded about any fDOM feature along the trapping level in [Figure 3.1.9](#).

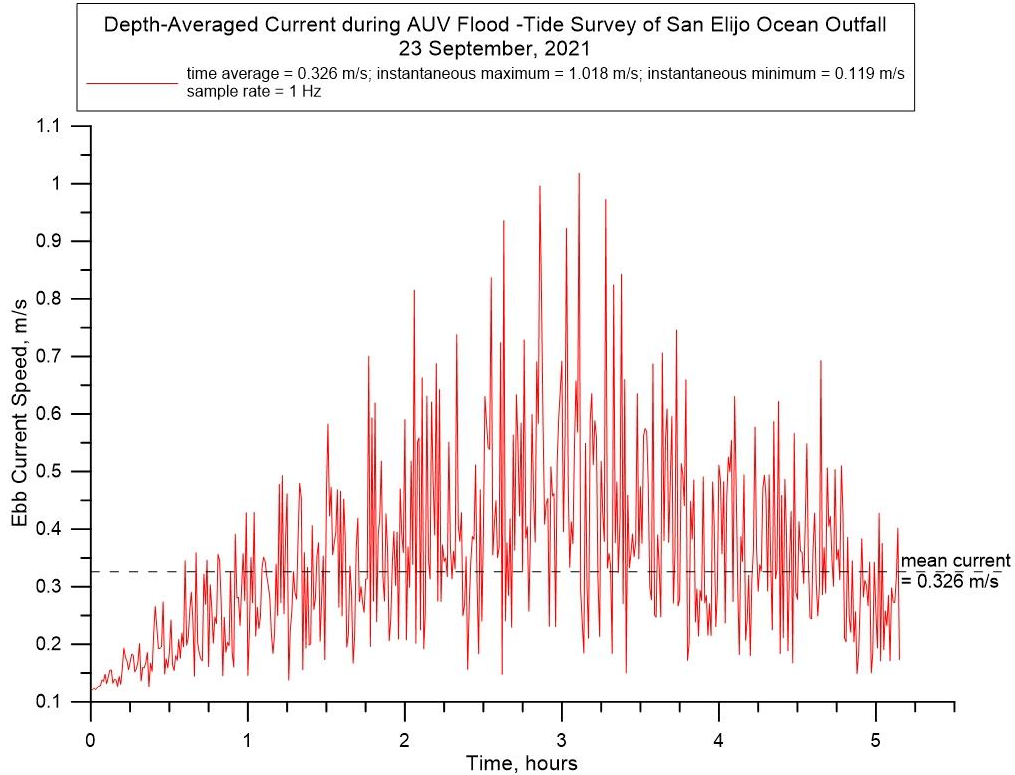


Figure 3.1.5: Time series of depth averaged current derived from ADCP measurements at SEOO during flood-tide AUV survey on 23 September 2021.

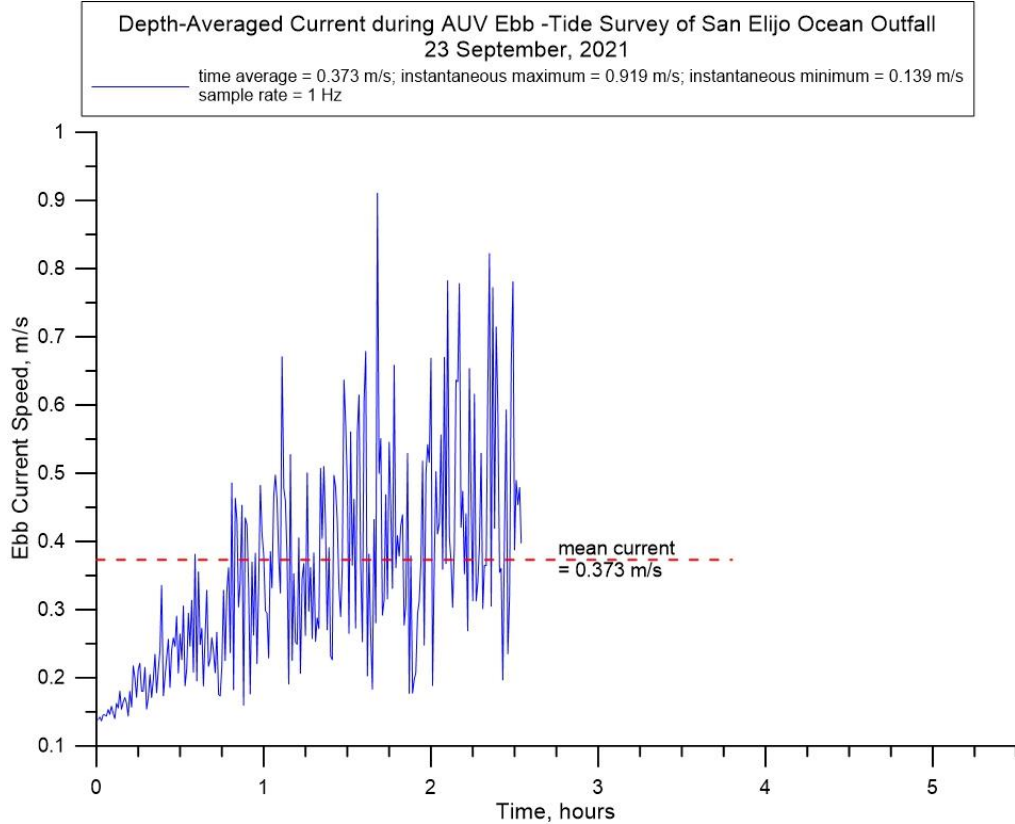


Figure 3.1.6: Time series of depth averaged current derived from ADCP measurements at SEOO during ebb-tide AUV survey on 23 September 2021.

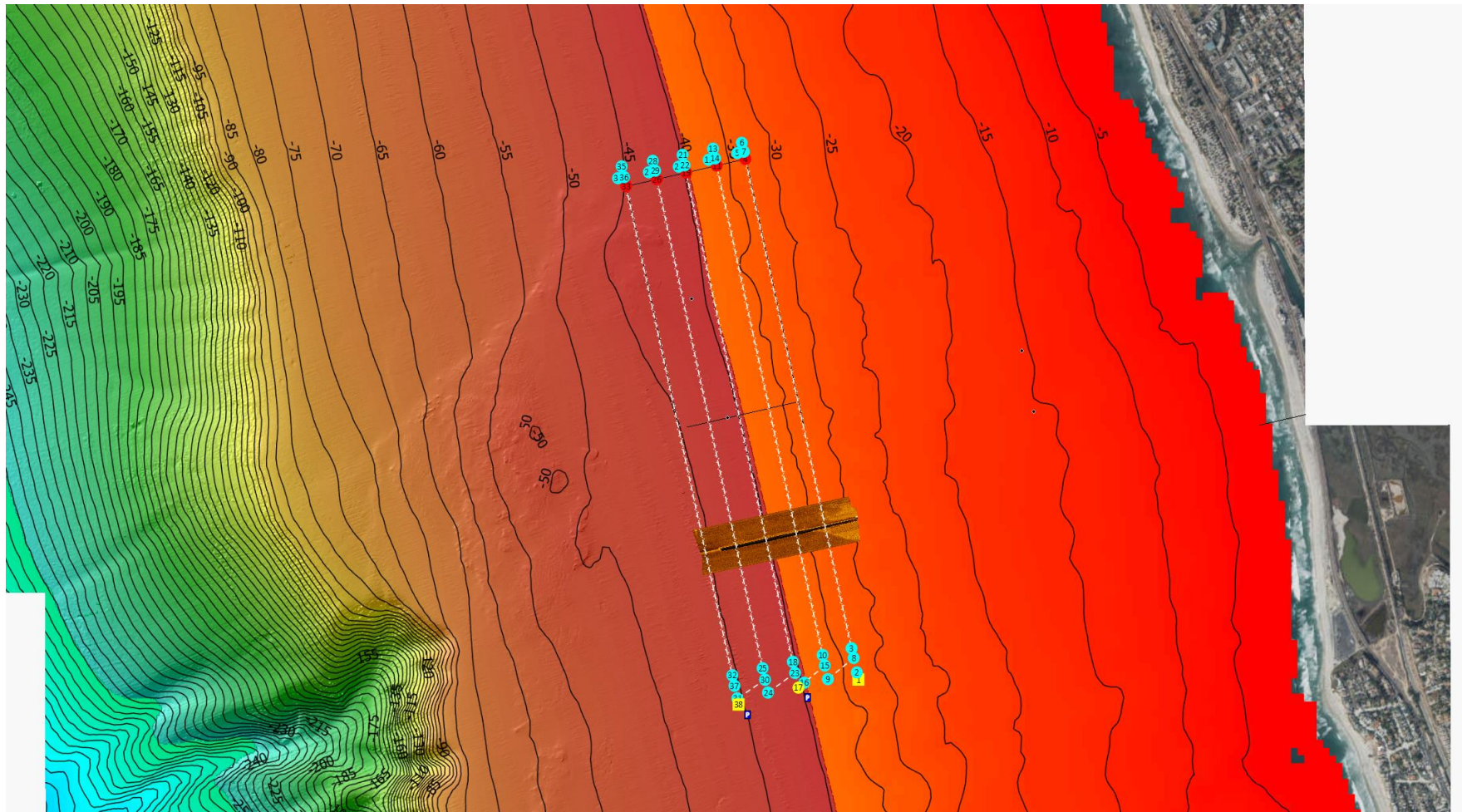


Figure 3.1.7: AUV track lines as planned for flood tide surveys of the discharge plume from SEOO.

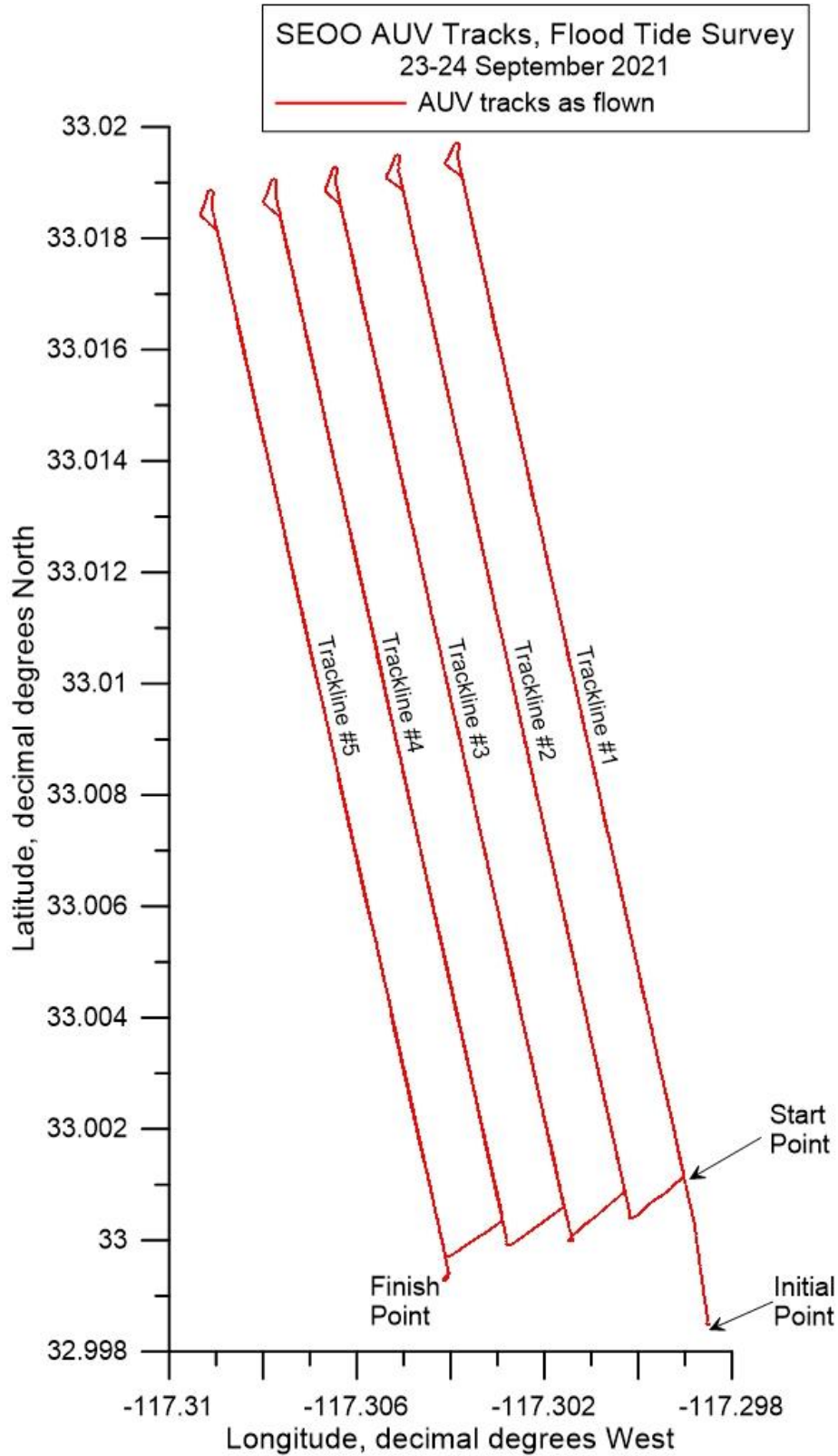


Figure 3.1.8: AUV track lines as flown during flood tide surveys of the discharge plume from SEOO. The total dimension of the AUV surveyed area on ebb tide was 2000 m in the along shore direction and 1000 m in the cross-shore direction or a total surveyed area of approximately 494.3 acres. Note, at 30° N latitude, 1° longitude = 93,453.2 m, while 1° latitude = 110,904.4 m.

Dispersion of fDOM at the Trapping Level, (depth = - 11.8m MSL)
San Elijo Ocean Outfall, Flood Tide, 23-24 September 2021

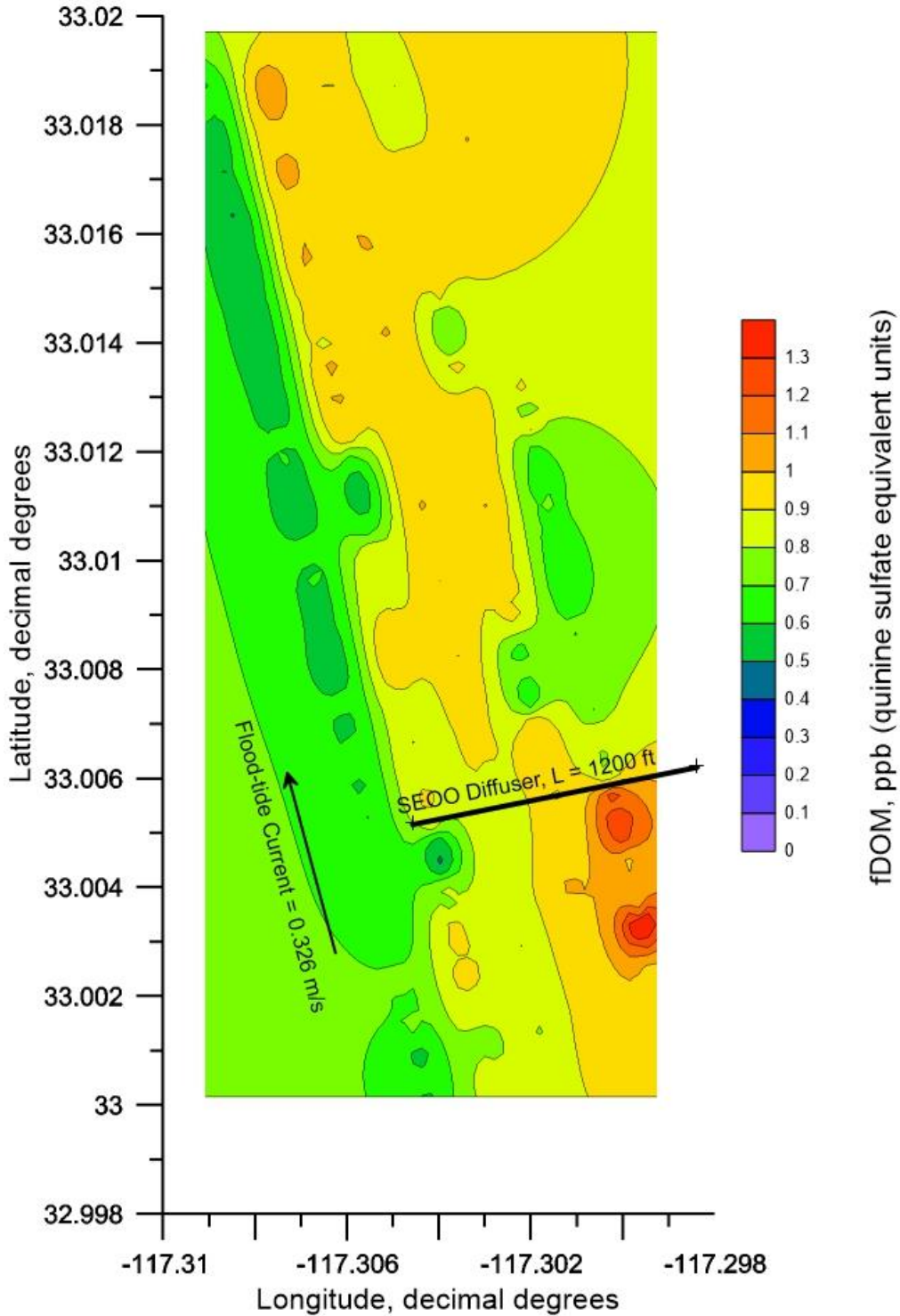


Figure 3.1.9: Contour plot of AUV measurements of fDOM at the trapping level during flood tide surveys of SEOO. SEOO discharge rate = 9.473 mgd; End-of-pipe discharge concentration of fDOM = 206.04 ppb (QSU); Trapping level (pycnocline depth) = 38.7 ft MSL; End of pipe salinity = 1.92 ppt; Mean flood tide current = 0.326 m/s (0.63 kts) toward the northwest.

To explore possible reasons for the failure to discover evidence of the SEOO plume at the trapping level during flood tide, a calibrated computational fluid dynamics (CFD) simulation was prepared using the AUV measurements of fDOM along track line #3 (cf. [Figure 3.1.8](#)) to examine vertical dispersion of the plume through the water column. The calibrated CFD simulation in [Figure 3.1.10](#) indicates that the SEOO plume drifts a significant distance horizontally near the seabed in the 0.326 kt flood tide current, before it rises and pancakes on the base of the trapping layer. As the plume drifts horizontally with the flood tide currents, it undergoes significant dilution before rising to the trapping level. As a result, fDOM concentrations at the trapping level are no more than $fDOM_{(x)} = 1.38$ ppb. [Figure 3.1.3](#) indicates that natural background concentrations of fDOM at the trapping level (11.8 m depth) during flood tide are $fDOM_{\infty} = 0.773$ ppb. Therefore, the signal to noise ratio of the fDOM at the trapping level in this CFD simulation was found to be only $SNR_{fDOM} = 0.78$, still below the lowest order significance threshold for detection (i.e., $SNR_{fDOM} \geq 1$). From this result it was concluded that the strongly stratified water column portrayed in the temperature/salinity profiles in [Figure 3.1.2](#), the SEOO plume was somewhat constrained from immediately rising and underwent sufficient dilution while it drifted horizontally in the flood current that the fDOM concentrations dropped below the significance threshold detection limit by the time the plume rose to the trapping level. Consequently, an alternative method was developed for mapping fDOM data from the AUV surveys of the SEOO.

The new fDOM mapping method involved displaying simultaneously all 65,920 fDOM measurements across all depths, including even those measured along the cross-shore tracks that connect with each of the 5 survey track lines, (cf. [Figure 3.1.8](#)). In this way it was anticipated that detectable portions of the SEOO plume could be found at certain depths and locations beneath the trapping level. [Figure 3.1.11](#) employs the new fDOM mapping technique with a full depth contour plot of AUV measurements of fDOM during flood tide surveys of the SEOO on 23 September 2021. These types of plots are referred to as *heat maps* in signal detection theory, (Schonhoff & Giordano, 2006). Inspection of [Figure 3.1.11](#) reveals that variations in fDOM concentrations across all depths surveyed by the AUV range from 0.2 ppb to 1.3 ppb. However, these fDOM variations exhibit horizontal structure, being arranged in a repeated banding pattern that does not appear to be spatially coherent with the alignment of the SEOO pipeline and diffuser but appears to align with the 5 track lines in the ebb tide survey pattern, (cf. [Figure 3.1.8](#)). It is likely that the repeated banding pattern in the fDOM heat map in [Figure 3.1.11](#) is a result of insufficient spatial resolution in fDOM sampling between the track lines, referred to as *spatial aliasing*, (Peterson, et al, 1954).

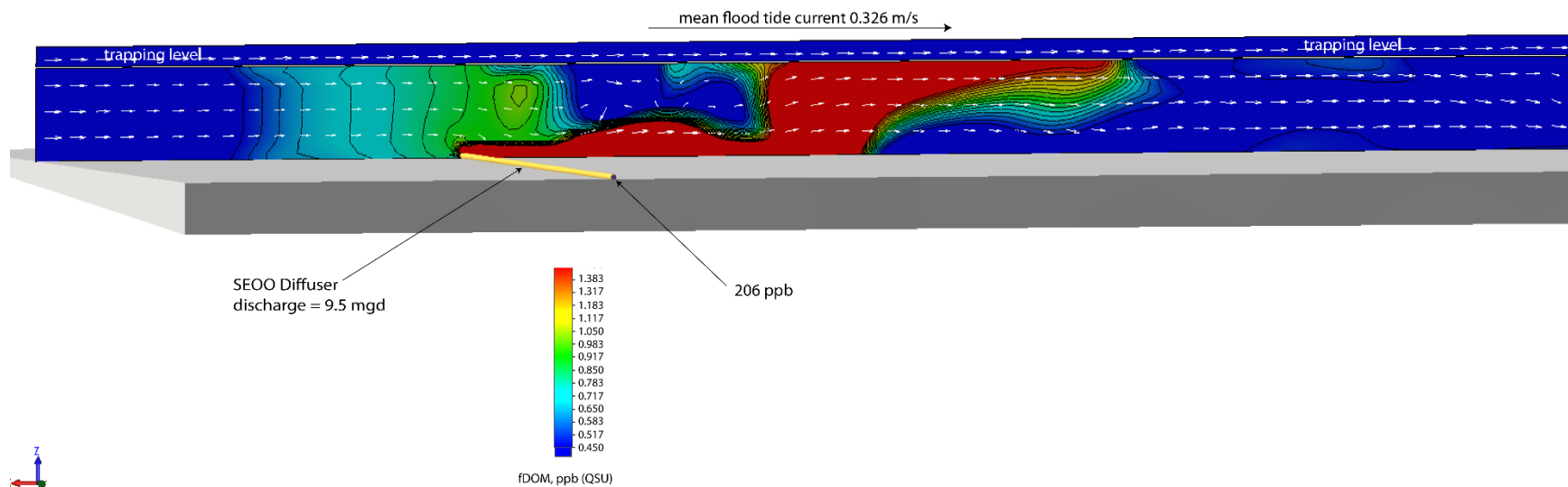


Figure 3.1.10: Calibrated CFD simulation of the plume dispersion through the water column from SEOO. CFD simulation calibrated to AUV measurements of fDOM along the track line #3 during flood tide as shown in [Figure 3.1.8](#). CFD simulation based on SEOO discharge rate = 9.5 mgd; End-of-pipe discharge concentration of fDOM = 206 ppb (QSU); End of pipe salinity = 1.92 psu; Trapping level (pycnocline depth) = 38.7 ft MSL; Mean flood tide current = 0.326 m/s (0.63 kts) toward the northwest; Ambient ocean fDOM concentration at the trapping level=0.45 to 0.65 ppb (QSU).

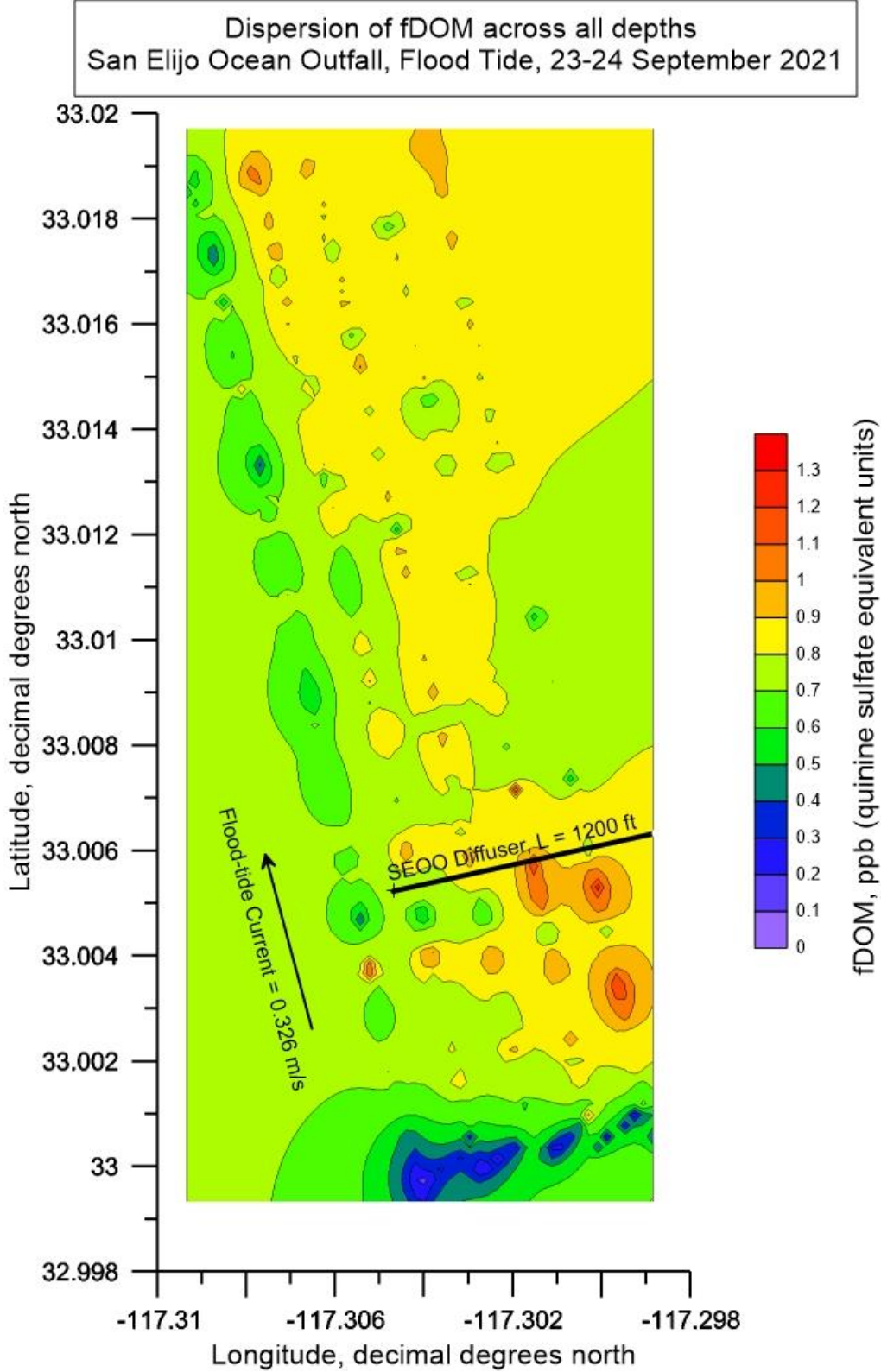


Figure 3.1.11: Full depth contour plot (aka, heat map) of AUV measurements of fDOM during surveys of SEOO during flood tide on 23 September 2021. Average SEOO discharge rate = 9.473 mgd during flood tide; End-of-pipe discharge concentration of fDOM = 206.04 ppb (QSU); End of pipe salinity = 1.92 psu; Trapping level (pycnocline depth) = 38.7 ft MSL; Mean flood tide current = 0.326 m/s (0.63 kts) toward the northwest.

The mechanism producing the blue bands in the fDOM heat map result from the AUV measurements near the apex of the dolphin style dive cycles, when the AUV is in the shallow water above the trapping layer where ambient fDOM concentrations are lower (cf [Figure 3.1.9](#)). Yellow, orange and red banding features in the fDOM heat map could be remnants of the SEOO plume at deeper depths along each track line. To assess whether this is plausible, the fDOM heat map in [Figure 3.1.11](#) is converted into a signal to noise ratio heat map in [Figure 3.1.12](#) by invoking equation (1) to convert the fDOM concentrations in [Figure 3.1.11](#) into corresponding SNR_{fDOM} patterns. Inspection of [Figure 3.1.12](#) reveals that the highest signal to noise ratio of the most elevated (orange/red) feature anywhere in the fDOM heat map is only a $SNR_{fDOM} \cong 0.68$, which does not meet the lowest order significance threshold for detection (i.e., $SNR_{fDOM} \geq 1$). Therefore, none of the elevated (orange or red) features in the fDOM heat map in [Figure 3.1.11](#) can be regarded as remnants of the SEOO flood tide plume. To verify this conclusion, the SNR_{fDOM} heat map in [Figure 3.1.12](#) was transposed into a dilution heat map in [Figure 3.1.13](#) using equation (2) under the assumption that the initial fDOM concentration is $fDOM_{(x=0)} = 206.04$ ppb. From that assumption, [Figure 3.1.13](#) indicates that the dilution factor (D_{fDOM}) for the fDOM features in [Figure 3.1.11](#) would range from $D_{fDOM} = 1,000$ to $D_{fDOM} = 30,000$, so that any toxic SEOO effluent constituents in the NPDES permit would be below quantifiable detection limits.

A potentially useful alternative plume observable might be salinity. [Figure 3.1.14](#) provides the salinity heat map generated from the AUV salinity measurements during the EOO ebb tide survey. Most of the features in the salinity heat map range from $S_{(x)} = 33.5$ psu to $S_{(x)} = 33.59$ psu. None of these salinity features in [Figure 3.1.14](#) appear to be spatially coherent with the SEOO pipeline or diffuser. The far-field depth averaged salinity from the salinity profile in [Figure 3.1.2](#) indicates that natural background salinity is $S_{\infty} = 33.44$ psu with a standard deviation of $\sigma = 0.093$ psu. Inserting these values into equation (1) indicates that the signal to noise ratio of the predominant salinity features in [Figure 3.1.14](#) range from $SNR_S = 0.0018$ to $SNR_S = 0.0033$, while the signal to noise ratio of the small scale salinity heat bubbles in [Figure 3.1.14](#) range from $SNR_S = 0.0044$ to $SNR_S = 0.0066$. Regardless, all the salinity features in [Figure 3.1.14](#) have signal to noise ratios significantly below the lowest order significance threshold for detection (i.e., $SNR_S \geq 1$) and consequently cannot be associated with plume fragments by any statistically meaningful measure. The conclusion that salinity is not a useful observable for tracking the SEOO plume was anticipated at the outset since the signal to noise ratio of the salinity signal at the point of discharge is only $SNR_{S(x=0)} = 0.97$, or less than lowest order significance threshold for detection.

Signal to Noise Ratio of fDOM across all depths
San Elijo Ocean Outfall, Flood Tide, 23-24 September 2021

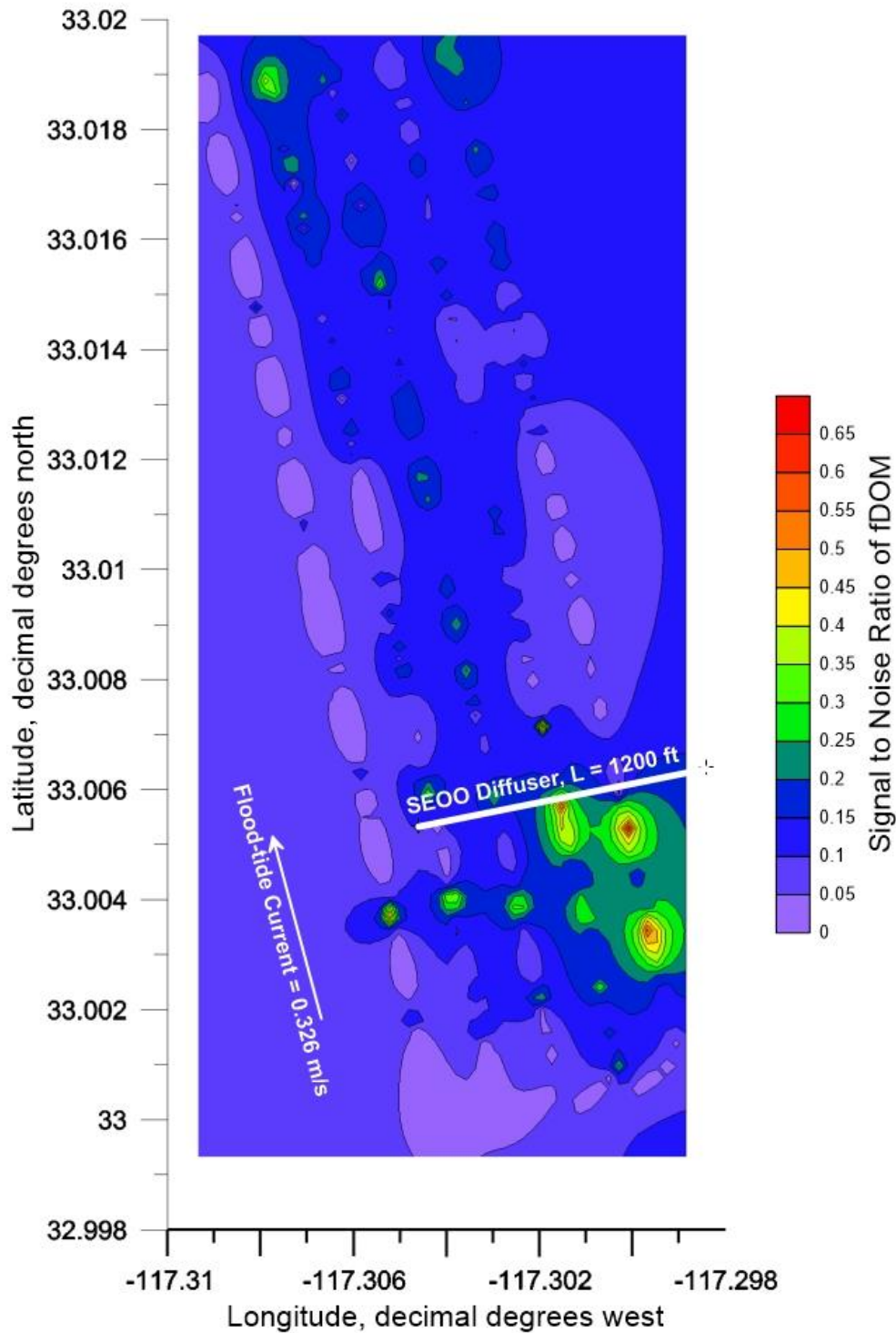


Figure 3.1.12: Full depth contour plot (aka, heat map) of the fDOM signal to noise ratio (SNR) from AUV surveys of SEOO during flood tide on 23 September 2021. Average SEOO discharge rate = 9.473 mgd during flood tide; End-of-pipe discharge concentration of fDOM = 206.04 ppb (QSU); End of pipe salinity = 1.92 psu; Trapping level (pycnocline depth) = 38.7 ft MSL; Mean flood tide current = 0.326 m/s (0.63 kts) toward the northwest.

Dilution Factor (Dm) of fDOM across all depths
San Elijo Ocean Outfall, Flood Tide, 23-24 September 2021

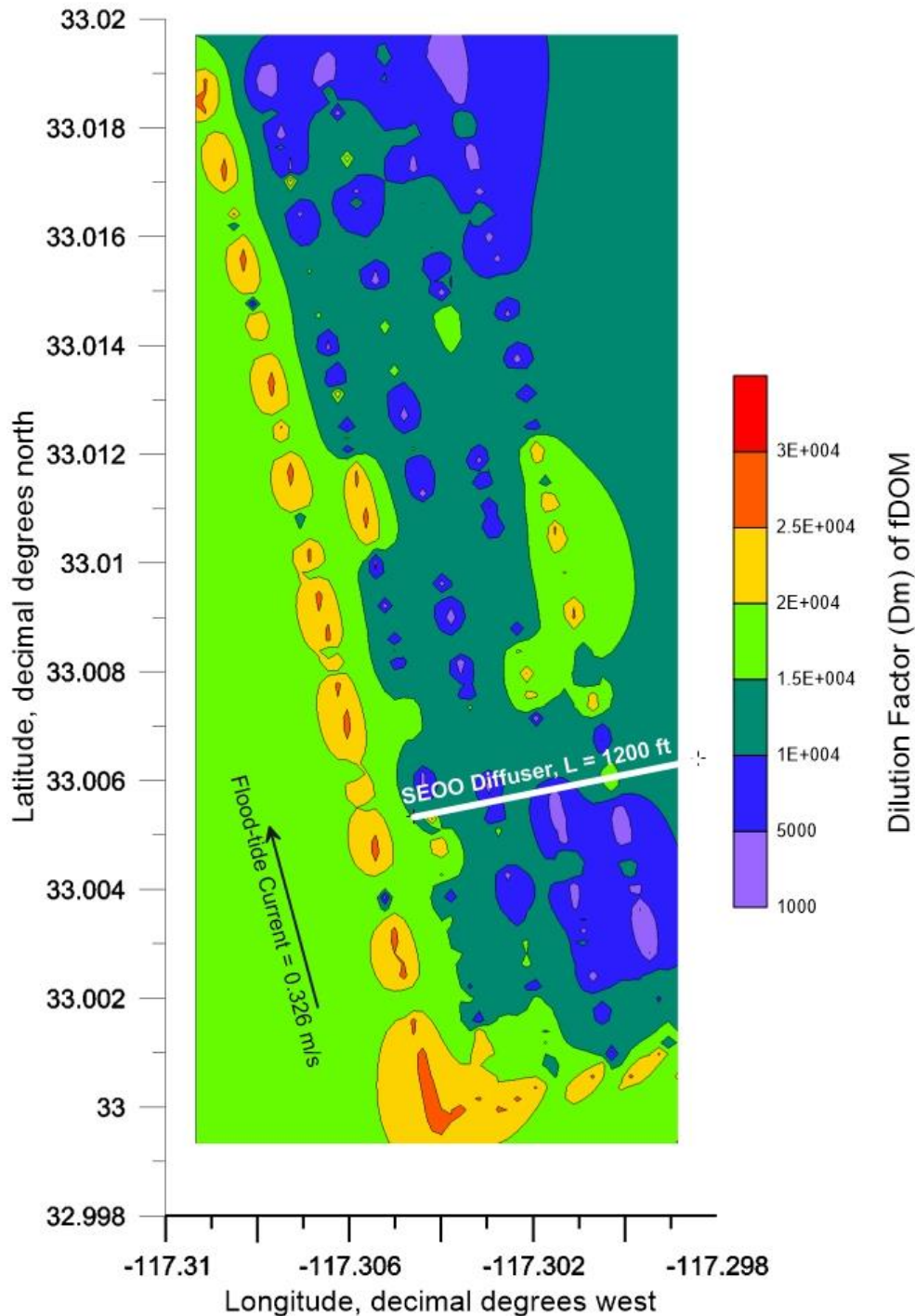


Figure 3.1.13: Full depth contour plot (aka, heat map) of the dilution factor (D_{fDOM}) of fDOM from AUV surveys of SEOO during flood tide on 23 September 2021. Average SEOO discharge rate = 9.473 mgd during flood tide; End-of-pipe discharge concentration of fDOM = 206.04 ppb (QSU); End of pipe salinity = 1.92 psu; Trapping level (pycnocline depth) = 38.7 ft MSL; Mean flood tide current = 0.326 m/s (0.63 kts) toward the northwest.

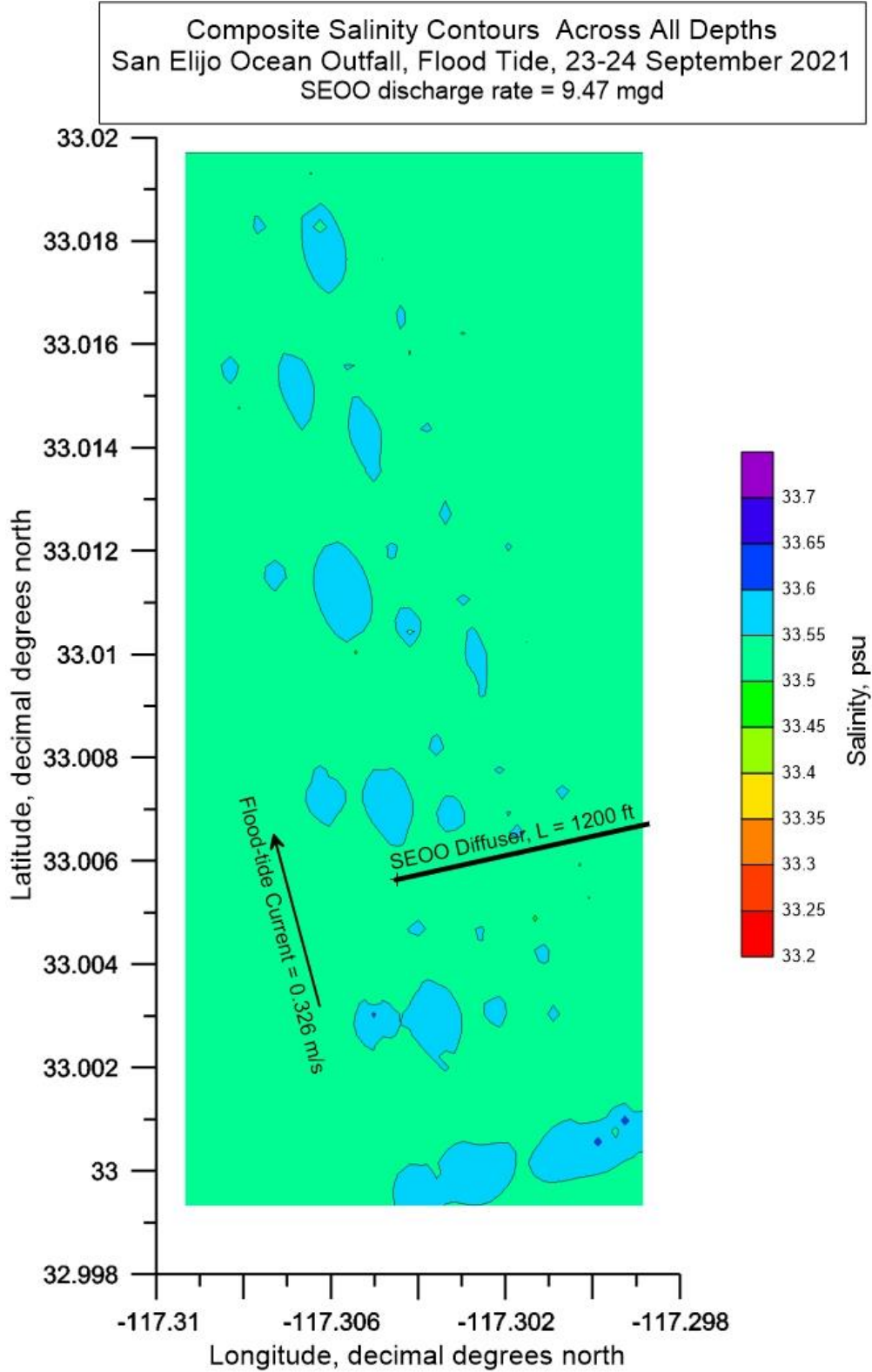


Figure 3.1.14: Full depth composite contour plot (aka, heat map) of salinity during AUV surveys of SEOO during flood tide on 23 September 2021. Average SEOO discharge rate = 9.473 mgd during flood tide; End of pipe salinity = 1.92 psu; Trapping level (pycnocline depth) = 38.7 ft MSL; Mean flood tide current = 0.326 m/s (0.63 kts) toward the northwest.

During the preceding ebb tide AUV survey, the survey tracks at the SEOO are reversed from those during flood tide. Hence, with the ebb current, survey track lines were biased toward the southeast (cf. [Figure 3.1.15](#)) to maximize the search area in the down-drift region of the ebb tide currents. However, problems with seawater in the fuel of the AUV support vessel were encountered at the beginning of the SEOO ebb tide survey. Several hours were required to clear the water from the fuel; and so only 3.22 hr remained within the 6.2 hr ebb tide window. Consequently, the SEOO ebb tide survey pattern was truncated to only 3 track lines shown as flown in [Figure 3.1.15](#). In spite of the un-planned abbreviation of the ebb tide survey, the as-flown track lines in [Figure 3.1.15](#) exhibit accurate repeatability of the outbound and return legs. The total dimension of the reduced AUV surveyed area on ebb tide was 2000 m in the along shore direction and 500 m in the cross-shore direction or a total surveyed area of approximately 247.2 acres.

During the ebb tide survey, the AUV collected 39,801 separate measurements of salinity and fDOM. The fDOM heat map generated from these 39,801 measurements of fDOM concentrations is plotted in [Figure 3.1.16](#). Inspection of [Figure 3.1.16](#) reveals that variations in fDOM concentrations across all depths surveyed by the AUV during ebb tide range again from 0.2 ppb to 1.3 ppb, (same as observed during flood tide). The fDOM variations during ebb tide in [Figure 3.1.16](#) also exhibit horizontal structure, being arranged in a repeated banding pattern that does not appear to be spatially coherent with the alignment of the SEOO diffuser, but does appear to align with the 3 track lines in the ebb tide survey pattern, (cf. [Figure 3.1.15](#)); again, likely due to spatial aliasing due to insufficient fDOM sampling resolution between the track lines, (cf. Peterson et al., 1954). The repeating dark-green/light-green bands in the fDOM heat map are small variations about the average natural back ground fDOM concentrations of $0.665 \text{ ppb} \leq fDOM_{\infty} \leq 0.673 \text{ ppb}$, consistent with [Figure 3.1.4](#). Within the repeating dark-green/light-green bands of the fDOM heat map are lines of small blue and orange bubbles of depressed and elevated fDOM concentration ranging between minimums of $fDOM_{\infty} \cong 0.3 \text{ ppb}$ and maximums of $fDOM_{\infty} \cong 0.9 \text{ ppb}$, which are also consistent with variations in natural background fDOM concentrations found at control stations SEOO-Ebb, (cf. [Figure 3.1.4](#)). Since these fDOM concentration bubbles follow the 3 AUV track lines, they are likely caused by depth variations along the dolphin stile dive cycles as the AUV yo-yo's between the shallow water above the trapping layer where ambient fDOM concentrations are lower, and the near bottom waters where fDOM concentrations are higher (cf. [Figure 3.1.4](#)). To assess whether these banding features due to spatial aliasing in the fDOM heat map could possibly contain remnants of the SEOO plume, the fDOM heat map in [Figure 3.1.16](#) is converted into a signal to noise ratio heat map in [Figure 3.1.17](#). This is done by invoking equation (1) to convert the fDOM concentrations in [Figure 3.1.16](#) into corresponding SNR_{fDOM} patterns. Inspection of [Figure 3.1.17](#) reveals that the highest signal to noise ratio anywhere in the [Figure 3.1.16](#) fDOM heat map is only a $SNR_{fDOM} \cong 0.7$, which does not meet the lowest order significance threshold for detection (i.e., $SNR_{fDOM} \geq 1$). Therefore, none of the features in the fDOM heat map in [Figure 3.1.16](#) can be regarded as remnants of the SEOO ebb-tide plume. To verify this conclusion, the SNR_{fDOM} heat map in [Figure 3.1.17](#) was transposed into a dilution heat map in [Figure 3.1.18](#) using equation (2) under the assumption that the initial fDOM concentration is $fDOM_{(x=0)} = 206.04 \text{ ppb}$. From that assumption, [Figure 3.1.18](#) indicates that the dilution factor (D_{fDOM}) for the ebb tide fDOM features in [Figure 3.1.16](#) would range from $D_{fDOM} = 1,000$ to $D_{fDOM} = 30,000$, the same as the dilutions for

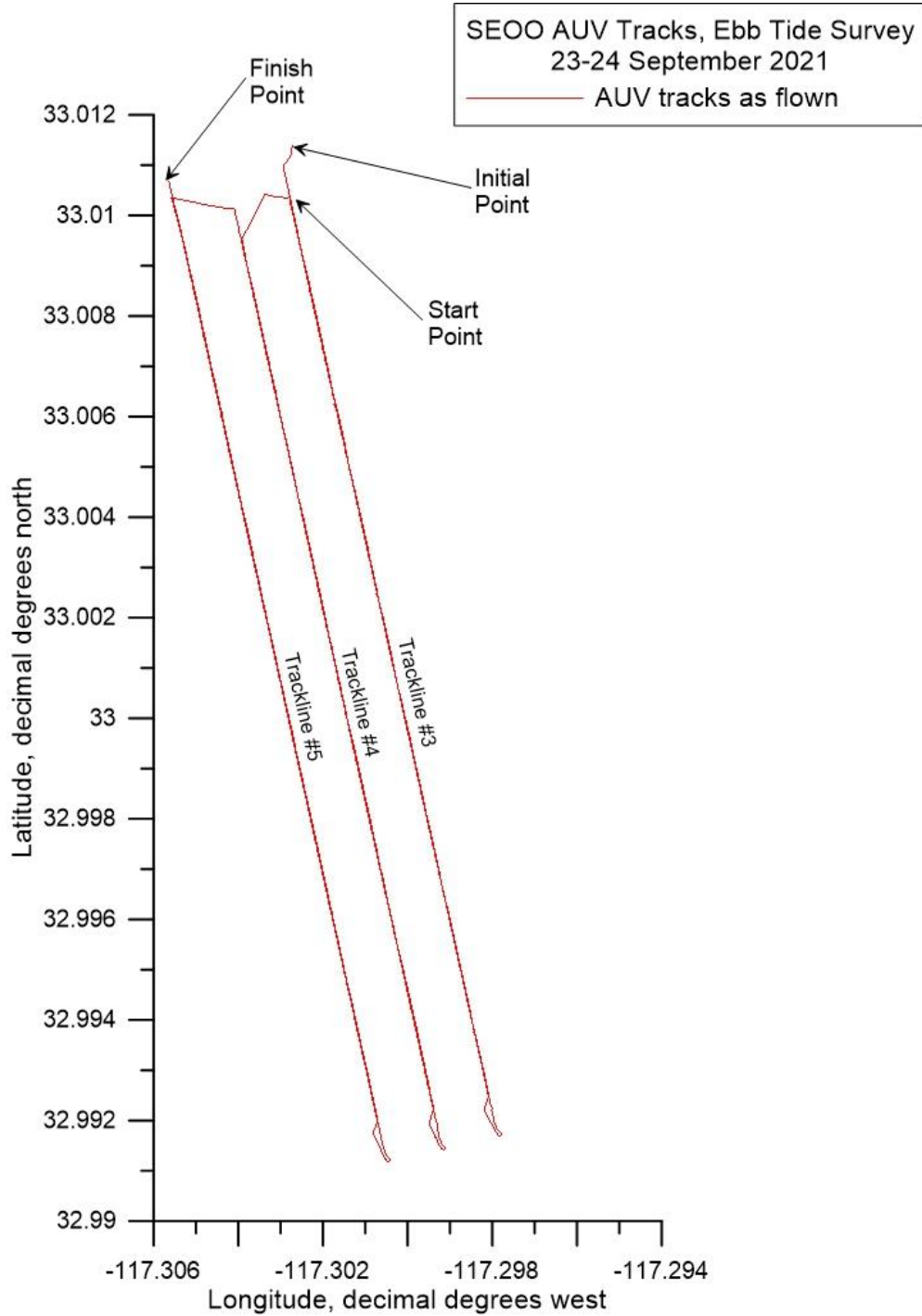


Figure 3.1.15: AUV track lines as flown during ebb tide surveys of the discharge plume from SEOO. Ebb tide survey was truncated to only 3 track lines due to problems with seawater in the fuel of the AUV support vessel. The total dimension of the AUV surveyed area on flood tide was 2000 m in the along shore direction and 500 m in the cross-shore direction or a total surveyed area of approximately 247.2 acres. Note, at 30° N latitude, 1° longitude = 93,453.2 m, while 1° latitude = 110,904.4 m.

Dispersion of fDOM across all depths
San Elijo Ocean Outfall, Ebb Tide, 23 September 2021

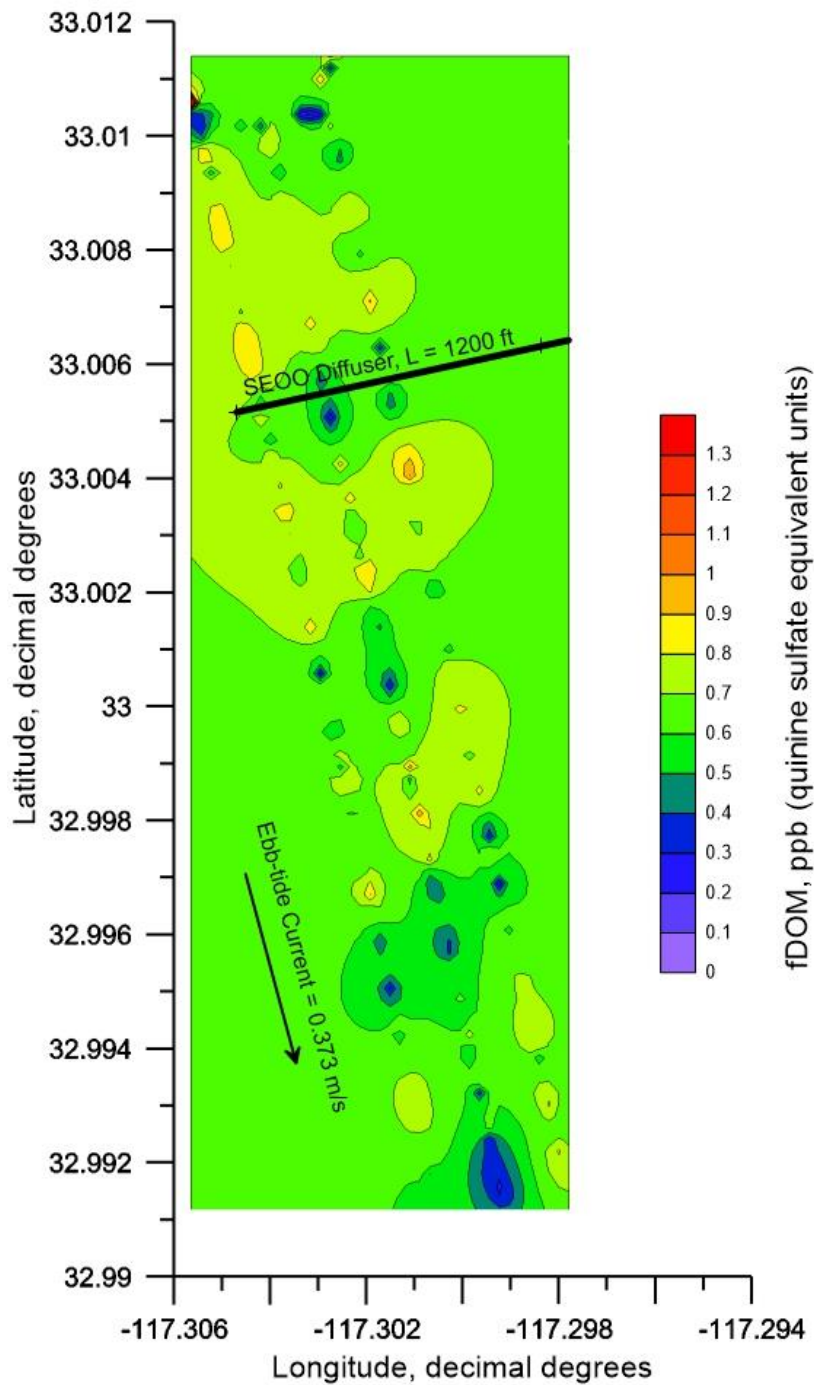


Figure 3.1.16: Full depth contour plot (aka, heat map) of AUV measurements of fDOM from surveys of the discharge plume from SEOO during ebb tide on 23 September 2021. Average SEOO discharge rate = 10.44 mgd during flood tide; End-of-pipe discharge concentration of fDOM = 206.04 ppb (QSU); End of pipe salinity = 1.87 psu Trapping level (pycnocline depth) = 38.7 ft MSL; Mean ebb tide current = 0.373 m/s (0.72 kts) toward the southeast.

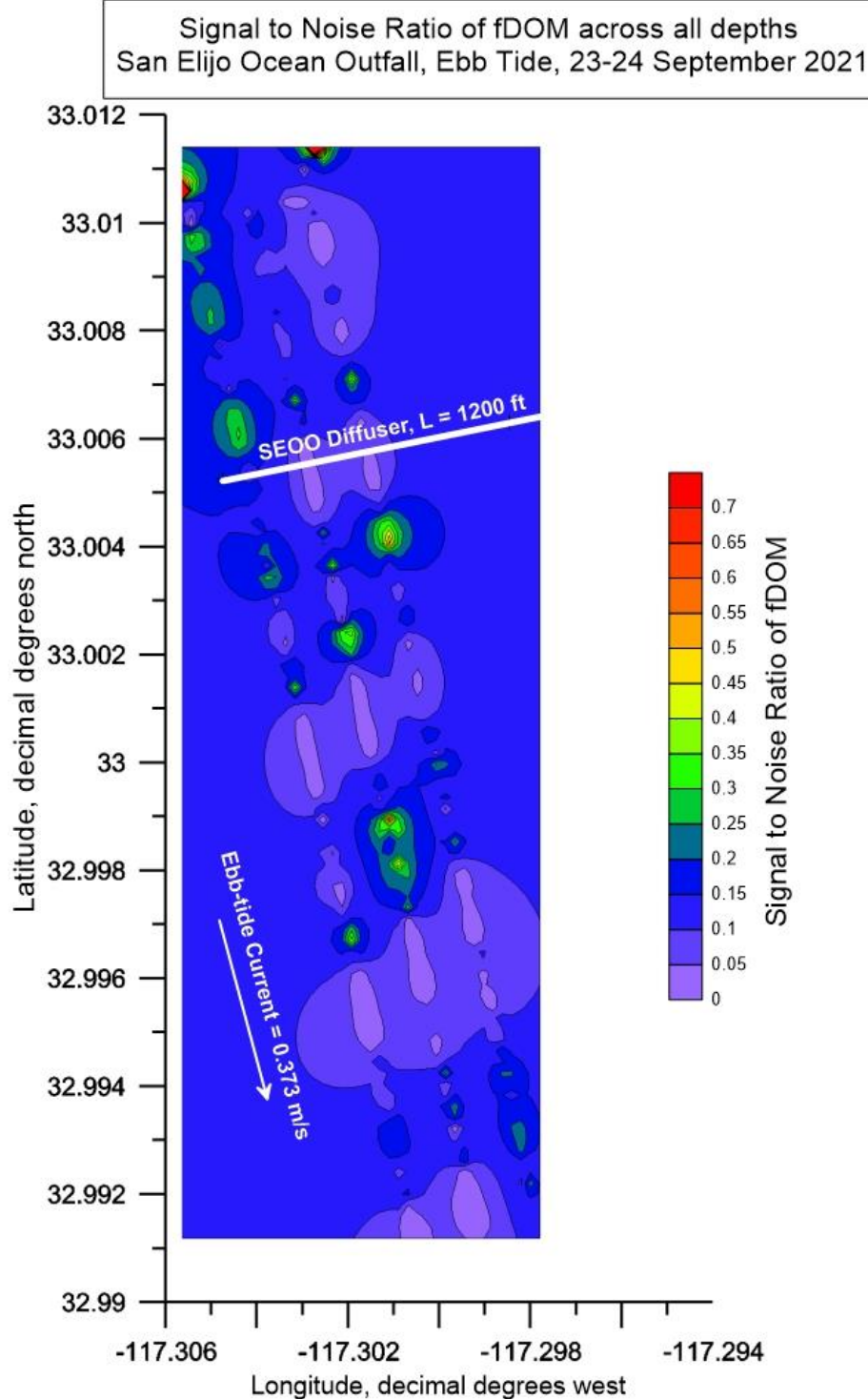


Figure 3.1.17: Full depth contour plot (aka, heat map) of the fDOM signal to noise ratio (SNR) from AUV surveys of the discharge plume from SEOO during ebb tide on 23 September 2021. Average SEOO discharge rate = 10.44 mgd during flood tide; End-of-pipe discharge concentration of fDOM = 206.04 ppb (QSU); End of pipe salinity = 1.87 psu Trapping level (pycnocline depth) = 38.7 ft MSL; Mean ebb tide current = 0.373 m/s (0.72 kts) toward the southeast.

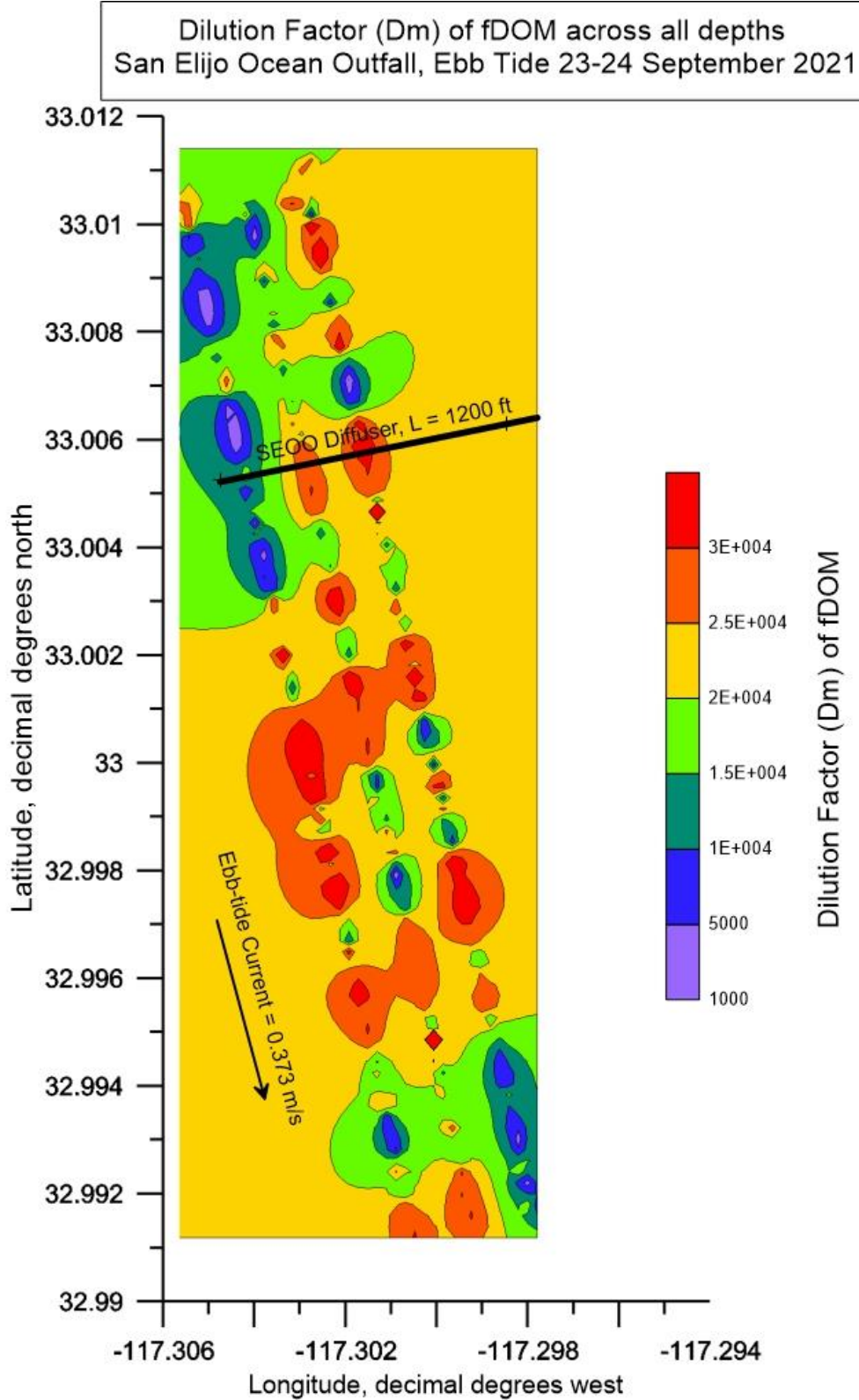


Figure 3.1.18: Full depth contour plot (aka, heat map) of the fDOM dilution factor (D_{fDOM}) from AUV surveys of the discharge plume from SEOO during ebb tide on 23 September 2021. Average SEOO discharge rate = 10.44 mgd during flood tide; End-of-pipe discharge concentration of fDOM = 206.04 ppb (QSU); End of pipe salinity = 1.87 psu Trapping level (pycnocline depth) = 38.7 ft MSL; Mean ebb tide current = 0.373 m/s (0.72 kts) toward the southeast.

fDOM features measured in the SEOO flood tide fDOM heat map in **Figure 3.1.13**. Hence, any regulated or unregulated toxic SEOO effluent constituents would be below quantifiable detection limits.

Salinity was considered a potentially useful alternative to CDOM for plume observation. **Figure 3.1.19** provides the salinity heat map generated from the AUV salinity measurements during the SEOO ebb tide survey. Most of the features in the salinity heat map range from $S_{(x)} = 33.5$ psu to $S_{(x)} = 33.55$ psu with some small random heat bubbles well to the northwest of the outfall reaching as high as $S_{(x)} = 33.6$ psu. None of these salinity features in **Figure 3.1.19** appear to be spatially coherent with the SEOO pipeline or diffuser. The far-field depth averaged salinity from the salinity profiles in **Figure 3.1.2** indicates that natural background salinity is $S_{\infty} = 33.44$ psu with a standard deviation of $\sigma = 0.094$ psu. Inserting these values into equation (1) indicates that the signal to noise ratio of the predominant salinity features in **Figure 3.1.19** range from $SNR_S = 0.0017$ to $SNR_S = 0.0033$, while the signal to noise ratio of the small scale salinity heat bubbles in **Figure 3.1.19** reach as high as $SNR_S = 0.0048$. Regardless, all the salinity features in **Figure 3.1.19** have signal to noise ratios significantly below the lowest order significance threshold for detection (i.e., $SNR_S \geq 1$) and consequently cannot be associated with plume fragments by any statistically meaningful measure. The conclusion that salinity is not a useful observable for tracking the EOO plume was anticipated in Section 1.0, since the signal to noise ratio of the salinity signal at the point of discharge is only $SNR_{S(x=0)} = 0.97$, or less than lowest order significance threshold for detection.

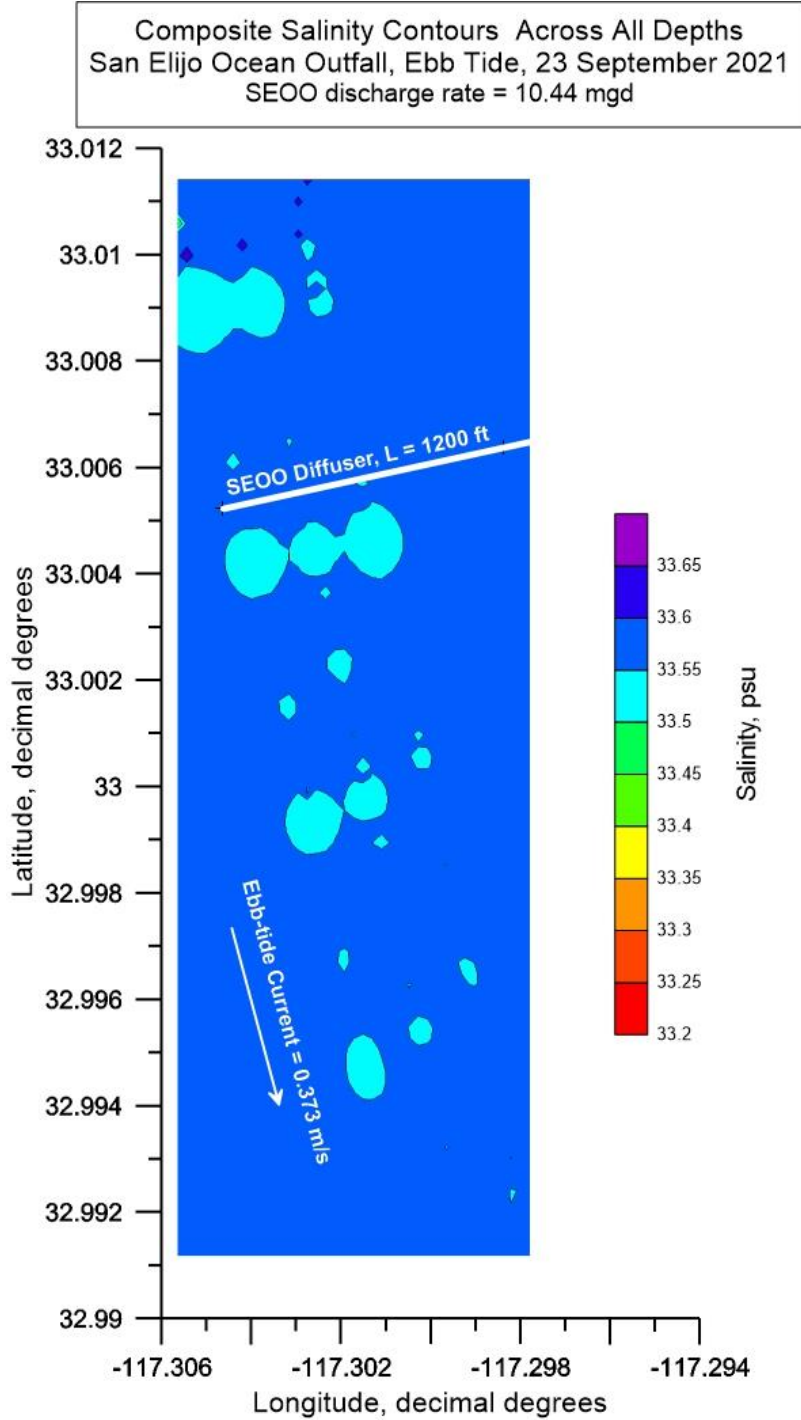


Figure 3.1.19: Full depth composite contour plot (aka, heat map) of salinity during AUV surveys of the discharge plume from SEOO during ebb tide on 23 September 2021. Average SEOO discharge rate = 10.44 mgd during ebb tide; End of pipe salinity = 1.92 psu; Trapping level (pycnocline depth) = 38.7 ft MSL; Mean ebb tide current = 0.373 m/s (0.72 kts) toward the southeast.

3.2 SECOND SEOO DEPLOYMENT – 21 DECEMBER 2021

The design of the SEOO survey boxes and the AUV track lines within those boxes was modified for the second AUV deployment on 21 December 2021. Based on the patterns of fDOM features found in the fDOM heat maps of the first deployments, it was determined that the distance surveyed in the long-shore direction could be reduced since no evidence of plume dispersion beyond 1,000 m from the SEOO had been found. By reducing the long-shore search range, additional survey area could be added to the inshore region to determine if there was any evidence of the plume drifting shoreward due to mass transport by shoaling internal waves. The modified survey plan still includes 2 separate AUV survey boxes (a flood tide box shown in orange in [Figure 3.2.1](#) and an ebb tide box shown in yellow) while the numbers of stationary water column monitoring stations (where CTD casts and ADCP velocity profiles are taken) was increased from 15 to 18 stations, (shown as green circles in [Figure 3.2.1](#)). The total dimension of the AUV surveyed area on either ebb or flood tide was 707.1 m in the longshore (shore parallel) direction and 1,414.2 m on the cross-shore (on/off shore) direction. Thus, the total area surveyed during both ebb and flood tide is approximately 494.2 acres. While this is only half the size of the ebb and flood tide survey boxes used during the first deployment in September 2021, it allows for increasing the numbers of track lines from 5 to 12 shore parallel AUV track lines at 108.8 m spacings within each survey box. This increase in numbers of track lines increases the horizontal resolution within each ebb and flood survey box by a factor of 2.4, thereby reducing or eliminating the spurious fDOM features that aligned with sparse track lines during the September 2021 deployments (cf. [Figure 3.1.11](#) and [Figure 3.1.16](#)). Those spurious features in the fDOM heat maps of the September 2021 deployments were the result of *spatial aliasing* which arises from insufficient sampling density in the spatial domain. To eliminate spatial aliasing, the AUV track line spacing must be no more than $\frac{1}{2}$ the length scale of the finest scale features in the fDOM spatial distribution, Peterson, et al, (1954). By increasing the horizontal resolution of the second deployment survey boxes by a factor of 2.4, it was anticipated that the spatial aliasing fDOM features encountered during the first deployment could be eliminated, or at least significantly muted.

As practiced during the first AUV deployment in September 2021, the new survey boxes in [Figure 3.2.1](#) were searched twice for the presence of the SEOO plume, (i.e., out and return). As before, the AUV is flown along a dolphin-style flight path when transiting outbound with the current (i.e., a yo-yo flight path diving and ascending through the water column between the sea bed and an apex halfway between the sea surface and the pycnocline). On the return legs of each track line (against the current), the AUV is flown at a constant depth immediately beneath the pycnocline (trapping level) where the maximum horizontal dispersion of the plume is expected, (cf. Baumgartner, 1994; Frick et al., 2003). Altogether, the AUV covers a distance of about 20.0 kilometers in about 5 hours within each survey box which is roughly the endurance limit of the AUV with fully charged batteries. The survey period is centered within each ebb or flood tide interval of 6.2 hours. The AUV batteries are changed during the 1.2 hour interval around slack water between ebb and flood tide intervals, allowing for AUV surveys of the SEOO over a complete semi-diurnal tide cycle.

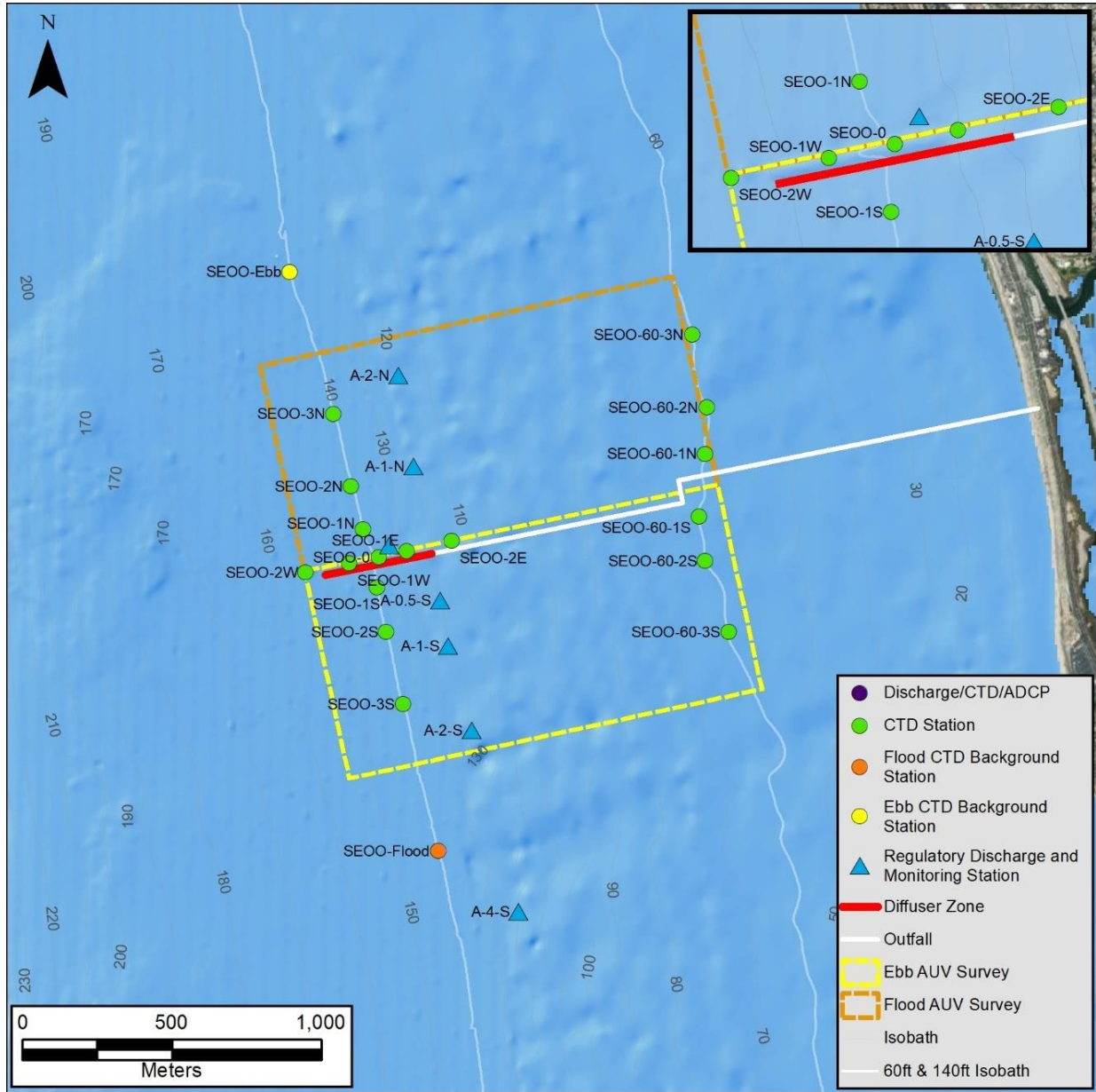


Figure 3.2.1: SEOO Survey boxes and sampling stations for second AUV deployment, 21 December 2021

The 18 stationary water column monitoring stations are distributed between the 140 ft and 60 ft depth contours around the SEOO, and provide vertical profiles of salinity, temperature, and fDOM water mass properties immediately prior to and during the AUV surveys. Measurements from the control stations SEOO-Ebb and SEOO-Flood provide far-field measurements of natural background (ambient) water-mass properties (salinity, temperature, and fDOM). The measurements of the fDOM at the 18 stationary monitoring stations were in units of RFU which were converted to QSU fDOM units using the second order polynomial in Figure 1.3.1. Figure 3.2.1 also shows a group of blue triangles around the EOO diffuser, indicating the locations of the offshore regulatory discharge monitoring stations used for NPDES permit compliance determination.

To establish the precise location of the San Elijo Ocean Outfall, a side-scan sonar survey of SEOO was performed prior to the AUV deployments on 19 December 2021 to obtain precision geo-referenced coordinates along the length of the pipeline and diffuser, (cf. [Figure 3.2.2](#)). This survey also located a concrete junction box where the inshore section of the SEOO pipeline joined the offshore section. Unfortunately, during the flood tide AUV survey of the SEOO the night of 21 December 2021, the AUV struck this concrete junction box and damaged the onboard fDOM and conductivity sensors, so that only the preceding ebb-tide survey of the SEOO on 21 December produced any useful data.

It was critical to the plume tracking effort to program the AUV to fly directly beneath the pycnocline during the return leg (against the current) along each of the 12 track lines within the ebb and flood survey boxes shown in [Figure 3.2.1](#). To locate the depth of the pycnocline, the CTD casts were performed prior to the AUV survey on 21 December 2021 and quickly processed to determine the salinity changes and temperature changes with depth, (cf. [Figure 3.2.3](#)). These CTD data showed a cold, nearly homogeneous surface layer, (about 6° C cooler than during the first deployment in September 2021) that mixed down to about 21 m depth, while the bottom layer remained about the same temperature as in September 2021. Consequently, the water column during the second deployment on 21 December 2021 was only weakly stratified (i.e., less stable than in September 2021) and the trapping level rose to only 4 m depth. Based on this finding, the AUV was programmed on its outbound dolphin-style legs (with the current) for dive cycle apex points set above the pycnocline at a depth of 2 m depth (-6.6 ft. MSL) and dive cycle bottoming points set at 2 m (-6.6 ft) above the seabed. The Iver3 AUV uses its bottom-locking sonar to determine the distance above the local seabed at any location within the survey box. Along the return leg of each track line (flown against the current), the AUV was programmed to fly at a constant depth of 6 m depth (-19.7 ft. MSL).

At the time of the ebb tide AUV survey on 21 December 2021, the SEOO was discharging 12.63 mgd of wastewater having an average discharge salinity of 1.097 psu and an average fDOM discharge concentration of 232.8 ppb (QSU), based on shoreside monitoring of the SEOO effluent, (see tabulations of SEOO shoreside monitoring data in Appendix B). The average SEOO discharge concentrations of fDOM are significantly higher (by more than 2 orders of magnitude) than the natural ocean background concentrations of fDOM measured at far-field control stations, SEOO-Ebb, which were profiled twice during the ebb tide event on 21 December 2021. Vertical profiles of natural background fDOM measured during ebb tide at SEOO-Ebb (cf. [Figure 3.2.4](#)) exhibited depth-averaged concentrations ranging between 0.301 ppb and 0.305 ppb. Consequently, the signal to noise ratio of the fDOM plume observable at any point of discharge along the EOO diffuser ranges between $SNR_{fDOM} = 762.3$ and $SNR_{fDOM} = 772.4$, based on the depth averaged concentrations of natural background fDOM measured at far-field control station, SEOO-Ebb, (cf. [Figure 3.2.4](#)), applied to equation (1). While profiles of natural background fDOM concentrations measured during ebb tide showed both random variations (noise) with some general vertical structure (with higher concentration near the bottom, declining near the surface), the standard deviations around the depth averaged fDOM concentrations were small, ranging between $\sigma = 0.027$ ppb and $\sigma = 0.050$ ppb, (cf. [Figure 3.2.4](#)).



Figure 3.2.2: Side-scan sonar survey of SEOO used to obtain precision coordinates along the length of the pipeline and diffuser

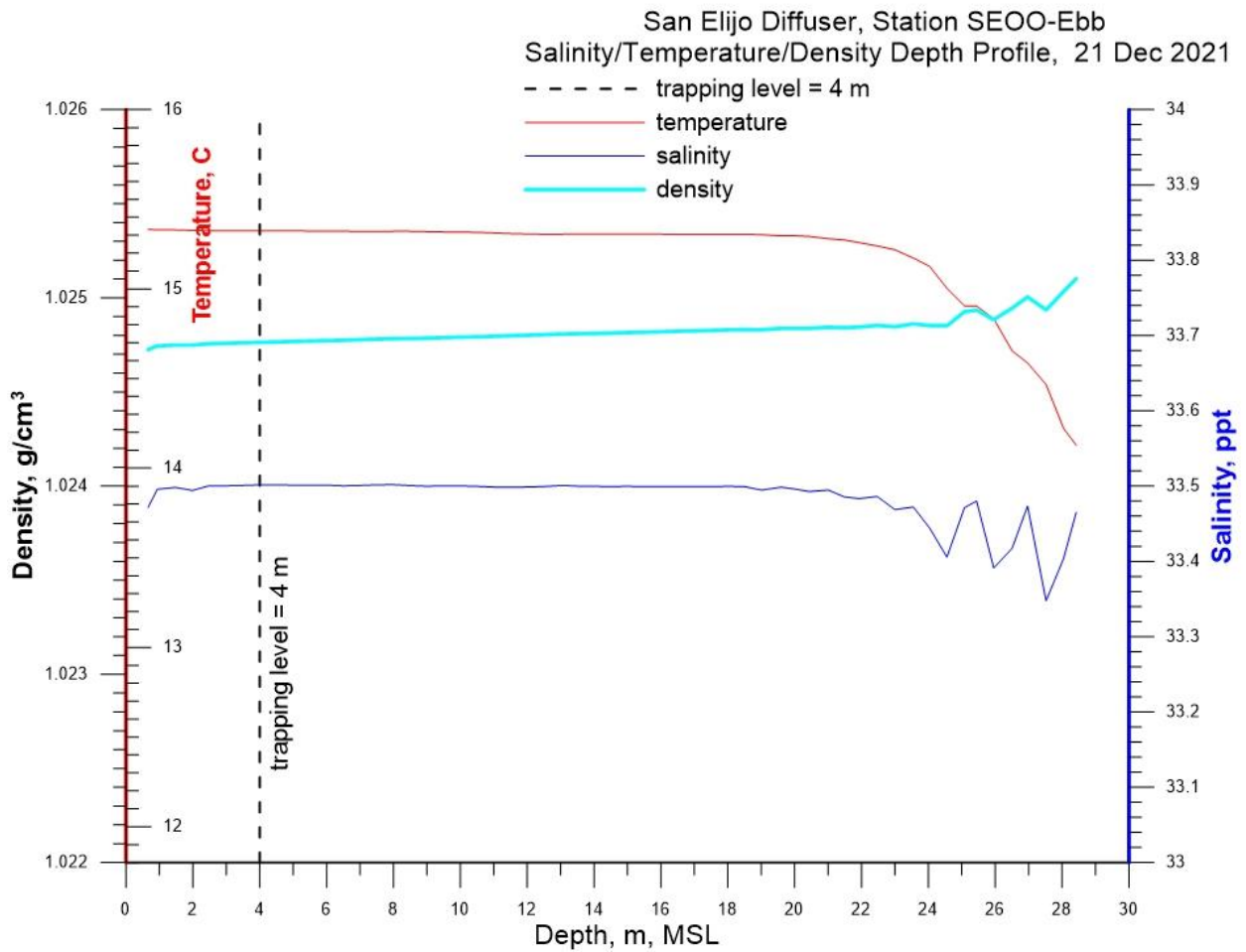


Figure 3.2.3: Salinity/Temperature/Density depth profiles derived from CTD casts on 19 December 2021 used to program the AUV survey of the plume dispersion from SEOO on 21 December 2021 during ebb tide.

Vertical Profiles of Natural Background fDOM
Station SEOO-EBB, 21 December 2021
2 km north of the San Elijo Ocean Outfall

— SEOO EBB-1, average = 0.301 ppb; maximum = 0.390 ppb; minimum = 0.164 ppb; $\sigma=0.050$
 — SEOO EBB-2, average = 0.305 ppb; maximum = 0.351 ppb; minimum = 0.233 ppb; $\sigma=0.027$

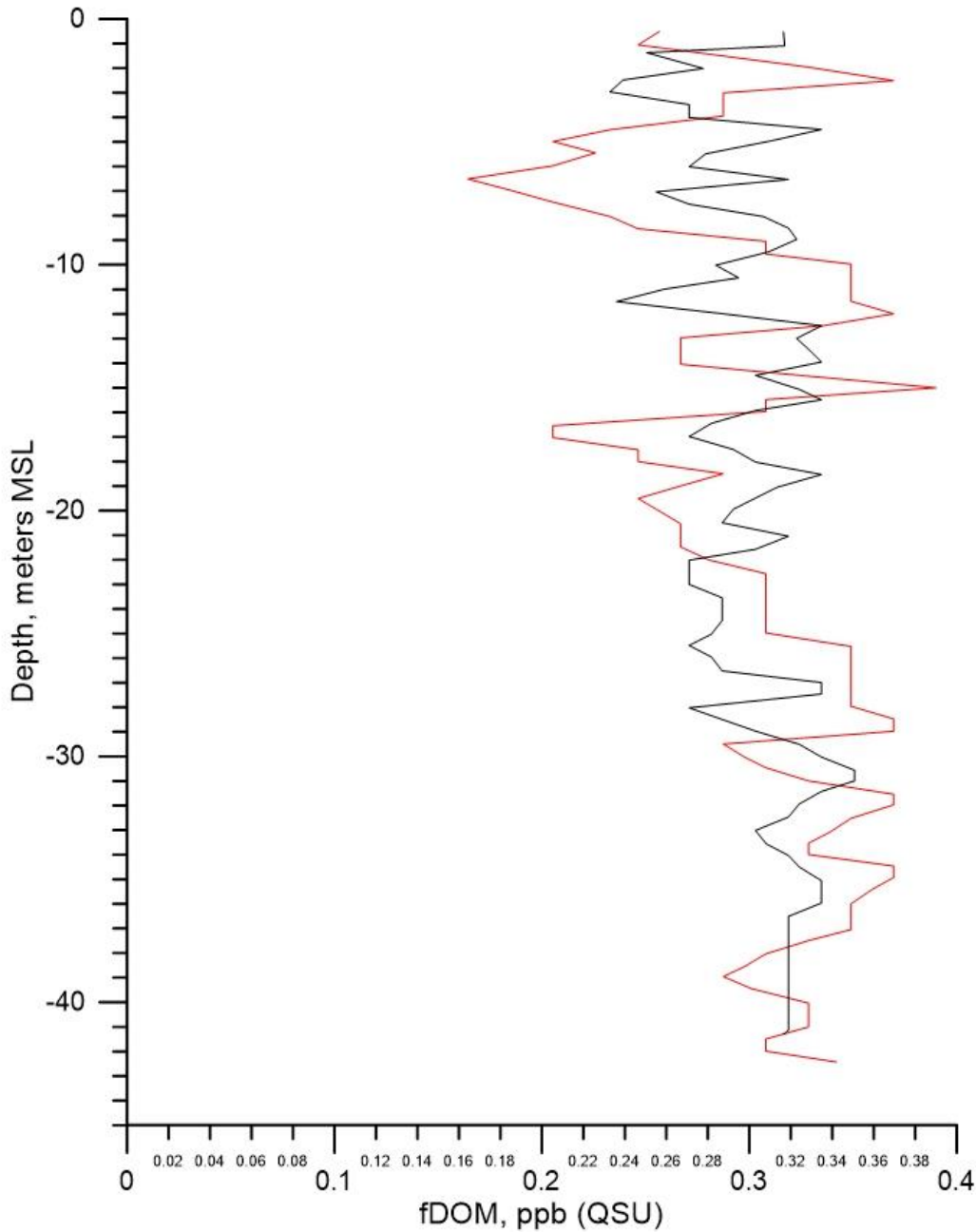


Figure 3.2.4: Vertical profiles of natural background fDOM concentrations measured during the second deployment at the far-field flood tide monitoring station “SEOO-EBB”, located 2 km northwest of SEOO along the -140 ft. MLLW depth contour, cf. yellow dot in Figure 3.2.1.

Mean ebb tide currents on 21 December 2021 at the far-field control station, SEOO-Ebb, were 0.263 m/s (0.51 kts) toward the southeast, based on ADCP data at far field monitoring station, SEOO-Ebb, (cf. [Figure 3.2.5](#)) located along the 140 ft depth contour at the yellow dot found up-drift (north) of the yellow AUV survey box shown in [Figure 3.2.1](#). These mean currents convey a net shore-parallel drift of the SEOO discharge plume. However, there are other transient short-lived current oscillations reaching 0.731 m/s (1.42 kts) in the ebb tide ADCP time series record on 21 December 2021. The current direction data in the ADCP record indicates these spikes of higher oscillatory currents were directed cross-shore, indicating they were due to shoaling internal waves. Because of the oscillatory nature of these internal wave current spikes, they produce no net drift of the SEOO discharge plume, but merely serve to smear the plume or break off pieces from the main body of the plume and smear or disperse those pieces in the cross-shore direction. These internal waves are excited by an extreme bathymetric feature that resulted in an abrupt narrowing of the continental shelf directly offshore of the SEOO diffuser, (cf. [Figure 3.1.7](#)). This abrupt narrowing of the shelf creates a cliff that is perpendicular to the shoreline along the shelf break and excites internal waves as the tidal currents flow across the escarpment formed by this cross-shore cliff, much like lee waves do in the atmosphere when storm winds blow over mountainous topography. The cross-shore oscillations of the internal waves that radiate outward from the shelf break, producing high current spikes in the ADCP records on 21 December 2021 (cf. [Figure 3.2.5](#)).

[Figure 3.2.6](#) displays accurate repeatability of the outbound and return legs along each of 12 track lines as flown by the AUV during ebb tide surveys of the SEOO on 21 December 2021. During this survey, the AUV collected 65,811 separate measurements of salinity and fDOM along a total distance surveyed of 21.2 km. The fDOM heat map generated from these 65,811 measurements of fDOM concentrations is plotted in [Figure 3.2.7](#). Inspection of [Figure 3.2.7](#) reveals that variations in fDOM concentrations across all depths surveyed by the AUV that range from $fDOM_{(x)} = 0.3$ ppb to 1.05 ppb. These fDOM variations exhibit weak banding along the 12 track lines from highly muted spatial aliasing relative to the September 2021 deployments. However, the fDOM heat map in [Figure 3.2.7](#) also exhibits a horizontal structure having high spatial coherence with the SEOO diffuser, with a singular, large fDOM (green area) centered 329.8 m down-drift (south) of the SEOO diffuser in which elevated fDOM concentrations are in the range of $fDOM_{(x)} = 0.5$ ppb to 1.05 ppb, or 65% to 246% higher than the depth-averaged natural background fDOM concentration $fDOM_{\infty}$ in [Figure 3.2.4](#). Moreover, the fDOM concentrations in the remainder of the surveyed area outside of this singular elevated fDOM feature are on the order of $fDOM_{\infty} \cong 0.3$ ppb, consistent with the depth-averaged natural background fDOM concentration in [Figure 3.2.4](#). Therefore, the primary elevated fDOM feature in [Figure 3.2.7](#) that is centered 329.8 m downstream (south) of the SEOO diffuser in the ebb tide current has the spatial coherence, structure, and contrast against natural background to possibly be a remnant of the SEOO discharge plume. To verify this hypothesis, the fDOM heat map in [Figure 3.2.7](#) is converted into a signal to noise ratio heat map in [Figure 3.2.8](#) by invoking equation (1) to convert the fDOM concentrations in [Figure 3.2.7](#) into corresponding SNR_{fDOM} patterns. Since only fDOM features having signal to noise ratios of unity or greater are possible remnants of the plume, [Figure 3.2.8](#) has been scaled to filter out features having $SNR_{fDOM} < 0.8$, where features having $0.8 \leq SNR_{fDOM} < 1.0$ are potentially diluted fragments or diluted outer edges of a plume remnants.

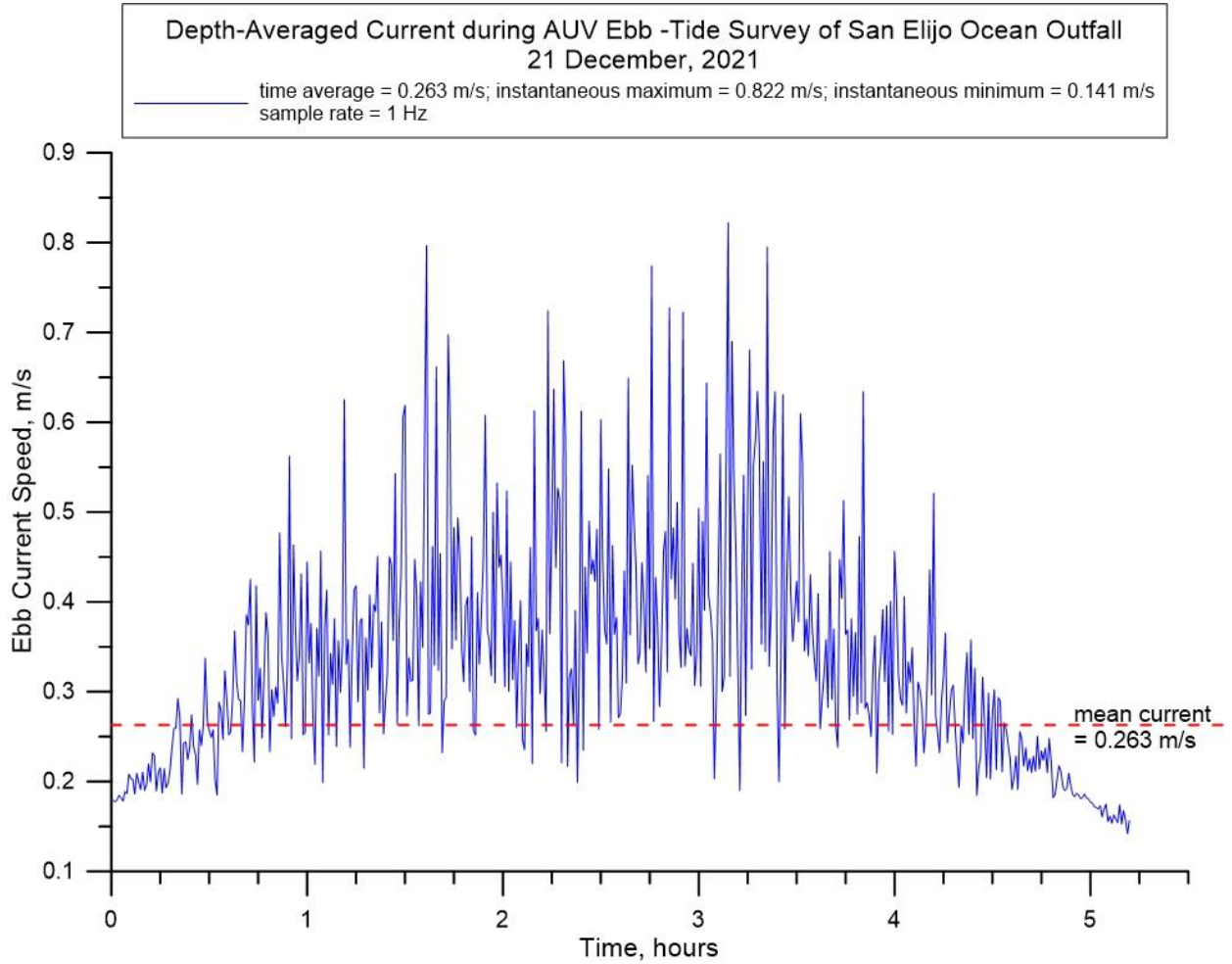


Figure 3.2.5: Time series of depth averaged current derived from ADCP measurements at SEOO during ebb-tide AUV survey on 21 December 2021.

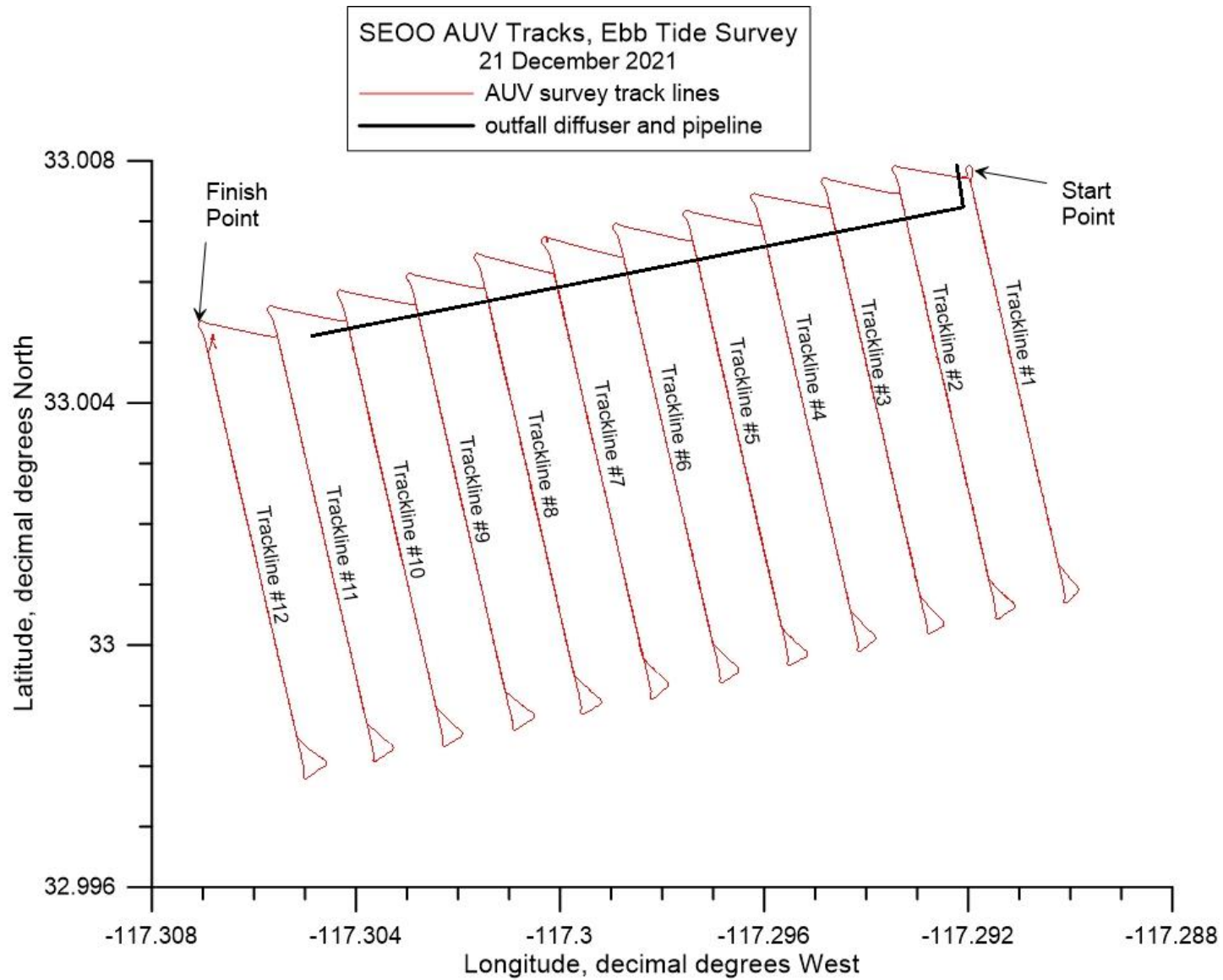


Figure 3.2.6: AUV track lines on 21 December 2021 as flown during ebb tide surveys of the discharge plume from SEOO. Note, at 30° N latitude, 1° longitude = 93,453.2 m, while 1° latitude = 110,904.4 m.

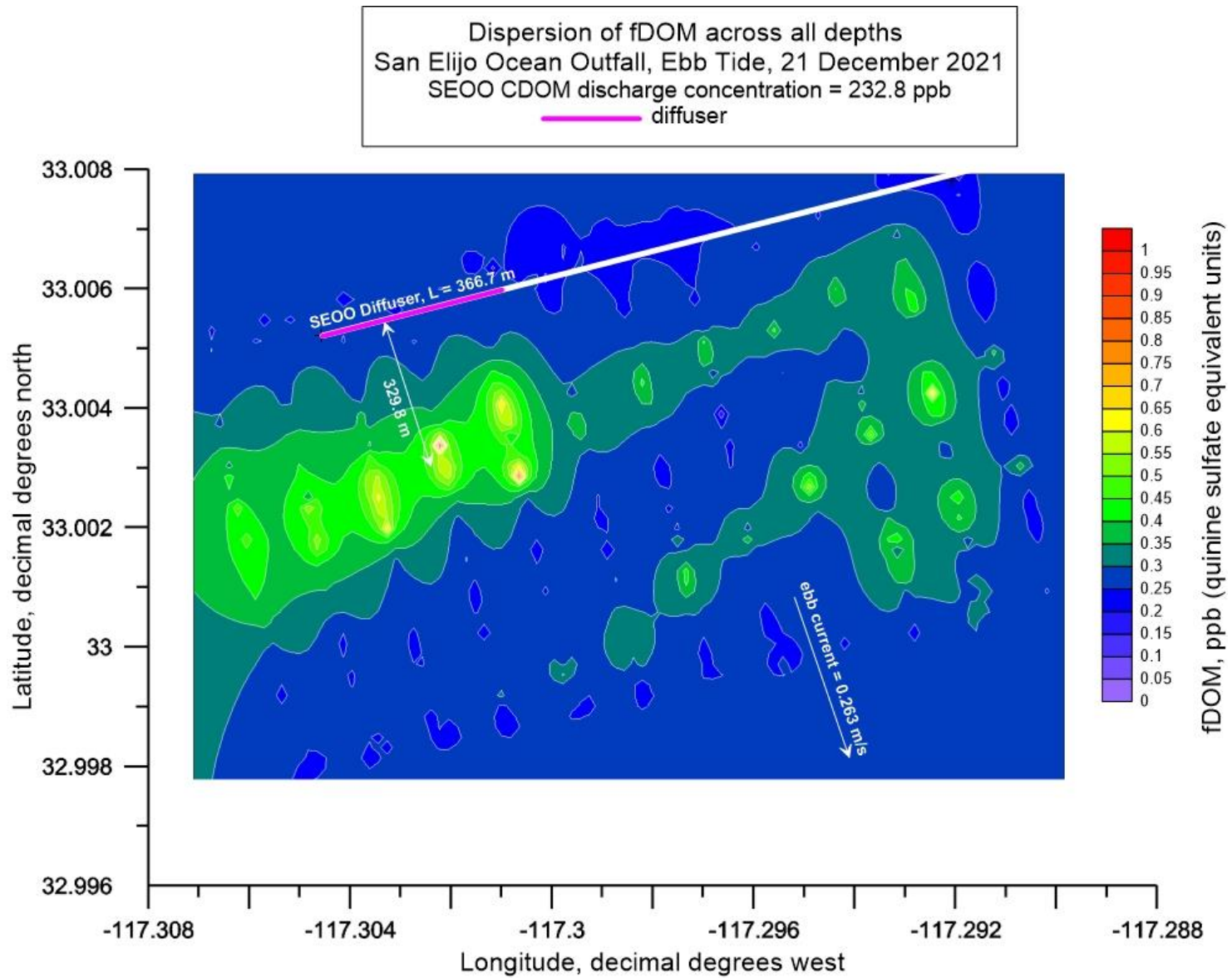


Figure 3.2.7: Full depth contour plot (aka, heat map) of AUV measurements of fDOM from surveys of SEOO during ebb tide on 21 December 2021. Average SEOO discharge rate = 12.63 mgd during flood tide; End-of-pipe discharge concentration of fDOM = 232.8 ppb (QSU); End of pipe salinity = 1.097 psu; Trapping level (pycnocline depth) = -13.1 ft MSL; Mean ebb tide current = 0.263 m/s (0.51 kts) toward the southeast.

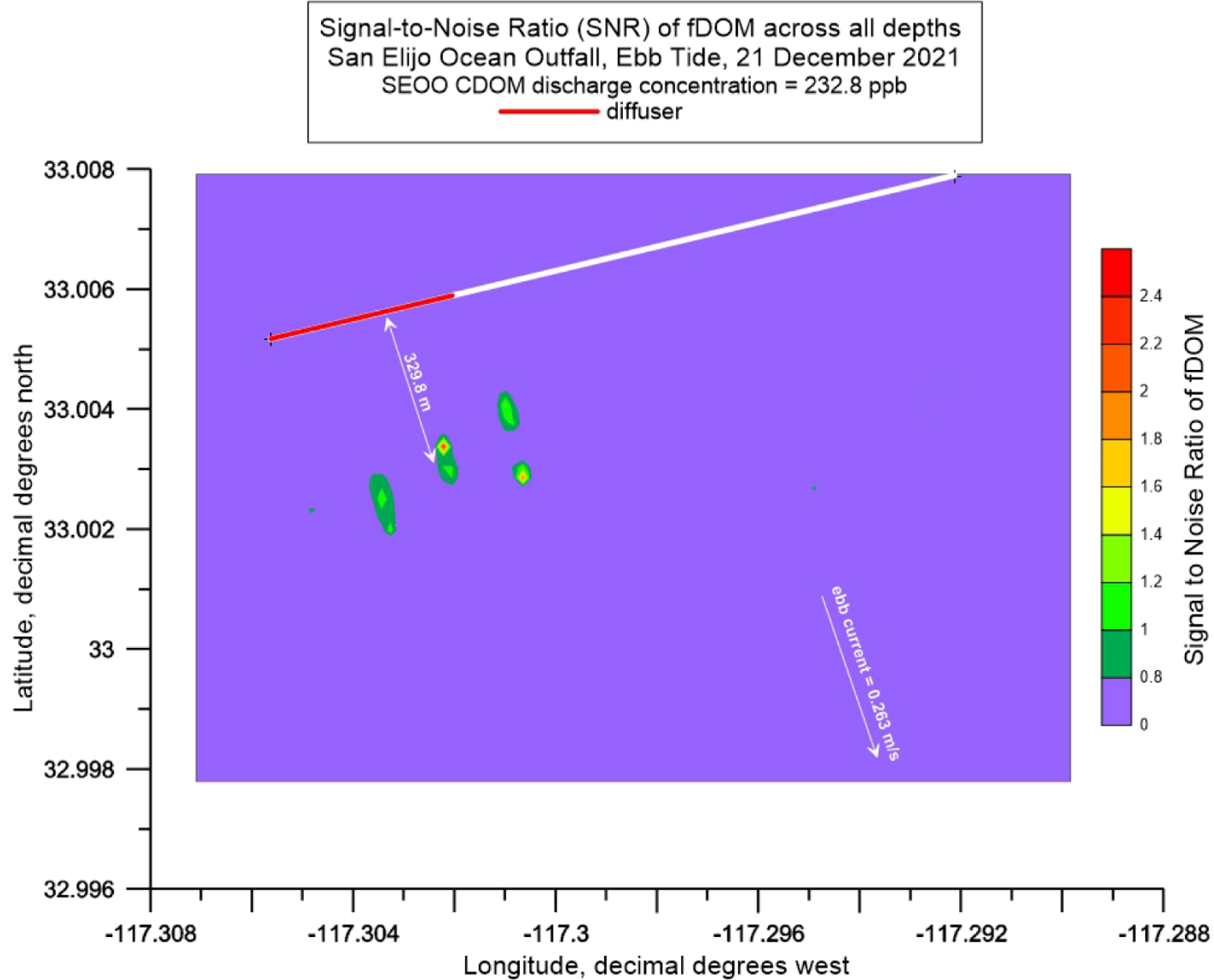


Figure 3.2.8: Full-depth contour plot (aka, heat map) of the signal to noise ratio (SNR) of fDOM during AUV surveys of SEOO during ebb tide on 21 December 2021. Average SEOO discharge rate = 12.63 mgd during flood tide; End-of-pipe discharge concentration of fDOM = 232.8 ppb (QSU); End of pipe salinity = 1.097 psu; Trapping level (pycnocline depth) = -13.1 ft MSL; Mean ebb tide current = 0.263 m/s (0.51 kts) toward the southeast.

Inspection of **Figure 3.2.8** reveals that the SNR of this suspected plume remnant ranges from $SNR_{fDOM} \cong 1$ along its outer perimeter, to as high as $SNR_{fDOM} \cong 2.46$ in its inner core 329.8 m downstream of the SEOO diffuser. Therefore, the elevated fDOM concentrations found centered 329.8 m downstream of the SEOO diffuser satisfy the lowest order significance threshold for detection, (i.e., $SNR_{fDOM} \geq 1$). Based on this detection metric, we conclude the SEOO discharge plume has been located 329.8 m downstream of the SEOO diffuser during ebb tide on 21 December 2021.

To assess minimum dilution levels in the SEOO plume fragment, the SNR_{fDOM} heat map in **Figure 3.2.8** was transposed into a dilution heat map in **Figure 3.2.9** using equation (2) on the basis that the initial fDOM concentration at the point of discharge is $fDOM_{(x=0)} = 232.8$ ppb. Equation (2) demonstrates that regions of high SNR will correspond to regions of low values of D_{fDOM} relative to the dilution elsewhere within the AUV survey area. **Figure 3.2.9** indicates that the dilution factor (D_{fDOM}) for the fDOM features would be no less than as $D_{fDOM} = 312:1$ in the inner core of the plume fragment, or a factor of 1.3 times greater than the initial dilution of $D_m = 237:1$ assigned within the current SEOO NPDES permits (Order Nos. R9-2018-0002 and R9-2018-0003). The dilution along the outer perimeter of the plume remnant ranges from $D_{fDOM} = 766:1$ to as much as 40,000:1. Elsewhere in the wake of the SEOO diffuser dilution ranges from $D_{fDOM} = 50,000:1$ to 70,000:1 so that any regulated or unregulated toxic SEOO effluent constituents would be below quantifiable detection limits within any plume remnants beyond 400 m from the outfall.

Figure 3.2.10 provides the salinity heat map generated from the AUV salinity measurements during the SEOO ebb tide survey. Most of the features in the ebb tide salinity heat map range from $S_{(x)} = 33.52$ psu in the core of the plume remnant to as high as $S_{(x)} = 33.6$ psu in isolated spots in the far-field of the SEOO diffuser. The far-field depth-averaged salinity from the salinity profile in **Figure 3.2.3** indicates that natural background salinity is $S_{\infty} = 33.5$ psu with a standard deviation of $\sigma = 0.032$ psu. Applying these salinity values to equation (1), the signal to noise ratio of the salinity features in **Figure 3.2.10** range from only $SNR_S = 0.0006$ to $SNR_S = 0.0029$. Therefore, all the salinity features in **Figure 3.2.10** have signal to noise ratios significantly below the lowest order significance threshold for detection (i.e., $SNR_S \geq 1$) and consequently cannot be associated with suspected plume remnants.

Despite the low signal to noise ratios in the salinity heat map in **Figure 3.2.10**, the fDOM heat map data in **Figure 3.2.7** and the corresponding signal to noise ratio data in **Figure 3.2.8** represents probable evidence of an SEOO plume remnant centered 329.8 m downstream (south) of the SEOO diffuser in the 0.263 m/s (0.51 kts) ebb tide current.

To further investigate this, a Plumes 20 (UM3) initial dilution simulation (see **Table 15**) was performed using the actual ebb tide currents of 0.263 m/s (0.51 kts) on 21 December 2021. The solution file listed in **Table 16** indicates a simulated SEOO initial dilution under these conditions of 388.6:1 at discharge flow of 12.63 mgd. The Plumes 20 (UM3) simulation also (see **Figure 3.2.11**) indicates that initial dilution is completed within a distance of approximately 120 meters of the SEOO diffuser, which is approximately 62% less than the horizontal distance to the SEOO plume remnant depicted in the fDOM heat map in **Figure 3.2.7** during ebb tide. Therefore, the plume tracking study of the SEOO discharge during ebb tide on 21 December 2021 indicates that the discharge plume may be detectable a couple of hundred meters

beyond the point where initial dilution is complete, albeit at high dilution ratios that are at least 766:1 and can exceed 10,000:1.

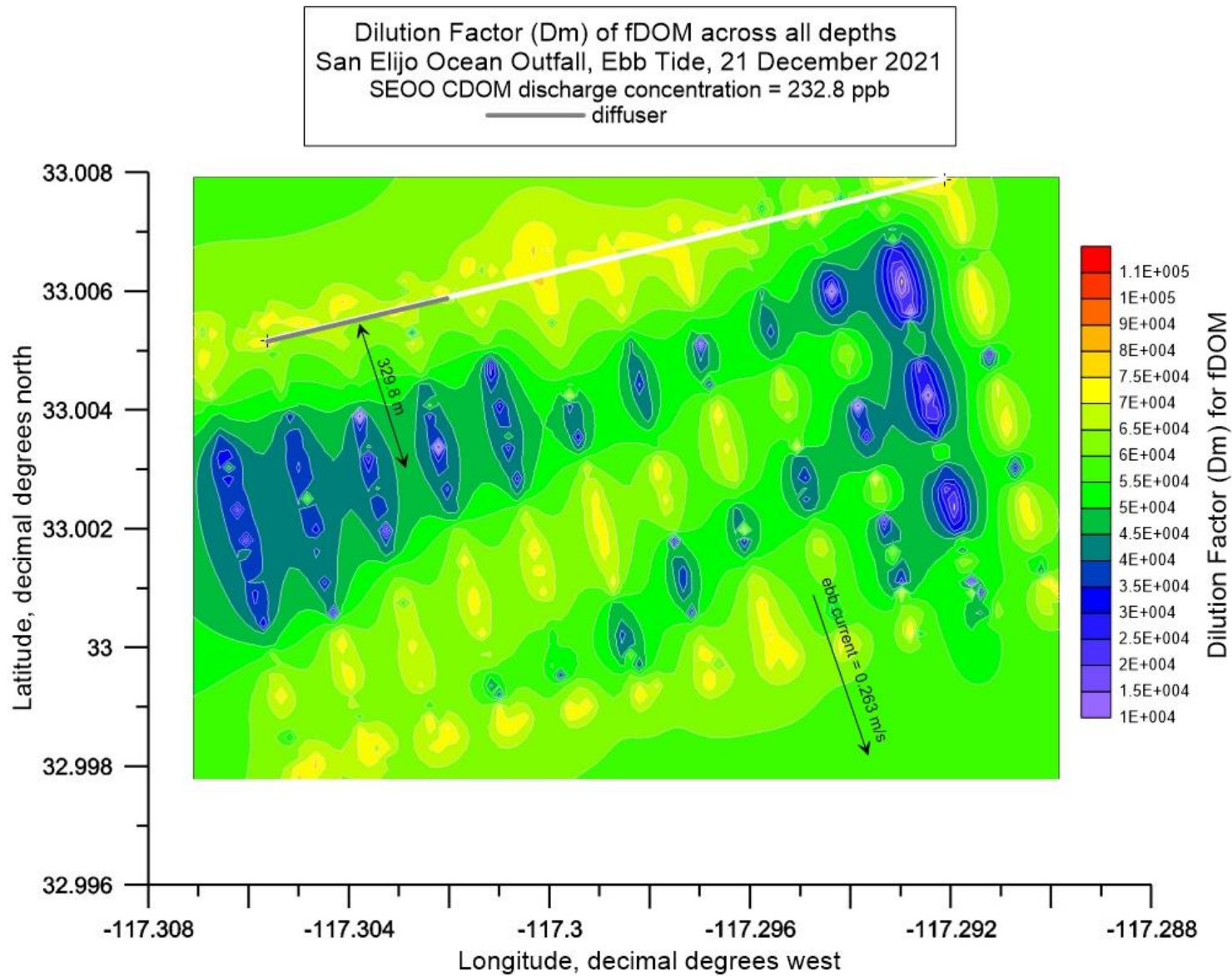


Figure 3.2.9: Full depth contour plot (aka, heat map) of the dilution factor, (D_{fDOM}) of fDOM during AUV surveys of SEOO during ebb tide on 21 December 2021. Average SEOO discharge rate = 12.63 mgd during flood tide; End-of-pipe discharge concentration of fDOM = 232.8 ppb (QSU); End of pipe salinity = 1.097 psu; Trapping level (pycnocline depth) = -13.1 ft MSL; Mean ebb tide current = 0.263 m/s (0.51 kts) toward the southeast.

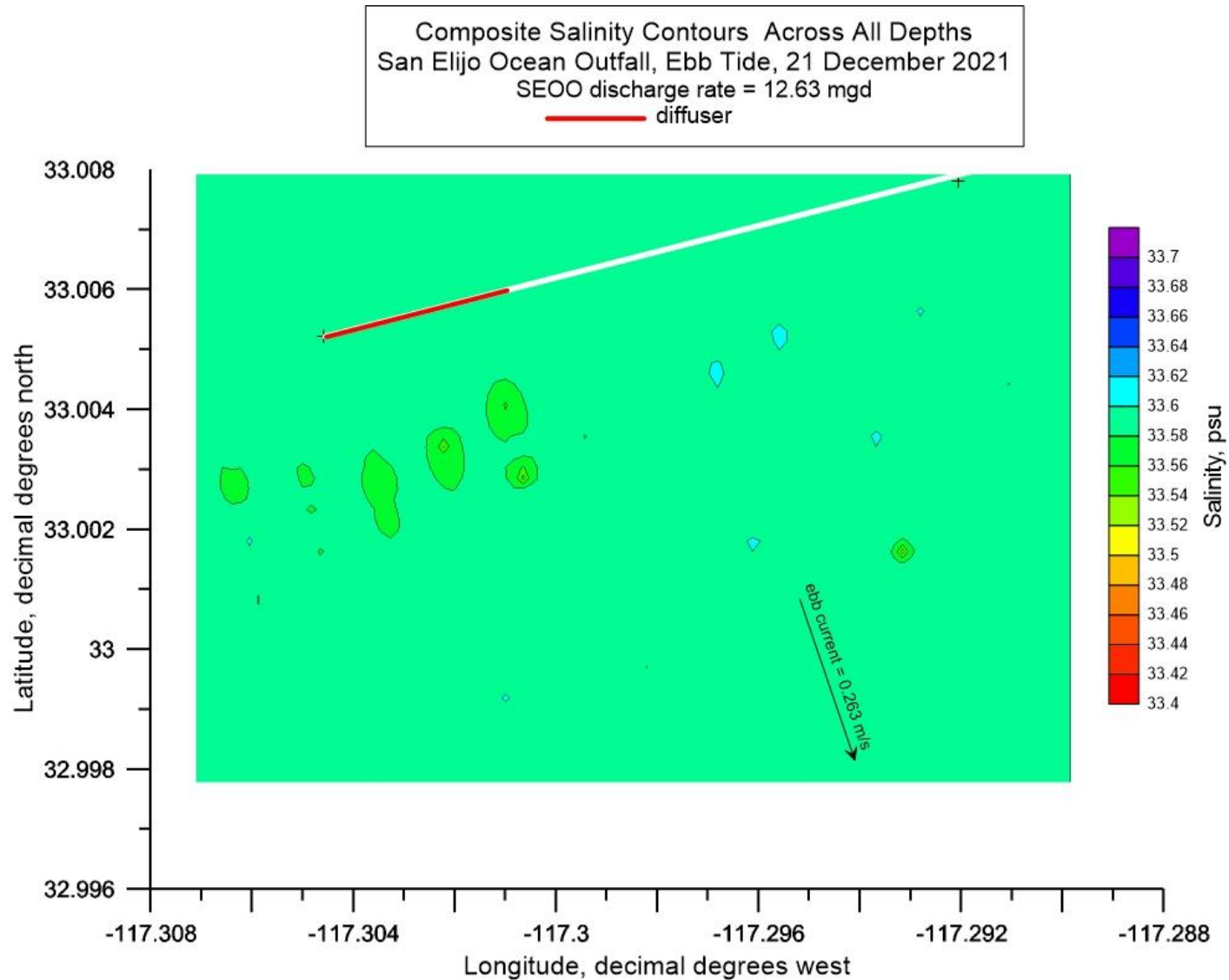


Figure 3.2.10: Full depth composite contour plot (aka, heat map) of salinity during AUV surveys of the discharge plume from SEOO during ebb tide on 21 December 2021. Average SEOO discharge rate = 12.63 mgd during flood tide; End-of-pipe discharge concentration of fDOM = 232.8 ppb (QSU); End of pipe salinity = 1.097 psu; Trapping level (pycnocline depth) = -13.1 ft MSL; Mean ebb tide current = 0.263 m/s (0.51 kts) toward the southeast.

Table 15: Plumes 20 (UM3) Initialization of SEOO Ebb Tide Ambient Conditions on 21 December 2021 with Ambient Current

Project "C:\Plumes20\SEOO_Ebb_21Dec_with-current_versio"-2"	
Model configuration items checked:	
Channel width (m)	100
Start case for graphs	1
Max detailed graphs	10 (limits plots that can overflow memory)
Elevation Projection Plane (deg)	0
Shore vector (m,deg)	not checked
Bacteria model:	Mancini (1978) coliform model
PDS sfc. model heat transfer	Medium
Equation of State	S, T
Similarity Profile	Default profile (k=2.0, ...)
Diffuser port contraction coefficient	1.0
Light absorption coefficient	0.16
Farfield increment (m)	200
UM3 aspiration coefficient	0.1
Output file:	text output tab
Output each ?? steps	25
Maximum dilution reported	10000
Text output format	Standard
Max vertical reversals	to max rise or fall

/ UM3. 4/19/2022 12:49:15 PM

Case 1; ambient file C:\Plumes20\SEOO_Ebb_21Dec_with-current_version-2.001.db; Diffuser table record 1:

Ambient Table:

Depth m	Amb-cur m/s	Amb-dir deg	Amb-sal psu	Amb-tem C	Amb-pol kg/kg	Decay s-1	Far-spd m/s	Far-dir deg	Disprsn m0.67/s2	Density sigma-T
0.0	0.263	0.0	33.50	15.28	2.8000E-10	0.0	0.0	0.0	0.0	24.77391
3.510	0.263	0.0	33.50	15.27	2.7500E-10	0.0	0.0	0.0	0.0	24.78057
6.466	0.263	0.0	33.50	15.24	2.4000E-10	0.0	0.0	0.0	0.0	24.78591
9.470	0.263	0.0	33.50	15.21	3.1000E-10	0.0	0.0	0.0	0.0	24.79147
12.52	0.263	0.0	33.50	15.15	3.3000E-10	0.0	0.0	0.0	0.0	24.80592
15.49	0.263	0.0	33.50	15.11	3.4000E-10	0.0	0.0	0.0	0.0	24.81486
18.53	0.263	0.0	33.46	14.98	3.0000E-10	0.0	0.0	0.0	0.0	24.81705
21.45	0.263	0.0	33.48	14.82	2.8000E-10	0.0	0.0	0.0	0.0	24.86070
24.51	0.263	0.0	33.41	14.46	3.0000E-10	0.0	0.0	0.0	0.0	24.88616
27.50	0.263	0.0	33.48	14.06	3.4000E-10	0.0	0.0	0.0	0.0	25.02182
30.51	0.263	0.0	33.41	13.67	3.3000E-10	0.0	0.0	0.0	0.0	25.05240
33.48	0.263	0.0	33.63	13.29	3.2000E-10	0.0	0.0	0.0	0.0	25.29523
36.51	0.263	0.0	33.48	13.05	3.4000E-10	0.0	0.0	0.0	0.0	25.22974
39.52	0.263	0.0	33.32	12.92	3.1000E-10	0.0	0.0	0.0	0.0	25.12819
42.50	0.263	0.0	33.49	12.27	3.2000E-10	0.0	0.0	0.0	0.0	25.38572

Diffuser Table:

P-diaVer (in)	angl (deg)	H- Angle (deg)	SourceX (m)	SourceY (m)	Ports ()	MZ-dis (m)	Isoplth (concent)	P-depth (ft)	Ttl-flo (MGD)	Eff-sal (psu)	Temp (C)	Polutnt (ppb)
2.0000	0.0	0.0	0.0	0.0	200.00	2000.0	0.0	140.00	12.630	1.0970	21.350	232.80

Table 16: Plumes 20 (UM3) Output of SEOO Dilution Factor (D_{fDOM}) during Ebb Tide on 21 December 2021 with Ambient Current (Final D_{fDOM} solution highlighted in yellow)

Simulation: Froude No: 11.86; Strat No: 2.74E-5; Spcg No: 10.97; k: 5.190; eff den (sigmaT) -1.188470; eff vel 1.365(m/s);

Depth Step	Amb-cur (ft)	Amb-sal (m/s)	P-dia (psu)	Polutnt (in)	Dilutn (ppb)	CL-diln (')	x-posn (')	y-posn (ft)	Iso dia	
									(ft)	(m)
0	140.0	0.263	33.49	2.000	232.8	1.000	1.000	0.0	0.0	0.0508;
1	140.0	0.263	33.49	2.026	226.9	1.026	1.000	0.0132	0.0	0.05146; bottom hit
25	140.0	0.263	33.49	3.075	142.6	1.634	1.000	0.268	0.0	0.0781;
50	140.0	0.263	33.49	4.632	87.57	2.665	1.332	0.689	0.0	0.1176;
75	140.0	0.263	33.49	6.782	53.71	4.355	2.178	1.376	0.0	0.1723;
100	139.8	0.263	33.49	9.629	32.94	7.129	3.564	2.483	0.0	0.2446;
125	139.7	0.263	33.49	13.29	20.23	11.68	5.840	3.897	0.0	0.3376;
150	139.4	0.263	33.49	17.94	12.47	19.14	9.572	5.600	0.0	0.4558;
168	139.1	0.263	33.48	22.04	8.834	27.33	13.67	7.090	0.0	0.5598; merging
175	139.0	0.263	33.48	23.87	7.734	31.39	16.05	7.814	0.0	0.6062;
200	138.3	0.263	33.47	32.04	4.843	51.49	29.09	11.71	0.0	0.8138;
225	137.2	0.263	33.45	43.99	3.080	84.46	56.30	18.23	0.0	1.1173;
250	135.3	0.263	33.42	62.73	2.005	138.5	92.36	28.94	0.0	1.5933;
275	132.2	0.263	33.36	94.00	1.348	227.3	151.5	47.67	0.0	2.3876;
280	131.5	0.263	33.35	102.6	1.251	250.9	167.3	53.24	0.0	2.6050; trap level
300	128.5	0.263	33.33	142.0	0.978	355.0	236.7	88.89	0.0	3.6065;
310	127.8	0.263	33.35	155.7	0.921	388.6	259.1	125.2	0.0	3.9558; local maximum rise or fall

Horiz plane projections in effluent direction: radius(m): 0.0; CL(m): 38.163

Lmz(m): 38.163

forced entrain 1 196.6 3.711 3.956 1.000

Rate sec-1 0.0 dy-1 0.0 kt: 0.0 Amb Sal 33.3462

12:49:15 PM. amb fills: 4

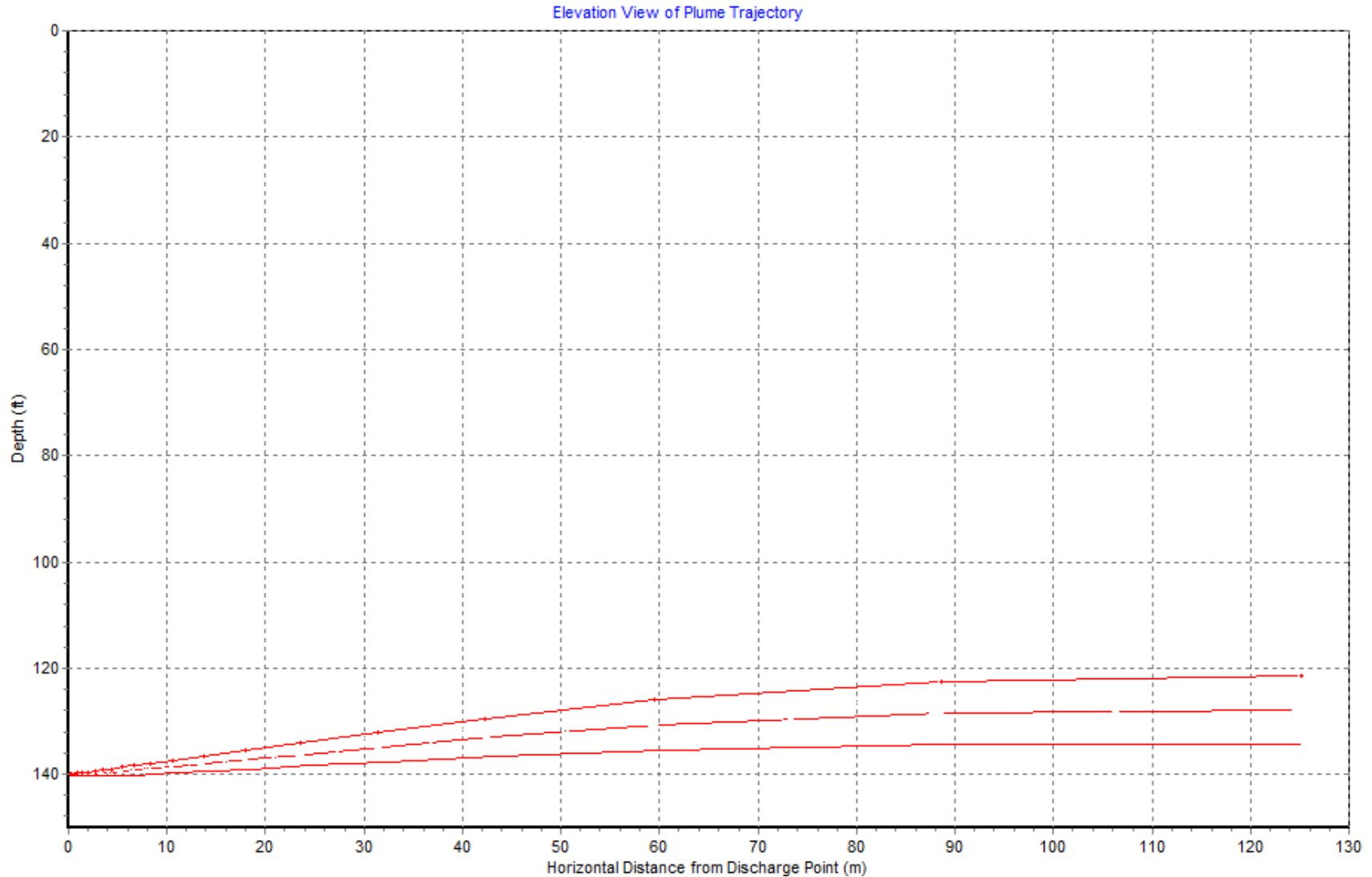


Figure 3.2.11: Plumes 20 solution of discharge plume trajectories for discharges of 12.63 mgd of SEOO effluent at discharge salinity of $S_{(x=0)} = 1.097$ psu, per operating conditions and water mass temperature/salinity profiles during flood tide on 21 December 2021. Plumes 20 simulation performed based on ambient current = 0.263 m/s per ADCP measurements. ZID is defined by the maximum horizontal excursion of trajectories from the origin. From the maximum horizontal spreading of the plume, the ZID extends from $X = 0.0$ m to $X = 126$ m so that ZID = 126 m.

3.3 THIRD SEOO DEPLOYMENT - 3 MARCH 2022

The design of the SEOO survey boxes was slightly modified for the third AUV deployment on 2 March 2022. Because the patterns of fDOM features that had SNR's exceeding unity and were spatially coherent with the SEOO diffuser did not extend beyond 300 to 400 m from the diffuser in the heat maps of the second deployments, it was decided to create 100 m of overlap between the ebb-tide and flood-tide survey boxes in the long-shore direction in order to increase resolution of suspected plume remnants. Within each overlapping ebb-tide and flood-tide survey box, the same track line pattern used during the second AUV deployments in December 2021 were retained, with 12 shore parallel track lines at 108.8 m spacings spread across 1,414.2 m in the cross-shore (on/off shore) direction with each track line measuring 707.1 m in length along the longshore (shore parallel) direction. This arrangement was found in the second SEOO deployment to provide sufficient horizontal resolution to suppress spatial aliasing of the fDOM sampling. The modified survey plan with overlapping ebb and flood tide survey boxes over the SEOO outfall is shown in [Figure 3.3.1](#), where again the flood tide box shown in orange and the ebb tide box is shown in yellow. The numbers of stationary water column monitoring stations (where CTD casts and ADCP velocity profiles are taken) remained the same as during the second deployment on 20 December 2021, with 18 stations distributed along the 160 ft and 60 ft depth contours (shown as green circles in [Figure 3.3.1](#)). The total dimension of the AUV surveyed area on either ebb or flood tide was 707.1 m in the longshore (shore parallel) direction and 1,414.2 m on the cross-shore (on/off shore) direction. However, the total area surveyed during both ebb and flood tide is reduced from 494.2 acres during the second deployment to 459.3 acres during the third deployment due to the 100 m of overlap between the ebb-tide and flood-tide survey boxes.

As practiced during the first and second AUV deployments in September and December 2021, the new survey boxes in [Figure 3.3.1](#), were searched twice for the presence of the SEOO plume, (i.e., out and return). As before, the AUV is flown along a dolphin-style flight path when transiting outbound with the current, i.e., a yo-yo flight path diving and ascending through the water column between the seabed and an apex halfway between the sea surface and the pycnocline, (cf. [Figure 1.2.2](#)). On the return legs of each track line, (against the current) the AUV is flown at a constant depth immediately beneath the pycnocline (trapping level) where the maximum horizontal dispersion of the plume is expected, (cf. Baumgartner, 1994; Frick et al., 2003). Altogether, the AUV covers a distance of about 20.0 kilometers in about 5 hours within each survey box which is roughly the endurance limit of the AUV with fully charged batteries. The survey period is centered within each ebb or flood tide interval of 6.2 hours. The AUV batteries are changed during the 1.2 hour interval around slack water between ebb and flood tide intervals, allowing for AUV surveys of the SEOO over a complete semi-diurnal tide cycle.

The 18 stationary water column monitoring stations are distributed between the 140 ft and 60 ft depth contours around the SEOO, and provide vertical profiles of salinity, temperature, and fDOM water mass properties immediately prior to and during the AUV surveys. Measurements from the control stations SEOO-Ebb and SEOO-Flood provide far-field measurements of natural background (ambient) water-mass properties (salinity, temperature, and fDOM). The measurements of the fDOM at the 18 stationary monitoring stations were in units of RFU which were converted to QSU fDOM units using the second order polynomial in [Figure 1.3.1](#).

It was critical to the plume tracking effort to program the AUV to fly directly beneath the pycnocline during the return leg (against the current) along each of the 12 track lines within the ebb and flood survey boxes shown in

Figure 3.3.1. To locate the depth of the pycnocline, the CTD casts were performed prior to the AUV survey on 1 March 2022 at monitoring stations EOO-Ebb and EOO-Flood and quickly processed to determine the salinity and temperature changes with depth, (cf. **Figure 3.3.2**). These CTD data showed a cold bottom layer with temperatures ranging from 11.4° C at the seabed, warming rapidly to 13° C at 3 m above the seabed, and then warming almost linearly to 14.7° C at the sea surface. The salinity reached 33.7 ppt near the seabed, declining to 33.48 ppt at about a depth of -27m MSL and then remained nearly constant between -27 m depth and the sea surface. Consequently, the density profile during the third AUV deployment was more typical of a continuously stratified water column rather than a two-layer system as prevailed during the first and second deployments with a cold bottom layer and warm surface mixed layer. Consequently, the trapping level was deep, at a depth of -26.9 m (88.26 ft) MSL, which is more typical of a worst-case dilution scenario, because initial dilution is arrested relatively close to the seabed. Based on this finding, the AUV was programmed on its outbound dolphin-style legs (with the current) for dive cycle apex points set halfway between the trapping level and the sea surface at a depth of the pycnocline at a depth of -13.45 m (-44.1 ft) MSL and dive cycle bottoming points set at 2 m (-6.6 ft) above the seabed. The Iver3 AUV uses its bottom-locking sonar to determine the distance above the local seabed at any location within the survey box. Along the return leg of each track line (flown against the current), the AUV was programmed to fly at a constant depth of -15.5 m depth (-50.8 ft) MSL.

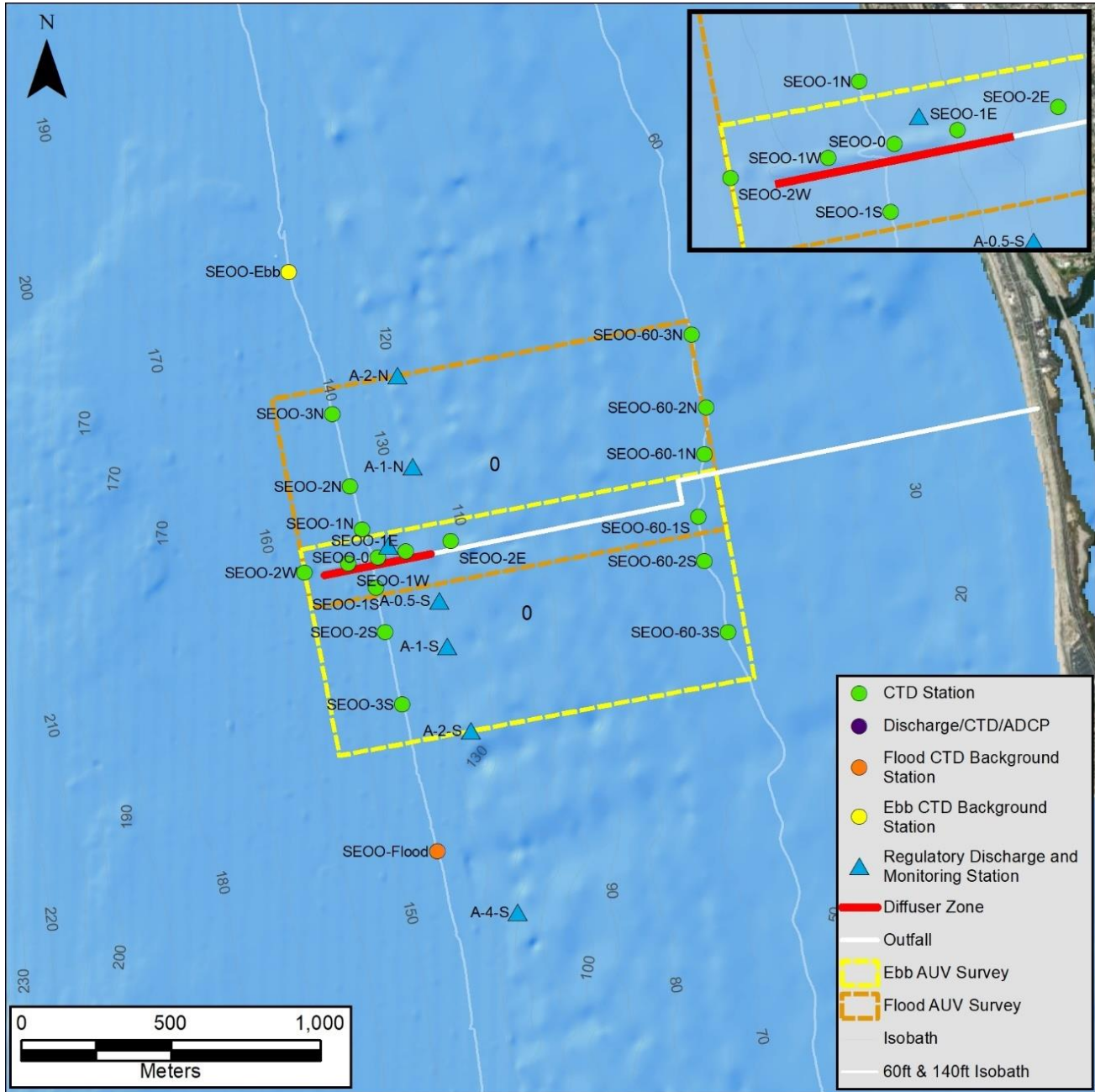


Figure 3.3.1: Survey boxes and sampling stations for the second AUV deployment, 3 March 2022, at the San Elijo Ocean Outfall

At the time of the ebb tide AUV survey on 2 March 2022, the SEOO was discharging on average 8.806 mgd of wastewater during ebb tide with an average daily discharge salinity of 0.71 psu and an average daily fDOM discharge concentration of 204.34 ppb (QSU), based on shoreside monitoring of the SEOO effluent, (see tabulations of SEOO shoreside monitoring data in Appendix-B). Later in the day during flood tide the SEOO average discharge rates increased to 11.851 mgd, while average discharge salinity and fDOM concentrations remained unchanged, (cf. Appendix-A). The average SEOO discharge concentrations of fDOM are significantly higher (by more than 2 orders of magnitude) than the natural ocean background concentrations of fDOM measured at far-field control stations, SEOO-Ebb and SEOO-Flood, which were profiled twice during each ebb and flood tide event on 2 March 2022. Vertical profiles of natural background fDOM measured during ebb tide at SEOO-Ebb (cf. [Figure 3.3.3](#)) exhibited depth-averaged concentrations ranging between 0.277 ppb and 0.279 ppb, but nearly doubled in the upper 3 m of the water column to 0.475 ppb to 0.520 ppb. This abrupt rise in ambient fDOM near the surface coincided with survey notations in the monitoring logs that a red tide was observed at monitoring stations SEOO-Ebb between the hours 0940 and 1030 PST and again along the 60 ft depth contour at inshore monitoring stations SEOO 60-3N, SEOO 60-2N, and SEOO 60-1N between the hours of 1000 and 1030 PST. Natural background fDOM measured later during flood tide on 2 March 2022 at SEOO-Flood (cf. [Figure 3.3.4](#)) declined to depth-averaged concentrations ranging between 0.234 ppb and 0.235 ppb with no abrupt rise in fDOM concentrations near the surface. Regardless, the signal to noise ratio of the fDOM plume observable at any point of discharge along the SEOO diffuser ranges between $SNR_{fDOM} = 392$ and $SNR_{fDOM} = 872$, based on the maximum and average concentrations of natural background fDOM measured at far-field control stations, SEOO-Ebb and SEOO-Flood ([Figure 3.3.3](#) and [Figure 3.3.4](#)), applied to equation (1). While profiles of natural background fDOM concentrations measured during both ebb and flood tide showed both random variations (noise) with some general vertical structure (with higher concentration near the surface during ebb tide, and declining near the surface during flood tide), the standard deviations around the depth averaged fDOM concentrations were small, ranging between $\sigma = 0.027$ ppb and $\sigma = 0.055$ ppb, (cf. [Figure 3.3.3](#) and [Figure 3.3.4](#)).

Mean ebb tide currents on 2 March 2022 at the far-field control station, SEOO-Ebb, were strong, 0.472 m/s (0.92 kts) toward the southeast, based on acoustic Doppler profiling (ADCP) at far field monitoring station, SEOO-Ebb, (cf. [Figure 3.3.5](#)) located up-drift of the yellow AUV survey box shown in [Figure 3.3.1](#). Mean current speeds reaching 1 knot are not typical of tidal currents in the Southern California Bight. An approaching extratropical frontal cyclone from the northwest on 2 March 2022 imparted a considerable wind-driven component to the local coastal currents, which when combined with the ebb tidal component induced a large net shore-parallel drift to the SEOO discharge plume directed toward the southeast. However, there are other transient short-lived current oscillations in the ebb tide ADCP time series record on 2 March 2022 that reached 1.35 m/s (2.62 kts), cf. [Figure 3.3.5](#). The current direction data in the ADCP record indicates these spikes of higher oscillatory currents were directed cross-shore, indicating they were due to shoaling surface gravity waves from the approaching storm, possibly combined with internal waves. Because of the oscillatory nature of these current spikes, they produce no net drift of the SEOO discharge plume, but merely serve to smear the plume or break off pieces from the main body of the plume and smear or disperse those pieces in the cross-shore direction.

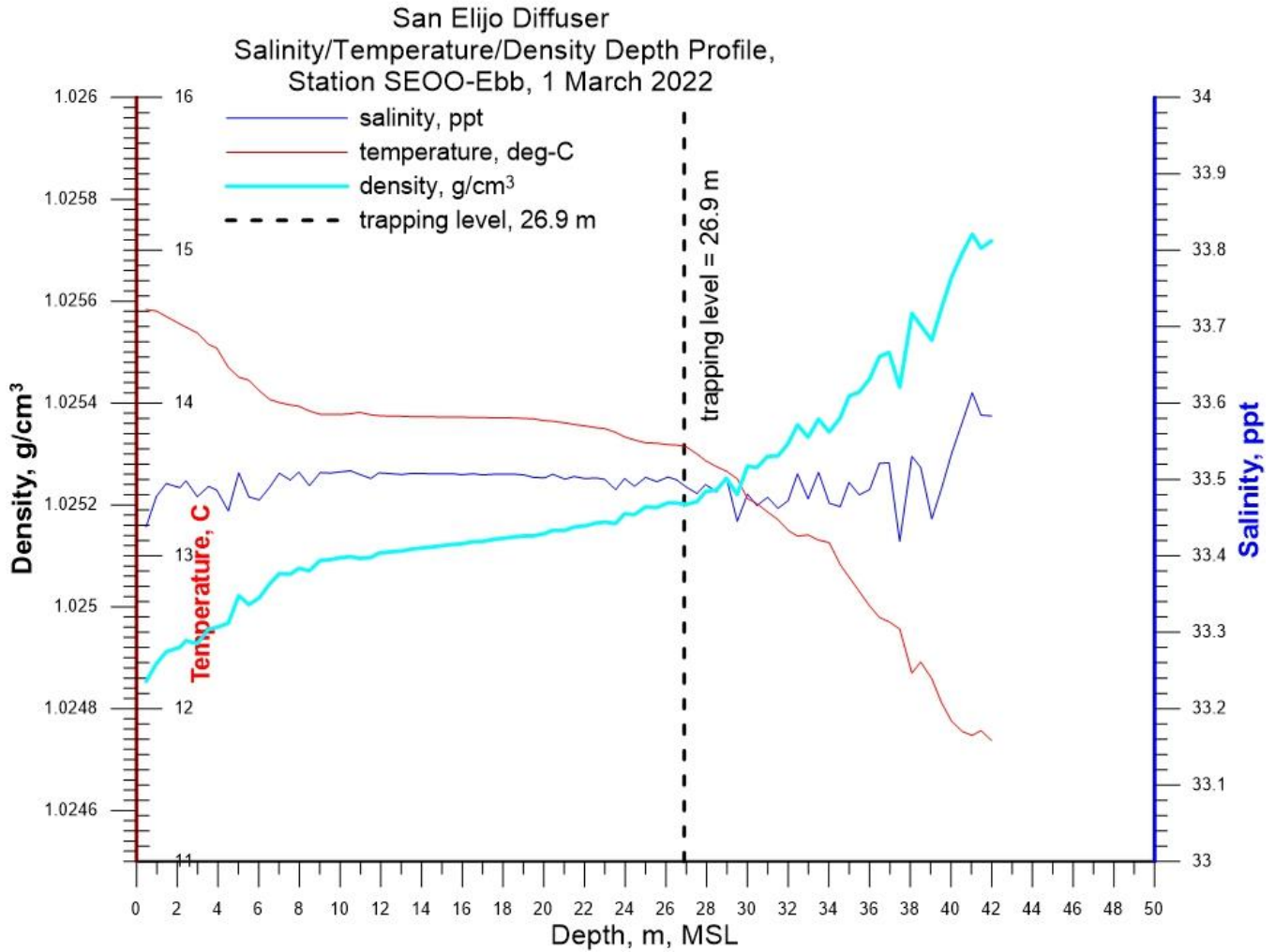


Figure 3.3.2: Salinity/Temperature/Density depth profiles derived from CTD casts on 1 March 2022 used to program the AUV survey of the plume dispersion from SEOO on 3 March 2021 during ebb and flood tides.

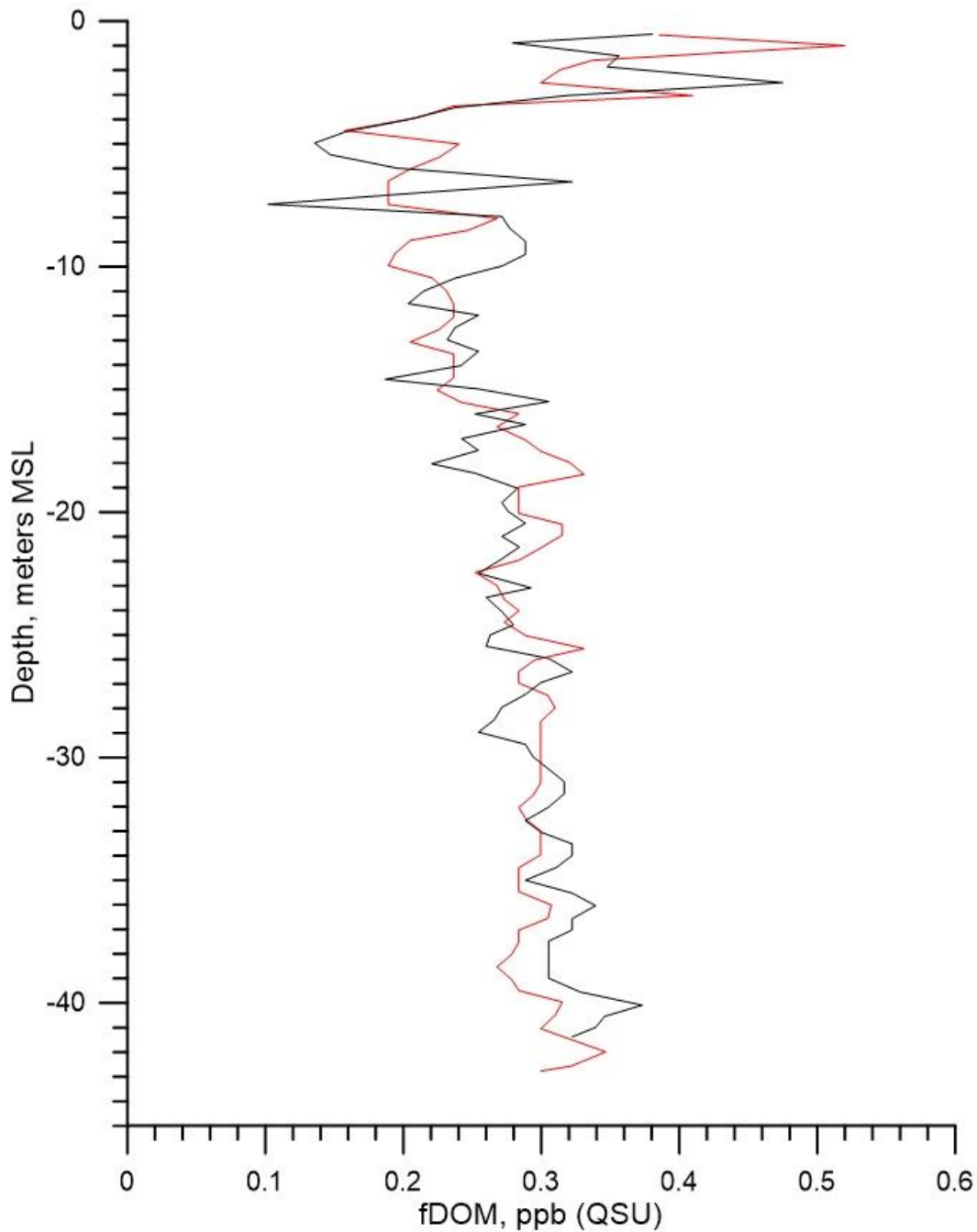


Figure 3.3.3: Vertical profiles of natural background fDOM concentrations measured during the third deployment at the far-field ebb tide monitoring station “SEOO-EBB”, located 2 km northwest of SEOO along the -140 ft. MLLW depth contour, cf. yellow dot in **Figure 3.3.1**

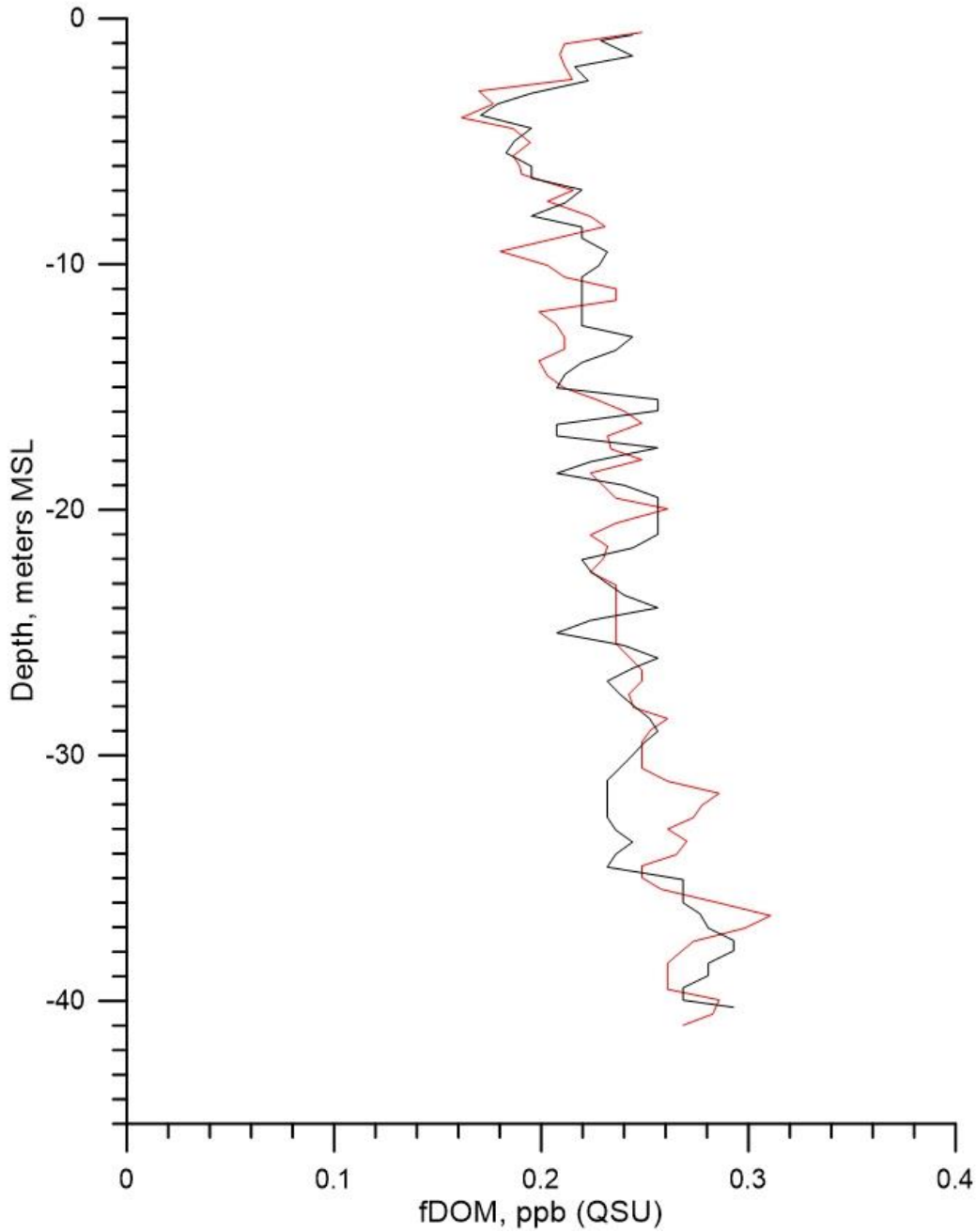


Figure 3.3.4: Vertical profiles of natural background fDOM concentrations measured during the third deployment at the far-field flood tide monitoring station “SEOO-Flood”, located 2 km southeast of SEOO along the -140 ft. MLLW depth contour, cf. orange dot in Figure 3.3.1

ADCP measurements of currents at far field monitoring station, SEOO-Flood, (cf. **Figure 3.3.6**) demonstrated that mean flood tide currents on 2 March 2022 were considerably less than the mean ebb tide currents, reaching only 0.301 m/s (0.58 kts) directed toward the northwest. This decline in the flood tide current ADCP record relative to the ebb tide current record earlier in the day is due to combination of factors. One of these factors is the flood tidal current component directed toward the northwest is flowing against the wind driven current component directed toward the southeast. The other factor is the fact that tidal currents along the coastline of the lower Southern California Bight do not reverse symmetrically between ebb and flood tide, but rather are *ebb-tide dominant*, imparting a net southeasterly drift to the SEOO discharge plume over a complete tidal day of 24.83 hrs. Transient oscillatory current spikes in the flood tide ADCP current record on 2 March 2022 were non the less significant, reaching 1.35m/s (2.62 kts) in the cross-shore direction, due to shoaling surface gravity waves from the approaching storm, in combination with internal waves. The internal waves are excited by an extreme bathymetric feature that resulted in an abrupt narrowing of the continental shelf directly offshore of the SEOO diffuser, (cf. **Figure 3.1.7**). This abrupt narrowing of the shelf creates a cliff that is perpendicular to the shoreline along the shelf break and excites internal waves as the tidal currents flow across the escarpment formed by this cross-shore cliff, much like lee waves do in the atmosphere when storm winds blow over mountainous topography. The cross-shore oscillations of the internal waves that radiate outward from the shelf break, adding to the high current spikes in the ADCP records on 3 March 2022 (cf. **Figure 3.3.5** and **Figure 3.3.6**).

Again, the ebb tide navigation precision of the AUV shown in **Figure 3.3.7** is excellent with accurate repeatability of the outbound and return legs of each track line. During this survey, the AUV collected 65,770 separate measurements of salinity and fDOM along a total distance surveyed of 21.2 km. The fDOM heat map generated from these 65,770 measurements of fDOM concentrations is plotted in **Figure 3.3.8**. **Figure 3.3.8** exhibits a small degree of banding in the fDOM distribution along the 12 track lines due to mild spatial aliasing. However, the fDOM heat map exhibits no horizontal structures having spatial coherence with the SEOO diffuser. Instead, there is a large mass of elevated fDOM along the -60 ft (-18.3 m) depth contour with a sharply defined frontal boundary located 685.9 m (2,250 ft) shoreward of the shoreward end of the SEOO diffuser. The fDOM concentrations across all depths within the survey area in **Figure 3.3.8** range from $fDOM_{(x)} = 0.09$ ppb to 1.2 ppb in isolated spots shoreward of the fDOM frontal boundary [685.9 m (2,250 ft) shoreward of the shoreward end of the SEOO diffuser]. The maximum fDOM concentrations within the fDOM front are as much as 330% higher than the depth-averaged natural background fDOM concentration monitoring station SEOO-flood where $fDOM_{\infty} = 0.279$ ppb (cf. **Figure 3.3.3**). The fDOM front in **Figure 3.3.8** is a relatively massive feature compared with all other elevated fDOM features discovered during the plume tracking field studies in September and December 2021 and is defined by 14,634 separate fDOM measurements having concentrations ranging between 0.56 ppb and 1.2 ppb. No other fDOM features having this high a concentration can be found anywhere else in the SEOO ebb-tide heat map in **Figure 3.3.8**. By contrast, fDOM concentrations seaward of the fDOM front, and in particular the wake of the SEOO diffuser are on the order of $fDOM_{\infty} \cong 0.1$ to 0.34 ppb, consistent with the depth variation of natural background fDOM concentration below -3 m depth plotted in **Figure 3.3.3**.

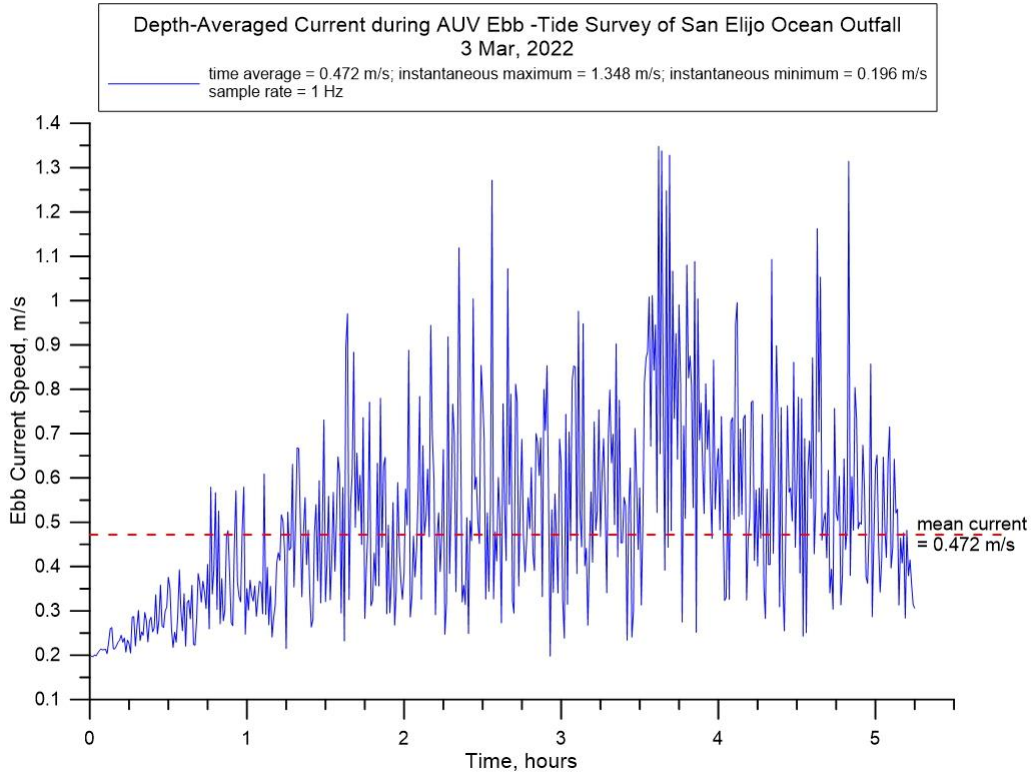


Figure 3.3.5: Time series of depth averaged current derived from ADCP measurements at SEOO during ebb-tide AUV survey on 21 December 2021.

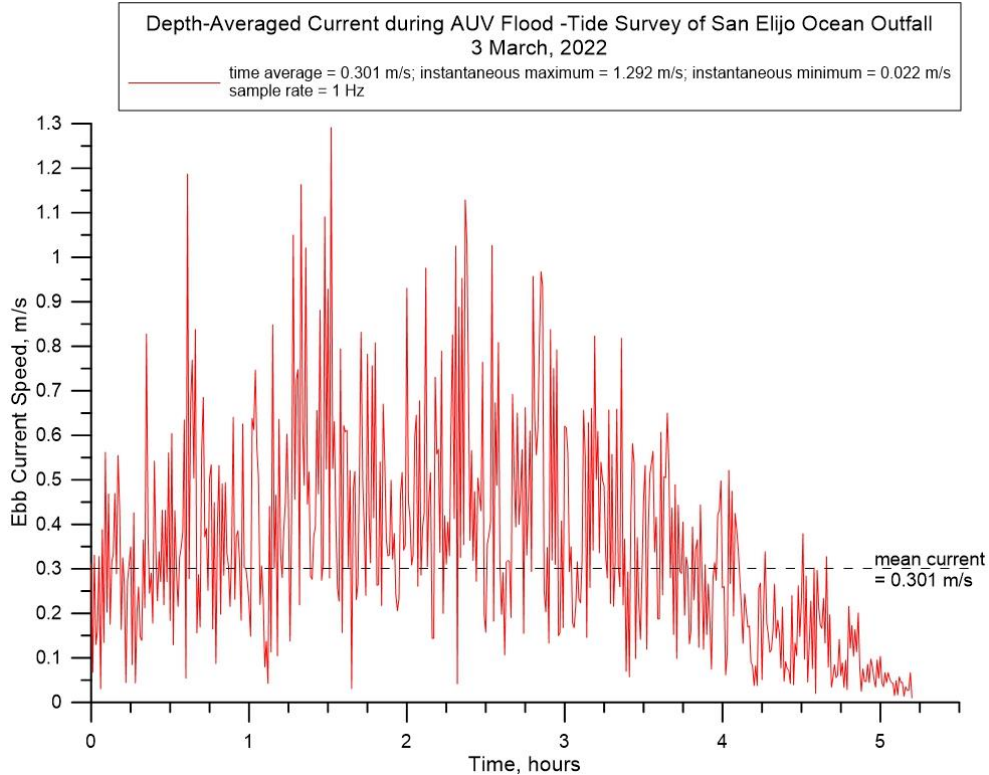


Figure 3.3.6: Time series of depth averaged current derived from ADCP measurements at SEOO during flood-tide AUV survey on 21 December 2021.

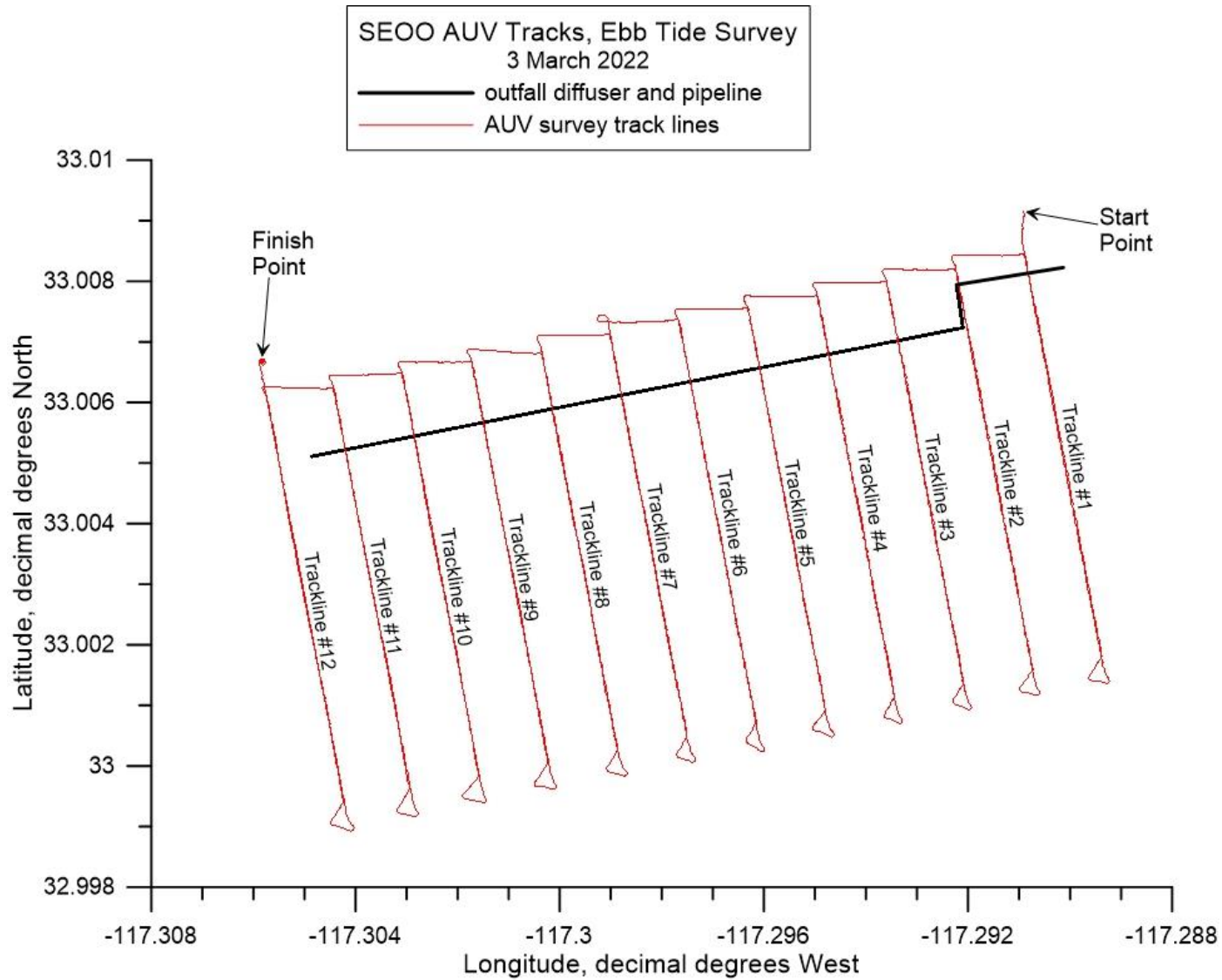


Figure 3.3.7: AUV track lines on 3 March 2022 as flown during ebb tide surveys of the discharge plume from SEOO. Note, at 30° N latitude, 1° longitude = 93,453.2 m, while 1° latitude = 110,904.4 m.

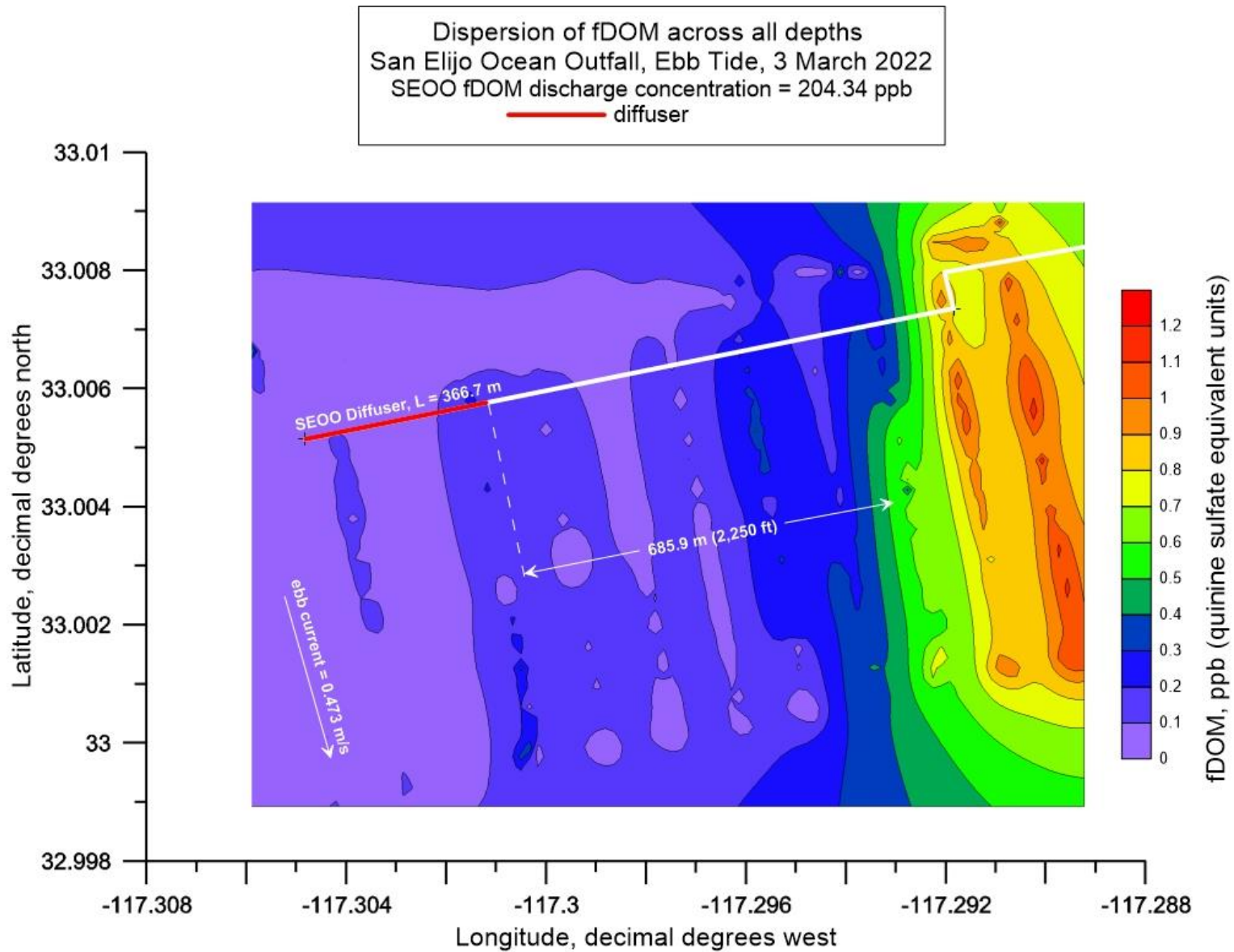


Figure 3.3.8: Full depth contour plot (aka, heat map) of AUV measurements of fDOM from surveys of SEOO during ebb tide on 3 March 2022. Average SEOO discharge rate = 8.806 mgd during ebb tide; End-of-pipe discharge concentration of fDOM = 204.34 ppb (QSU); End of pipe salinity = 0.71 psu; Trapping level (pycnocline depth) = 26.9 m (-88.3 ft) MSL; Mean ebb tide current = 0.472 m/s (0.92 kts) toward the southeast.

The probable reason for finding no remnants of the SEOO plume are the relatively low SEOO flow rates (8.806 mgd) discharged into the extremely high mean currents 0.473 m/s (0.92 kts) flowing shore-parallel in combination with transient wave surges as high as 1.35 m/s (2.62 kts) flowing obliquely to the mean current, thereby exposing the SEOO plume to high velocity shearing rates. This shearing by the ambient currents breaks up the plume into fragments and greatly accelerates dilution rates. Plumes 20 of the 21 December 2021 ebb event (**Table 15** and **Table 16**) found minimum dilutions of 388.6:1 in substantially less current (0.263 m/s or 0.51 kts and at higher discharge rates (12.63 mgd) than occurred during ebb tide on 3 March 2022. Since dilution increases with increasing current and decreasing discharge rates, it is sensible that no evidence of the SEOO discharge plume was found during ebb tide on 3 March 2022.

To further explore this hypothesis, the fDOM heat map in **Figure 3.3.8** is converted into a signal to noise ratio heat map in **Figure 3.3.9** by invoking equation (1) to convert the fDOM concentrations into corresponding SNR_{fDOM} patterns. Again, since only fDOM features having signal to noise ratios of unity or greater are possible remnants of the plume, **Figure 3.3.9** has been scaled to filter out features having $SNR_{fDOM} < 0.8$, where features having $0.8 \leq SNR_{fDOM} < 1.0$ are potentially diluted fragments or diluted outer edges of a plume remnants. Inspection of **Figure 3.3.9** reveals that the signal to noise ratio in the wake of the SEOO plume range from $SNR_{fDOM} \cong 0$ to 0.2, indicating no presence of any plume remnant downstream of the diffuser since the lowest order significance threshold for detection is: $SNR_{fDOM} \geq 1$. Inshore, signal to noise ratios within the fDOM front range from $SNR_{fDOM} \cong 1.01$ to 3.3 in various places within the core of the fDOM front. Therefore, regardless of the source of the fDOM front located 685.9 m (2,250 ft) shoreward of the shoreward end of the SEOO diffuser, that feature is certainly real and satisfies the lowest order significance threshold for detection, (i.e., $SNR_{fDOM} \geq 1$), by a considerable degree. Based on this detection metric, we conclude there is no detectible trace of the EOO plume during ebb tide on 3 March 2020, but there is a considerable inshore water mass with elevated fDOM that has a well-defined frontal boundary separating it from the deeper waters surrounding the SEOO diffuser.

To assess whether there is any possibility that the SEOO discharge could be the source of the fDOM front in **Figure 3.3.8**, the SNR_{fDOM} heat map in **Figure 3.3.9** was transposed into a dilution heat map in **Figure 3.3.10** using equation (2) on the basis that the initial fDOM source concentrations in the fDOM front are the same as the fDOM concentrations discharged by the SEOO diffuser, namely: $fDOM_{(x=0)} = 204.34$ ppb. Equation (2) teaches that the regions of high SNR will correspond to regions of low values of D_{fDOM} relative to the dilution elsewhere within the AUV survey area. **Figure 3.3.10** indicates that the dilution factor (D_m) for the fDOM front would be no less than as $D_{fDOM} = 221:1$ in various places within the core of the fDOM front. The dilution along the outer perimeter of the fDOM front, the dilution ranges from $D_{fDOM} = 933:1$ to as much as 20,000:1 along the frontal boundary. Elsewhere in the wake of the SEOO diffuser (e.g., down current) dilution ranges from $D_{fDOM} = 3,344:1$ to as high as 80,000:1, even 148,655:1. Given that fDOM dilutions are at least 3,344:1 in the nearfield of the diffuser; it would be impossible for dilutions to be as low as 221:1, at a distance of 2,250 ft. from the SEOO, if the SEOO were the source of the fDOM front.

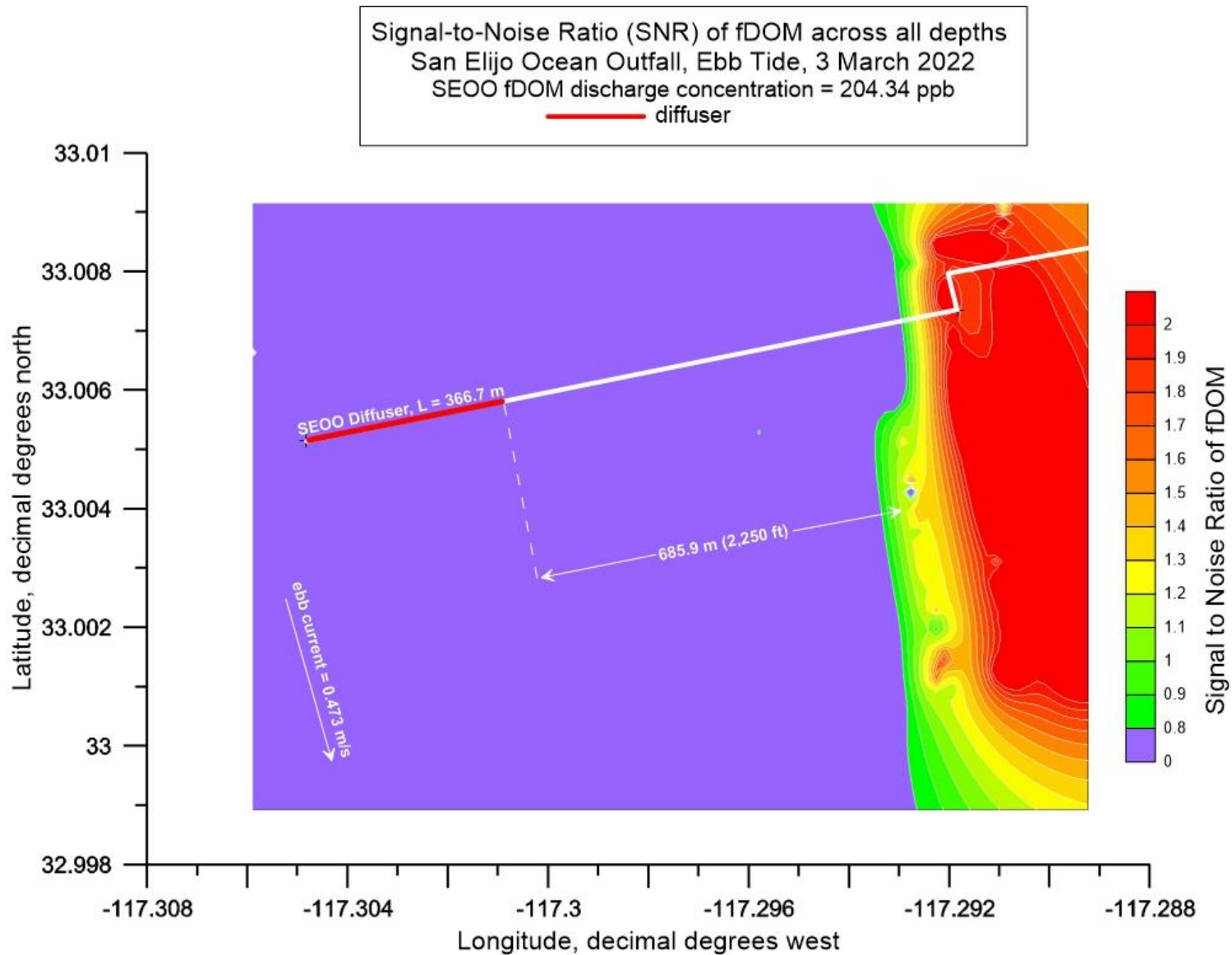


Figure 3.3.9: Full-depth contour plot (aka, heat map) of the signal to noise ratio (SNR) of fDOM during AUV surveys of SEOO during ebb tide on 3 March 2022. Average SEOO discharge rate = 8.806 mgd during ebb tide; End-of-pipe discharge concentration of fDOM = 204.34 ppb (QSU); End of pipe salinity = 0.71 psu; Trapping level (pycnocline depth) = -26.9 m (-88.3 ft) MSL; Mean ebb tide current = 0.473 m/s (0.92 kts) toward the southeast.

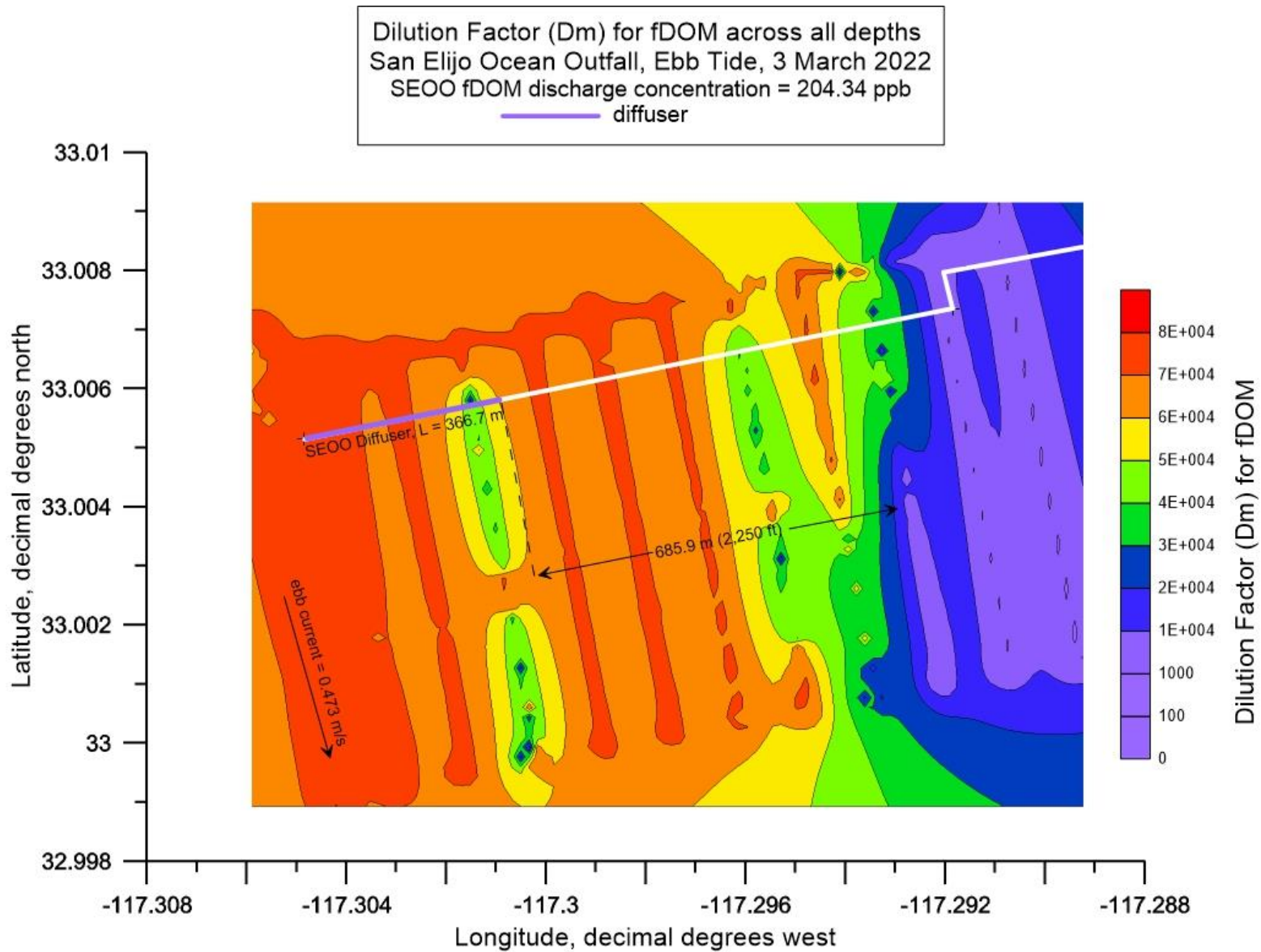


Figure 3.3.10: Full depth contour plot (aka, heat map) of the dilution factor, (D_{fDOM}) of fDOM during AUV surveys of SEOO during ebb tide on 3 March 2022. Average SEOO discharge rate = 8.806 mgd during ebb tide; End-of-pipe discharge concentration of fDOM = 204.34 ppb (QSU); End of pipe salinity = 0.71 psu; Trapping level (pycnocline depth) = -26.9 m (-88.3 ft) MSL; Mean ebb tide current = 0.473 m/s (0.92 kts) toward the southeast.

Given the observations of a red tide at inshore monitoring stations SEOO 60-3N, SEOO 60-2N, and SEOO 60-1N, the most likely source of the fDOM front that is so prominent in [Figure 3.3.8](#) through [Figure 3.3.10](#) would be tidal discharges from the recently restored San Elijo Lagoon, (cf. [Figure 3.3.11](#)). Algal blooms in coastal lagoons and bays are common in Southern California and the tidal inlet of the San Elijo Lagoon is located 660 m (2,165 ft.) north of the headworks of the San Elijo Ocean Outfall, (cf. [Figure 3.3.11](#)). Based on the nearest NOAA tide gage (Scripps Pier, NOAA #941-0230) higher-high water was +3.14 ft MSL at 0930 PST on 3 March 2022, and lower low water was -3.27 ft MSL at 1548 PST, so that the tidal range in the ocean during ebb tide on 3 March 2022 was 6.41 ft. However, this is not the tidal range in the lagoon. Lower low water elevations in the lagoon are truncated by the sill in inlet channel. The San Elijo Lagoon Restoration plan requires that the inlet channel be maintained at an elevation of no less than -1.5 ft MSL, (cf. AECOM, 2016). Consequently, the tidal range during ebb tide in the lagoon on 3 March 2022 was actually 4.64 ft. In flood tide on March 3 2022 began with lower low water at -3.27 ft MSL and ended at 2200 PST with a lower-high water level of 2.39 ft MSL, so that the tidal range in the ocean during flood tide was 5.66 ft, but due to tidal muting by the inlet channel sill, tidal range in the lagoon during flood tide was only 3.89 ft.

The storage rating curve for the recently restored San Elijo Lagoon is plotted in [Figure 3.3.12](#), based on the San Elijo Lagoon Restoration grading plan, (cf. AECOM, 2016). Plotting the water level changes between higher-high water and the inlet channel elevation indicates that the San Elijo Lagoon discharged 645 acre ft during the 6.3 hour ebb tide event on 3 March 2022. This is the equivalent of a 768 mgd discharge into the nearshore waters of the SEOO, which is 87 times greater than the discharge rate from the SEOO (8.806 mgd) during ebb tide on 3 March 2022

To determine if the fDOM front discovered by the AUV during ebb tide on 3 March 2022 could be due to tidal discharges from the San Elijo Lagoon, the CORMIX v-11 mixing model was used to simulate the tidal discharge plume. CORMIX is supported by both US EPA as well as the SWRCB, and has demonstrated high predictive skill in simulating shoreline discharges along open ocean coastlines (cf. Frick et al., 2003). The latest version of CORMIX (version-11) was initialized for the bathymetry, measured ebb currents, ([Figure 3.3.5](#)), and discharge rates derived from the storage rating curve ([Figure 3.3.12](#)) during ebb tide on 3 March 2022. The fDOM concentration of the lagoon waters was not known, so successive iterations with CORMIX v-11 were performed varying the fDOM discharge concentration until predicted fDOM discharge concentrations along the -60 ft (-18.3 m) MSL depth contour were matching the AUV measurements of $fDOM_{(x)} \cong 1.2$ ppb at the same depth. The lagoon fDOM concentration that gave the closest match to the AUV measurements was $fDOM_{(lagoon)} \cong 198$ ppb, which is roughly comparable to the SEOO discharge concentration of $fDOM_{(x=0)} = 204.34$ ppb. The resulting “calibrated” CORMIX-v11 simulation of the San Elijo discharge plume is plotted on [Figure 3.3.13](#). The 1.2 ppb isoline of the CORMIX plume follows approximately the frontal boundary of the fDOM front discovered by the AUV in [Figure 3.3.8](#), and extends an additional 2 km (1.24 miles) downstream beyond the SEOO diffuser and pipeline in the 0.473 m/s (0.92 kts) ebb tide current. This result, in combination with AUV data and observations of an inshore red tide, is strong evidence that the fDOM front, defined by a sharp frontal boundary 685.9 m (2,250 ft) inshore of the shoreward end of the SEOO diffuser, was not caused by the SEOO, but rather was a signature of the tidal discharge plume from the San Elijo Lagoon.

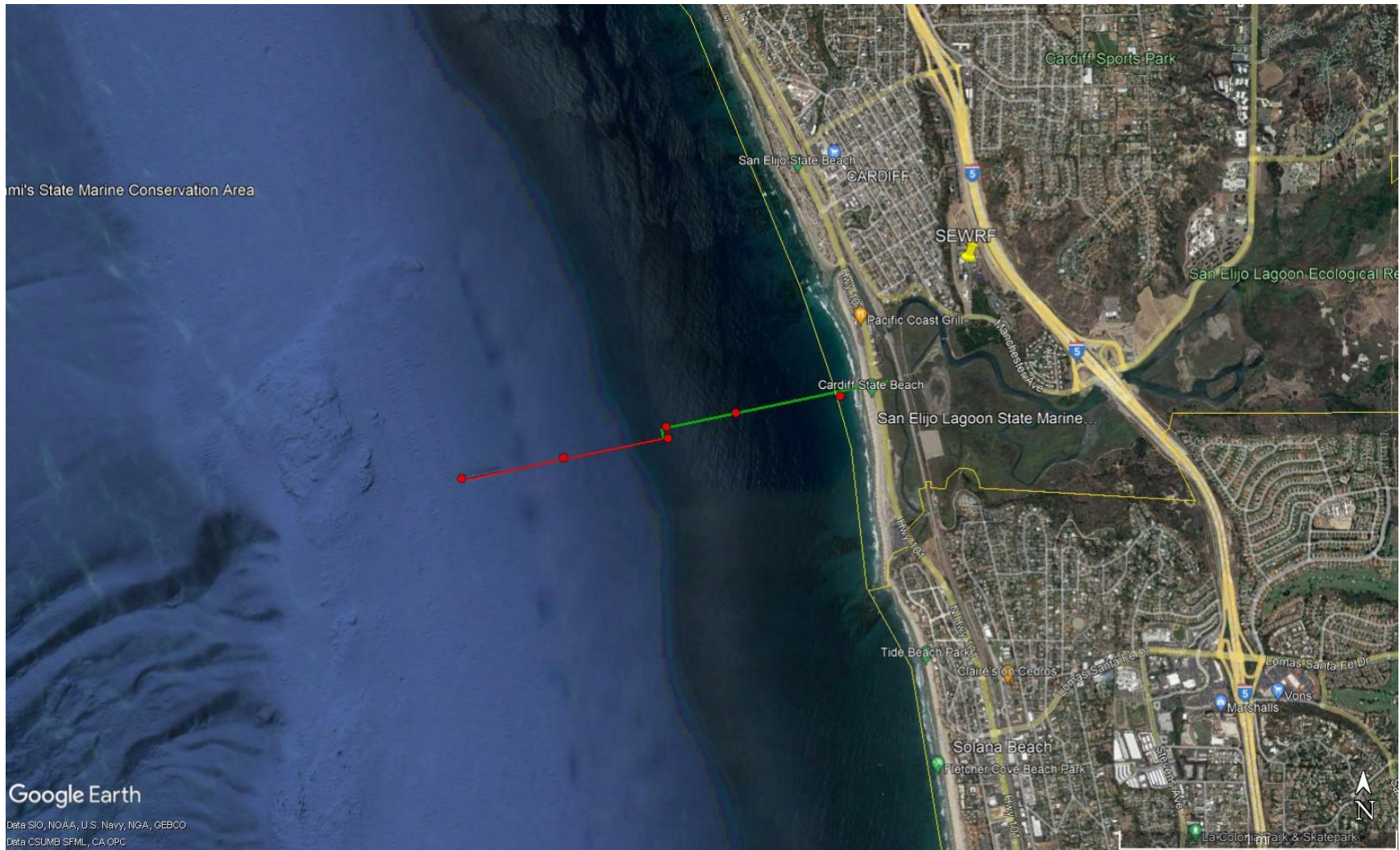


Figure 3.3.11: Google Earth image of the San Elijo Lagoon whose tidal inlet is located 660 m (2,165 ft.) north of the headworks of the San Elijo Ocean Outfall, (located by the green and red lines).

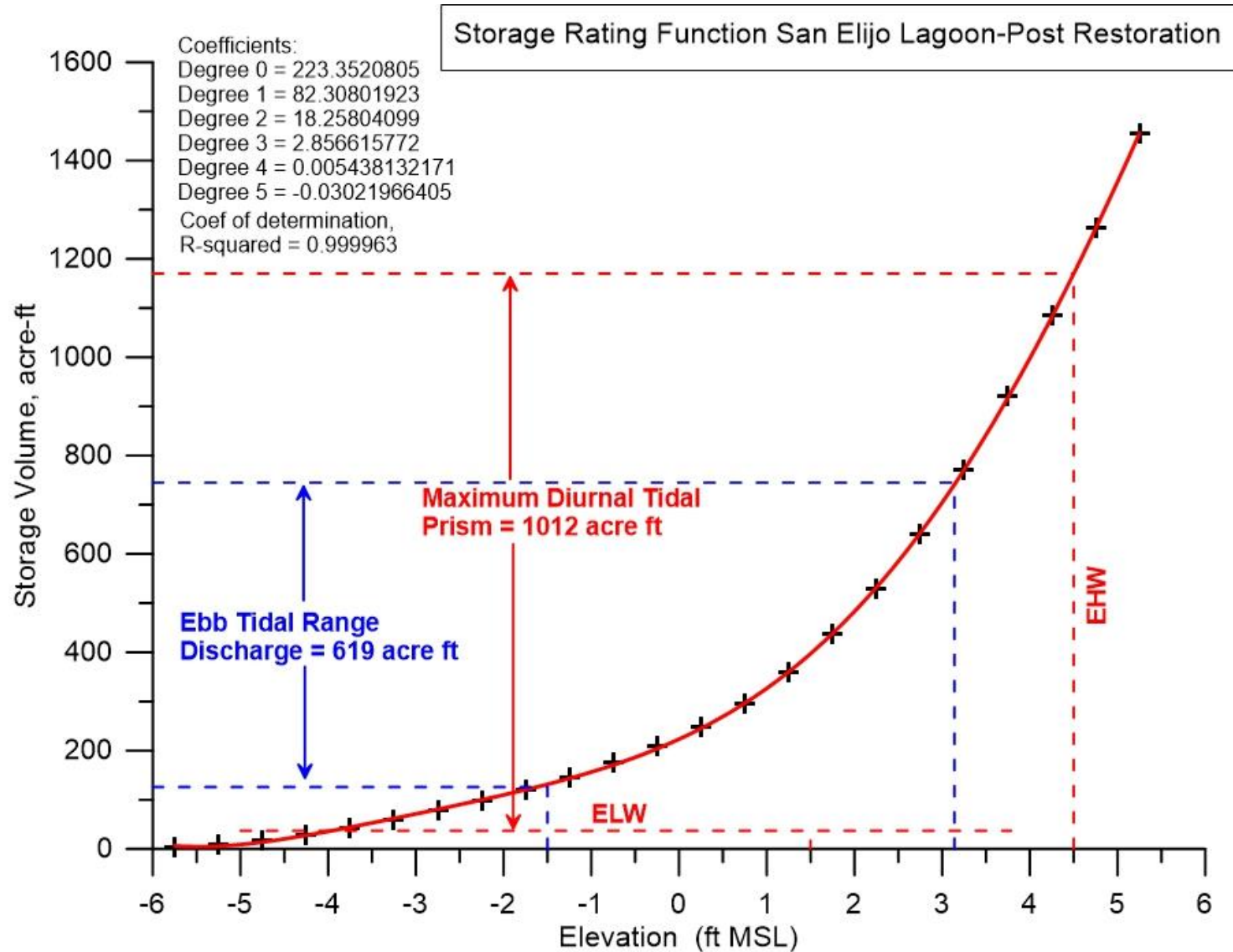


Figure 3.3.12: Storage rating function of the newly restored San Dieguito Lagoon, (cf. AECOM, 2016, “Environmental Impact Report/Environmental Impact Statement for the San Elijo Lagoon Restoration Project”). Annotations in blue designate the tidal range and tidal discharge volume from the lagoon during ebb tide on 3 March 2022

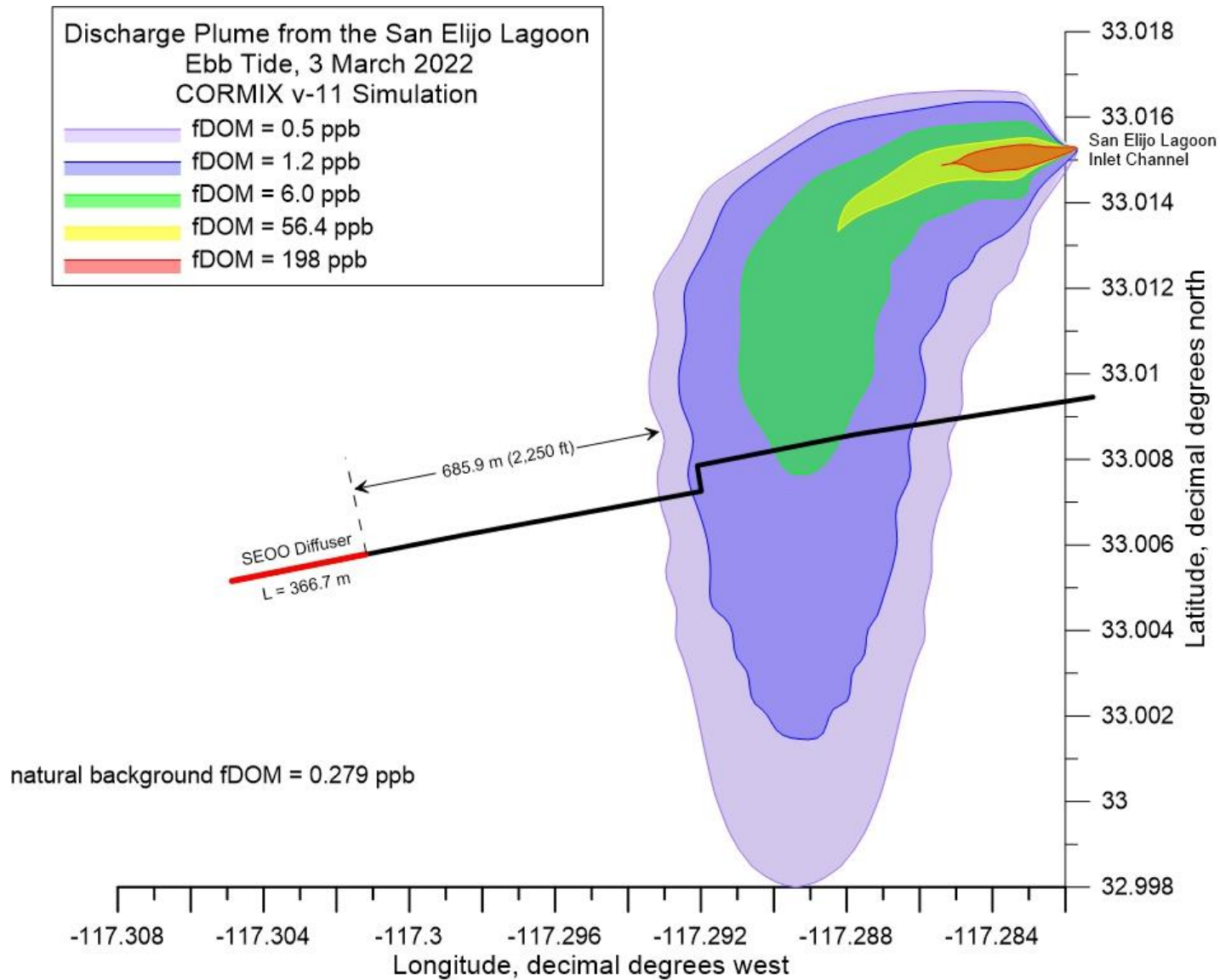


Figure 3.3.13: CORMIX v-11 Simulation of the discharge plume from the San Elijo Lagoon during ebb tide on 3 March 2022. Average SEOO discharge rate = 8.806 mgd during ebb tide; End-of-pipe discharge concentration of fDOM = 204.34 ppb (QSU); End of pipe salinity = 0.71 psu; Trapping level (pycnocline depth) = -26.9 m (-88.3 ft) MSL; Mean ebb tide current = 0.472 m/s (0.92 kts) toward the southeast.

On the following flood tide on 3 March 2021, the orange survey box in **Figure 3.3.1** was flown by the AUV with accurate repeatability of the outbound and return legs along each of 12 track lines, (cf. **Figure 3.3.14**). During this survey, the AUV collected 66,568 separate measurements of salinity and fDOM along a total distance surveyed of 21.2 km. The fDOM heat map generated from these 65,770 measurements of fDOM concentrations is plotted in **Figure 3.3.15**. **Figure 3.3.15** exhibits a small degree of banding in the fDOM distribution along the 12 track lines due to mild spatial aliasing. As during the preceding ebb tide, the fDOM heat map during flood tide exhibits no horizontal structures having spatial coherence with the SEOO diffuser. Instead, there is a large mass of elevated fDOM along the -60 ft (-18.3 m) depth contour with a well-defined frontal boundary located 579.7 m (1,902 ft) shoreward of the shoreward end of the SEOO diffuser. Concentrations in the fDOM front are noticeably reduced relative to the concentrations observed during the preceding ebb tide (cf. **Figure 3.3.8**), with concentrations along the frontal boundary generally on the order of $fDOM_{(x)} \cong 0.4$ ppb to 0.47 ppb, reaching as high as $fDOM_{(x)} = 0.79$ ppb in isolated spots shoreward of the fDOM frontal boundary [579.7 m (1,902 ft) shoreward of the shoreward end of the SEOO diffuser]. The maximum fDOM concentrations within the fDOM front are as much as 236% higher than the depth-averaged natural background fDOM concentration at monitoring station SEOO-flood where $fDOM_{\infty} = 0.235$ ppb (cf. **Figure 3.3.4**). The fDOM front in **Figure 3.3.15** is a relatively massive feature compared with all other elevated fDOM features discovered during the plume tracking field studies in September and December 2021, and is defined by 15,336 separate fDOM measurements having concentrations ranging between 0.47 ppb and 0.79 ppb. No other fDOM features having this high a concentration can be found anywhere else in the SEOO flood-tide heat map in **Figure 3.3.15**. By contrast, fDOM concentrations seaward of the fDOM front, and in particular the wake of the SEOO diffuser are on the order of $fDOM_{\infty} \cong 0.1$ to 0.31 ppb, consistent with the depth variation of natural background fDOM concentration below -3 m depth plotted in **Figure 3.3.4**.

The probable reason for finding no remnants of the SEOO plume are the relatively low SEOO flow rates (11.851 mgd) discharged into a moderately strong mean currents 0.301 m/s (0.58 kts) flowing shore-parallel in combination with transient wave surges as high as 1.29 m/s (2.51 kts) flowing obliquely to the mean current, thereby exposing the SEOO plume to high velocity shearing rates. This shearing by the ambient currents breaks up the plume into fragments and greatly accelerates dilution rates. Plumes 20 of the 21 December 2021 ebb event (**Table 15** and **Table 16**) found minimum dilutions of 388.6:1 in substantially less current (0.263 m/s or 0.51 kts) and at higher discharge rates (12.63 mgd) than occurred during flood tide on 3 March 2022. Since dilution increases with increasing current and decreasing discharge rates, it is sensible that no evidence of the SEOO discharge plume was found during flood tide on 3 March 2022.

To further explore this hypothesis, the fDOM heat map in **Figure 3.3.15** is converted into a signal to noise ratio heat map in **Figure 3.3.16** by invoking equation (1) to convert the fDOM concentrations into corresponding SNR_{fDOM} patterns. Again, since only fDOM features having signal to noise ratios of unity or greater are possible remnants of the plume, **Figure 3.3.16** has been scaled to filter out features having $SNR_{fDOM} < 0.8$, where features having $0.8 \leq SNR_{fDOM} < 1.0$ are potentially diluted fragments or diluted outer edges of a plume remnants. Inspection of **Figure 3.3.16** reveals that the signal to noise ratio in the wake of the SEOO plume range from $SNR_{fDOM} \cong 0$ to 0.2, indicating no presence of any plume remnant downstream of the diffuser since the lowest order significance threshold for detection is: $SNR_{fDOM} \geq 1$. Inshore, signal to noise ratios within the fDOM front range from $SNR_{fDOM} \cong 1.01$ to 2.36 in various places within the core of the fDOM front. Therefore, regardless of

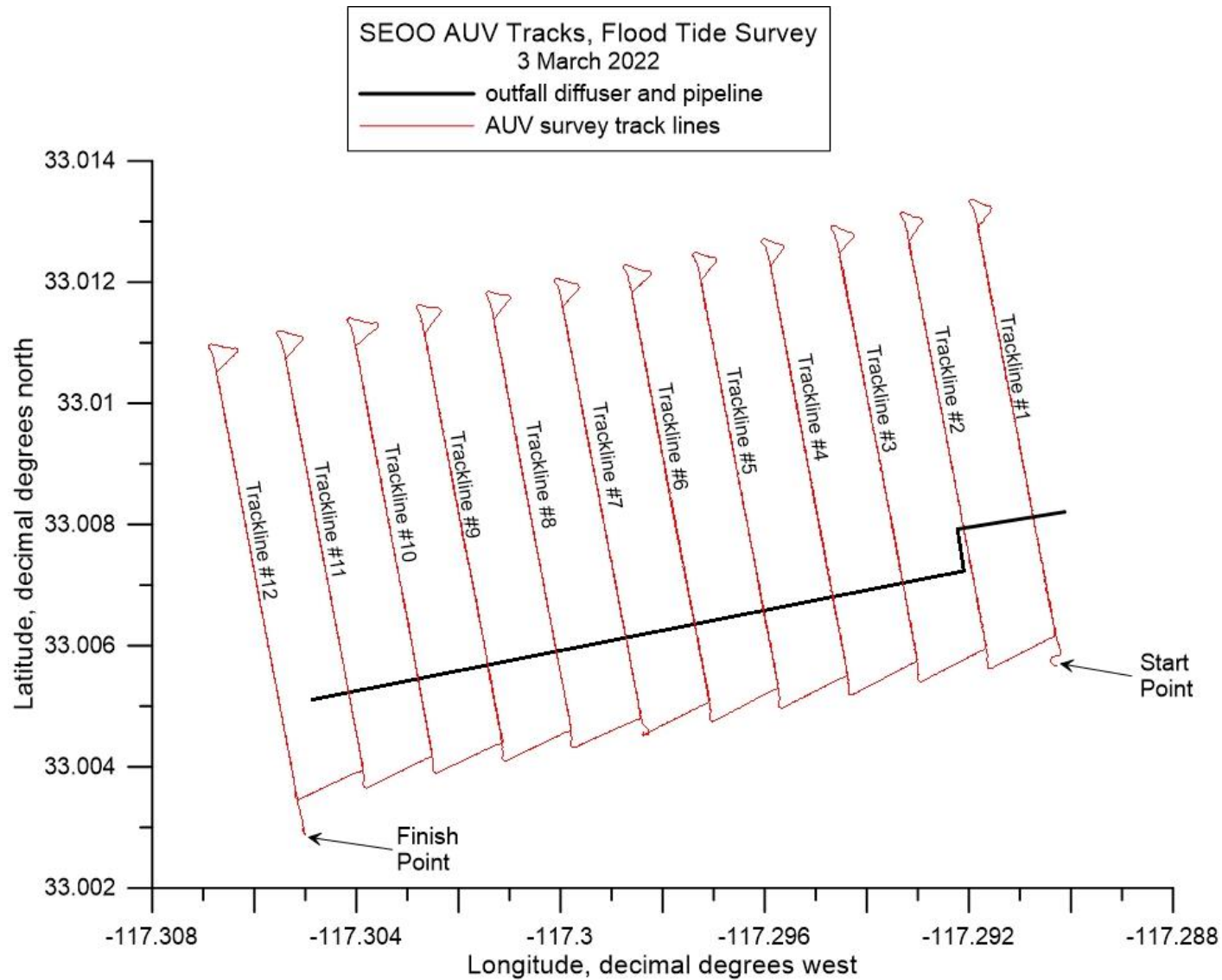


Figure 3.3.14: AUV track lines on 3 March 2022 as flown during flood tide surveys of the discharge plume from SEOO. Note, at 30° N latitude, 1° longitude = 93,453.2 m, while 1° latitude = 110,904.4 m.

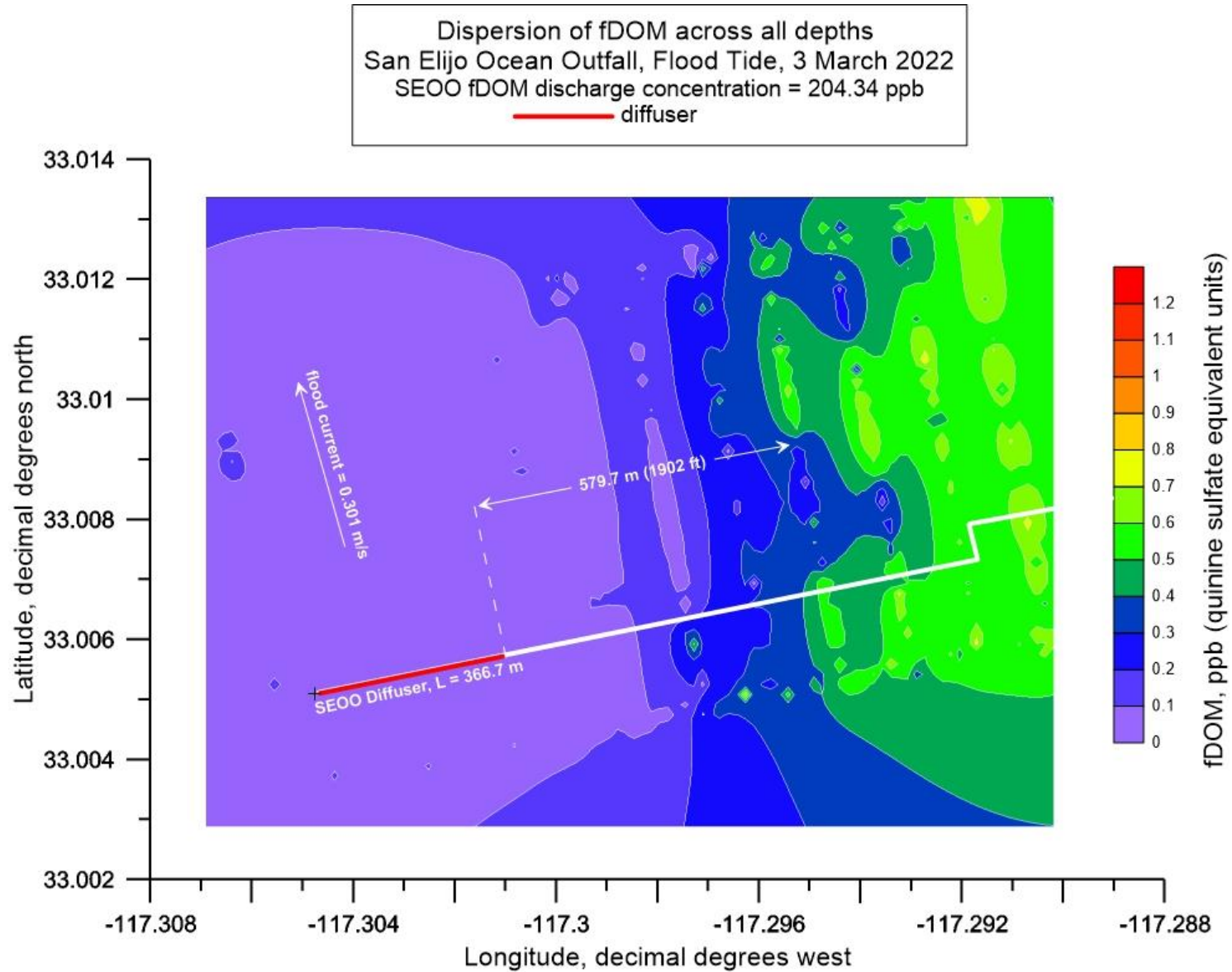


Figure 3.3.15: Full depth contour plot (aka, heat map) of AUV measurements of fDOM from surveys of SEOO during flood tide on 3 March 2022. Average SEOO discharge rate = 11.851 mgd during flood tide; End-of-pipe discharge concentration of fDOM = 204.34 ppb (QSU); End of pipe salinity = 0.71 psu; Trapping level (pycnocline depth) = -26.9 m (-88.3 ft) MSL; Mean flood tide current = 0.301 m/s (0.58 kts) toward the northwest.

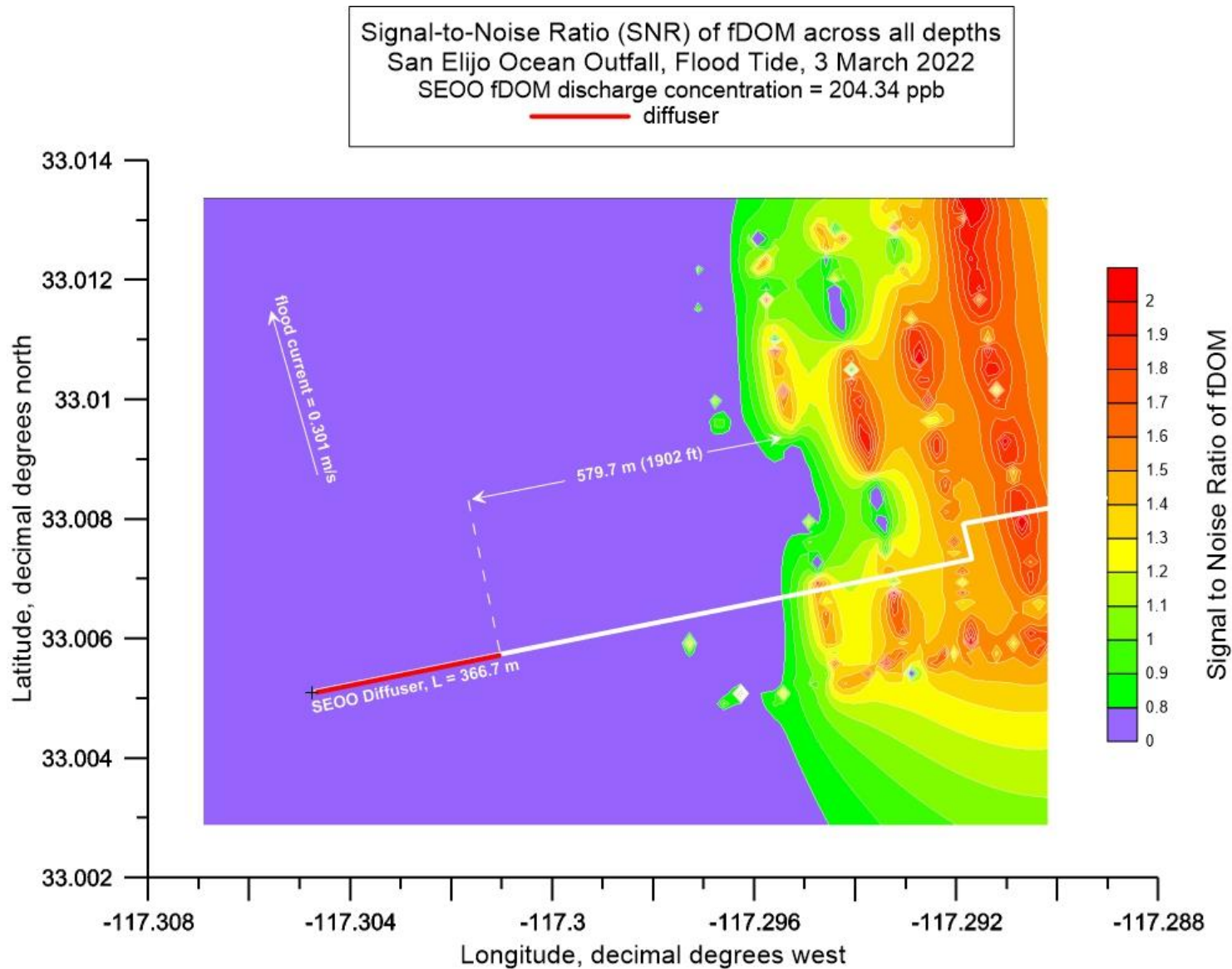


Figure 3.3.16: Full-depth contour plot (aka, heat map) of the signal to noise ratio (SNR) of fDOM during AUV surveys of SEOO during flood tide on 3 March 2022. Average SEOO discharge rate = 11.851 mgd during flood tide; End-of-pipe discharge concentration of fDOM = 204.34 ppb (QSU); End of pipe salinity = 0.71 psu; Trapping level (pycnocline depth) = -26.9 m (-88.3 ft) MSL; Mean flood tide current = 0.301 m/s (0.58 kts) toward the northwest.

the source of the fDOM front, (now located 579.7 m [1,902 ft] shoreward of the shoreward end of the SEOO diffuser during flood tide), that feature is certainly real and satisfies the lowest order significance threshold for detection, (i.e., $SNR_{fDOM} \geq 1$), by a considerable degree. Based on this detection metric, we conclude there is no detectible trace of the EOO plume during flood tide on 3 March 2020, but there is a considerable inshore water mass with elevated fDOM that has a well-defined frontal boundary separating it from the deeper waters surrounding the SEOO diffuser.

To assess whether there is any possibility that the SEOO discharge might be the source of the fDOM front in **Figure 3.3.15**, the SNR_{fDOM} heat map in **Figure 3.3.16** was transposed into a dilution heat map in **Figure 3.3.17** using equation (2) on the basis that the initial fDOM source concentrations in the fDOM front are the same as the fDOM concentrations discharged by the SEOO diffuser, namely: $fDOM_{(x=0)} = 204.34$ ppb. Equation (2) demonstrates that regions of high SNR will correspond to regions of low values of D_{fDOM} relative to the dilution elsewhere within the AUV survey area. **Figure 3.3.17** indicates that the dilution factor (D_m) for the fDOM front would be no less than as $D_{fDOM} = 267:1$ in various places within the core of the fDOM front. The dilution along the outer perimeter of the fDOM front, the dilution ranges from $D_{fDOM} = 1,237:1$ to as much as 40,000:1 along the frontal boundary. Elsewhere in the wake of the SEOO diffuser dilution ranges from $D_{fDOM} = 2,721:1$ to as high as 100,000:1, even 129,503:1. Given that fDOM dilutions are at least 2,721:1 in the nearfield of the diffuser; it would be impossible for dilutions to be as low as 267:1, at a distance of 2,250 ft. from the SEOO, if the SEOO were the source of the fDOM front.

Since fDOM signal to noise and dilution data clearly rule out the SEOO as the possible source of fDOM front discovered by the AUV during flood tide, we examine the possibility that the ebb tide discharges from the San Elijo Lagoon could linger long enough down-coast in the inshore waters to the south and be subsequently advected back up-coast on the ensuing flood tide at concentrations comparable to those discovered by the AUV in **Figure 3.3.15**. There are several considerations that support this hypothesis, including: 1) observations of a red tide at inshore monitoring stations SEOO 60-3N, SEOO 60-2N, and SEOO 60-1N; 2) the CORMIX model results show the lagoon discharge plume extends at least 2 km to the south beyond the SEOO; 3) the lagoon discharge plume contains a huge amount of water, the equivalent of a 768 mgd; 4) the fDOM front had spread further offshore during flood tide and concentrations within the front during AUV survey in **Figure 3.3.15** are roughly 1/3 the concentrations discovered in the fDOM front during the preceding flood tide survey, consistent with dilution occurring in the lagoon discharge plume as it aged between ebb and flood tide; and 5) a significant amount of the lagoon's ebb tide discharge remains in the inshore waters even at the completion of following flood tide event.

Consideration #5 above is supported by the fact that the tidal range in the lagoon during ebb tide on 3 March 2022 was 4.64 ft but was only 3.89 ft during the following flood tide. To determine what effect this disparity in tidal range has on the tidal exchange volume during flood tide, the storage rating curve for the restored San Elijo Lagoon has been annotated in **Figure 3.3.18** for the water elevation changes during flood tide on 3 March 2022. Although flood tide in the ocean began with water levels rising from the daily lower-low water level of -3.27 ft MSL, inshore waters did not begin flowing into the lagoon until the ocean water levels rose above the elevation of the inlet channel sill of the lagoon which is at -1.5 ft. Flood tide ended when ocean water levels reached the daily lower-high water level of + 2.42 ft MSL. During that 6.3 hr long flood tide event, 454 acre ft of inshore waters

flowed back into the lagoon, or an influx equivalent to 563 mgd, as compared to 768 mgd of lagoon water discharged into the nearshore during the preceding ebb tide. Therefore, as much as 205 mgd of lagoon water remained in the inshore waters around the inlet to San Elijo Lagoon by the end of the flood tide event on 3 March 2022. Since the AUV flood tide survey began at the most inshore tacklines near the -60 ft (-18.3 m) MSL depth contour, (i.e., track lines #1 - #4 in [Figure 3.3.14](#)), probably only 151 mgd of inshore water had flowed into the lagoon while the AUV was traversing through the fDOM front, implying that as much as 617 mgd of lagoon water remained in the inshore waters around the inlet to San Elijo Lagoon.

To determine if the fDOM front with its diminished concentrations during flood tide AUV survey on 3 March 2022 could be due to the lingering ebb-tidal discharges from the San Elijo Lagoon, the CORMIX v-11 mixing model was used to simulate the evolution of the residual lagoon discharge plume during the following flood tide. CORMIX v-11 was initialized using the measured flood tide ocean currents ([Figure 3.3.6](#)) and lagoon influx rates derived from the storage rating curve ([Figure 3.3.18](#)) during flood tide on 3 March 2022. Initial conditions on the fDOM source at the beginning of the flood tide simulation were specified from the CORMIX solution of the lagoon's ebb-tide discharge plume in [Figure 3.3.13](#) from the preceding ebb tide. The resulting CORMIX-v11 simulation of the residual San Elijo discharge plume influxing the lagoon during flood is plotted on [Figure 3.3.19](#). The 0.4 ppb isoline of the CORMIX plume follows approximately the frontal boundary of the fDOM front discovered by the AUV during flood tide in [Figure 3.3.15](#), and only a small portion of the frontal boundary of the plume extends about 400 m south along the -60 ft (-18.3 m) MSL depth contour in the vicinity of the dogleg section of the SEOO pipeline. The preponderance of the residual lagoon plume extends northward in the 0.301 m/s (0.58 kts) flood tide current. In the inshore portions the residual San Elijo plume, fDOM concentrations are significantly diminished relative to those in the ebb-tide discharge plume simulation in [Figure 3.3.13](#). Concentrations of fDOM in the inner core of the plume near the lagoon inlet are reduced to 115 ppb from 198 ppb during the preceding discharge cycle. In general, there is significant fidelity between the CORMIX flood tide simulation of the San Elijo Lagoon plume ([Figure 3.3.19](#)) and the measured fDOM front in [Figure 3.3.15](#). This result, in combination with AUV data and observations of an inshore red tide, is strong evidence that the fDOM front, defined by a frontal boundary located 579.7 m (1,902 ft) inshore of the shoreward end of the SEOO diffuser, was not caused by the SEOO, but rather was a signature of the tidal purging of San Elijo Lagoon.

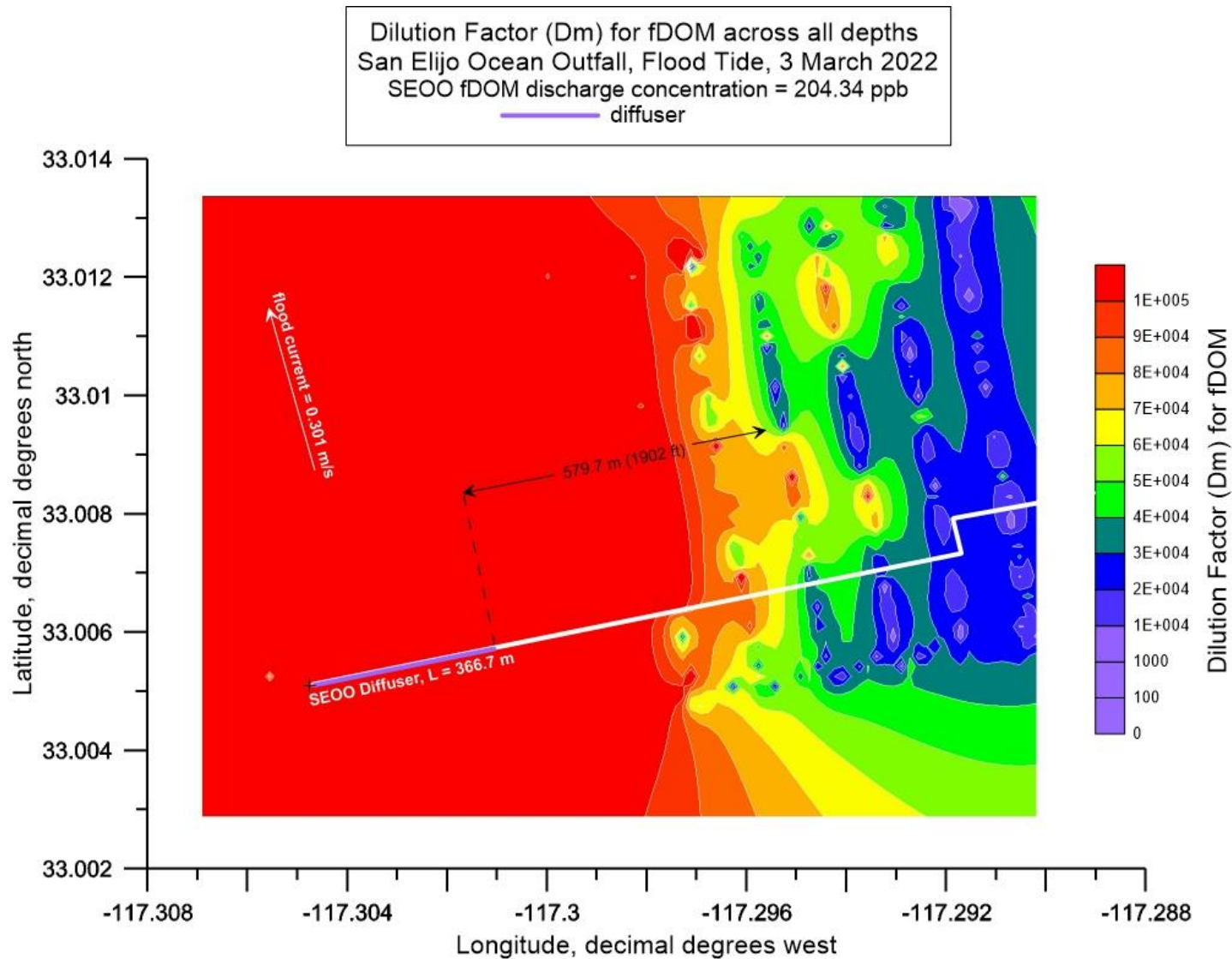


Figure 3.3.17: Full depth contour plot (aka, heat map) of the dilution factor, (D_{fDOM}) of fDOM during AUV surveys of SEOO during flood tide on 3 March 2022. Average SEOO discharge rate = 11.851 mgd during flood tide; End-of-pipe discharge concentration of fDOM = 204.34 ppb (QSU); End of pipe salinity = 0.71 psu; Trapping level (pycnocline depth) = -26.9 m (-88.3 ft) MSL; Mean flood tide current = 0.301 m/s (0.58 kts) toward the northwest.

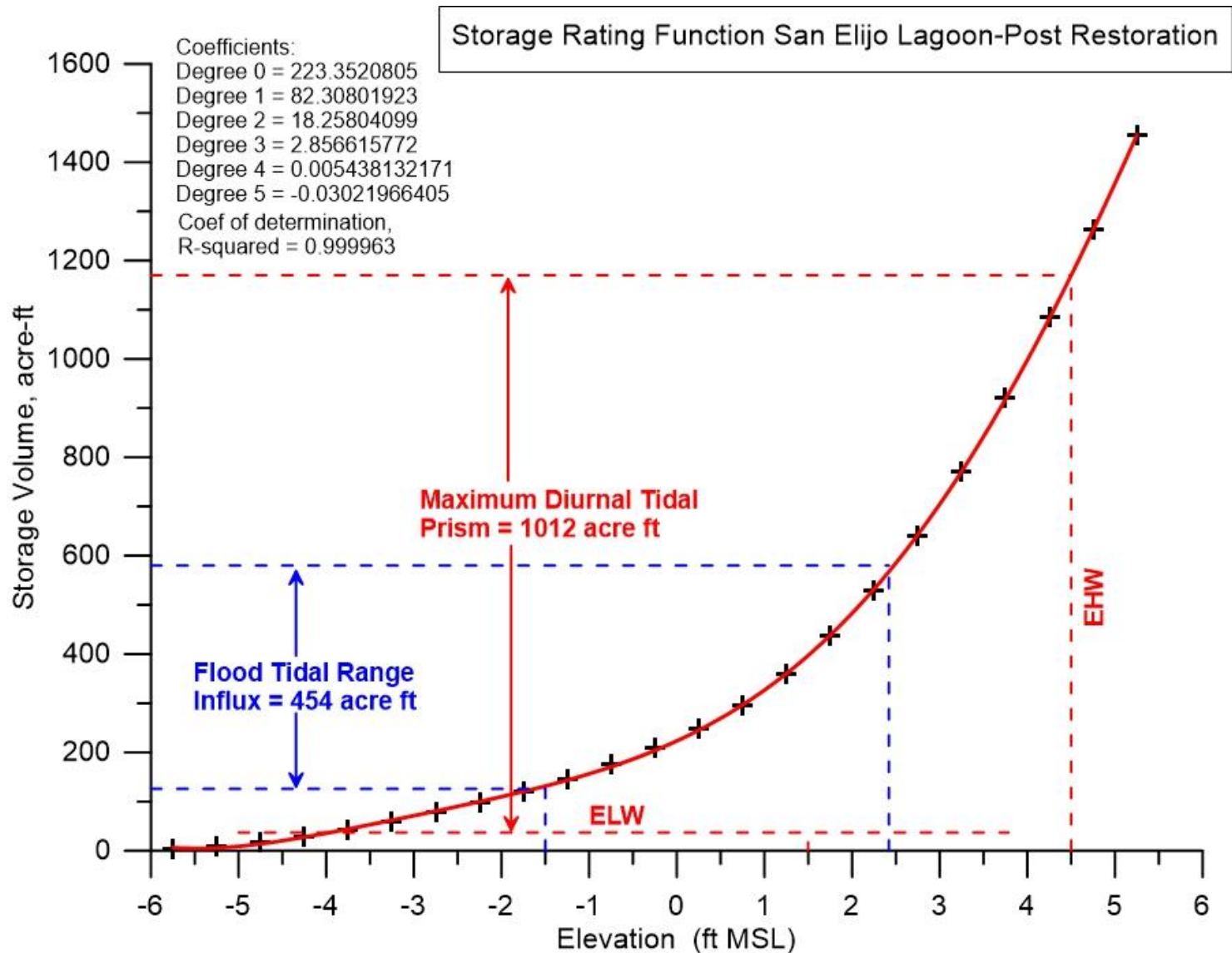


Figure 3.3.18: Storage rating function of the newly restored San Dieguito Lagoon, (cf. AECOM, 2016, “Environmental Impact Report/Environmental Impact Statement for the San Elijo Lagoon Restoration Project”). Annotations in blue designate the tidal range and tidal influx volume from the lagoon during flood tide on 3 March 2022.

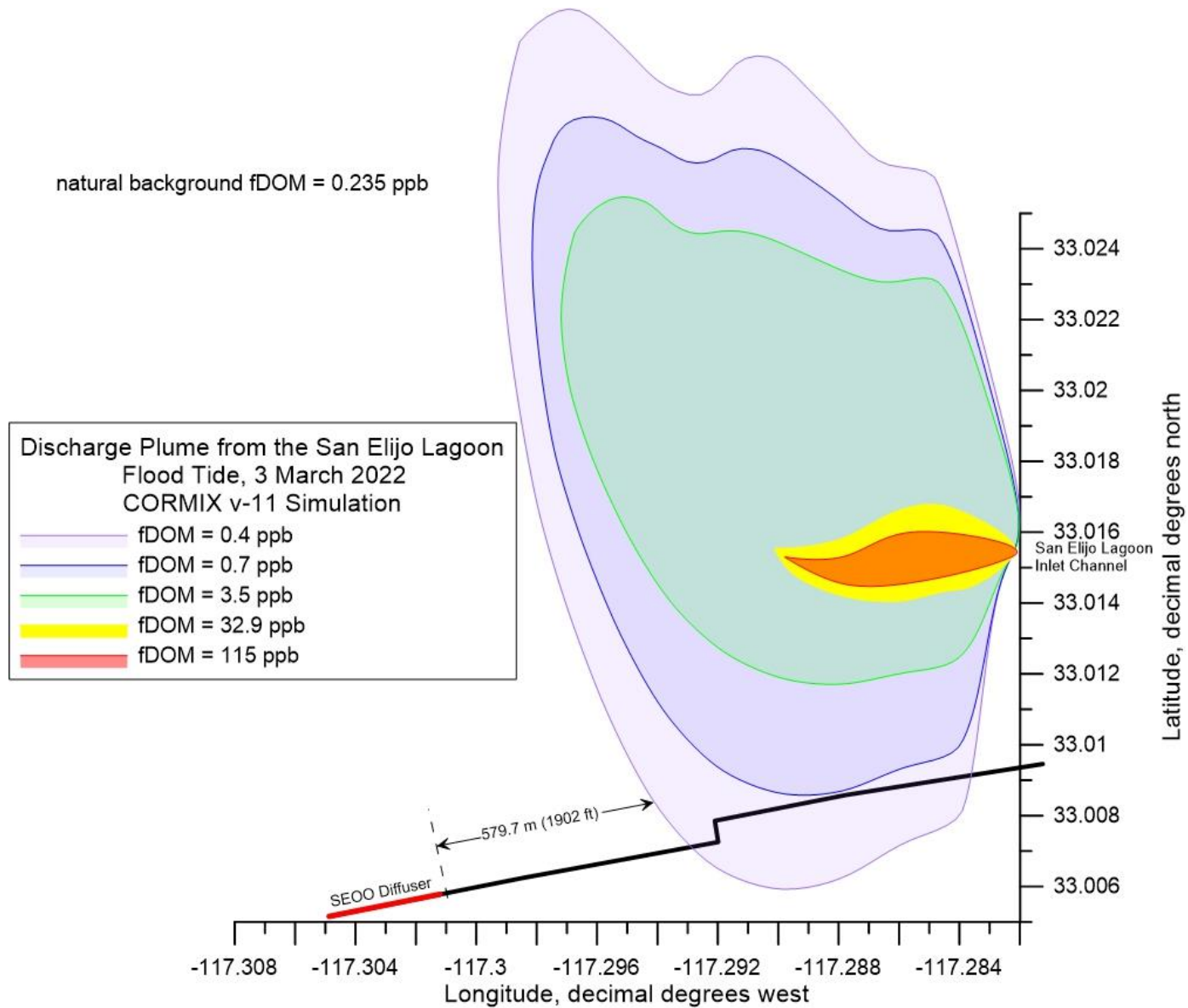


Figure 3.3.19: CORMIX v-11 Simulation of the discharge plume from the San Elijo Lagoon during flood tide on 3 March 2022. Average SEOO discharge rate = 11.851 mgd during flood tide; End-of-pipe discharge concentration of fDOM = 204.34 ppb (QSU); End of pipe salinity = 0.71 psu; Trapping level (pycnocline depth) = -26.9 m (-88.3 ft) MSL; Mean flood tide current = 0.301 m/s (0.58 kts) toward the northwest.

4 NPDES PERMIT DISCUSSION

Based on the June 2020 joint PTMP for the SEOO and EOO, along with plume tracking requirements in the SEOO and EOO NPDES permits (RWQCB Order Nos. R9-2018-0002, R9-2018-0003 and R9-2018-0059), the plume tracking program was intended to address, at minimum, the following questions:

(1) Are the current monitoring locations and methods adequate to determine whether the wastewater plume is encroaching on water recreational areas, including, but not limited to, areas used for swimming, scuba diving, surfing, and fishing? If not, what monitoring locations and/or methods are more appropriate?

Based on the findings of the plume tracking field studies in September 2021, December 2021 and March 2022, the wastewater plumes were never found inshore of the shoreward end of the either the SEOO or the EOO diffusers. What is discharged offshore stays offshore.

The current monitoring stations for the SEOO (cf. [Figure 4.1](#)) and EOO (cf. blue triangles in [Figure 2.3.1](#)) are more than adequate to confirm that the outfall wastewater plumes are encroaching on water recreational areas. No additional monitoring stations are required for that purpose. Further, evidence that the outfall discharges remain offshore is sufficiently strong as to question why shore-based monitoring is required at all. The lack of need for such shore-based bacteriological monitoring as part of the SEOO and EOO NPDES outfall permits is supported by the fact that the existing near-shore SEOO and EOO receiving water monitoring stations (located between the shore and the outfall discharge point) consistently show compliance with Ocean Plan body contact recreational standards. Additionally, elimination of offshore sample locations greater than 2,000 ft from the ocean outfall should be considered, as no evidence of the discharge was recorded greater than 1,082 ft from the SEOO diffuser.

SEOO plume tracking measurements using an AUV never produced evidence of the discharge plume further than 329.8 m (1,082 ft) from the SEOO diffuser in a shore parallel direction. The criteria for plume detection were based on signal detection metrics that require the measurements of a plume tracer that must have a signal to noise ratio of at least unity in order to identify the presence of the plume. As a result, it may be concluded that the SEOO inshore monitoring stations (T, N, and S stations) are best suited for monitoring effects caused by shoreline discharges. In support of this conclusion, the inshore AUV survey plume tracking measurements in March 2022 detected the discharge of the San Elijo Lagoon whose frontal boundary was along the -60 ft. MSL depth contour in the vicinity the N-monitoring stations in [Figure 4.1](#).

EEO plume tracking measurements of fDOM and salinity using AUV sensors never found evidence of the discharge plume further than 669.8 m (2,197 ft) from the EOO diffuser in a shore parallel direction. The plume was never found inshore of the shoreward end of the EOO diffuser. Based on this finding, the present disposition of the NPDES offshore monitoring stations for the EOO (blue triangles in [Figure 2.1.1](#), [Figure 2.2.1](#), and [Figure 2.3.1](#)) appear to be adequate to determine whether the wastewater plume is encroaching on water recreational areas.

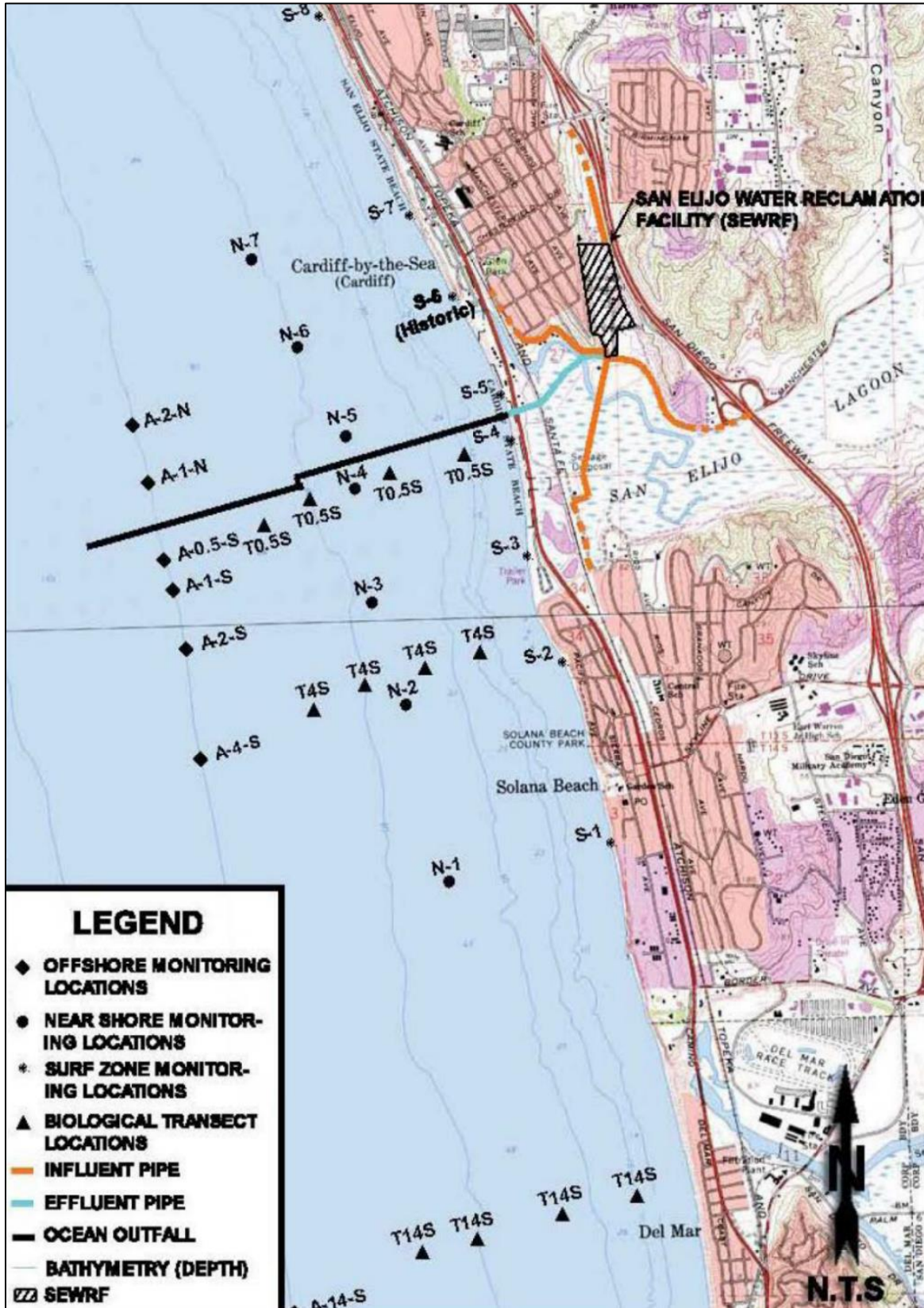


Figure 4.1: NPDES permit monitoring stations for SEOO, per CA0107999; Order Nos. R9-2018-0002 and R9-2018-0003.

(2) Is the removal of the SEOO Surf Zone monitoring location S-6 (historical) still appropriate?

Based on the findings of the plume tracking field studies in September 2021, December 2021 and March 2022, removal of the SEOO Surf Zone monitoring location S-6 (historical) remains appropriate. Further, as documented above, available evidence indicates that the SEOO and EOO discharges remain offshore (carried upcoast/downcoast), and that shore-based discharges remain near the shore (also carried upcoast/downcoast). As a result, SEOO and EOO shore stations appear to be of little use in assessing outfall discharge effects and instead the stations record effects from shore-based sources. Removal of SEOO Surf Zone Station S-6 is appropriate.

(3) How does the brine discharge from the MFRO Facility and San Elijo Water Reclamation Facility and future brine discharges (along with increased recycled water use and decreased outfall discharge flows) affect the dynamics of the wastewater plume and initial dilution?

This question is being further evaluated as part of a SEOO initial dilution study that is being performed pursuant to requirements in Order Nos. R9-2018-0002 and R9-2018-0003. Data developed as part of initial dilution modeling performed in this plume tracking study, however, indicate that brine discharges from the MFRO Facility and San Elijo Water Reclamation Facility will not have a significant impact on the dynamics of the SEOO wastewater plume and initial dilution. Similarly, existing and proposed brine discharges to the EOO are unlikely to discernibly affect initial dilution.

(4) Does the wastewater plume have the potential to interact with wastewater plumes from other ocean outfalls or other sources of pollution, such as storm water and outflows from the San Elijo Lagoon?

Based on the findings of the plume tracking field studies in September 2021, December 2021 and March 2022, the SEOO and EOO wastewater plumes have no potential to interact with each other or with wastewater plumes from other ocean outfalls or other sources of pollution, such as storm water and outflows from the San Elijo Lagoon or Agua Hedionda Lagoon. The plume tracking measurements using an AUV to acquire more than 66,000 measurements of plume tracers (fDOM and salinity) never found evidence of the SEOO discharge plume further than 329.8 m (1,082 ft) from the SEOO diffuser in a shore parallel direction, and no further than 669.8 m (2,197 ft) from the EOO diffuser in a shore parallel direction. At either outfall, the wastewater plumes were never found inshore of the shoreward end of the either the SEOO diffuser or the EOO diffuser. AUV survey plume tracking measurements of fDOM in March 2022 presented convincing evidence of the shore-based discharge of the San Elijo Lagoon, whose frontal boundary was detected 685.9 m (2,250 ft) shoreward of the shoreward end of the SEOO diffuser during ebb tide near the -60 ft. MSL depth contour. The lagoon discharge, however, did not impinge on the SEOO discharge.

(5) What is the fate of the wastewater plume in typical and atypical oceanographic conditions, and when and under what conditions is the wastewater plume no longer distinguishable from ambient receiving water?

The plume tracking field studies in September 2021 were conducted under typical late summer/fall oceanographic conditions when the water column was strongly stratified, forming a two-layer water mass with a well-defined pycnocline at 8 m depth (-26.2 ft. MSL). Ambient background concentrations of fDOM were high, averaging 0.639 ppb to 0.776 ppb. With the high ambient fDOM concentrations under typical summer oceanographic conditions, the discharge plumes of the SEOO and EOO could not be distinguished from the ambient receiving water. Additionally, salinity was found to be useless as a plume tracer due to its low SNR at the point of discharge.

The plume tracking field studies in December 2021 were conducted after the passage of a dry cold front (post-storm conditions that included high winds. At this time, a cold, nearly homogeneous surface layer, (about 6° C cooler than during the first deployment in September 2021) existed down to approximately a 25 m depth, while the bottom layer remained about the same temperature as in September 2021. Consequently, the water column during December 2021 was only weakly stratified (i.e., less stable than in September 2021) and the trapping level rose to within 4 m of the sea surface. However, ambient background concentrations of fDOM were relatively low, averaging 0.294 ppb to 0.310 ppb. Due to the low ambient fDOM concentrations, the discharge plumes of the SEOO and EOO could be easily distinguished from the ambient receiving water with high signal to noise ratios reaching $SNR_{fDOM} \cong 2.46$ in the inner core of the SEOO wastewater plume located 329.8 m (1,082 ft) downstream of the SEOO diffuser in a shore parallel direction; and as high as $SNR_{fDOM} = 3.39$ in the inner core of the EOO wastewater plume, located 393.9 m (1,292 ft) downstream of the EOO diffuser in a shore parallel direction.

The plume tracking field studies in March 2022 were conducted to characterize late winter/early spring conditions. The conditions included a cold bottom layer having temperatures ranging from 11.4° C at the seabed, warming rapidly to 13° C at 3 m above the seabed, and then warming almost linearly to 14.7° C at the sea surface. The salinity reached 33.7 ppt near the seabed, declining to 33.48 ppt at about a depth of -27 m MSL; and then remained nearly constant between -27 m depth and the sea surface. The density profile during the third AUV deployment represented a stable, continuously stratified water column rather than a two-layer system as prevailed during the first and second deployments in September and December 2021. Consequently, the trapping level during March 2022 was deep, at a depth of -26.9 m (-88.26 ft) MSL, which is more typical of a worst-case dilution scenario, because initial dilution is arrested relatively close to the seabed. Nonetheless, ambient background concentrations of fDOM were low averaging 0.170 ppb to 0.279 ppb. In spite of the low ambient background concentrations of fDOM, the discharge remained difficult to distinguish from the ambient receiving water because of strong currents in the presence of an approaching extratropical frontal cyclone from the northwest. Mean currents (on the order of 1 kts) were flowing shore-parallel in combination with transient wave surges as high as 1.53 kts flowing obliquely to the mean current, thereby exposing the wastewater discharges to high velocity shearing rates. This shearing by the ambient currents broke up the wastewater plumes into small fragments. Small plume fragments with signal to noise ratios of $SNR_{fDOM} \cong 2.3$ in the inner core were detected at the EOO, located 669.8 m downstream of the diffuser in a shore parallel direction. No plume fragments could be detected at the SEOO during the March 2022 AUV surveys.

(6) What parameters are most useful for assessing the presence of a wastewater plume?

The AUV deployments indicated that fDOM can be an effective parameter in indicating the possible or probable presence of remnants of the SEOO and EOO discharges. Bacteriological parameters (e.g., fecal coliform and enterococcus) can be combined with fDOM to provide additional evidence of the presence of the discharge plumes.

At present, small, low-power electronic sensors capable of being carried aboard an AUV are only capable of measuring potential plume traces such as salinity and fDOM (the component of colored dissolved organic matter that fluoresces). Salinity was found to be useless as a plume tracer. Signal to noise ratios of salinity measurements during the plume tracking study never exceeded $SNR_S \cong 0.008$. This is due to fact that effluent salinity at the point of discharge is typically about 1 to 1.5 psu, compared with natural background ocean salinity which averages 33.5 psu; so that the signal to noise ratio of salinity at the point of discharge is on the order of $SNR_S \approx 0.96$, less than the threshold of detection by signal detection metrics. On the other hand, effluent fDOM at the point of discharge is typically in the range of 200 to 300 ppb, significantly greater than natural background ocean fDOM which is typically in the range of 1 ppb. Consequently, the signal to noise ratio of fDOM at the point of discharge is typically no less than $SNR_{fDOM} \approx 199$. Signal to noise ratios of fDOM features believed to be the wastewater plume were found to be in the range of $SNR_{fDOM} \cong 2$ to 3. This means the fDOM concentrations of features believed to be the wastewater plume were 3 to 4 times greater than the ambient background fDOM concentrations.

(7) What is the variability in the degree of initial dilution that occurs under typical and atypical oceanographic conditions?

The plume tracking field studies in September 2021 that were conducted under typical late summer oceanographic conditions were unable to detect the wastewater plumes from either the SEOO or the EOO due to high ambient concentrations of fDOM. Therefore, no conclusion could be drawn regarding the degree of initial dilution that occurs under typical late summer oceanographic conditions.

The plume tracking field studies in December 2021 that were conducted under typical dry weather winter oceanographic conditions detected fDOM features of the SEOO wastewater plume having initial dilution ratios as high as 311:1 in the inner core of the plume, or a factor of 1.3 times greater than the minimum month dilution of $D_m = 237:1$ assigned in the current SEOO NPDES permits (Order Nos. R9-2018-0002 and R9-2018-0003). At the EOO initial dilution ratio of the fDOM features of the wastewater plume were no less than as $D_m = 215:1$ in the inner core of the plume, or a factor of 1.5 times greater than the minimum month dilution of $D_m = 144:1$ assigned within the current EOO permit (Order No. RS-2018-0059).

The plume tracking field studies in March 2022 coincided with worst case (maximum trapping depth) oceanographic conditions. The March 2022 field studies were unable to detect the wastewater plume from the SEOO due to high ambient currents and surges that sheared the plume into small undetectable fragments. At the EOO, fDOM-derived dilutions within wastewater plume fragments were at least 477:1 in the core of the plume fragments, or a factor of 3.18 times greater than the minimum month dilution of $D_m = 144:1$ assigned within the EOO NPDES permit (No. Order No. RS-2018-0059).

THIS PAGE INTENTIONALLY LEFT BLANK



5 SUMMARY OF FINDINGS

This project consisted of field studies with supporting dilution modeling to address questions posed in the SEOO/EOO PTMP and NPDES permits. To address these questions, observables of the outfall effluent that were tracked during field studies in September 2021 (1st Deployment), December 2021 (2nd Deployment), and March 2022 (3rd Deployment) included salinity and colored dissolved organic matter (CDOM), and its surrogate fDOM, which is the portion of *colored dissolved organic matter* (CDOM) that fluoresces. Salinity and fDOM were tracked across 459 to 988 acres of ocean surrounding the EOO and SEOO by an Iver3 autonomous underwater vehicle (AUV) supported by 15 to 18 stationary monitoring stations using fDOM sensors, conductivity/ temperature/depth (CTD) sensors and acoustic doppler current profilers (ADCPs). Advantages to sampling the EOO and SEOO with an AUV included the ability to run pre-programmed survey track lines to efficiently cover a large survey area with high density sampling that produces as many as 65,000 to 68,500 separate measurements of fDOM and salinity. These AUV survey results produce high-resolution, three-dimensional data models of the outfall plumes and receiving waters.

Signal detection theory was used to differentiate between the outfall discharge plume and the surrounding ambient water mass. Plume detectability was approached as a signal-to-noise problem which is measured by the signal to noise ratio, SNR ; where the noise is the ambient (aka, *natural ocean background*) concentrations of salinity or fDOM; and the signal is the difference between the ambient concentrations of salinity or fDOM and the measured concentrations of salinity or fDOM. Signal detection theory teaches that the lowest order significance threshold for detection arises when $SNR \geq 1$.

During the first AUV deployments (21-23 September 2021), natural ocean background levels of fDOM were somewhat elevated in the range of 0.64 parts per billion (ppb) to 0.77 ppb due to high biological activity in warm water during the long summer days. With these high ambient fDOM concentrations, the highest signal to noise ratio of any fDOM feature anywhere in the 988.4 acres of ocean water mass surveyed around the SEOO was only a $SNR_{fDOM} \cong 0.68$ to 0.70, which does not meet the lowest order significance threshold for detection, namely $SNR_{fDOM} \geq 1$. Because of the high natural receiving water concentrations of fDOM during this September 2021 deployment, SNR_{fDOM} ratios were insufficient to detect or reliably discern remnants of either the SEOO discharge plumes. However, the EOO was discharging about 2.5 times more effluent than the SEOO, and signal to noise ratios in the 988.4 acres of ocean water mass surveyed around the EOO reached $1.0 \leq SNR_{fDOM} \leq 1.5$ in several small plume remnants located between 33 m and 588 m of the downstream side of the EOO diffuser. Dilution factors in these plume remnants were no less than 260:1, or about 80.5% higher than the assigned minimum month dilution of $D_m = 144:1$ established in the current NPDES permit for the EOO (No. CA0107395; Order No. RS-2018-0059).

Based on fDOM patterns measured during the first AUV deployments, the resolution of the survey pattern was increased by a factor of 2.4. This was accomplished by reducing the distance between survey track lines and increasing the number of track lines from 5 to 12. However, because the battery capacity of the Iver3 AUV limited the total distance traveled to about 20 km, the length of each track line was reduced resulting in a reduction of the total area surveyed from 998.4 acres to 494.2 acres. The second AUV deployments 20-21 December 2021 occurred after passage of a dry cold front that brought strong onshore winds the week prior. Natural ocean background levels of fDOM dropped to only about 0.3 ppb. With

these reduced background fDOM concentrations, singular, large fDOM features were discovered 268 meters (m) to 394 m down-drift in the shore parallel direction from both the EOO and SEOO diffusers. The signal to noise ratios of these fDOM features ranged from $SNR_{fDOM} \cong 1.2$ along the outer perimeter of the suspected plume remnants, to as high as $SNR_{fDOM} \cong 3$ in the inner core of the suspected plume remnants, thereby readily satisfying the lowest order significance threshold for detection, (i.e., $SNR_{fDOM} \geq 1$). Based on this detection metric, we conclude remnants of the EOO and SEOO discharge plumes had been discovered. Due to the relatively small variation between discharge salinity and ocean background salinity, it was learned that salinity is an unsatisfactory tracer of the plumes because it always produced signal to noise ratios several orders of magnitude less than unity.

The probable detection of discharge remnants during the December 2021 fDOM surveys (located several hundred meters down-drift from the EOO and SEOO in the shore parallel direction) prompted the question of how much additional dilution had occurred within these remnants after the completion of initial dilution. The initial approach to this question involved performing initial dilution simulations with Plumes 20 (UM3) using the actual ambient currents on 20-21 December 2021. Under these conditions, the simulated initial dilution for the EOO was in excess of 310:1, while the initial dilution for the SEOO was simulated at more than 390:1. In concert with these dilution simulations the plume tracking study of the EOO and SEOO discharges on 20-21 December 2021 indicates that the discharge plume from each outfall can be detectable a couple of hundred meters beyond the point where initial dilution is complete. Dilution ratios associated with such suspected plume remnants, however, are high and range from $D_{fDOM} = 766:1$ and greater at the SEOO to $D_{fDOM} = 638:1$ and greater at the EOO.

The third AUV deployments at the SEOO and EOO on 2-3 March 2022 utilized a slightly modified AUV survey pattern having the same horizontal resolution as that used during the second deployments but included 100 m of overlap between the ebb-tide and flood-tide survey boxes in the long-shore direction in order to increase resolution of any suspected plume remnants found close to the outfall diffusers. This overlap reduced the total area surveyed during the third deployments to 459.3 acres. The third AUV deployments occurred about 32 hours prior to the arrival of an extratropical frontal cyclone, approaching from the northwest that generated strong southward flowing wind-driven currents, which when combined with tidal currents and wave surges produced strong velocity shear across the plumes, causing them to break up into small fragments. Furthermore, the water column exhibited strong, continuous, stable stratification between the sea surface and the seabed, resulting in a deep trapping level that arrested initial dilution at a relatively short distance above the seabed. However, ambient fDOM background concentrations were low, ranging between 0.170 ppb and 0.279 ppb during the third deployments, favoring detection of any plume fragments that survived in the strong current shear. However, the plume was not detectable at the SEOO and only small fragments of a plume were found at the EOO that were located 332 m to 670 m down-drift from the EOO diffuser in the shore parallel direction. Minimum dilution ratios in these plume fragments were never less than $D_{fDOM} = 477:1$ in the core of the EOO plume fragments discovered on 2 March 2022, which is a factor of 3.18 times greater than the minimum month initial dilution assigned in the current NPDES permit for the EOO (Order No. R9-2018-0059).

The most obvious feature evident within the 459.3 acres surveyed around the SEOO was the ebb-tide discharge plume from the San Elijo Lagoon. The fDOM feature identified as a tidal purge from the lagoon was substantial, comprised of 14,000 to 15,000 separate fDOM measurements with a sharp frontal

boundary located 579 m to 686 m inshore of the shoreward end of the SEOO diffuser. The conclusion that the source of the fDOM front was ebb tide discharges from the San Elijo Lagoon was verified by CORMIX v-11 simulations of shoreline discharges at the location of the inlet to San Elijo Lagoon and supported by field observations of a red tide located inshore, beginning along the -60 ft depth contour.

THIS PAGE INTENTIONALLY LEFT BLANK

6 CONCLUSIONS

Based on the three (3) AUV deployment field studies and supporting dilution modeling of discharges from the SEOO during summer, winter, and early spring oceanographic conditions, the resultant conclusions are provided below:

- The existing SEOO diffuser system is very effective in mixing the discharge water with ambient ocean water, ensuring the dispersion of the discharge. SEOO dilutions estimated using fDOM are consistently and significantly greater than the minimum monthly initial dilution assigned in Order No. R9-2018-0003.
- The presence of a SEOO plume could not be confirmed in two of the three deployments around the outfall. When detected, the presence of small pockets of the diluted SEOO discharge were only detectable using the sensitive parameter fDOM and were confined to within a few hundred meters (a thousand feet) down current from the SEOO diffuser.
- The SEOO discharge stays offshore and moves parallel to the shoreline. No significant net onshore movement of discharged water occurs. Effects of the SEOO discharge are not observed beyond several hundred feet inshore of the SEOO diffuser and the SEOO discharge has no potential to impact water quality in nearshore and surf zone waters.
- Shore based discharges stay onshore and do not mix with offshore discharges. Tidal exchanges within the San Elijo Lagoon are significant in volume and represent the most significant shore-based flow element affecting nearshore waters inshore from the SEOO. Shore sample stations are useful for detecting effects of shore-based discharges (such as tidal exchange flows from San Elijo Lagoon) but are not useful for monitoring offshore discharges.
- Conductivity, temperature, and salinity cannot be used to track the SEOO plume due to the efficiency of the diffuser and rapid dilution, but they represent valuable parameters for estimating plume trapping depths due to stratification.
- fDOM may be used as an indicator of SEOO plume presence providing that the signal-to-noise ratio is considered due to the variation of background fDOM naturally occurring in the ocean, but the presence of fDOM by itself is not proof of the presence of the outfall discharge.
- The offshore sample locations more than 4,000 feet from the SEOO are too remote from the SEOO to be of use in assessing the outfall-related effects, but stations 4,000 feet from the SEOO may represent valuable reference stations for background data.
- This plume tracking study effectively answered the questions that were outlined in Order No. 2018-0003 and no further effort is required.

Based on the three (3) AUV deployment field studies and supporting dilution modeling of discharges from the EOO during summer, winter, and early spring oceanographic conditions, the resultant conclusions are provided below:

- The existing EOO diffuser system is very effective in mixing the discharge water with ambient ocean water, ensuring the dispersion of the discharge. EOO dilutions estimated using fDOM are consistently and significantly greater than the minimum monthly initial dilution assigned in Order No. R9-2018-0059.



- The presence of a EOO plume could not be confirmed in one of the three deployments around the outfall. When detected, the presence of patches of the diluted EOO discharge were only detectable using the sensitive parameter fDOM and were confined to within a few hundred meters (a thousand feet) down current from the EOO diffuser.
- The EOO discharge stays offshore and moves parallel to the shoreline. No significant net onshore movement of discharged water occurs. Effects of the EOO discharge are not observed beyond several hundred feet inshore of the EOO diffuser and the EOO discharge has no potential to impact water quality in nearshore and surf zone waters.
- Shore based discharges stay onshore and do not mix with offshore discharges. Tidal exchanges within the Agua Hedionda and Batiquitos Lagoons are significant in volume and represent the most significant shore-based flow element affecting nearshore waters inshore from the EOO. Shore sample stations are useful for detecting effects of shore-based discharges (such as tidal exchange flows from Agua Hedionda and Batiquitos Lagoons) but are not useful for monitoring offshore discharges.
- Conductivity, temperature, and salinity cannot be used to track the EOO plume due to the efficiency of the diffuser and rapid dilution, but they represent valuable parameters for estimating plume trapping depths due to stratification.
- fDOM may be used as an indicator of EOO plume presence providing that the signal-to-noise ratio is considered due to the variation of background fDOM naturally occurring in the ocean, but the presence of fDOM by itself is not proof of the presence of the outfall discharge.
- The offshore sample locations more than 4,000 feet from the EOO are too remote from the EOO to be of use in assessing the outfall-related effects, but stations 4,000 feet from the EOO may represent valuable reference stations for background data.

7 REFERENCES

- Baumgartner, D. J., Frick, W. E., and Roberts, P. J. W., 1994. "Dilution Models for Effluent Discharges (Third Edition)." U.S. Environmental Protection Agency, Office of Research and Development, EPA/600/R-94/086
- Coble, P. 2007, "Marine Optical Biogeochemistry: The Chemistry of Ocean Color". *Chemical Reviews*. Vol. 107 No. 2, p 402–418. doi:10.1021/cr050350
- AECOM, 2016, "Environmental Impact Report/Environmental Impact Statement for the San Elijo Lagoon Restoration Project" Final: SCH #2011111013, Prepared for: U.S. Army Corps of Engineers, and County of San Diego Department of Parks and Recreation, 894 pp.
- Frick, W.E., Roberts, P., Davis, L., Keyes, J., Baumgartner, D., George, K., 2003, "Dilution models for effluent discharges, Forth Addition," U.S. Environmental Protection Agency, Standards and Applied Science Division Office of Science and Technology, 148 pp
- Frick, W.E., Roberts, P., Davis, L., Keyes, J., Baumgartner, D., George, K., 2003, "Dilution models for effluent discharges, Forth Addition", U.S. Environmental Protection Agency, Standards and Applied Science Division Office of Science and Technology, 148 pp.
- Frick, W., Ahmed, A., George, K., Laputz, A., Pelletie, G., and Roberts, P., 2010. "On Visual Plumes and Associated Applications." MWW 2010 6th International Conference on Marine Waste Water Discharges and Coastal Environment, C. Avanzini, ed. Langkawi, Malaysia
- Peterson, W.; Birdsall, T.; Fox, W., 1954, "The theory of signal detectability." *Transactions of the IRE Professional Group on Information Theory*. 4 (4): 171-212. doi:10.1109/TIT.1954.1057460.
- RWQCB, 2005, *Waste Discharge Requirements for the San Elijo Joint Powers Authority, San Elijo Water Reclamation Facility Discharge to the Pacific Ocean via the San Elijo Ocean Outfall, NPDES No. CA0107999; Order No. R9-2005-0100*, California Regional Water Quality Control Board, San Diego Region, 108 pp.
- RWQCB, 2018, *Waste Discharge Requirements for the City of Escondido Hale Avenue Resources Recovery Facility and Membrane Filtration/Reverse Osmosis Facility Discharge to the Pacific Ocean through the San Elijo Ocean Outfall, NPDES No. CA0107981; Order No. R9-2018-0002*, California Regional Water Quality Control Board, San Diego Region, 146 pp.
- RWQCB, 2018, *Waste Discharge Requirements for the Encina Wastewater Authority Encina Water Pollution Control Facility and Satellite Wastewater Treatment Plants Discharge to the Pacific Ocean through the Encina Ocean Outfall, NPDES No. CA0107395; Order No. RS-2018-0059*, California Regional Water Quality Control Board, San Diego Region, 147 pp.
- RWQCB, 2018, *Waste Discharge Requirements for the San Elijo Joint Powers Authority, San Elijo Water Reclamation Facility Discharge to the Pacific Ocean through the San Elijo Ocean Outfall, NPDES No. CA0107999; Order No. R9-2018-0003*, California Regional Water Quality Control Board, San Diego Region, 132 pp.
- San Elijo Joint Powers Authority, City of Escondido and Encina Wastewater Authority, 2020, *Plume Tracking Monitoring Plan, San Elijo Ocean Outfall, Encina Ocean Outfall*. 39 pp.
- Schonhoff, T.A. and Giordano, A.A., 2006, *Detection and Estimation Theory and Its Applications*. New Jersey: Pearson Education, ISBN 0-13-089499-0.

Stanislaw, Harold; Todorov, Natasha, 1999, "Calculation of signal detection theory measures". *Behavior Research Methods, Instruments, & Computers*. 31 (1): 137–149. [doi:10.3758/BF03207704](https://doi.org/10.3758/BF03207704)

SWRCB, 2019, State Water Resources Control Board. California Ocean Plan, *Water Quality Control Plan, Ocean Waters of California*, 117 pp.

**APPENDIX-A:
Discharge Logs
for the EOO
on 21 September,
20 December 2021,
and 2 March 2022**

THIS PAGE INTENTIONALLY LEFT BLANK

EOO Discharge Log – 21 September 2021

Date	Quantity (MGD)	Date	Quantity (MGD)	Date	Quantity (MGD)
09/21/2021 12:00:00 AM	13.620	09/21/2021 10:45:00 AM	23.336	09/21/2021 10:00:00 PM	24.904
09/21/2021 12:15:00 AM	12.255	09/21/2021 11:00:00 AM	24.176	09/21/2021 10:15:00 PM	23.393
09/21/2021 12:30:00 AM	11.250	09/21/2021 11:15:00 AM	22.121	09/21/2021 10:30:00 PM	13.549
09/21/2021 12:45:00 AM	11.010	09/21/2021 11:30:00 AM	22.774	09/21/2021 10:45:00 PM	13.245
09/21/2021 1:00:00 AM	10.421	09/21/2021 11:45:00 AM	22.496	09/21/2021 11:00:00 PM	17.111
09/21/2021 1:15:00 AM	9.266	09/21/2021 12:00:00 PM	21.716	09/21/2021 11:15:00 PM	21.308
09/21/2021 1:30:00 AM	8.265	09/21/2021 12:15:00 PM	21.529	09/21/2021 11:30:00 PM	19.714
09/21/2021 1:45:00 AM	7.590	09/21/2021 1:00:00 PM	19.241	09/21/2021 11:45:00 PM	17.453
09/21/2021 2:00:00 AM	11.805	09/21/2021 1:15:00 PM	20.501	09/22/2021 12:00:00 AM	16.448
09/21/2021 2:15:00 AM	11.501	09/21/2021 1:30:00 PM	17.636	09/22/2021 12:15:00 AM	16.823
09/21/2021 2:30:00 AM	11.456	09/21/2021 1:45:00 PM	19.451	09/22/2021 12:30:00 AM	18.829
09/21/2021 2:45:00 AM	9.589	09/21/2021 2:00:00 PM	20.276	09/22/2021 12:45:00 AM	18.979
09/21/2021 3:00:00 AM	9.615	09/21/2021 2:15:00 PM	24.446	09/22/2021 1:00:00 AM	19.185
09/21/2021 3:15:00 AM	8.175	09/21/2021 2:30:00 PM	23.783	09/22/2021 1:15:00 AM	14.213
09/21/2021 3:30:00 AM	9.630	09/21/2021 2:45:00 PM	23.633	09/22/2021 1:30:00 AM	12.465
09/21/2021 3:45:00 AM	8.085	09/21/2021 3:00:00 PM	23.040	09/22/2021 1:45:00 AM	14.749
09/21/2021 4:00:00 AM	7.609	09/21/2021 3:15:00 PM	24.000	09/22/2021 2:00:00 AM	14.749
09/21/2021 4:15:00 AM	8.756	09/21/2021 3:30:00 PM	16.841	09/22/2021 2:15:00 AM	16.706
09/21/2021 4:30:00 AM	11.029	09/21/2021 3:45:00 PM	16.290	09/22/2021 2:30:00 AM	16.215
09/21/2021 4:45:00 AM	12.581	09/21/2021 4:00:00 PM	17.198	09/22/2021 3:15:00 AM	15.739
09/21/2021 5:00:00 AM	10.616	09/21/2021 4:15:00 PM	17.055	09/22/2021 3:30:00 AM	17.404
09/21/2021 5:15:00 AM	11.974	09/21/2021 4:30:00 PM	15.964	09/22/2021 3:45:00 AM	18.015
09/21/2021 5:30:00 AM	12.675	09/21/2021 4:45:00 PM	17.505	09/22/2021 4:00:00 AM	17.655
09/21/2021 5:45:00 AM	12.761	09/21/2021 5:00:00 PM	16.894	09/22/2021 4:15:00 AM	17.355
09/21/2021 6:00:00 AM	11.850	09/21/2021 5:15:00 PM	16.575	09/22/2021 4:30:00 AM	16.305
09/21/2021 6:15:00 AM	13.676	09/21/2021 5:30:00 PM	15.923	09/22/2021 4:45:00 AM	15.251
09/21/2021 6:30:00 AM	12.011	09/21/2021 5:45:00 PM	16.350	09/22/2021 5:00:00 AM	13.530
09/21/2021 6:45:00 AM	11.978	09/21/2021 6:00:00 PM	18.236	09/22/2021 5:15:00 AM	12.244
09/21/2021 7:00:00 AM	13.361	09/21/2021 6:15:00 PM	17.565	09/22/2021 5:30:00 AM	11.490
09/21/2021 7:15:00 AM	16.751	09/21/2021 6:30:00 PM	18.998	09/22/2021 5:45:00 AM	12.514
09/21/2021 7:30:00 AM	13.714	09/21/2021 6:45:00 PM	18.926	09/22/2021 6:00:00 AM	11.314
09/21/2021 7:45:00 AM	11.396	09/21/2021 7:00:00 PM	19.451	09/22/2021 6:15:00 AM	13.781
09/21/2021 8:00:00 AM	14.955	09/21/2021 7:15:00 PM	20.932	09/22/2021 6:30:00 AM	13.838
09/21/2021 8:15:00 AM	16.080	09/21/2021 7:30:00 PM	20.993	09/22/2021 6:45:00 AM	11.558
09/21/2021 8:30:00 AM	18.731	09/21/2021 7:45:00 PM	22.057	09/22/2021 7:00:00 AM	8.381
09/21/2021 8:45:00 AM	22.316	09/21/2021 8:00:00 PM	22.838	09/22/2021 7:15:00 AM	7.905
09/21/2021 9:00:00 AM	24.341	09/21/2021 8:15:00 PM	23.839	09/22/2021 7:30:00 AM	9.705
09/21/2021 9:15:00 AM	24.525	09/21/2021 8:30:00 PM	24.124	09/22/2021 7:45:00 AM	10.766
09/21/2021 9:30:00 AM	25.384	09/21/2021 8:45:00 PM	25.125	09/22/2021 8:00:00 AM	15.270
09/21/2021 9:45:00 AM	23.801	09/21/2021 9:00:00 PM	25.613	09/22/2021 8:15:00 AM	17.936
09/21/2021 10:00:00 AM	23.505	09/21/2021 9:15:00 PM	24.248	09/22/2021 8:30:00 AM	19.275
09/21/2021 10:15:00 AM	24.037	09/21/2021 9:30:00 PM	26.318		
09/21/2021 10:30:00 AM	24.037	09/21/2021 9:45:00 PM	26.055		

Discharge of fDOM from EOO, 21-22 September 2021

Date	Time	fDOM (ppb)	Temperature °C	Salinity (psu)	conductivity (µS/cm)
21-Sep-21	0800	228.26	23.8	0.81	1616
	0900	246.16	23.4	0.81	1611
	1000	250.9	23.10	0.81	1613
	1100	245.6	23	0.81	1616
	1200	246.8	23	0.82	1615
	1300	245.10	23	0.82	1629
	1400	240.67	22.9	0.83	1649
	1500	233.49	22.9	0.86	1695
	1600	239.53	22.9	0.89	1753
	1700	247.40	22.8	0.89	1765
	1800	253.22	22.9	0.89	1759
	1900	264.5	22.9	0.89	1757
	2000	266.73	23	0.89	1763
22-Sep-21	2100	267.6	23	0.89	1767
	2200	268.32	23.1	0.89	1758
	2300	264.61	23.2	0.88	1746
	0000	263.05	23.1	0.88	1736
	0100	257.16	23.4	0.87	1725
	0200	254.78	23.50	0.87	1716
	0300	248.49	23.7	0.86	1700
	0400	245.57	23.9	0.85	1684
	0500	238.58	24	0.84	1666
	0600	227.84	24.2	0.83	1653
	0700	224.62	24.1	0.83	1644
	Average	248.71	23.28	0.85	1693
	SD	12.97	0.44	0.03	59
	Min	224.62	22.8	0.81	1611
	Max	268.32	24.2	0.89	1767

EOO Discharge Rates – 20 December 2021

Date	QUANTITY (MGD)	Date	QUANTITY (MGD)
12/20/2021 12:00:00 AM	20.578125	12/21/2021 3:00:00 AM	17.854687
12/20/2021 1:00:00 AM	21.015938	12/21/2021 4:00:00 AM	19.891876
12/20/2021 2:00:00 AM	18.33375	12/21/2021 5:00:00 AM	19.772812
12/20/2021 3:00:00 AM	16.543125	12/21/2021 6:00:00 AM	18.980625
12/20/2021 4:00:00 AM	18.478125	12/21/2021 7:00:00 AM	14.595938
12/20/2021 5:00:00 AM	18.022501	12/21/2021 8:00:00 AM	21.876562
12/20/2021 6:00:00 AM	15.207188	12/21/2021 9:00:00 AM	28.0125
12/20/2021 7:00:00 AM	14.000625	12/21/2021 10:00:00 AM	30.504375
12/20/2021 8:00:00 AM	22.632187	12/21/2021 11:00:00 AM	27.868126
12/20/2021 9:00:00 AM	28.65	12/21/2021 12:00:00 PM	26.83125
12/20/2021 10:00:00 AM	31.95375	12/21/2021 1:00:00 PM	24.883125
12/20/2021 11:00:00 AM	33.023438	12/21/2021 2:00:00 PM	23.762814
12/20/2021 12:00:00 PM	33.419064	12/21/2021 3:00:00 PM	21.938438
12/20/2021 1:00:00 PM	31.15875	12/21/2021 4:00:00 PM	24.13875
12/20/2021 2:00:00 PM	30.023438	12/21/2021 5:00:00 PM	25.054688
12/20/2021 3:00:00 PM	22.254375	12/21/2021 6:00:00 PM	27.2025
12/20/2021 4:00:00 PM	20.4375	12/21/2021 7:00:00 PM	28.355625
12/20/2021 5:00:00 PM	21.250313	12/21/2021 8:00:00 PM	29.744062
12/20/2021 6:00:00 PM	23.210625	12/21/2021 9:00:00 PM	30.442501
12/20/2021 7:00:00 PM	24.36375	12/21/2021 10:00:00 PM	29.951248
12/20/2021 8:00:00 PM	27.305624	12/21/2021 11:00:00 PM	28.209375
12/20/2021 9:00:00 PM	27.396563	12/22/2021 12:00:00 AM	24.414375
12/20/2021 10:00:00 PM	26.460938	12/22/2021 1:00:00 AM	20.62875
12/20/2021 11:00:00 PM	23.541563	12/22/2021 2:00:00 AM	18.695625
12/21/2021 12:00:00 AM	22.035	12/22/2021 7:00:00 AM	10.47375
12/21/2021 1:00:00 AM	23.145939	12/22/2021 8:00:00 AM	18.681562
12/21/2021 2:00:00 AM	20.548124		

Discharge of fDOM from EOO, 21-22 December 2021

Date	Time	CDOM (ppb)	Temperature °C	Salinity psu	Conductivity (µS/cm)
21-Dec-21	0830	167.68	13.76	0.79	1574
	0930	199.69	10.36	0.78	1552
	1030	149.44	8.67	0.77	1539
	1130	122.47	8.49	0.82	1620
	1230	221.37	8.41	0.82	16.27
	1330	197.47	8.36	0.81	1617
	1430	159.37	8.3	0.84	1670
	1530	224.89	8.95	0.87	1727
	1630	232.64	9.16	0.87	1728
	1730	213.26	8.68	0.87	1729
	1830	254.51	8.52	0.87	1731
	1930	255.39	8.55	0.87	1722
	2030	236.19	8.8	0.86	1707
	2130	244.97	8.76	0.86	1699
22-Dec-21	2230	257.34	8.84	0.86	1703
	2330	256.29	8.8	0.86	1702
	0030	252.22	8.93	0.86	1704
	0130	235.82	8.96	0.86	1707
	0230	236.57	8.88	0.86	1698
	0330	218.22	9.06	0.85	1683
	0430	231.23	8.96	0.84	1674
	0530	228.7	8.59	0.84	1665
	0630	211.21	8.66	0.83	1652
	0730	223.15	8.75	0.83	1647
		Average	217.50	9.01	0.84
	SD	37.21	1.09	0.03	56
	Min	112.47	8.3	0.77	1539
	Max	257.34	13.76	0.87	1731

Wastewater Discharge Rates from the EOO, 1-3 March 2022
Encina_EE1

Date	QUANTITY (MGD)	Date	QUANTITY (MGD)
03/01/2022 12:00:00 AM	20.315624	03/02/2022 1:00:00 PM	26.265938
03/01/2022 1:00:00 AM	16.112812	03/02/2022 2:00:00 PM	26.019375
03/01/2022 2:00:00 AM	11.697187	03/02/2022 3:00:00 PM	24.165937
03/01/2022 3:00:00 AM	10.110937	03/02/2022 4:00:00 PM	24.19125
03/01/2022 4:00:00 AM	9.16875	03/02/2022 5:00:00 PM	24.015
03/01/2022 5:00:00 AM	8.551875	03/02/2022 6:00:00 PM	25.549686
03/01/2022 6:00:00 AM	8.644688	03/02/2022 7:00:00 PM	27.184687
03/01/2022 7:00:00 AM	14.117813	03/02/2022 8:00:00 PM	29.599688
03/01/2022 8:00:00 AM	25.363125	03/02/2022 9:00:00 PM	30.151875
03/01/2022 9:00:00 AM	30.865313	03/02/2022 10:00:00 PM	28.697813
03/01/2022 10:00:00 AM	32.766563	03/02/2022 11:00:00 PM	23.811562
03/01/2022 11:00:00 AM	29.744999	03/03/2022 12:00:00 AM	16.791561
03/01/2022 12:00:00 PM	24.1275	03/03/2022 1:00:00 AM	12.248437
03/01/2022 1:00:00 PM	22.663126	03/03/2022 2:00:00 AM	7.660312
03/01/2022 2:00:00 PM	22.155937	03/03/2022 3:00:00 AM	5.390625
03/01/2022 3:00:00 PM	21.332813	03/03/2022 4:00:00 AM	5.9615626
03/01/2022 4:00:00 PM	20.430939	03/03/2022 5:00:00 AM	6.9196873
03/01/2022 5:00:00 PM	19.888124	03/03/2022 6:00:00 AM	6.837188
03/01/2022 6:00:00 PM	21.253124	03/03/2022 7:00:00 AM	12.515625
03/01/2022 7:00:00 PM	23.890312	03/03/2022 8:00:00 AM	24.100313
03/01/2022 8:00:00 PM	26.198437	03/03/2022 9:00:00 AM	30.47625
03/01/2022 9:00:00 PM	29.46	03/03/2022 10:00:00 AM	30.157501
03/01/2022 10:00:00 PM	28.425938	03/03/2022 11:00:00 AM	30.820312
03/01/2022 11:00:00 PM	24.141563	03/03/2022 12:00:00 PM	28.60875
03/02/2022 12:00:00 AM	19.230938	03/03/2022 1:00:00 PM	25.940626
03/02/2022 1:00:00 AM	13.550625	03/03/2022 2:00:00 PM	23.717812
03/02/2022 2:00:00 AM	9.516562	03/03/2022 3:00:00 PM	23.235937
03/02/2022 3:00:00 AM	5.8509374	03/03/2022 4:00:00 PM	22.979063
03/02/2022 4:00:00 AM	5.685	03/03/2022 5:00:00 PM	21.720001
03/02/2022 5:00:00 AM	5.5003123	03/03/2022 6:00:00 PM	22.994062
03/02/2022 6:00:00 AM	6.9487495	03/03/2022 7:00:00 PM	26.575314
03/02/2022 7:00:00 AM	11.513437	03/03/2022 8:00:00 PM	28.816875
03/02/2022 8:00:00 AM	24.125626	03/03/2022 9:00:00 PM	29.749687
03/02/2022 9:00:00 AM	28.341562	03/03/2022 10:00:00 PM	28.8525
03/02/2022 10:00:00 AM	29.2275	03/03/2022 11:00:00 PM	25.865139
03/02/2022 11:00:00 AM	27.620625		
03/02/2022 12:00:00 PM	27.002811		

Discharge of fDOM from the EOO, 2-3 March 2022

Date	Time	CDOM (ppb)	°C	psu	conductivity (µS/cm)
2-Mar-22	800	241.49	12.10	0.77	1.520
	900	253.01	11.32	0.78	1.548
	1000	256.20	11.50	0.78	1.540
	1100	253.28	11.31	0.78	1.547
	1200	255.48	11.19	0.78	1.555
	1300	252.59	10.77	0.79	1.573
	1400	251.24	11.90	0.81	1.599
	1500	251.40	11.41	0.76	1.517
	1600	254.25	11.74	0.79	1.572
	1700	266.72	11.57	0.81	1.595
	1800	273.52	11.80	0.69	1.377
	1900	261.03	12.02	0.66	1.326
	2000	268.23	11.79	0.63	1.268
	2100	270.82	10.68	0.64	1.250
3-Mar-22	2200	270.99	11.80	0.61	1.230
	2300	273.87	11.08	0.62	1.254
	2400	271.66	11.35	0.62	1.241
	0100	272.52	11.35	0.62	1.255
	0200	277.00	11.40	0.61	1.236
	0300	274.15	11.72	0.87	1.715
	0400	-	-	0.59	1.190
	0500	255.94	11.48	0.59	1.197
	0600	259.98	11.72	0.59	1.187
	0700	256.63	11.26	0.61	1.129
		Average	261.83	11.49	0.70
	SD	9.93	0.36	0.09	0.177
	Min	241.49	10.68	0.59	1.129
	Max	277	12.1	0.87	1.715

**APPENDIX-B:
Discharge Logs
for the SEOO
on 23 September,
21 December 2021,
and 3 March 2022**

THIS PAGE INTENTIONALLY LEFT BLANK

SEOO Total Discharge Rates - 23-24 September 2021

Date/Time	SEJPA Flow (mgd) Calculated	Total Outfall Flow (mgd) Calculated	Escondido Flow (mgd) metered	Escondido TDS meter (mg/L)	SEJPA TDS meter (mg/L)
9/23/2021 9:00	0.120	1.510	1.389	1,089	1,106
9/23/2021 9:15	0.113	1.491	1.394	1,089	1,103
9/23/2021 9:30	0.087	1.477	1.393	1,090	1,108
9/23/2021 9:45	0.129	1.518	1.398	1,090	1,110
9/23/2021 10:00	0.095	5.949	5.853	1,085	1,109
9/23/2021 10:15	0.131	6.085	5.963	1,078	1,116
9/23/2021 10:30	0.106	7.462	7.366	1,080	1,111
9/23/2021 10:45	0.095	8.740	8.649	1,089	1,119
9/23/2021 11:00	0.098	7.318	7.218	1,091	1,124
9/23/2021 11:15	0.124	5.307	5.174	1,091	1,121
9/23/2021 11:30	0.096	4.800	4.711	1,091	1,134
9/23/2021 11:45	0.097	4.619	4.532	1,094	1,133
9/23/2021 12:00	0.126	4.603	4.487	1,095	1,137
9/23/2021 12:15	0.140	1.941	1.820	1,099	1,148
9/23/2021 12:30	0.599	1.990	1.385	1,102	1,141
9/23/2021 12:45	1.249	2.634	1.388	1,105	1,146
9/23/2021 13:00	1.339	2.727	1.389	1,106	1,160
9/23/2021 13:15	1.354	4.725	3.376	1,108	1,168
9/23/2021 13:30	1.327	5.266	3.937	1,112	1,174
9/23/2021 13:45	1.365	5.264	3.904	1,116	1,178
9/23/2021 14:00	1.329	5.169	3.837	1,119	1,180
9/23/2021 14:15	1.332	5.119	3.783	1,119	1,181
9/23/2021 14:30	1.357	2.901	1.534	1,121	1,182
9/23/2021 14:45	2.320	3.704	1.389	1,123	1,182
9/23/2021 15:00	2.516	3.909	1.387	1,124	1,181
9/23/2021 15:15	2.207	8.092	5.885	1,129	1,181
9/23/2021 15:30	1.359	7.270	5.914	1,148	1,179
9/23/2021 15:45	1.342	7.676	6.341	1,185	1,177
9/23/2021 16:00	1.330	7.635	6.305	1,206	1,174
9/23/2021 16:15	1.344	5.598	4.250	1,263	1,171
9/23/2021 16:30	1.322	8.400	7.075	1,328	1,169
9/23/2021 16:45	0.910	7.440	6.537	1,349	1,165
9/23/2021 17:00	0.269	6.618	6.345	1,409	1,162
9/23/2021 17:15	0.352	7.295	6.948	1,495	1,159
9/23/2021 17:30	0.717	7.769	7.049	1,827	1,156
9/23/2021 17:45	1.195	7.694	6.502	2,191	1,153
9/23/2021 18:00	1.378	8.369	6.987	2,016	1,152
9/23/2021 18:15	1.294	8.141	6.843	1,819	1,150
9/23/2021 18:30	1.414	8.266	6.840	1,575	1,148
9/23/2021 18:45	1.255	7.334	6.072	1,286	1,146
9/23/2021 19:00	1.378	8.779	7.397	1,179	1,144
9/23/2021 19:15	1.320	8.672	7.362	1,128	1,141
9/23/2021 19:30	1.342	8.888	7.551	1,083	1,139

Date/Time	SEJPA Flow (mgd) Calculated	Total Outfall Flow (mgd) Calculated	Escondido Flow (mgd) metered	Escondido TDS meter (mg/L)	SEJPA TDS meter (mg/L)
9/23/2021 19:45	1.356	8.992	7.640	1,068	1,137
9/23/2021 20:00	1.333	9.124	7.788	1,069	1,135
9/23/2021 20:15	1.351	9.473	8.133	1,189	1,133
9/23/2021 20:30	1.351	9.796	8.446	1,540	1,131
9/23/2021 20:45	1.311	10.385	9.073	1,718	1,130
9/23/2021 21:00	0.823	9.832	9.008	1,700	1,128
9/23/2021 21:15	0.237	9.241	9.029	1,251	1,126
9/23/2021 21:30	0.382	8.537	8.163	1,249	1,123
9/23/2021 21:45	0.209	8.616	8.423	1,252	1,114
9/23/2021 22:00	0.038	8.401	8.396	1,263	1,100
9/23/2021 22:15	0.030	9.543	9.591	1,228	1,101
9/23/2021 22:30	0.044	8.937	8.901	1,247	1,102
9/23/2021 22:45	0.007	9.741	9.769	1,255	1,103
9/23/2021 23:00	0.035	9.379	9.376	1,246	1,106
9/23/2021 23:15	0.255	10.141	9.889	1,255	1,103
9/23/2021 23:30	0.509	11.378	10.858	1,253	1,102
9/23/2021 23:45	0.439	10.441	9.994	1,239	1,103

SEOO Total fDOM Discharge Concentrations, 23-24 September 2021

Date	Time	fDOM (ppb)	Temperature (°C)	Salinity (psu)	conductivity (µS/cm)
23-Sep-21	0900	190.52	24.59	0.98	1942
23-Sep-21	1000	205.67	18.10	0.99	1959
23-Sep-21	1100	202.94	24.39	1.03	2040
23-Sep-21	1200	216.14	24.86	1.55	2970
23-Sep-21	1300	204.10	24.92	1.00	1972
23-Sep-21	1400	205.72	24.96	1.00	1961
23-Sep-21	1500	205.56	24.99	1.16	2270
23-Sep-21	1600	215.90	24.95	1.42	2750
23-Sep-21	1700	208.54	25.00	1.02	2010
23-Sep-21	1800	206.18	25.17	1.01	1986
23-Sep-21	1900	204.44	25.36	1.07	2110
23-Sep-21	2000	198.37	25.50	0.98	1933
23-Sep-21	2100	206.38	25.96	0.98	1936
23-Sep-21	2200	200.53	25.92	0.98	1928
23-Sep-21	2300	204.51	25.87	0.99	1952
24-Sep-21	0000	203.46	25.94	0.98	1936
24-Sep-21	0100	196.34	25.95	0.98	1940
24-Sep-21	0200	187.62	25.77	1.13	2220
24-Sep-21	0300	151.56	25.69	0.99	1953
24-Sep-21	0400	188.50	25.42	0.98	1931
24-Sep-21	0500	244.93	25.10	1.40	2710
24-Sep-21	0600	212.32	24.96	1.25	2430
24-Sep-21	0700	214.05	24.94	1.24	2410
24-Sep-21	0800	211.95	24.74	1.23	2400
	Average	206.04	24.96	1.10	2152
	SD	15.85	1.53	0.17	305
	Min	151.56	18.10	0.98	1928
	Max	244.93	25.96	1.55	2970

SEOO Total Discharge Rates - 21 December 2021

Date/Time	SEJPA Flow (mgd)	Total Outfall Flow (mgd)	Date/Time	SEJPA Flow (mgd)	Total Outfall Flow (mgd)
12/21/2021 9:00	1.850	6.388	12/21/2021 19:45	3.162	15.271
12/21/2021 9:15	1.778	6.715	12/21/2021 20:00	3.213	15.325
12/21/2021 9:30	1.834	7.142	12/21/2021 20:15	3.162	15.444
12/21/2021 9:45	1.751	7.383	12/21/2021 20:30	3.212	15.574
12/21/2021 10:00	1.836	7.811	12/21/2021 20:45	3.167	15.768
12/21/2021 10:15	1.789	8.488	12/21/2021 21:00	3.185	15.776
12/21/2021 10:30	1.815	9.231	12/21/2021 21:15	3.170	15.924
12/21/2021 10:45	1.781	9.893	12/21/2021 21:30	3.217	16.001
12/21/2021 11:00	1.800	10.395	12/21/2021 21:45	3.137	15.955
12/21/2021 11:15	1.794	12.459	12/21/2021 22:00	3.218	16.079
12/21/2021 11:30	1.808	14.164	12/21/2021 22:15	3.136	15.889
12/21/2021 11:45	1.810	15.395	12/21/2021 22:30	3.204	15.811
12/21/2021 12:00	2.933	16.174	12/21/2021 22:45	2.987	15.682
12/21/2021 12:15	2.939	16.132	12/21/2021 23:00	2.950	15.549
12/21/2021 12:30	1.857	15.399	12/21/2021 23:15	2.934	15.319
12/21/2021 12:45	1.782	14.113	12/21/2021 23:30	3.267	15.445
12/21/2021 13:00	1.832	13.767	12/21/2021 23:45	2.822	15.312
12/21/2021 13:15	1.708	13.874	12/22/2021 0:00	2.984	15.197
12/21/2021 13:30	1.852	14.109	12/22/2021 0:15	2.965	15.132
12/21/2021 13:45	1.761	13.980	12/22/2021 0:30	2.988	14.955
12/21/2021 14:00	1.818	14.173	12/22/2021 0:45	2.941	14.738
12/21/2021 14:15	1.746	14.023	12/22/2021 1:00	3.001	14.355
12/21/2021 14:30	1.802	14.187	12/22/2021 1:15	2.988	14.075
12/21/2021 14:45	2.132	14.558	12/22/2021 1:30	2.999	13.759
12/21/2021 15:00	3.182	15.301	12/22/2021 1:45	2.973	13.238
12/21/2021 15:15	3.150	15.309	12/22/2021 2:00	2.992	12.799
12/21/2021 15:30	3.246	15.326	12/22/2021 2:15	2.971	12.445
12/21/2021 15:45	3.176	14.892	12/22/2021 2:30	2.997	12.239
12/21/2021 16:00	3.214	13.580	12/22/2021 2:45	2.964	12.016
12/21/2021 16:15	3.145	12.764	12/22/2021 3:00	2.984	11.983
12/21/2021 16:30	3.245	12.654	12/22/2021 3:15	2.978	11.775
12/21/2021 16:45	3.055	12.438	12/22/2021 3:30	2.976	11.535
12/21/2021 17:00	3.161	12.564	12/22/2021 3:45	2.999	11.282
12/21/2021 17:15	3.104	12.532	12/22/2021 4:00	2.992	11.145
12/21/2021 17:30	3.200	13.496	12/22/2021 4:15	2.980	11.065
12/21/2021 17:45	3.136	14.531	12/22/2021 4:30	2.996	10.790
12/21/2021 18:00	3.188	14.727	12/22/2021 4:45	2.982	10.570
12/21/2021 18:15	3.158	14.722	12/22/2021 5:00	2.994	10.374
12/21/2021 18:30	3.226	14.695	12/22/2021 5:15	2.978	10.013
12/21/2021 18:45	3.147	14.711	12/22/2021 5:30	2.994	9.756
12/21/2021 19:00	3.236	14.808	12/22/2021 5:45	2.972	9.438
12/21/2021 19:15	3.118	14.822	12/22/2021 6:00	2.976	9.215
12/21/2021 19:30	3.229	15.072	12/22/2021 6:15	2.999	9.088

Date/Time	SEJPA Flow (mgd)	Total Outfall Flow (mgd)
12/22/2021 6:30	2.994	8.944
12/22/2021 6:45	1.627	7.714
12/22/2021 7:00	1.461	7.948
12/22/2021 7:15	0.893	7.427
12/22/2021 7:30	1.021	7.344
12/22/2021 7:45	1.335	7.217
12/22/2021 8:00	1.691	6.783

Date/Time	SEJPA Flow (mgd)	Total Outfall Flow (mgd)
12/22/2021 8:15	1.965	7.009
12/22/2021 8:30	1.999	8.511
12/22/2021 8:45	1.968	8.818
12/22/2021 9:00	2.655	9.648
Average	2.644	12.633
Max	3.267	16.174

SEOO Total fDOM Discharge Concentrations, 21 December 2021

Date	Time	CDOM (ppb)	temperature (°C)	salinity (psu)	conductivity (µS/cm)	% Escondido	% San Elijo
21-Dec-21	0900	393.15	19.15	1.00	1964	71.00	29.00
21-Dec-21	1000	392.96	19.10	0.95	1864	76.00	23.00
21-Dec-21	1100	300.25	19.04	0.98	1930	83.00	17.00
21-Dec-21	1200	226.78	19.02	0.93	1835	82.00	18.00
21-Dec-21	1300	145.38	19.22	0.90	1772	87.00	13.00
21-Dec-21	1400	383.44	19.27	0.90	1780	87.00	13.00
21-Dec-21	1500	168.80	19.06	0.90	1775	79.00	21.00
21-Dec-21	1600	371.72	19.04	0.90	1780	76.00	24.00
21-Dec-21	1700	350.22	18.97	0.92	1809	75.00	25.00
21-Dec-21	1800	121.70	18.99	0.91	1798	78.00	22.00
21-Dec-21	1900	144.94	18.96	0.90	1782	78.00	22.00
21-Dec-21	2000	375.35	19.02	0.91	1803	79.00	21.00
21-Dec-21	2100	375.84	19.05	0.92	1807	80.00	20.00
21-Dec-21	2200	134.91	19.03	0.90	1786	80.00	20.00
21-Dec-21	2300	130.39	19.05	0.90	1776	81.00	19.00
22-Dec-21	0000	194.13	19.08	0.90	1777	80.00	20.00
22-Dec-21	0100	125.70	19.09	0.90	1776	79.00	21.00
22-Dec-21	0200	150.35	19.03	0.90	1779	77.00	23.00
22-Dec-21	0300	152.32	19.06	0.90	1772	75.00	25.00
22-Dec-21	0400	265.41	19.11	0.90	1779	73.00	27.00
22-Dec-21	0500	166.23	19.38	0.90	1782	71.00	29.00
22-Dec-21	0600	145.41	19.71	0.97	1915	68.00	32.00
22-Dec-21	0700	223.01	20.26	0.98	1928	82.00	18.00
	0800	147.8	19.98	0.99	1938	75.00	25.00
	Average	232.76	19.19	0.92	1821	78.00	21.96
	SD	104.48	0.33	0.03	64	4.67	4.66
	Min	121.7	18.96	0.9	1772	68	13
	Max	393.15	20.26	1	1964	87	32

SEOO Total Discharge Rates – 3-4 March 2022

Date/Time	SEJPA Flow (mgd)	Total Outfall Flow (mgd)	Escondido Flow (mgd)	Escondido TDS (mg/L)	SEJPA TDS (mg/L)	Combined TDS (mg/L) Calculated	% Escondido	% San Elijo	1000 mL Esco	1000 mL San Elijo
3/3/2022 9:00	1.688	3.789	2.097	955	1,130	1,032	55%	45%	554	445
3/3/2022 9:15	1.718	3.777	2.062	954	1,131	1,035	55%	45%	546	455
3/3/2022 9:30	1.678	3.795	2.117	954	1,133	1,033	56%	44%	558	442
3/3/2022 9:45	1.728	4.033	2.303	954	1,136	1,031	57%	43%	571	428
3/3/2022 10:00	1.679	4.309	2.629	956	1,138	1,027	61%	39%	610	390
3/3/2022 10:15	1.736	4.994	3.257	960	1,140	1,023	65%	35%	652	348
3/3/2022 10:30	1.670	5.858	4.191	966	1,142	1,017	72%	29%	715	285
3/3/2022 10:45	1.690	7.266	5.577	972	1,146	1,013	77%	23%	768	233
3/3/2022 11:00	1.704	8.253	6.551	980	1,151	1,016	79%	21%	794	206
3/3/2022 11:15	1.691	9.163	7.477	991	1,155	1,022	82%	18%	816	185
3/3/2022 11:30	1.734	9.927	8.200	1,003	1,159	1,031	83%	17%	826	175
3/3/2022 11:45	1.391	10.875	9.476	1,019	1,164	1,037	87%	13%	871	128
3/3/2022 12:00	1.727	12.953	11.216	1,051	1,167	1,066	87%	13%	866	133
3/3/2022 12:15	1.699	13.059	11.355	1,097	1,172	1,106	87%	13%	869	130
3/3/2022 12:30	1.706	13.527	11.821	1,194	1,174	1,192	87%	13%	874	126
3/3/2022 12:45	1.676	13.358	11.687	1,237	1,178	1,230	87%	13%	875	126
3/3/2022 13:00	1.657	13.368	11.699	1,207	1,181	1,203	88%	12%	875	124
3/3/2022 13:15	1.703	13.460	11.764	1,147	1,184	1,152	87%	13%	874	126
3/3/2022 13:30	1.721	13.658	11.946	1,088	1,187	1,101	87%	13%	875	126
3/3/2022 13:45	1.717	13.490	11.780	1,044	1,190	1,063	87%	13%	873	127
3/3/2022 14:00	1.670	13.238	11.569	1,011	1,192	1,034	87%	13%	874	126
3/3/2022 14:15	1.699	13.193	11.482	984	1,194	1,010	87%	13%	870	129
3/3/2022 14:30	1.676	13.113	11.435	961	1,195	991	87%	13%	872	128
3/3/2022 14:45	1.705	13.073	11.379	942	1,196	976	87%	13%	870	130
3/3/2022 15:00	1.679	12.922	11.237	926	1,198	961	87%	13%	870	130
3/3/2022 15:15	1.718	12.618	10.885	913	1,198	950	86%	14%	863	136
3/3/2022 15:30	1.619	11.411	9.788	901	1,198	943	86%	14%	858	142
3/3/2022 15:45	1.357	10.720	9.357	892	1,197	930	87%	13%	873	127
3/3/2022 16:00	1.352	10.621	9.270	884	1,197	924	87%	13%	873	127
3/3/2022 16:15	1.357	10.427	9.070	877	1,196	919	87%	13%	870	130

Date/Time	SEJPA Flow (mgd)	Total Outfall Flow (mgd)	Escondido Flow (mgd)	Escondido TDS (mg/L)	SEJPA TDS (mg/L)	Combined TDS (mg/L)	Calculated % Escondido	% San Elijo	1000 mL Esco	1000 mL San Elijo
3/3/2022 16:30	1.247	10.077	8.829	870	1,195	910	88%	12%	876	124
3/3/2022 16:45	1.337	10.069	8.729	862	1,194	906	87%	13%	867	133
3/3/2022 17:00	1.105	9.745	8.635	855	1,193	893	89%	11%	886	113
3/3/2022 17:15	1.374	10.259	8.889	850	1,191	896	87%	13%	866	134
3/3/2022 17:30	1.383	10.318	8.937	843	1,189	890	87%	13%	866	134
3/3/2022 17:45	1.391	10.540	9.154	838	1,186	884	87%	13%	868	132
3/3/2022 18:00	1.208	10.477	9.274	835	1,184	876	89%	12%	885	115
3/3/2022 18:15	1.774	11.232	9.464	834	1,181	889	84%	16%	843	158
3/3/2022 18:30	2.535	11.762	9.226	836	1,178	910	78%	22%	784	216
3/3/2022 18:45	2.620	12.774	10.154	838	1,174	907	79%	21%	795	205
3/3/2022 19:00	1.818	12.455	10.638	843	1,171	891	85%	15%	854	146
3/3/2022 19:15	1.407	12.531	11.121	849	1,169	885	89%	11%	887	112
3/3/2022 19:30	1.484	12.611	11.129	856	1,166	892	88%	12%	882	118
3/3/2022 19:45	1.447	12.564	11.120	864	1,162	899	89%	12%	885	115
3/3/2022 20:00	1.374	12.862	11.487	880	1,159	910	89%	11%	893	107
3/3/2022 20:15	0.996	12.761	11.757	889	1,155	909	92%	8%	921	78
3/3/2022 20:30	0.557	12.473	11.920	895	1,149	907	96%	4%	956	45
3/3/2022 20:45	0.577	12.602	12.031	893	1,145	905	95%	5%	955	46
3/3/2022 21:00	0.539	12.735	12.199	889	1,143	900	96%	4%	958	42
3/3/2022 21:15	0.584	12.842	12.259	888	1,140	900	95%	5%	955	45
3/3/2022 21:30	0.537	13.052	12.502	891	1,137	900	96%	4%	958	41
3/3/2022 21:45	0.587	13.287	12.703	896	1,134	907	96%	4%	956	44
3/3/2022 22:00	0.585	13.408	12.814	903	1,131	912	96%	4%	956	44
3/3/2022 22:15	0.780	13.702	12.924	906	1,128	919	94%	6%	943	57
3/3/2022 22:30	1.282	13.765	12.477	909	1,126	929	91%	9%	906	93
3/3/2022 22:45	1.446	14.340	12.897	913	1,124	935	90%	10%	899	101
3/3/2022 23:00	1.307	14.103	12.796	917	1,121	936	91%	9%	907	93
3/3/2022 23:15	1.289	14.109	12.826	920	1,119	938	91%	9%	909	91
3/3/2022 23:30	1.327	14.034	12.704	920	1,116	938	91%	9%	905	95
3/3/2022 23:45	1.358	14.134	12.770	920	1,114	938	90%	10%	903	96
3/4/2022 0:00	1.373	13.974	12.600	921	1,112	939	90%	10%	902	98

Date/Time	SEJPA Flow (mgd)	Total Outfall Flow (mgd)	Escondido Flow (mgd)	Escondido TDS (mg/L)	SEJPA TDS (mg/L)	Combined TDS (mg/L) Calculated	% Escondido	% San Elijo	1000 mL Esco	1000 mL San Elijo
3/4/2022 0:15	1.438	13.709	12.271	920	1,109	939	90%	10%	895	105
3/4/2022 0:30	1.458	13.455	11.999	919	1,107	939	89%	11%	892	108
3/4/2022 0:45	2.583	13.832	11.249	921	1,104	955	81%	19%	813	187
3/4/2022 1:00	2.611	14.361	11.746	924	1,101	956	82%	18%	818	182
3/4/2022 1:15	2.012	14.932	12.913	928	1,099	951	86%	13%	865	135
3/4/2022 1:30	1.411	14.048	12.630	931	1,096	947	90%	10%	899	100
3/4/2022 1:45	1.480	13.247	11.767	933	1,092	951	89%	11%	888	112
3/4/2022 2:00	1.435	12.737	11.305	935	1,089	953	89%	11%	888	113
3/4/2022 2:15	2.669	13.085	10.417	938	1,078	967	80%	20%	796	204
3/4/2022 2:30	3.789	13.811	10.019	944	1,030	967	73%	27%	725	274
3/4/2022 2:45	3.836	13.615	9.782	948	1,052	977	72%	28%	718	282
3/4/2022 3:00	3.802	13.173	9.365	950	1,070	984	71%	29%	711	289
3/4/2022 3:15	3.839	12.968	9.131	953	1,076	989	70%	30%	704	296
3/4/2022 3:30	3.627	12.808	9.184	955	1,077	989	72%	28%	717	283
3/4/2022 3:45	3.811	12.924	9.111	955	1,078	991	70%	29%	705	295
3/4/2022 4:00	3.806	13.663	9.850	956	1,077	989	72%	28%	721	279
3/4/2022 4:15	3.791	13.839	10.045	958	1,077	990	73%	27%	726	274
3/4/2022 4:30	3.810	13.768	9.954	958	1,076	991	72%	28%	723	277
3/4/2022 4:45	3.802	13.770	9.958	958	1,076	990	72%	28%	723	276
3/4/2022 5:00	3.775	13.136	9.358	959	1,076	992	71%	29%	712	287
3/4/2022 5:15	3.796	12.925	9.129	959	1,075	993	71%	29%	706	294
3/4/2022 5:30	3.794	12.824	9.034	958	1,074	993	70%	30%	704	296
3/4/2022 5:45	3.818	12.719	8.904	958	1,074	993	70%	30%	700	300
3/4/2022 6:00	3.767	12.547	8.772	957	1,073	991	70%	30%	699	300
3/4/2022 6:15	3.800	12.517	8.721	959	1,072	994	70%	30%	697	304
3/4/2022 6:30	3.780	12.335	8.555	962	1,070	995	69%	31%	694	306
3/4/2022 6:45	3.804	11.976	8.172	964	1,069	997	68%	32%	682	318
3/4/2022 7:00	3.813	11.610	7.800	969	1,067	1,002	67%	33%	672	328
3/4/2022 7:15	3.816	11.359	7.542	973	1,062	1,003	66%	34%	664	336
3/4/2022 7:30	3.794	11.173	7.377	975	1,057	1,003	66%	34%	660	340
3/4/2022 7:45	4.726	11.584	6.854	977	1,060	1,010	59%	41%	592	408

Date/Time	SEJPA Flow (mgd)	Total Outfall Flow (mgd)	Escondido Flow (mgd)	Escondido TDS (mg/L)	SEJPA TDS (mg/L)	Combined TDS (mg/L) Calculated	% Escondido	% San Elijo	1000 mL Esco	1000 mL San Elijo
3/4/2022 8:00	3.402	10.140	6.738	980	1,056	1,005	66%	34%	665	335
3/4/2022 8:15	2.101	9.511	7.416	982	1,054	999	78%	22%	780	221
3/4/2022 8:30	2.104	9.199	7.100	983	1,064	1,002	77%	23%	772	229
3/4/2022 8:45	1.787	8.634	6.850	972	1,069	993	79%	21%	793	207
3/4/2022 9:00	1.269	8.134	6.866	962	1,070	979	84%	16%	844	156
Average	2.065	11.752	9.686	944	1,130	975	81%	19%		
Max	4.726	14.932	12.924	1,237	1,198	1,230	96%	45%		

SEOO Total fDOM Discharge Concentrations, 3-4 March 2022

Date	Time	CDOM (ppb)	°C	psu	conductivity (µS/cm)	% Econdido	% San Elijo
3-Mar-22	0900	216.10	20.02	0.77	1.526	55.00	45.00
	1000	221.53	19.77	0.78	1.545	61.00	39.00
	1100	218.23	20.22	0.77	1.536	79.00	21.00
	1200	220.79	20.41	0.92	1.810	87.00	13.00
	1300	210.80	20.50	0.74	1.481	88.00	12.00
	1400	203.49	20.50	0.64	1.278	87.00	13.00
	1500	201.55	20.53	0.65	1.298	87.00	13.00
	1600	210.24	20.46	0.67	1.352	87.00	13.00
	1700	210.60	20.46	0.67	1.336	89.00	11.00
	1800	147.12	20.48	0.66	1.328	89.00	12.00
	1900	211.79	20.44	0.69	1.388	85.00	15.00
	2000	211.50	20.53	0.7	1.409	89.00	11.00
	2100	206.63	20.72	0.7	1.394	96.00	4.00
	2200	202.38	20.75	0.70	1.408	96.00	4.00
2300	182.96	20.65	0.73	1.455	91.00	9.00	
2400	209.54	20.62	0.71	1.422	90.00	10.00	
4-Mar-22	0100	208.70	20.52	0.72	1.438	82.00	18.00
	0200	210.71	20.67	0.72	1.434	89.00	11.00
	0300	206.37	20.40	0.70	1.403	71.00	29.00
	0400	203.10	20.42	0.69	1.383	72.00	28.00
	0500	200.58	20.45	0.69	1.379	71.00	29.00
	0600	195.11	20.42	0.70	1.397	70.00	30.00
	0700	197.88	20.31	0.70	1.401	67.00	33.00
	0800	196.48	20.23	0.71	1.428	66.00	34.00
	Average	204.34	20.44	0.71	1.426	81.00	19.04
	SD	14.98	0.22	0.06	0.106	11.42	11.39
	Min	147.12	19.77	0.64	1.278	55	4
	Max	221.53	20.75	0.92	1.810	96	45

**APPENDIX-C:
EEO - Plumes 20
Text file Output**

THIS PAGE INTENTIONALLY LEFT BLANK

Table 6: Plumes 20 (UM3) Initialization of EOO Ebb tide Ambient Conditions on 21 December 2021 with Ambient Current

Project "C:\Plumes20\EOO_Ebb_21Dec2021_1_with-current"

Model configuration items checked:

- Channel width (m) 100
- Start case for graphs 1
- Max detailed graphs 10 (limits plots that can overflow memory)
- Elevation Projection Plane (deg) 0
- Shore vector (m,deg) not checked
- Bacteria model : Mancini (1978) coliform model
- PDS sfc. model heat transfer : Medium
- Equation of State : S, T
- Similarity Profile : Default profile (k=2.0, ...)
- Diffuser port contraction coefficient 1
- Light absorption coefficient 0.16
- Farfield increment (m) 200
- UM3 aspiration coefficient 0.1
- Output file: text output tab
- Output each ?? steps 25
- Maximum dilution reported 10000
- Text output format : Standard
- Max vertical reversals : to max rise or fall

/ UM3. 4/19/2022 1:09:10 PM

Case 1; ambient file C:\Plumes20\EOO_Ebb_21Dec2021_1_with-current.001.db; Diffuser table record 1:

Ambient Table:

Depth	Amb-cur	Amb-dir	Amb-sal	Amb-tem	Amb-pol	Decay	Far-spdx	Far-dir	Disprsn	Density
m	m/s	deg	psu	C	kg/kg	s-1	m/s	deg	m0.67/s2	sigma-T
0.0	0.304	0.0	33.51	15.34	3.0000E-10	0.0	0.0	0.0	0.0	24.76877
3.465	0.304	0.0	33.51	15.34	2.9000E-10	0.0	0.0	0.0	0.0	24.77234
6.389	0.304	0.0	33.51	15.33	2.5000E-10	0.0	0.0	0.0	0.0	24.77418
9.479	0.304	0.0	33.51	15.30	2.8000E-10	0.0	0.0	0.0	0.0	24.78128
12.52	0.304	0.0	33.51	15.28	2.8000E-10	0.0	0.0	0.0	0.0	24.78438
15.53	0.304	0.0	33.51	15.28	2.1000E-10	0.0	0.0	0.0	0.0	24.78515
18.50	0.304	0.0	33.51	15.25	2.5000E-10	0.0	0.0	0.0	0.0	24.79055
21.44	0.304	0.0	33.50	15.23	2.6000E-10	0.0	0.0	0.0	0.0	24.79126
24.48	0.304	0.0	33.41	15.04	2.5000E-10	0.0	0.0	0.0	0.0	24.76392
27.48	0.304	0.0	33.48	14.50	3.0000E-10	0.0	0.0	0.0	0.0	24.93144
30.52	0.304	0.0	33.32	13.82	3.1000E-10	0.0	0.0	0.0	0.0	24.94873
33.47	0.304	0.0	33.12	12.61	2.9000E-10	0.0	0.0	0.0	0.0	25.03897
36.47	0.304	0.0	33.31	12.15	3.1000E-10	0.0	0.0	0.0	0.0	25.26924
39.47	0.304	0.0	33.55	12.42	3.2000E-10	0.0	0.0	0.0	0.0	25.40460
42.55	0.304	0.0	33.53	12.19	3.4000E-10	0.0	0.0	0.0	0.0	25.43855
45.55	0.304	0.0	33.53	12.19	3.7000E-10	0.0	0.0	0.0	0.0	25.43780
48.68	0.304	0.0	33.55	12.08	3.7300E-10	0.0	0.0	0.0	0.0	25.46989

Diffuser table:

P-diaVer	angl	H-Angle	SourceX	SourceY	Ports	MZ-dis	Isoplth	P-depth	Ttl-flo	Eff-sal	Temp	Polutnt
(in)	(deg)	(deg)	(ft)	(ft)	()	(m)(concent)	(ft)	(MGD)	(psu)	(C)	(ppb)	
2.7750	0.0	0.0	0.0	0.0	138.00	2000.0	0.0	155.75	31.200	0.9600	19.380	217.50

Table 7: Plumes 20 (UM3) Output of EOO Dilution Factor (Dm) during Ebb Tide on 21 December 2021 with Ambient Current (Final Dm solution highlighted in yellow)

Simulation:

Froude No: 18.81; Strat No: 3.88E-5; Spcg No: 7.909; k: 8.351; eff den (sigmaT) -0.874719; eff vel 2.539(m/s);

Depth	Amb-cur	Amb-sal	P-dia	Eff-sal	Polutnt	Dilutn	CL-diln	x-posn	y-posn	Iso dia
Step (ft)	(m/s)	(psu)	(in)	(psu)	(ppb)	()	()	(ft)	(ft)	(m)
0	155.8	0.304	33.54	2.775	0.960	217.5	1.000	1.000	0.0	0.0
25	155.7	0.304	33.54	4.403	14.05	131.7	1.654	1.000	0.376	0.0
50	155.7	0.304	33.54	6.814	21.66	80.89	2.697	1.348	0.958	0.0
75	155.7	0.304	33.54	10.31	26.30	49.64	4.408	2.204	1.893	0.0
100	155.6	0.304	33.54	15.15	29.13	30.47	7.216	3.608	3.412	0.0
125	155.4	0.304	33.54	21.60	30.85	18.75	11.82	5.911	5.878	0.0
127	155.4	0.304	33.54	22.19	30.96	18.04	12.30	6.149	6.114	0.0
150	154.8	0.304	33.54	30.49	31.90	11.59	19.38	10.73	9.943	0.0
175	153.6	0.304	33.54	43.63	32.54	7.214	31.78	21.10	16.17	0.0
200	151.5	0.304	33.54	64.44	32.93	4.547	52.12	34.75	25.26	0.0
225	148.0	0.304	33.53	99.36	33.17	2.920	85.49	56.99	38.83	0.0
250	142.4	0.304	33.53	159.0	33.31	1.924	140.2	93.49	59.72	0.0
275	133.4	0.304	33.54	259.9	33.40	1.308	230.1	153.4	92.82	0.0
293	123.8	0.304	33.42	374.3	33.43	1.015	328.6	219.0	129.9	0.0
300	120.5	0.304	33.33	425.0	33.43	0.941	367.5	245.0	145.5	0.0
325	115.9	0.304	33.24	512.6	33.41	0.850	430.1	286.7	179.6	0.0
339	115.4	0.304	33.23	526.6	33.40	0.839	439.4	292.9	194.6	0.0

Horiz plane projections in effluent direction: radius(m): 0.0; CL(m): 59.330
Lmz(m): 59.330
forced entrain 1 210.4 12.30 13.38 1.000
Rate sec-1 0.0 dy-1 0.0 kt: 0.0 Amb Sal 33.2259
;
1:09:16 PM. amb fills: 4

Table 8: Plumes 20 (UM3) Initialization of EOO Flood tide Ambient Conditions on 21 December 2021 with Ambient Current

Project "C:\Plumes20\EOO_Flood_21Dec2021_1_with-current"

Model configuration items checked:

- Channel width (m) 100
- Start case for graphs 1
- Max detailed graphs 10 (limits plots that can overflow memory)
- Elevation Projection Plane (deg) 0
- Shore vector (m,deg) not checked
- Bacteria model : Mancini (1978) coliform model
- PDS sfc. model heat transfer : Medium
- Equation of State : S, T
- Similarity Profile : Default profile (k=2.0, ...)
- Diffuser port contraction coefficient 1
- Light absorption coefficient 0.16
- Farfield increment (m) 200
- UM3 aspiration coefficient 0.1
- Output file: text output tab
- Output each ?? steps 25
- Maximum dilution reported 10000
- Text output format : Standard
- Max vertical reversals : to max rise or fall

/ UM3. 4/18/2022 3:59:52 PM

Case 1; ambient file C:\Plumes20\EOO_Flood_21Dec2021_1_with-current.001.db; Diffuser table record 1:

Ambient Table:

Depth	Amb-cur	Amb-dir	Amb-sal	Amb-tem	Amb-pol	Decay	Far-spd	Far-dir	Disprsn	Density
m	m/s	deg	psu	C	kg/kg	s-1	m/s	deg	m0.67/s2	sigma-T
0.0	0.211	0.0	33.50	15.19	3.4000E-10	0.0	0.0	0.0	0.0	24.79668
3.490	0.211	0.0	33.51	15.17	3.2000E-10	0.0	0.0	0.0	0.0	24.80573
6.487	0.211	0.0	33.51	15.17	3.1000E-10	0.0	0.0	0.0	0.0	24.80744
9.540	0.211	0.0	33.51	15.16	3.1000E-10	0.0	0.0	0.0	0.0	24.80995
12.54	0.211	0.0	33.51	15.16	3.0000E-10	0.0	0.0	0.0	0.0	24.81068
15.56	0.211	0.0	33.51	15.15	3.3000E-10	0.0	0.0	0.0	0.0	24.81273
18.48	0.211	0.0	33.50	15.13	3.2000E-10	0.0	0.0	0.0	0.0	24.81177
21.48	0.211	0.0	33.50	15.11	3.1000E-10	0.0	0.0	0.0	0.0	24.81839
24.44	0.211	0.0	33.48	14.99	3.2000E-10	0.0	0.0	0.0	0.0	24.82382
27.50	0.211	0.0	33.49	14.69	3.0900E-10	0.0	0.0	0.0	0.0	24.89472
30.57	0.211	0.0	33.46	14.35	3.3000E-10	0.0	0.0	0.0	0.0	24.94822
33.46	0.211	0.0	33.36	14.04	3.1000E-10	0.0	0.0	0.0	0.0	24.93718
36.47	0.211	0.0	33.37	13.02	3.5000E-10	0.0	0.0	0.0	0.0	25.15306
39.44	0.211	0.0	33.43	12.53	3.3000E-10	0.0	0.0	0.0	0.0	25.29416
42.53	0.211	0.0	33.53	12.19	3.2000E-10	0.0	0.0	0.0	0.0	25.43855
45.46	0.211	0.0	33.57	11.83	2.8000E-10	0.0	0.0	0.0	0.0	25.53567
48.68	0.211	0.0	33.58	11.80	3.2000E-10	0.0	0.0	0.0	0.0	25.55021

Diffuser table:

P-dia	Ver angl	H-Angle	SourceX	SourceY	Ports	MZ-dis	Isoplth	P-depth	Ttl-flo	Eff-sal	Temp	Polutnt
(in)	(deg)	(deg)	(ft)	(ft)	()	(m)(concent)	(ft)	(MGD)	(psu)	(C)	(ppb)	
2.7750	0.0	0.0	0.0	0.0	138.00	2000.0	0.0	155.75	29.700	0.9600	19.380	217.50

Table 9: Plumes 20 (UM3) Output of EOO Dilution Factor (Dm) during Flood Tide on 21 December 2021 with Ambient Current (Final Dm solution highlighted in yellow)

Simulation:

Froude No: 17.87; Strat No: 4.20E-5; Spcg No: 7.909; k: 11.45; eff den (sigmaT) -0.874719; eff vel 2.417(m/s);

Depth Step (ft)	Amb-cur (m/s)	Amb-sal (psu)	P-dia (in)	Eff-sal (psu)	Polutnt (ppb)	Dilutn ()	CL-diln (ft)	x-posn (ft)	y-posn (m)	Iso dia
0	155.8	0.211	33.58	2.775	0.960	217.5	1.000	1.000	0.0	0.07049;
25	155.7	0.211	33.58	4.444	14.05	131.7	1.653	1.000	0.374	0.0 0.1129;
50	155.7	0.211	33.58	6.971	21.68	80.89	2.695	1.348	0.957	0.0 0.1771;
75	155.7	0.211	33.58	10.73	26.32	49.61	4.406	2.203	1.889	0.0 0.2726;
100	155.6	0.211	33.58	16.10	29.16	30.43	7.212	3.606	3.386	0.0 0.4088;
121	155.4	0.211	33.58	22.08	30.66	20.21	10.92	5.459	5.316	0.0 0.5609; merging;
125	155.3	0.211	33.58	23.42	30.88	18.69	11.82	6.008	5.784	0.0 0.5948;
150	154.4	0.211	33.58	33.93	31.94	11.53	19.37	11.22	9.781	0.0 0.8619;
175	152.7	0.211	33.58	49.96	32.58	7.148	31.76	21.17	15.43	0.0 1.2689;
200	149.7	0.211	33.57	76.20	32.97	4.474	52.09	34.73	23.37	0.0 1.9355;
225	144.7	0.211	33.56	121.4	33.20	2.842	85.44	56.96	35.00	0.0 3.0837;
250	136.9	0.211	33.51	201.3	33.33	1.858	140.2	93.44	53.26	0.0 5.1126;
265	130.7	0.211	33.45	277.3	33.37	1.473	187.5	125.0	69.76	0.0 7.0433; trap level;
275	127.7	0.211	33.42	324.0	33.38	1.336	213.3	142.2	79.26	0.0 8.2287;
300	123.4	0.211	33.40	402.1	33.38	1.176	254.3	169.5	98.79	0.0 10.214;
325	121.8	0.211	33.39	438.7	33.38	1.121	272.4	181.6	116.2	0.0 11.143;
331	121.8	0.211	33.39	441.5	33.38	1.118	273.8	182.5	120.3	0.0 11.215; local maximum rise or fall;

Horiz plane projections in effluent direction: radius(m): 0.0; CL(m): 36.666

Lmz(m): 36.666

forced entrain 1 129.2 10.36 11.21 1.000

Rate sec-1 0.0 dy-1 0.0 kt: 0.0 Amb Sal 33.3863

;

3:59:52 PM. amb fills: 4

Table 10: Plumes 20 (UM3) Initialization of EOO Ebb tide Ambient Conditions on 2 March with Ambient Current

Project "C:\Plumes20\EEO_Ebb_With-Current_2Mar2022"

Model configuration items checked:

Channel width (m) 100
 Start case for graphs 1
 Max detailed graphs 10 (limits plots that can overflow memory)
 Elevation Projection Plane (deg) 0
 Shore vector (m,deg) not checked
 Bacteria model : Mancini (1978) coliform model
 PDS sfc. model heat transfer : Medium
 Equation of State : S, T
 Similarity Profile : Default profile (k=2.0, ...)
 Diffuser port contraction coefficient 1
 Light absorption coefficient 0.16
 Farfield increment (m) 200
 UM3 aspiration coefficient 0.1
 Output file: text output tab
 Output each ?? steps 10
 Maximum dilution reported 10000
 Text output format : Standard
 Max vertical reversals : to max rise or fall

Ambient Table:

Depth	Amb-cur	Amb-dir	Amb-sal	Amb-tem	Amb-pol	Decay	Far-spd	Far-dir	Disprsn	Density
m	m/s	deg	psu	C	kg/kg	s-1	m/s	deg	m0.67/s2	sigma-T
0.0	0.526	0.0	33.47	14.70	3.6000E-10	0.0	0.0	0.0	0.0	24.87799
3.534	0.526	0.0	33.45	14.30	1.7000E-10	0.0	0.0	0.0	0.0	24.95378
6.535	0.526	0.0	33.48	14.15	2.2200E-10	0.0	0.0	0.0	0.0	25.00789
9.510	0.526	0.0	33.48	14.02	1.6700E-10	0.0	0.0	0.0	0.0	25.03189
12.55	0.526	0.0	33.49	13.96	1.7000E-10	0.0	0.0	0.0	0.0	25.05283
15.45	0.526	0.0	33.50	13.91	2.0900E-10	0.0	0.0	0.0	0.0	25.06862
18.47	0.526	0.0	33.50	13.90	2.6200E-10	0.0	0.0	0.0	0.0	25.07033
21.49	0.526	0.0	33.50	13.78	2.0500E-10	0.0	0.0	0.0	0.0	25.09644
24.51	0.526	0.0	33.49	13.72	2.3500E-10	0.0	0.0	0.0	0.0	25.10051
27.47	0.526	0.0	33.48	13.43	2.4800E-10	0.0	0.0	0.0	0.0	25.15101
30.51	0.526	0.0	33.55	13.23	2.3500E-10	0.0	0.0	0.0	0.0	25.24583
33.47	0.526	0.0	33.55	13.23	2.5500E-10	0.0	0.0	0.0	0.0	25.24688
36.54	0.526	0.0	33.59	13.07	2.0900E-10	0.0	0.0	0.0	0.0	25.30754
39.54	0.526	0.0	33.59	13.05	2.6500E-10	0.0	0.0	0.0	0.0	25.31448
42.43	0.526	0.0	33.51	11.97	2.3500E-10	0.0	0.0	0.0	0.0	25.46085
45.47	0.526	0.0	33.68	11.43	2.4900E-10	0.0	0.0	0.0	0.0	25.69300
48.41	0.526	0.0	33.66	11.04	2.5800E-10	0.0	0.0	0.0	0.0	25.75193

Diffuser table:

P-dia	Ver	angl	H-Angle	SourceX	SourceY	Ports	MZ-dis	Isoplth	P-depth	Ttl-flo	Eff-sal	Temp	Polutnt
(in)	(deg)	(deg)	(ft)	(ft)	()	(m)	(concent)	(ft)	(MGD)	(psu)	(C)	(ppb)	
2.7750	0.0	0.0	0.0	0.0	138.00	2000.0	0.0	155.75	27.600	0.8200	20.420	261.80	

Table 11: Plumes 20 (UM3) Output of EOO Dilution Factor (Dm) during Ebb Tide on 2 March 2022 with Ambient Current (Final Dm solution highlighted in yellow)

Simulation:

Froude No: 16.45; Strat No: 4.72E-5; Spcg No: 7.909; k: 4.269; eff den (sigmaT) -1.196681; eff vel 2.246(m/s);

Depth Amb-cur Amb-sal P-dia Eff-sal Polutnt Dilutn CL-diln x-posn y-posn Iso dia

Step (ft) (m/s) (psu) (in) (psu) (ppb) () () (ft) (ft) (m)

0	155.8	0.526	33.67	2.775	0.820	261.8	1.000	1.000	0.0	0.0	0.07049;
10	155.7	0.526	33.67	3.295	6.985	213.8	1.225	1.000	0.138	0.0	0.08369;
20	155.7	0.526	33.67	3.895	11.78	176.1	1.487	1.000	0.292	0.0	0.09894;
30	155.7	0.526	33.67	4.588	15.71	145.0	1.807	1.000	0.478	0.0	0.1165;
40	155.7	0.526	33.67	5.380	18.94	119.3	2.197	1.099	0.703	0.0	0.1367;
50	155.7	0.526	33.67	6.281	21.58	98.12	2.673	1.336	0.978	0.0	0.1595;
60	155.7	0.526	33.67	7.299	23.75	80.68	3.252	1.626	1.315	0.0	0.1854;
70	155.7	0.526	33.67	8.442	25.54	66.33	3.959	1.979	1.729	0.0	0.2144;
80	155.7	0.526	33.67	9.717	27.00	54.52	4.820	2.410	2.243	0.0	0.2468;
90	155.7	0.526	33.67	11.13	28.20	44.82	5.870	2.935	2.886	0.0	0.2828;
100	155.6	0.526	33.67	12.70	29.18	36.84	7.150	3.575	3.694	0.0	0.3225;
110	155.6	0.526	33.67	14.42	29.99	30.29	8.710	4.355	4.670	0.0	0.3663;
120	155.5	0.526	33.67	16.32	30.65	24.91	10.61	5.306	5.786	0.0	0.4145;
130	155.4	0.526	33.67	18.40	31.19	20.49	12.93	6.465	7.032	0.0	0.4674;
140	155.3	0.526	33.67	20.69	31.64	16.86	15.76	7.878	8.414	0.0	0.5254;
146	155.2	0.526	33.67	22.16	31.86	15.00	17.74	8.870	9.313	0.0	0.5629; merging;
150	155.2	0.526	33.67	23.21	32.00	13.88	19.20	9.741	9.993	0.0	0.5896;
160	155.0	0.526	33.67	26.11	32.30	11.44	23.40	12.28	12.07	0.0	0.6631;
170	154.7	0.526	33.67	29.43	32.55	9.432	28.52	15.59	14.67	0.0	0.7474;
180	154.4	0.526	33.67	33.26	32.75	7.786	34.76	19.95	17.83	0.0	0.8448;
190	154.0	0.526	33.67	37.73	32.91	6.435	42.37	25.83	21.66	0.0	0.9584;
200	153.5	0.526	33.67	43.01	33.05	5.326	51.64	33.97	26.26	0.0	1.0924;
210	152.9	0.526	33.67	49.30	33.16	4.416	62.94	41.96	31.78	0.0	1.2523;
220	152.1	0.526	33.67	56.89	33.25	3.670	76.72	51.15	38.39	0.0	1.4449;
230	151.2	0.526	33.68	66.12	33.33	3.057	93.51	62.34	46.33	0.0	1.6794;
240	150.1	0.526	33.68	77.44	33.39	2.554	114.0	75.99	55.85	0.0	1.9671;
250	148.8	0.526	33.68	91.40	33.44	2.141	138.9	92.63	67.34	0.0	2.3217;
260	147.2	0.526	33.65	108.7	33.48	1.802	169.4	112.9	81.32	0.0	2.7603;
270	145.3	0.526	33.62	130.1	33.51	1.524	206.5	137.6	98.88	0.0	3.3040;
279	143.3	0.526	33.58	153.7	33.53	1.316	246.7	164.5	119.5	0.0	3.9036; trap level;
280	143.0	0.526	33.58	156.6	33.53	1.295	251.7	167.8	122.2	0.0	3.9777;
290	140.5	0.526	33.53	189.4	33.53	1.106	306.8	204.5	157.3	0.0	4.8116;
300	138.7	0.526	33.51	220.1	33.53	0.991	353.9	236.0	208.5	0.0	5.5897;
303	138.7	0.526	33.51	224.0	33.53	0.981	359.0	239.3	223.6	0.0	5.6900; local maximum rise or fall;

Horiz plane projections in effluent direction: radius(m): 0.0; CL(m): 68.152

Lmz(m): 68.152

forced entrain 1 173.6 5.188 5.690 1.000

Rate sec-1 0.0 dy-1 0.0 kt: 0.0 Amb Sal 33.5134;

3:38:38 PM. amb fills: 4

Table 12: Plumes 20 (UM3) Initialization of EOO flood tide Ambient Conditions on 2 March with Ambient Current

Project "C:\Plumes20\EOO_Flood_With-Current_2Mar2022" memo

Model configuration items checked:

Channel width (m) 100
 Start case for graphs 1
 Max detailed graphs 10 (limits plots that can overflow memory)
 Elevation Projection Plane (deg) 0
 Shore vector (m,deg) not checked
 Bacteria model : Mancini (1978) coliform model
 PDS sfc. model heat transfer : Medium
 Equation of State : S, T
 Similarity Profile : Default profile (k=2.0, ...)
 Diffuser port contraction coefficient 1
 Light absorption coefficient 0.16
 Farfield increment (m) 200
 UM3 aspiration coefficient 0.1
 Output file: text output tab
 Output each ?? steps 10
 Maximum dilution reported 10000
 Text output format : Standard
 Max vertical reversals : to max rise or fall

Ambient Table:

Depth	Amb-cur	Amb-dir	Amb-sal	Amb-tem	Amb-pol	Decay	Far-spd	Far-dir	Disprsn	Density
m	m/s	deg	psu	C	kg/kg	s-1	m/s	deg	m0.67/s2	sigma-T
0.0	0.261	0.0	33.47	14.70	3.6000E-10	0.0	0.0	0.0	0.0	24.87799
3.534	0.261	0.0	33.45	14.30	1.7000E-10	0.0	0.0	0.0	0.0	24.95378
6.535	0.261	0.0	33.48	14.15	2.2200E-10	0.0	0.0	0.0	0.0	25.00789
9.510	0.261	0.0	33.48	14.02	1.6700E-10	0.0	0.0	0.0	0.0	25.03189
12.55	0.261	0.0	33.49	13.96	1.7000E-10	0.0	0.0	0.0	0.0	25.05283
15.45	0.261	0.0	33.50	13.91	2.0900E-10	0.0	0.0	0.0	0.0	25.06862
18.47	0.261	0.0	33.50	13.90	2.6200E-10	0.0	0.0	0.0	0.0	25.07033
21.49	0.261	0.0	33.50	13.78	2.0500E-10	0.0	0.0	0.0	0.0	25.09644
24.51	0.261	0.0	33.49	13.72	2.3500E-10	0.0	0.0	0.0	0.0	25.10051
27.47	0.261	0.0	33.48	13.43	2.4800E-10	0.0	0.0	0.0	0.0	25.15101
30.51	0.261	0.0	33.55	13.23	2.3500E-10	0.0	0.0	0.0	0.0	25.24583
33.47	0.261	0.0	33.55	13.23	2.5500E-10	0.0	0.0	0.0	0.0	25.24688
36.54	0.261	0.0	33.59	13.07	2.0900E-10	0.0	0.0	0.0	0.0	25.30754
39.54	0.261	0.0	33.59	13.05	2.6500E-10	0.0	0.0	0.0	0.0	25.31448
42.43	0.261	0.0	33.51	11.97	2.3500E-10	0.0	0.0	0.0	0.0	25.46085
45.47	0.261	0.0	33.68	11.43	2.4900E-10	0.0	0.0	0.0	0.0	25.69300
48.41	0.261	0.0	33.66	11.04	2.5800E-10	0.0	0.0	0.0	0.0	25.75193

Diffuser table:

P-dia	Ver angl	H-Angle	SourceX	SourceY	Ports	MZ-dis	Isoplth	P-depth	Ttl-flo	Eff-sal	Temp	Polutnt
(in)	(deg)	(deg)	(ft)	(ft)	()	(m)(concent)	(ft)	(MGD)	(psu)	(C)	(ppb)	
2.7750	0.0	0.0	0.0	0.0	138.00	2000.0	0.0	155.75	24.200	0.8200	20.420	261.80

Table 13: Plumes 20 (UM3) Output of EOO Dilution Factor (Dm) during Flood Tide on 2 March 2022 with Ambient Current (Final Dm solution highlighted in yellow)

Simulation:

Froude No: 14.42; Strat No: 4.72E-5; Spcg No: 7.909; k: 7.544; eff den (sigmaT) -1.196681; eff vel 1.969(m/s);

Depth Amb-cur Amb-sal P-dia Eff-sal Polutnt Dilutn CL-diln x-posn y-posn Iso dia

Step (ft) (m/s) (psu) (in) (psu) (ppb) () () (ft) (ft) (m)

0 155.8 0.261 33.67 2.775 0.820 261.8 1.000 1.000 0.0 0.0 0.07049;

Ambient species greater than plume isopleth value, physical boundary graphed

10 155.7 0.261 33.67 3.328 6.979 213.8 1.225 1.000 0.132 0.0 0.08453;

20 155.7 0.261 33.67 3.982 11.77 176.1 1.487 1.000 0.282 0.0 0.1011;

30 155.7 0.261 33.67 4.751 15.71 145.0 1.807 1.000 0.463 0.0 0.1207;

40 155.7 0.261 33.67 5.652 18.93 119.3 2.197 1.098 0.682 0.0 0.1436;

50 155.7 0.261 33.67 6.701 21.58 98.14 2.672 1.336 0.946 0.0 0.1702;

60 155.7 0.261 33.67 7.913 23.75 80.69 3.252 1.626 1.265 0.0 0.2010;

70 155.7 0.261 33.67 9.305 25.53 66.34 3.958 1.979 1.651 0.0 0.2363;

80 155.7 0.261 33.67 10.89 27.00 54.53 4.819 2.410 2.120 0.0 0.2766;

90 155.6 0.261 33.67 12.68 28.19 44.83 5.869 2.934 2.691 0.0 0.3222;

100 155.6 0.261 33.67 14.70 29.18 36.85 7.148 3.574 3.388 0.0 0.3733;

110 155.5 0.261 33.67 16.94 29.98 30.30 8.708 4.354 4.205 0.0 0.4303;

120 155.4 0.261 33.67 19.44 30.65 24.91 10.61 5.305 5.099 0.0 0.4937;

130 155.2 0.261 33.67 22.19 31.19 20.49 12.93 6.464 6.054 0.0 0.5637; merging;

140 155.0 0.261 33.67 25.35 31.63 16.86 15.75 8.194 7.219 0.0 0.6439;

150 154.7 0.261 33.67 28.99 32.00 13.89 19.20 10.44 8.651 0.0 0.7363;

160 154.3 0.261 33.67 33.20 32.30 11.44 23.40 13.42 10.35 0.0 0.8433;

170 153.8 0.261 33.67 38.14 32.55 9.434 28.51 17.48 12.34 0.0 0.9688;

180 153.2 0.261 33.67 43.99 32.75 7.787 34.75 23.17 14.68 0.0 1.1173;

190 152.5 0.261 33.67 51.01 32.91 6.435 42.36 28.24 17.42 0.0 1.2956;

200 151.6 0.261 33.68 59.52 33.05 5.326 51.63 34.42 20.65 0.0 1.5118;

210 150.5 0.261 33.68 69.95 33.16 4.416 62.93 41.95 24.45 0.0 1.7768;

220 149.2 0.261 33.68 82.83 33.26 3.669 76.70 51.14 28.96 0.0 2.1038;

230 147.5 0.261 33.66 98.82 33.33 3.056 93.50 62.33 34.33 0.0 2.5099;

240 145.6 0.261 33.62 118.8 33.39 2.552 114.0 75.98 40.83 0.0 3.0182;

250 143.4 0.261 33.58 143.9 33.43 2.139 138.9 92.61 48.88 0.0 3.6563;

260 140.7 0.261 33.54 175.6 33.45 1.799 169.3 112.9 59.26 0.0 4.4598;

262 140.1 0.261 33.53 182.8 33.45 1.738 176.2 117.5 61.74 0.0 4.6442; trap level;

270 137.9 0.261 33.52 213.2 33.46 1.537 203.5 135.7 72.32 0.0 5.4150;

280 135.8 0.261 33.54 245.2 33.47 1.383 231.2 154.1 85.12 0.0 6.2286;

290 134.4 0.261 33.55 269.2 33.48 1.293 251.3 167.5 97.78 0.0 6.8377;

300 133.7 0.261 33.56 284.3 33.48 1.244 263.6 175.8 110.2 0.0 7.2219;

308 133.5 0.261 33.56 290.0 33.48 1.228 **268.0** 178.6 120.1 0.0 7.3655; local maximum rise or fall;

Horiz plane projections in effluent direction: radius(m): 0.0; CL(m): 36.603

Lmz(m): 36.603

forced entrain 1 128.4 6.782 7.366 1.000

Rate sec-1 0.0 dy-1 0.0 kt: 0.0 Amb Sal 33.5577;

4:50:50 PM. amb fills: 4

**APPENDIX-D:
SEOO - Plumes 20
Text file Output**



SAN ELIJO

JOINT POWERS
AUTHORITY



ENCINA
WASTEWATER
AUTHORITY



*Plume Tracking Field and Model Analysis of Discharges
from the Encina Ocean Outfall and San Elijo Ocean Outfall*

THIS PAGE INTENTIONALLY LEFT BLANK

Table 15: Plumes 20 (UM3) Initialization of SEOO Ebb Tide Ambient Conditions on 21 December 2021 with Ambient Current

Project "C:\Plumes20\SEOO_Ebb_21Dec_with-current_version-2"

Model configuration items checked:

- Channel width (m) 100
- Start case for graphs 1
- Max detailed graphs 10 (limits plots that can overflow memory)
- Elevation Projection Plane (deg) 0
- Shore vector (m,deg) not checked
- Bacteria model : Mancini (1978) coliform model
- PDS sfc. model heat transfer : Medium
- Equation of State : S, T
- Similarity Profile : Default profile (k=2.0, ...)
- Diffuser port contraction coefficient 1.0
- Light absorption coefficient 0.16
- Farfield increment (m) 200
- UM3 aspiration coefficient 0.1
- Output file: text output tab
- Output each ?? steps 25
- Maximum dilution reported 10000
- Text output format : Standard
- Max vertical reversals : to max rise or fall

/ UM3. 4/19/2022 12:49:15 PM

Case 1; ambient file C:\Plumes20\SEOO_Ebb_21Dec_with-current_version-2.001.db; Diffuser table record 1:

Ambient Table:

Depth	Amb-cur	Amb-dir	Amb-sal	Amb-tem	Amb-pol	Decay	Far-sp	Far-dir	Disprsn	Density
m	m/s	deg	psu	C	kg/kg	s-1	m/s	deg	m0.67/s2	sigma-T
0.0	0.263	0.0	33.50	15.28	2.8000E-10	0.0	0.0	0.0	0.0	24.77391
3.510	0.263	0.0	33.50	15.27	2.7500E-10	0.0	0.0	0.0	0.0	24.78057
6.466	0.263	0.0	33.50	15.24	2.4000E-10	0.0	0.0	0.0	0.0	24.78591
9.470	0.263	0.0	33.50	15.21	3.1000E-10	0.0	0.0	0.0	0.0	24.79147
12.52	0.263	0.0	33.50	15.15	3.3000E-10	0.0	0.0	0.0	0.0	24.80592
15.49	0.263	0.0	33.50	15.11	3.4000E-10	0.0	0.0	0.0	0.0	24.81486
18.53	0.263	0.0	33.46	14.98	3.0000E-10	0.0	0.0	0.0	0.0	24.81705
21.45	0.263	0.0	33.48	14.82	2.8000E-10	0.0	0.0	0.0	0.0	24.86070
24.51	0.263	0.0	33.41	14.46	3.0000E-10	0.0	0.0	0.0	0.0	24.88616
27.50	0.263	0.0	33.48	14.06	3.4000E-10	0.0	0.0	0.0	0.0	25.02182
30.51	0.263	0.0	33.41	13.67	3.3000E-10	0.0	0.0	0.0	0.0	25.05240
33.48	0.263	0.0	33.63	13.29	3.2000E-10	0.0	0.0	0.0	0.0	25.29523
36.51	0.263	0.0	33.48	13.05	3.4000E-10	0.0	0.0	0.0	0.0	25.22974
39.52	0.263	0.0	33.32	12.92	3.1000E-10	0.0	0.0	0.0	0.0	25.12819
42.50	0.263	0.0	33.49	12.27	3.2000E-10	0.0	0.0	0.0	0.0	25.38572

Diffuser table:

P-dia	Ver angl	H-Angle	SourceX	SourceY	Ports	MZ-dis	Isoplth	P-depth	Ttl-flo	Eff-sal	Temp	Polutnt
(in)	(deg)	(deg)	(m)	(m)	()	(m)(concent)	(ft)	(MGD)	(psu)	(C)	(ppb)	
2.0000	0.0	0.0	0.0	0.0	200.00	2000.0	0.0	140.00	12.630	1.0970	21.350	232.80

Table 16: Plumes 20 (UM3) Output of SEOO Dilution Factor (Dm) during Ebb Tide on 21 December 2021 with Ambient Current (Final Dm solution highlighted in yellow)

Simulation:

Froude No: 11.86; Strat No: 2.74E-5; Spcg No: 10.97; k: 5.190; eff den (sigmaT) -1.188470; eff vel 1.365(m/s);

Step (ft)	Amb-cur (m/s)	Amb-sal (psu)	P-dia (in)	Polutnt (ppb)	Dilutn ()	CL-diln ()	x-posn (ft)	y-posn (ft)	Iso dia (m)
0	140.0	0.263	33.49	2.000	232.8	1.000	1.000	0.0	0.0508;
1	140.0	0.263	33.49	2.026	226.9	1.026	1.000	0.0132	0.0 0.05146; bottom hit;
25	140.0	0.263	33.49	3.075	142.6	1.634	1.000	0.268	0.0 0.0781;
50	140.0	0.263	33.49	4.632	87.57	2.665	1.332	0.689	0.0 0.1176;
75	140.0	0.263	33.49	6.782	53.71	4.355	2.178	1.376	0.0 0.1723;
100	139.8	0.263	33.49	9.629	32.94	7.129	3.564	2.483	0.0 0.2446;
125	139.7	0.263	33.49	13.29	20.23	11.68	5.840	3.897	0.0 0.3376;
150	139.4	0.263	33.49	17.94	12.47	19.14	9.572	5.600	0.0 0.4558;
168	139.1	0.263	33.48	22.04	8.834	27.33	13.67	7.090	0.0 0.5598; merging;
175	139.0	0.263	33.48	23.87	7.734	31.39	16.05	7.814	0.0 0.6062;
200	138.3	0.263	33.47	32.04	4.843	51.49	29.09	11.71	0.0 0.8138;
225	137.2	0.263	33.45	43.99	3.080	84.46	56.30	18.23	0.0 1.1173;
250	135.3	0.263	33.42	62.73	2.005	138.5	92.36	28.94	0.0 1.5933;
275	132.2	0.263	33.36	94.00	1.348	227.3	151.5	47.67	0.0 2.3876;
280	131.5	0.263	33.35	102.6	1.251	250.9	167.3	53.24	0.0 2.6050; trap level;
300	128.5	0.263	33.33	142.0	0.978	355.0	236.7	88.89	0.0 3.6065;
310	127.8	0.263	33.35	155.7	0.921	388.6	259.1	125.2	0.0 3.9558; local maximum rise or fall;

Horiz plane projections in effluent direction: radius(m): 0.0; CL(m): 38.163

Lmz(m): 38.163

forced entrain 1 196.6 3.711 3.956 1.000

Rate sec-1 0.0 dy-1 0.0 kt: 0.0 Amb Sal 33.3462

;

12:49:15 PM. amb fills: 4